2.4 Hydrology

2.4.1 Hydraulic Description

Subsection 2.4.1.1 provides a general overview of the topography and hydrology in the site vicinity. Subsection 2.4.1.2 provides a discussion of the hydrosphere at Fermi 3 including local watersheds.

2.4.1.1 Site and Facilities

The Fermi site is located in the northeastern corner of Monroe County in southern Michigan, near the northern border of Ohio about 32 km (20 mi) north of the Michigan/Ohio border. The U.S./Canada international border runs through Lake Erie about 11 km (7 mi) east of the Fermi site. The Fermi site is on the west bank of Lake Erie, approximately 39 km (24 mi) northeast of Toledo, Ohio and 48 km (30 mi) southwest of Detroit, Michigan. The Fermi site encompasses approximately 510 hectares (1,260 acres), of which approximately 122 hectares (302 acres) will be utilized for the construction and operation of Fermi 3. Fermi 3 will be situated further inland than Fermi 2, approximately 0.40 km (0.25 mi) west of Lake Erie's shoreline.

The topography of the site is flat to gentle rolling plain. Site elevations range from the level of Lake Erie to approximately 7.6 m (25 ft) above the lake level on the western edge of the site. The topography on the Fermi site is relatively level in the undeveloped areas, with an elevation range of approximately 3 m (10 ft) over the site according to U.S. Geological Survey (USGS) topographic maps. Figure 2.4-209 and Figure 2.4-210 show USGS topographic maps of the 12-km (7.5-mi) vicinity and the Fermi property boundary, respectively. Lake Erie has an elevation of approximately 174 m (571 ft), while the area around the Fermi site ranges from 176 to 183 m (577 to 600 ft). The existing plant grade of elevation 177.7 m (583.0 ft) plant grade datum will be altered to 179.8 m (590.0 ft) plant grade datum. Fermi 3 safety-related facilities will be at a nominal grade of 180.0 m (590.5 ft) plant grade datum.

As described in Section 1.2, the plant arrangement is composed of nine principal plant structures: the Reactor Building, Control Building, Firewater Service Complex, Ancillary Diesel Building, Fuel Building, Turbine Building, Radwaste Building, Electrical Building, and Service Building. The Reactor/Fuel Building (RB/FB), Control Building (CB), and Fire Water Service Complex (FWSC) are the only three Seismic Category I structures of Fermi 3. A site plan showing the relative locations of the various Fermi 3 structures is shown on Figure 2.4-211. Seismic information pertaining to the Fermi site and vicinity is discussed in Subsection 2.5.1.

Lake Erie is the primary makeup water source for the CIRC, PSWS, and Fire Protection System (FPS). Additional water needs for potable water and makeup demineralizer water are supplied by the Frenchtown Township municipal water supply. Fermi 3 will utilize the intake bay currently in use by Fermi 2 and a newly constructed pump house to draw water from Lake Erie. Fermi 2 will continue to use both the intake bay and its current pumping location. Blowdown water and neutralized demineralizer waste will be discharged through a newly constructed outfall pipe.

Storm water runoff from the existing Fermi site flows to three drainage outlets, two ponds (Pond 1 and Stagnant Pond), and a drainage outfall pipe (Figure 2.4-214). Storm water runoff from the Fermi 3 final grade will flow into onsite drop inlets within the local drainage system, discharging to an outfall pipe. The outfall pipe discharges to an overflow canal which then enters the North Lagoon. The North Lagoon discharges to Swan Creek which feeds Lake Erie. Runoff may also drain by sheet flow to the North Lagoon and South Lagoon. (Figure 2.4-215 and Figure 2.4-217) The effects of Probable Maximum Precipitation (PMP) on site runoff are described in Subsection 2.4.2.

Soil characteristics are discussed in Subsection 2.5.4.

2.4.1.2 Hydrosphere

The Great Lakes Region is depicted in Figure 2.4-204. This region includes much of the Canadian Province of Ontario and eight U.S. states that border the Great Lakes: New York, Pennsylvania, Ohio, Indiana, Michigan, Illinois, Wisconsin, and Minnesota. Figure 2.4-206 depicts the hydrological pattern of the Great Lakes system. The following sections describe the hydrosphere surrounding Fermi 3 in more detail. The flooding potential of streams and rivers near the Fermi site is discussed in Subsection 2.4.3.

2.4.1.2.1 Swan Creek Watershed

The Fermi site is located within the 275 km^2 (106 mi^2) Swan Creek Watershed (Figure 2.4-208), which has an elliptical-shaped basin trending northwest-southeast. The mouth of Swan Creek is located approximately 1.6 km (1 mi) north of the Fermi site. The Swan Creek Watershed is the smallest drainage basin within the region and is bordered by the Huron River Basin to the north and the River Raisin Basin to the south. The Swan Creek Watershed contributes a small water flow to the relatively large water capacity of Lake Erie; however, under flood conditions it may have an impact locally at the site (Subsection 2.4.3).

2.4.1.2.2 Lake Erie

A regional view of Lake Erie and its major tributaries is shown on Figure 2.4-203. Furthermore, Figure 2.4-205 shows the 12-km (7.5-mi) perimeter with water bodies and land features identified. The 60,600 km^2 (23,400 mi^2) Lake Erie Drainage Basin is a sub-basin of the 774,000 km^2 (299,000 mi^2) Great Lakes Drainage Basin. The bathymetry of Lake Erie is shown on Figure 2.4-202. Figure 2.4-201 and Figure 2.4-202 show that Lake Erie is identified mainly by three separate basins:

- The western basin of Lake Erie is a very shallow basin with an average depth of 7.4 m (24 ft). The western basin is partially restricted from the rest of Lake Erie by a chain of barrier beaches and islands.
- The central basin of Lake Erie is uniform in depth with an average depth of 18.3 m (60 ft) and maximum depth of 25 m (82 ft).

- The eastern basin of Lake Erie is a small, relatively deep basin. The average depth in the eastern basin is 25 m (82 ft) with a maximum depth of 64 m (210 ft).

Figure 2.4-203 depicts the Lake Erie Drainage Basin and its twelve main tributaries: the Ashtabula River, Black River, Buffalo River, Clinton River, Cuyahoga River, Detroit River, Maumee River, Presque isle Bay, River Raisin, Rouge River, St Clair River, and the Wheatley Harbour.

Lake Erie is the shallowest, warmest, most southern and most biologically productive of all the Great Lakes. It supports more than eleven million people and eleven major ports and spans approximately 388 km (241 mi) with a breadth of 92 km (57 mi). The length of its shoreline is approximately 1,402 km (871 mi). Lake Erie has an average depth of 19 m (62 ft), a maximum depth of approximately 64 m (210 ft), a water surface area of approximately 25,670 km^2 (9,910 mi^2), and a volume of approximately 484 km^3 (116 mi^3) (Reference 2.4-202). The retention time of Lake Erie is 2.6 years, which is the shortest of all the Great Lakes (Reference 2.4-201). The lake is slow and meandering, and its velocity varies due to wind currents and seasonal climate change. The average flow rate of Lake Erie, according to data recorded by the U.S. Army Corps of Engineers (USACE), is 5,710 m^3/s (201,750 cfs) (Reference 2.4-217).

The Fermi site is protected by a shoreline barrier against the high water levels of Lake Erie. The rock shore barrier is located in front of Fermi 2 and Fermi 3 along the shore between Plant Coordinate System Grid N6800 and N7800. The rock shore barrier crest elevation is 178 m (583 ft) plant grade datum. The barrier is significant and historically functioned in keeping the shoreline bordering the site from eroding inland. Accordingly, a detailed analysis of local erosion characteristics and sediment transport is not necessary. Potential effects due to storm surge and seiche flooding are described in Subsection 2.4.3.

2.4.1.2.3 Detroit River

The Detroit River is the largest and most important tributary for the western basin of Lake Erie as it provides approximately 80 percent of Lake Erie's water inflow (Reference 2.4-219). The water quality of the western basin of the lake for the most part is similar to the Detroit River. The river has four monitoring stations which have been established by the National Oceanic and Atmospheric Administration (NOAA). The stations are located in Windmill Point, MI; Fort Wayne, MI; Wyandotte, MI; and Gibraltar, MI, listed from north to south with the Gibraltar station being the closest to the Fermi site. The outlet mouth of the Detroit River is approximately 26.6 km (16.5 mi) northeast of the Fermi site.

The Detroit River is about 51 km (32 mi) long from its head at the Windmill Point Light to its mouth at the Detroit River Light in Lake Erie. The decrease in water level from Lake St. Clair to Lake Erie is approximately 1 m (3 ft). The average velocity of the Detroit River has been estimated to be approximately 0.1 m/s (0.3 fps) in the winter months and as high as 0.2 m/s (0.5 fps) during summer months (Reference 2.4-220). The annual average flow-rate for the Detroit River during 2006 was 4,999 m^3/s (176,538 cfs).

2.4.1.2.4 Stony Creek

The Stony Creek Watershed is located in Washtenaw County and Monroe County in Southeastern Michigan. Stony Creek empties into the western basin of Lake Erie approximately 5 km (3 mi) southwest of the Fermi site. The watershed for Stony Creek is shown on Figure 2.4-208.

Stony Creek has a drainage area of approximately 326 km^2 (126 mi^2). There is no anticipated interface between Stony Creek and the construction and operation of Fermi 3. However, Stony Creek does impact sediment and other water quality characteristics within the western basin of Lake Erie in the vicinity of the Fermi site.

2.4.1.2.5 River Raisin

The River Raisin is located in the extreme southeastern portion of Michigan's Lower Peninsula and flows in a generally southeast direction, discharging into the western basin of Lake Erie at Monroe Harbor, approximately 9.6 km (6 mi) southwest of the Fermi 3 site. The river is approximately 185 km (115 mi) long, and its drainage area comprises approximately 2,770 km^2 (1,070 mi^2) of Southeast Michigan.

There is no anticipated interface between River Raisin and the construction and operation of Fermi 3. However, the River Raisin does impact sediment and other water quality characteristics within the western basin of Lake Erie in the vicinity of the Fermi site.

2.4.1.2.6 Additional Surface-Water Considerations

The site contains a man-made water basin that supports the functioning of the circulating water system for Fermi 2. Fermi 3 will not make use of this water basin, and the construction and operation of Fermi 3 will not impact this water basin. In addition, the site contains two Quarry Lakes that were established following rock quarry operations in support of site development activities for the construction of Fermi 2. Fermi 3 will not make use of the Quarry Lakes. The only impact to the Quarry Lakes may be minor temporary drawdown due to construction dewatering (Subsection 2.4.12.2.5.1)

There are no significant impoundments, reservoirs, estuaries, or oceans located in the region that needs to be considered when analyzing the hydrological impacts on the construction and operation of Fermi 3.

2.4.1.2.7 Water-Control Structures

Lake Erie is part of the larger network of the five Great Lakes. The outflows from two of the five Great Lakes (Lake Superior and Lake Ontario) are regulated by control structures. These outflows vary in accordance with their respective regulation plans. The outflows from Lake Michigan, Lake Huron and Lake Erie are not regulated; rather, they are controlled exclusively by the hydraulic characteristics of their outlet rivers (Reference 2.4-207). No control structures that would affect Lake Erie are expected to be constructed during the construction or operation of Fermi 3.

2.4.1.2.8 Surface-Water Use

Lake Erie is the principal source of water to the operation of Fermi 3. The most important Lake Erie parameter with respect to water use is the lake water level. Fermi 3 has been designed to operate at full capacity assuming the lowest historical water level at the plant basin intake. Low water considerations, including historical low lake levels, are discussed in Subsection 2.4.11.

There are two categories of surface-water use: withdrawal (non-consumptive) and consumption:

- "Withdrawal" refers to water drawn from surface or groundwater sources that is eventually returned to the area from where it came.
- "Consumption" refers to water that is withdrawn but not returned to the region.

In the Great Lakes Basin, non-consumptive withdrawals comprise 95 percent of water use, and consumption comprises only 5 percent. The vast majority of withdrawals, 90 percent, are from lakes, while 5 percent is withdrawn from streams and 5 percent from groundwater sources. The Great Lakes Basin has nine main sectors of water consumption: Public Water Supply, Self-Supply Domestic, Self-Supply Irrigation, Self-Supply Livestock, Self-Supply Industrial, Self-Supply Thermoelectric (Fossil Fuel), Self-Supply Thermoelectric (Nuclear), Hydroelectric, and Self-Supply Other. The most recent data collected concerning these sectors has been by the Great Lakes Commission (Reference 2.4-216).

The main sectors of water consumption regarding the region of influence from the construction and operation of Fermi 3, according to the MDEQ, are the following: Power Generation (Nuclear), Power Generation (Fossil Fuel), Public Water Supply, Agricultural Irrigation, Self-Supply Industrial, and Golf Course Irrigation. Water withdrawal information from years 2000 through 2006 for Monroe County is shown on Table 2.4-205. Table 2.4-206 and Table 2.4-207 show the 2005 and 2006 Monroe County water-use reports for these sectors. Table 2.4-208 shows the 2006 Monroe County water capacity report for these sectors. Table 2.4-206 through Table 2.4-208 show that the current water use for Fermi 2 is relatively small, representing approximately 3 percent of the overall water used by the three power generation facilities located nearby.

The actual withdrawals and consumption of Great Lakes water have decreased by 48 percent in the past two decades. The decrease is largely a result of technological innovations, many of which improve the quality of water discharged back to the basin. However, the public data on withdrawals overstates certain consumptive uses. For example, hydroelectric utilities routinely are cited among the largest users of Great Lakes water. In fact, all but one percent of billions of gallons of water utilized to drive turbine generators are returned to the basin. Considering hydroelectric use, the volume of Great Lakes withdrawals decreases from 3.20 billion m^3 (845 billion gallons) per day to 0.17 billion m^3 (45 billion gallons) per day, a 95 percent difference (Reference 2.4-208).

The degree of impact for each sector is shown on Figure 2.4-207 which displays the total withdrawal rates for each sector for the years of 2000 through 2004. On Figure 2.4-207, the Power Generation sector includes power generation from all fuel types. Furthermore, the yearly water

usage of withdrawals and consumption for Lake Erie are shown on Table 2.4-201 through Table 2.4-204. By comparing the quantity of withdrawals within the vicinity of Fermi 3 (Table 2.4-205) with the water supply of Lake Erie (Table 2.4-209), it is seen that the current water usage by the Power Generation sector is relatively small. A conservative quantity of withdrawals for Monroe County is approximately 2.5 billion m^3 (670 billion gallons) per year. The net water supply for Lake Erie in 2005 was approximately 177 billion m^3 (46,661 billion gallons) for the year. Thus, withdrawals comprise approximately 1.4 percent of the total Lake Erie supply.

2.4.1.2.9 Groundwater Use

Groundwater is not anticipated to be used at Fermi 3. Subsection 2.4.12 fully describes the regional and local groundwater.

2.4.2 Floods

Subsection 2.4.2.1 identifies the flood history at the Fermi 3 site. Subsection 2.4.2.2 describes the considerations used to determine the Probable Maximum Flood (PMF) for the site and shows that safety related facilities are located above the worst potential flood consideration. Subsection 2.4.2.3 describes the model used to estimate the local PMP runoff water levels, describes the capacity of drainage facilities, and shows that safety related facilities are adequately protected.

2.4.2.1 Flood History

Due to its proximity to the site, Lake Erie is the primary surface-water body to potentially impact Fermi 3. The Fermi site is located outside the realm of significant impact due to the flooding of local streams and rivers. The PMF of Swan Creek is discussed in Subsection 2.4.3. Following is a description of historical flooding of Lake Erie and other bodies of water surrounding Fermi 3.

Lake Erie

Lake Erie is in the Lake Erie Drainage Basin, which is a sub-basin of the Great Lakes Drainage Basin. The Lake Erie Drainage Basin is shown on Figure 2.4-203. The western basin of Lake Erie, along which Fermi 3 is located, is a very shallow basin with an average depth of 7.4 m (24 ft) and is partially restricted from the rest of Lake Erie by a chain of barrier beaches and islands.

Approximately 80 percent of Lake Erie's total inflow is from the Detroit River, 11 percent from precipitation, and the remaining 9 percent from tributaries flowing through watersheds in Michigan, Ohio, Pennsylvania, New York, and Ontario. Outflows from Lake Erie are not regulated; rather, outflows are controlled by the hydraulic characteristics of its outlet rivers.

The topography of the site is flat to gentle rolling plain and is located in the Swan Creek watershed, which is the smallest drainage basin within the region. The Swan Creek watershed has an elliptical-shaped basin, trending northwest-southeast, and generally distributes a small flow of water when compared to the capacity of Lake Erie.

The water levels of Lake Erie have been recorded from 1860 to the present by the Great Lakes Environmental Research Laboratory (GLERL). Extreme water levels, obtained from the Fermi Power Plant gauging station (ID 9063090), from 1967 to 2007, are shown on Figure 2.4-212. The data for these extreme water levels are shown on Table 2.4-210. The highest recorded water level of these extremes is 175.79 m (576.73 ft) NAVD 88, occurring in 1973 and 1985. Table 2.4-210 also lists the lowest recorded water level, of 171.9 m (563.9 ft) NAVD 88, which occurred in 1967 (Reference 2.4-228, Reference 2.4-234).

Recent flooding occurred within the Great Lakes Basin between 1985 and 1987. Precipitation over the entire Great Lakes Basin between November 1984 and April 1985 was 20 percent above average, and from May to December of 1985, precipitation was 27 percent above average. The 1985 spring runoff was 20 to 65 percent above normal, the highest in 20 years. The gauging station (ID 9063090) at the Fermi site on Lake Erie recorded a peak water level of 175.71 m (576.47 ft) IGLD 85 on March 31, 1985.

On December 2, 1985, a storm with winds gusting up to 100 km/hour (62.14 mph) severely affected shorelines with western exposures. The peak elevation at the Fermi site during this storm event was 174.4 m (572.1 ft) IGLD 85. A later storm event caused a peak elevation of Lake Erie at the Fermi site of 175.7 m (576.4 ft) IGLD 85, recorded on February 7, 1986. Furthermore, a peak elevation of 175.6 m (576.0 ft) IGLD 85 was recorded on January 19, 1987.

Swan Creek

Swan Creek, located north of the Fermi site, typically experiences maximum flow rates in the spring and minimum flow rates in late summer. At its mouth (Section 16, T6S, R10E, Frenchtown Township, Monroe County) Swan Creek has a drainage area of approximately 275 km^2 (106 mi^2). The 10, 2, 1, 0.5, and 0.2 percent peak flow rates are estimated to be 70, 100, 120, 130, and 140 m^3/s (2500, 3700, 4100, 4600, and 5000 cfs), respectively (Reference 2.4-232)

Stony Creek

Stony Creek is located about 5 km (3 mi) southwest of the Fermi site. It typically experiences maximum flow rates in the spring and minimum flow rates in late summer. The 10, 2, 1, 0.5, and 0.2 percent peak flows are estimated to be 50, 80, 100, 120, and 140 m^3/s (1800, 2900, 3600, 4100, and 4900 cfs), respectively (Reference 2.4-233).

River Raisin

The River Raisin, located about 9.6 km (6 mi) southwest of the Fermi site, typically experiences maximum annual flooding in April and May. The largest flood (records begin in 1938) of the River Raisin occurred on March 29, 1950, and the second largest occurred on April 6, 1947. The 10, 2, 1, 0.5, and 0.2 percent chance peak flows are estimated to be 280, 420, 480, 540, and 650 m^3/s (10000, 15000, 17000, 19000, and 23000 cfs), respectively (Reference 2.4-241)

Given the topography, regional location, and historical climatology of the Swan Creek Watershed, snowmelt factors will pose no significant impacts on flooding.

2.4.2.2 Flood Design Considerations

The design basis PMF is the most severe combination of critical meteorological and hydrologic conditions that are reasonably possible in the region being analyzed. The design basis PMF for Fermi 3 was determined by considering a number of flooding possibilities. Those applicable to the Fermi site include the local PMP runoff water levels (Subsection 2.4.2.3), the PMF of streams and rivers (Subsection 2.4.3), probable maximum surge and seiche flooding (Subsection 2.4.5), and flooding due to ice effects (Subsection 2.4.7). Each of these flooding scenarios was investigated in conjunction with the local streams and lakes per guidelines of ANSI/ANS-2.8-1992 (Reference 2.4-226). The highest water level determined from these flooding possibilities is selected as the design basis PMF and becomes a site parameter, as noted in Table 2.0-1, Envelope of ESBWR Standard Plant Site Parameters (Reference 2.4-225).

Flooding possibilities not considered in determination of the design basis PMF include flooding due to potential dam failures (Subsection 2.4.4) and flooding due to tsunami (Subsection 2.4.6). Landslides are also not likely to occur on the site (Subsection 2.5.5). Supporting information for these conclusions is described in the corresponding sections. Generally, these conclusions are based on the topography, geography, and location of the site within the Swan Creek watershed.

The most severe flooding combination possibility at the Fermi 3 site is caused by a potential high surge from Lake Erie. Details of the surge analysis are discussed in Subsection 2.4.5. Based on this analysis, safety-related structures and component elevations at the Fermi 3 site are established at elevation 179.6 m (589.3 ft) NAVD 88.

2.4.2.3 Effects of Local Intense Precipitation

The existing site area uses three drainage outlets, two ponds (Pond 1 and Stagnant Pond), and a drainage outfall pipe to handle storm discharge (Figure 2.4-214). Storm water runoff from the Fermi 3 final grade will possibly flow toward two lagoons (North Lagoon and South Lagoon) and also into onsite drop inlets within the local drainage system discharging to an outfall pipe. The outfall pipe discharges to an overflow canal which then enters the North Lagoon. The North Lagoon will discharge to Swan Creek which feeds Lake Erie, and the South Lagoon will discharge directly to Lake Erie. Figure 2.4-214 and Figure 2.4-215 show the distribution of flows for typical storm events on the existing site area and the final grade area, respectively. Figure 2.4-217 shows the distribution of flows assuming that all local underground storm drains and culverts are completely clogged. The drainage areas for storm water conveyance facilities around the Fermi 3 site are less than 2.6 km^2 (1 mi^2).

The following assumptions were used in the local PMP analysis. Further explanation can be found later in this section.

- All culverts and storm drains are completely clogged.
- The entire raised elevation (Areas S1+S2+S3+N1+N2) plus Area N3 concentrates through Area N3.
- A rectangular channel will collect the concentrated flow in Area N3 creating a backwater effect.

The backwater effect caused by the local PMP was considered and is discussed later in this section. The effect of snowmelt on the local PMP was considered and is discussed later in this section as well.

PMP is defined as the greatest depth of precipitation for a given duration that is physically possible over a given size storm area at a particular geographical location at a certain time of the year, as defined by Hydro-Meteorological Report (HMR) No. 55A. The PMP values for the 275 km^2 (106 mi^2) Swan Creek watershed were developed using HMR No. 51 and No. 52, which were published by NOAA (Reference 2.4-227). These regional PMP values are presented in Subsection 2.4.3. HMR No. 52 lists the multiplying factors to convert the 26 km^2 (10 mi^2) area PMP values to relative 2.6 km^2 (1 mi^2) PMP values. The derived PMP depths and durations are shown in Table 2.4-211. The corresponding PMP intensity duration curve is shown in Figure 2.4-213.

The specific flow-rate for the Fermi 3 site was calculated using the PMP intensity duration curve with the rational method. The rational method is used to determine peak runoff rates from specified areas. The rational method is given by Equation 1:

$$Q = k * C * I * A \qquad \text{[Eq. 1]}$$

where:

Q = runoff in cfs
k = constant = 1 for English units
C = unitless coefficient of runoff
I = intensity in inches/hour
A = drainage area in acres

Rainfall duration is assumed to be equal or greater than the time of concentration for each site drainage area. The corresponding intensity is determined using Figure 2.4-213. The coefficient of runoff, C, is assumed to equal 1.0 in order to conservatively estimate runoff and account for saturated antecedent conditions.

Storm runoff results for typical design storms, such as the 10-, 25-, 50-, and 100-year storms, are shown in Table 2.4-212 and Table 2.4-213 for the existing sub-basin drainage area and the final grade area, respectively. US Department of Agriculture, “Urban Hydrology for Small Watersheds,” Technical Release 55 (TR-55), dated June 1986, (Reference 2.4-298) provides methods for determining the time of concentration. Various methods in TR-55 include equations for sheet flow,

shallow concentrated flow, and streamflow. For the Fermi 3 raised area, the streamflow component was not applicable and therefore not included. Thus, the time of concentration for the onsite subbasins was calculated using the equations from TR-55 for sheet flow and shallow concentrated flow. Consistent with TR-55, the time of concentration is determined using the sheet flow equation for the first 300 feet of the flow path. After 300 feet, the time of concentration is determined using the shallow concentrated flow method. The total time of concentration is the sum of the sheet flow and shallow concentrated flow components.

The equations used are shown below.

Sheet Flow

$$T_{c1} = \frac{[0.007(Ln)^{0.8}]}{(P_2^{0.5} s^{0.4})}$$

Where:

T_{c1}= Time of concentration, hr
n = Manning roughness coefficient (Table 3-1, Smooth Surfaces, UFSAR Reference 2.4-298)
L = Flow length, ft
P_2= 2-year, 24-hour rainfall, inches (Reference 2.4-306, Isopluvial Chart 44)
s = Overland slope, ft/ft

Shallow Concentrated Flow

$$T_{c2} = \frac{L}{V}$$

Where:

T_{c2}= Shallow concentrated flow time of concentration, s

L= Flow length, ft

V= Average velocity, ft/s (Figure 3-1, “Paved” in Reference 2.4-298)

Total Time of Concentration

$$T_t = T_{c1} + T_{c2}$$

Where:

T_{c1}= Sheet flow time of concentration, min

T_{c2}= Shallow concentrated flow time of concentration, min

Table 2.4-214 compares the runoff of the existing site drainage area and the final grade site area for each design storm event. The additional runoff from the typical storm events will have a minimal impact on the site due to the size and slope of the outfall pipe, the final grade design storm flow distribution, and local site topography.

The NRCS Dimensionless Unit Hydrograph Method (Reference 2.4-238) was also used to calculate the one-hour unit hydrograph and the composite flood hydrograph for the 2.6 km^2 (1 mi^2) drainage area of the Fermi 3 site. This hydrograph is shown on Figure 2.4-216.

Manning's Equation was used to estimate a boundary channel depth that will be required to receive the local runoff from the PMP storm (Reference 2.4-227, Reference 2.4-229 through Reference 2.4-231). Manning's Equation is given by Equation 2, as follows:

$$Q = (k * A * R^{2/3} * s^{1/2}) / n \qquad \text{[Eq. 2]}$$

where:

Q = discharge in cfs
k = constant equal to 1.49 for English units
R = hydraulic radius = A/P_w
A = cross sectional flow area in square ft
P_w = wetted perimeter in ft
s = slope of hydraulic grade line in ft/ft
n = Manning's roughness coefficient for open channel flow

The channel characteristics used for the Manning's Equation were a bottom width of 23 m (75 ft), vertical sides, a slope of 0.006, and a roughness coefficient of 0.013.

Development of the local PMP runoff water level used a PMP depth at five minutes duration, corresponding to an intensity of 177 cm/hr (69.6 inches/hr) (Figure 2.4-213). Table 2.4-213 shows that the time of concentration (duration) are all greater than 5 minutes. Therefore, the 5 minute duration for the entire site is conservative. The most conservative method of calculation evaluates the potential impact on the safety related area of 7.59 hectares (18.76 acres), which is the final grade area without considering discharge section N3 (Table 2.4-213). The area used in the rational method was the combination of the safety related area and drainage area N3 because this total area may potentially impact the safety related structures from backwater during the local PMP storm. This total area is 18.10 hectares (44.72 acres). Due to the minimal 0.6 percent slope within the 10.51 hectare (25.96 acre) N3 area, the storm-runoff from the local PMP storm could create a backwater scenario due to the storm runoff leaving the 8 percent slope of the safety related area at a higher velocity than the 0.6 percent slope of the N3 drainage area. Using the rational method, the corresponding runoff for this area is 88.1 m^3/s (3,112 cfs). For this discharge, Manning's equation

predicts a runoff depth of 0.79 m (2.59 ft), using the channel characteristics described above. This depth is the local PMP runoff water level.

The effects of snowmelt on the local drainage were also evaluated. For local drainage on the plant site, the PMP 5-min intensity of 177 cm/hr (69.6 inches/hour) was used to estimate snowmelt. Snowmelt was estimated to be 3.92 cm (1.54 inches) during the 5-minute maximum rainfall intensity, thus producing a rainfall intensity equivalent of 47.0 cm/hour (18.5 inches/hour). The total equivalent intensity product of the PMP on snow is then 224 cm/hour (88.1 inches/hour).

Following the same procedure explained earlier in this section, the Rational Method and Manning's equation were used respectively to calculate runoff and flow depths. When accounting for snowmelt the calculated discharge was 110 m^3/s (3,880 cfs) and the flow depth was 0.91 m (2.97 ft). The existing plant grade is at elevation 177.3 m (581.8 ft) NAVD 88 and the nominal plant grade of safety related structures is at elevation 179.6m (589.3 ft) NAVD 88. Therefore, the Fermi 3 nominal plant grade elevation would be approximately 1.38 m (4.53 ft) above the local PMP runoff flood level. No safety related structures would be impacted by flooding due to the local PMP runoff.

Given that the existing plant grade is at elevation 177.3 m (581.8 ft) NAVD 88, the most conservative water level due to PMP runoff at the Fermi 3 site is approximately 178.2 m (584.67 ft) NAVD 88. The nominal Fermi 3 plant grade of safety related structures is 179.6 m (589.3 ft) NAVD 88. Therefore, the Fermi 3 nominal plant grade elevation is approximately 1.4 m (4.5 ft) above the local PMP runoff flood level. Accordingly, no safety related structures will flood due to PMP runoff.

To prevent erosion on the 8% slopes of the elevated area, a storm water collection system will be designed to collect the runoff before it has a chance to reach the slopes. Figure 2.4-215 shows the conceptual storm water collection plan. The runoff will be collected in drop inlets where it will make its way to an outfall pipe at the north canal. Therefore the only runoff that the slopes will see is from direct rainfall onto the slopes. The slope area is small which will result in a small runoff. The small runoff spread over the length of the boundary of the elevated area will result in very low velocities. Erosion does not occur at very low velocities. **[START COM FSAR-2.4-002]** Detailed design will incorporate best industry practices included in "The Guidebook of Best Management Practices for Michigan Watersheds" to provide added erosion protection to the slopes, even though they are receiving very little runoff. These practices include mulching, seeding, sodding, soil management, trees, shrubs, and ground covers. To be conservative, erosion protection methods selected will be based on runoff velocities for a local PMP condition not taking credit for the storm water drains. Where necessary, erosion protection will be provided for breaking waves during a postulated surge/seiche event.**[END COM FSAR-2.4-002]**

2.4.3 Probable Maximum Flood on Streams and Rivers

This section determines the PMF of the Swan Creek Watershed, which is located hydrologically above Fermi 3. The guidance of ANSI/ANS-2.8-1992, which is the latest available standard, was used in determining the PMF (Reference 2.4-235).

The Swan Creek Watershed is shown on Figure 2.4-208 (Reference 2.4-240). It has a drainage area of approximately 275 km^2 (106 mi^2). Swan Creek, the main outlet for this watershed and a minor tributary of the western basin of Lake Erie, is located approximately 1.6 km (1 mi) northeast of Fermi 3. Swan Creek is currently ungauged. Consequently, there is no recorded flow data pertaining to historical storm events. However, historical flow rates have been estimated by the Michigan Department of Environmental Quality (MDEQ) using the Drainage Area Ratio (DAR) method on Plum Brook watershed, gauge 04163500, near Utica, MI. The lowest 95 percent and 50 percent exceedance, the harmonic mean, and the 90-day once in 10-year flow (90Q10) for Swan Creek are estimated to be 0, 0.08, 0.13, and 0.03 m^3/s (0, 2.8, 4.6, and 0.9 cfs), respectively. Monthly 50 percent and 95 percent exceedance flows and monthly mean flows are shown on Table 2.4-215.

The MDEQ estimated the Swan Creek peak flow rates from the FEMA Flood Insurance study for Monroe County, Michigan (Reference 2.4-300). The hydrology analysis, as stated in Reference 2.4-300, page 12, was carried out using TR-20, a computer program that utilizes the parameters of land use, soil types, topography, and precipitation in the development of peak flow rates. The Swan Creek 10 percent, 2 percent, 1 percent, 0.5 percent, and 0.2 percent peak flow rates are estimated to be 70, 100, 120, 130, and 140 m^3/s (2500, 3700, 4100, 4600, and 5000 cfs), respectively (Reference 2.4-244).

Other streams and rivers near the Fermi site include Stony Creek, about 5 km (3 mi) southwest, the River Raisin about 9.6 km (6 mi) southwest, and the Huron River about 9.25 km (5.75 mi) north. These water bodies are far enough away from the site that even the most severe flooding would not cause a potential hazard to Fermi 3.

On site flooding due to runoff is covered in Subsection 2.4.2. Seismic information is discussed in detail in Subsection 2.5.1. Seismic events are not expected to have an impact on flooding at the site.

2.4.3.1 Probable Maximum Precipitation

The PMF of Swan Creek was determined based on PMP estimates. The PMP was developed according to the procedures outlined in Hydrometeorological Report (HMR) No. 51 (Reference 2.4-236). The PMP values were estimated based on the size of the Swan Creek Watershed drainage area, in accordance with the procedures outlined in HMR No. 51.

HMR No. 51 data used to generate depth-area-duration curves consisted of historical precipitation maps based on 6 to 72-hour rainfall storms for various watershed areas located east of the 105th meridian. The evaluated watershed areas ranged from 26 to 26,000 km^2 (10 to 10,000 mi^2). The Swan Creek Watershed depth-area-duration curves from 6 to 72-hour rainfall storms were produced by interpolating this data.

As indicated in ANSI/ANS-2.8-1992, an antecedent storm condition was assumed. Furthermore, the isohyetal pattern was oriented over the watershed to obtain the maximum precipitation volume

over the entire drainage area. The evaluation yielded a PMP of 79.8 cm (31.4 inches) for the watershed. Table 2.4-216 presents the PMP values for the Swan Creek Watershed.

Guidance from ANSI/ANS-2.8-1992 was followed in determining the time distribution of the PMP. The incremental PMP values were grouped in a critical time sequence that represented the most significant potential rainfall impact within the watershed. This sequence was chosen based on historical rainfall events and the land characteristics of the watershed. During the first 24 to 30 hours of rainfall, the infiltration and storage capacity factors have a greater effect on rainfall water-flow than after 30 hours, so sequencing the maximum 24 hour period before 30 hours is not conservative. Moreover, sequencing the maximum 24 hour period at the end of the 72-hour rainstorm is not conservative due to the time of concentration of the watershed. The most conservative sequence is shown on Table 2.4-217. This sequence includes the maximum rainfall between 30 to 54 hours of the 72-hour storm.

The evaluation of the impact of snowmelt is organized around requirements stated in ANSI/ANS-2.8-1992 Sections 5.2 and 5.3. Initial snowpack is assumed to cover the whole watershed with no significant variation of temperature or snow depth. The critical sequence of meteorological factors affecting melt are described in the explanation of the equation used. Rainfall total and time distribution was calculated using the Probable Maximum Storm (HMR52) software (Reference 2.4-302). Loss and runoff conditions are estimated using the NRCS curve number (CN) method.

-Hourly PMP

A detailed PMP analysis was done to evaluate the impacts of snowmelt in the PMF analysis on Swan Creek Watershed. The HMR52 software package by the Hydrologic Engineering Center of the U.S. Army Corps of Engineers was used to determine the PMP with hourly precipitation depths.

Inputs to the HMR52 software are as follows:

- Figure 2.4-258 shows the watershed boundary, including the x and y coordinates (Miles, state plane Michigan South).
- The recommended storm orientation used was 250º (Figure 8, Reference 2.4-301)
- Depth-Area-Duration data (Figures 16 through 47, Reference 2.4-302) is summarized in Table 2.4-237.
- The SA (input) card in the software was used to steer the program to calculate the storm size and orientation that produces the maximum precipitation. As calculated iteratively these values are respectively 100 Mi2 and 311º. These parameters were hard coded on the last run of the model.
- The 1-hr to 6-hr ratio used is 0.302 (Figure 39, Reference 2.4-301). This value is needed to provide a 60 min (1-hr) temporal distribution of the PMP.

Figure 2.4-259 shows the PMP hyetograph resulting from the input to the software.

-Snowmelt

The U.S. Army Corps of Engineers EM 1110-2-1406 “Runoff from Snowmelt” (Reference 2.4-303) was used as guidance for computing snowmelt runoff. The lumped model approach was used, which assumes the progression of each variable through time can be a single computational algorithm that represents the entire basin. The sources of energy affecting snow melt include short-wave and long-wave net radiation, convection from the air, vapor condensation, and conduction from the ground, as well as energy contained in rainfall.

Whenever sufficient energy is available, some snow (ice) will melt and form liquid water (snowmelt). Snowmelt is held as a liquid in the interstices between snow grains and will increase snow water content. Snowpack is considered “ripe” when it is isothermal at 0 degrees Celsius (32 degrees F) and saturated. Estimates of snowmelt amounts are derived through the use of energy balance equations. Generalized equations were adapted to varying degrees of forest cover. For the Fermi 3 site in Michigan the equation for open or partly forested areas was used. (Equation 5-19, Reference 2.4-303):

$$M = (0.029+0.0084kV+0.007Pr)(T_a-32)+0.09$$

Where,

M = snowmelt, in/day

k = basin wind coefficient

V = wind velocity, miles/hr

Pr = rate of precipitation, in/day

T_a = temperature of saturated air, ºF

This equation assumes constant shortwave radiation and ground melt. The atmosphere was assumed to be saturated, which allows the option to equate dew-point temperature to air temperature. This assumption would be valid under PMP conditions. For the 2-year wind speed we evaluated historical data used for the surge and seiche analysis, Section 2.4.5, and chose a max value from the hourly readings for a more conservative calculation.

A value of one was used for the basin wind coefficient k, which represents unforested plains (some wooded areas exist in the watershed but in lieu of a detailed analysis of land cover, a conservative value of the coefficient was used). Precipitation rate was calculated from the PMP hyetograph (Figure 2.4-259).

A plausible scenario is that snow has fallen and temperatures remain low enough to allow snow accumulation on the ground through winter, and at the beginning of spring a saturated air mass with high temperature produces a rainfall event of the magnitude of the PMP. Inspection of historical monthly temperature averages and maxima showed that April is a month where relatively high temperatures can occur after freezing or lower temperatures have been maintained. These conditions are required for the PMP on snow to occur, so the April values were used.

The wind velocity and temperature was calculated by performing a statistical analysis of historical wind velocities and dewpoints measured in April at the Detroit Metropolitan Airport meteorological station. During a PMP event it is assumed that rainwater temperature is equal to air temperature (Reference 2.4-303) and that dewpoints are representative of air temperature (Reference 2.4-226). The maximum hourly windspeeds and dewpoints for the month of April were compiled for each year on record (34 years, 1961-1995). An extreme value frequency analysis was done to determine the hourly windspeed with an annual (in April) exceedance probability of 50% (2-yr hourly windspeed) and the hourly dewpoint with an annual (in April) exceedance probability of 1% (100-yr dewpoint). The estimated max 2-yr windspeed and the 100-yr dewpoint are respectively 52.3 Km/h (32.5 mph) and 20.6 ºC (69.1 ºF). In lieu of a detailed analysis of temporal variations of windspeeds and dewpoints the max hourly values were assumed to be constant over the 72hr PMP (a conservative assumption).

Figure 2.4-260 shows results of the snowmelt analysis in the form of total depth of rain and snowmelt available for runoff during the PMP on snow event.

-Runoff and Streamflow

Runoff and runoff transformation into streamflow calculations were run using HEC-HMS 3.1.0 software using the CN method. A CN of 98 was used to represent completely saturated ground conditions, a conservative but plausible situation under “ripe” snow conditions. Initial abstractions where calculated using the NRCS default (Ia = 0.2 S, where S = (1000 – 10 CN) / CN = 0.2 in) The transformation into streamflow was done using the NRCS Dimensionless Unit Hydrograph. The NRCS unit hydrograph lag time (t_{lag}) can be estimated from the time of concentration (t_c) where, t_{lag} = 3/5 t_c. Using the methods discussed in UFSAR Subsection 2.4.3.3, the time of concentration for the Swan Creek watershed was 16.4 hours, and the lag time was 9.84 hours (590.4 minutes). A time interval of 1-hr was selected for the calculations in HEC-HMS.

The estimated peak discharge at the downstream end of Swan Creek due to the PMP on snow was 4.76 x 10^3 m^3/s (1.68 x 10^5 cfs). Figure 2.4-261 summarizes the HEC-HMS run results.

-Water Surface Elevations

The HEC-RAS model as described in UFSAR Subsection 2.4.3.5 was used to determine the water surface elevation at the plant site that would result from the PMP on snow runoff.

To evaluate the impact of the worst possible condition the downstream boundary conditions of the model were set to the maximum surge and seiche (still water elevation of 178.4 m (585.4 ft) NAVD 88). This setting provides an extreme combination of conditions that would exceed the three scenarios proposed in Reference 2.4-226. The flow modeled was 4.76 x 10^3 m^3/s (1.68 x 10^5 cfs), resulting from PMP on snow runoff.

The modeling results show that at station 19+36.913 (Fermi 3 site) the water surface elevation would be 178.46 m (585.51 ft) NAVD 88 (Figure 2.4-262). The nominal plant grade of safety related structures is 179.62 m (589.3 ft) NAVD 88. Therefore, the Fermi 3 nominal plant grade elevation would be approximately 1.15 m (3.8 ft) above the Swan Creek PMP on snow flood level. Accordingly, no safety related structures would be impacted by flooding due to the PMP on snow pack.

2.4.3.2 Precipitation Losses

Estimates of precipitation losses for the Swan Creek Watershed are required to determine the direct runoff hydrograph. Surface soils in the Swan Creek drainage area are largely comprised of lacustrine clays, which have a low infiltration capacity. Winter initial losses typically vary from 0 to 0.5 cm (0 to 0.2 inches), and winter infiltration losses typically vary from 0.03 to 0.5 cm/hr (0.01 to 0.2 inches/hr). Summer initial losses typically vary from 1.3 to 3.1 cm (0.5 to 1.2 inches), and minimum summer infiltration losses are approximately 0.1 cm/hr (0.05 inches/hr).

In determining the PMF, the NRCS method was used in calculating the losses. The curve number (CN) for each type of landuse (30 percent small grain, 30 percent forage and pasture, 25 percent row crops, and 15 percent wooded land and building) of the watershed was determined assuming a soil type of Type D. The CN for each landuse was 82, 89, 82, and 83 respectively. The composite curve number for the watershed was 84.25. This value was used to calculate a storage capacity of 4.75 cm (1.87 inches). The storage capacity was used to calculate an initial abstraction of 0.97 cm (0.38 inches). The average infiltration rate was calculated to be 0.08 cm/hr (0.03 inches/hr) for the entire 72- hr probable maximum storm. These precipitation losses for the 72-hour period specify the general soil behavior of lacustrine clays within the region during wet antecedent conditions, when the moisture capacity of the topsoil is essentially saturated. Even though these losses were calculated, they were not applied to the Swan Creek watershed PMF hydrograph. Essentially the watershed was assumed to be completely impervious. This produced a more conservative peak flow rate for the PMF.

A separate analysis was performed for the effects of snowmelt on the PMP. To represent completely saturated ground conditions caused by snow cover a SCS curve number of 98 was assumed in the

calculation of the losses. The initial abstraction was calculated to be 0.1 cm (0.04 inches) using the NRCS method.

2.4.3.3 Runoff and Stream Course Models

ANSI/ANS-2.8-1992 lists the three pertinent alternative combinations to be evaluated in determining the PMF level.

Alternative I

1. One-half PMF or 500-year flood, whichever is less.
2. Surge and seiche from the worst regional hurricane or windstorm with wind wave activity.
3. 100-year or maximum controlled level of waterbody, whichever is less.

Alternative II

1. PMF.
2. 25-year surge and seiche with wind wave activity.
3. 100-year or maximum controlled level of waterbody, whichever is less.

Alternative III

1. 25-year flood.
2. Probable maximum surge and seiche with wind wave activity.
3. 100-year or maximum controlled level of waterbody, whichever is less.

The Natural Resources Conservation Service (NRCS) Dimensionless Unit Hydrograph method (Reference 2.4-238) was used to generate the PMF flow rate for the Swan Creek Watershed. This method is well-documented and considered a Best Management Practice (BMP) in design (Reference 2.4-239). In hydrograph analysis, the storm hyetograph (rainfall input function) is converted to the direct runoff hydrograph (output) using a unit hydrograph (transfer function). The land use of the area is estimated as follows: 30 percent small grain, 30 percent forage and pasture, 25 percent row crops, and 15 percent wooded land and buildings. These values were implemented into the unit hydrograph model. The time of concentration (T_C) is the time of travel from the most remote (timewise) point hydraulically in the watershed to the watershed outlet or other design point (Reference 2.4-237). In this analysis, T_C was estimated using the Kirpich equation (Reference 2.4-243). The Kirpich equation is given by Equation 3, as follows:

$$T_C = 5.735 * L^{0.77} * Y^{-0.385} \qquad \text{[Eq. 3]}$$

where:

T_C = Time of concentration in minutes

L = Length in mi
Y = Slope in ft per ft

The ordinates of the NRCS dimensionless unit hydrograph are given on Table 2.4-218. Linear interpretation of these ordinates was used to develop the unit hydrograph for the Swan Creek Watershed that represents the distribution of 72-hour PMP. The unit hydrograph developed for the Swan Creek Watershed is the hydrograph of direct runoff that results from one inch of excess rainfall generated uniformly over the watershed at a constant rate every six hours.

Subsection 2.4.3.4 gives the PMF flow, generated by the NRCS unit hydrograph method, which is used in the analysis of Alternative II. The Lake Erie elevation calculated for Alternative II was the 100-year lake level of 175.3 m (575.1 ft) NAVD 88 combined with the 25-year surge and seiche with wind wave activity, predicted to be 0.9 m (3.2 ft) above the lake level (Table 2.4-222) by the U.S. Army Corps of Engineers. This 25-year surge is a conservative estimate, corresponding to the 33-year surge shown on Table 2.4-222. The calculated Lake Erie elevation with surge for Alternative II is therefore 176.2 m (578.3 ft) NAVD 88. Subsection 2.4.5 describes the methods used to determine the 100-year lake level. This PMF evaluation and subsequent water level determination fulfills Alternative II.

Alternative I is fulfilled by evaluation of the 500-year flood for Swan Creek, which is estimated by the MDEQ to be 140 m^3/s (5,000 cfs) (Subsection 2.4.3). The Lake Erie elevation calculated for Alternative I was the 100-year lake level of 175.3 m (575.1 ft) NAVD 88 combined with the surge and seiche from the worst regional windstorm with wind wave activity. The 100-year surge for the month of December was used to represent the seiche from the worst regional wind storm in this analysis. The calculated 100-year storm surges vary by month and range from 1.6 ft in August to 4.0 feet in December (Table 2.4-222). The exceedance probability of the combination of events used in the Fermi 3 analysis to satisfy Alternative I in ANSI/ANS-2.8-1992, Section 9.2.3.2 is 2 x 10-7 per year, which is less frequent than 1 x 10^{-6} sited in ANSI/ANS-2.8-1992, Section 9.2, as the bases for the event combinations. Using the 100-year storm surge of 4.0 feet, the predicted water surface elevation for Alternative I was 176.6 m (579.4 ft) NAVD88 (580.6 ft PD, plant datum).

As reported in the Shore Protection Manual (Reference 2.4-249), the maximum recorded rise for Toledo was 1.9 m (6.3 ft). Because of differences in shoreline configuration and bathymetry, this same rise might not have occurred at the Fermi Site. However, if a seiche of 6.3 was used in the Alternative I analysis, the predicted water surface elevation would be approximately 177.3 m (581.7 ft) NAVD 88 (582.9 ft PD).

Alternative III is fulfilled by analysis of the probable maximum surge and seiche with wind wave activity. Subsection 2.4.5 covers Probable Maximum Surge and Seiche Flooding in depth. The resulting maximum still-water elevation from Subsection 2.4.5 is 178.4 m (585.4 ft) NAVD 88. This

is the Lake Erie water elevation calculated for Alternative III. The flow used under this scenario was the 25-year flood, estimated to be 90 m^3/s (3,100 cfs) from MDEQ predictions (Subsection 2.4.3).

Figure 2.4-263 shows the still water elevations for all three alternatives. On Figure 2.4-263 the seiche height of 6.3 feet was used in place of the 100-year storm surge of 4.0 ft for Alternative I (identified as Alternative IA). Alternative III has the highest still water level of all alternatives evaluated. The other alternatives vary between 1.1 to 2.1 m (3.8 to 6.8 ft) less than Alternative III.

2.4.3.4 Probable Maximum Flood Flow

Q_{PMF} represents the Swan Creek Watershed discharge during the PMF calculated from a 72-hour PMP rainfall event. The 6-hour unit hydrograph and composite flood hydrograph of the Swan Creek Watershed are shown in Figure 2.4-219. Q_{PMF} is approximately 3,200 m^3/s (113,200 cfs). This is the estimated flow of Swan Creek as it enters Lake Erie.

There are no dams existing within the Swan Creek Watershed that would produce measurable effects on Lake Erie water levels. Subsection 2.4.4 discusses potential dam failures.

2.4.3.5 Water Level Determination

The water surface profiles for all three alternatives were determined by using the HEC-RAS Version 4.0 Beta 2008 software (Reference 2.4-242). A Digital Terrain Model (DTM) was developed using U.S. Quad Map data loaded in the ArcGIS 9 ArcMap Version 9.2 software. After locating the Swan Creek Watershed within the ArcGIS software (Reference 2.4-223), the HEC-GeoRAS Version 4 software (Reference 2.4-241) was used to survey the features in the watershed model in order to represent the most conservative PMP rainfall analysis and generate a water surface profile. Figure 2.4-218 shows the cross sections used within the Swan Creek Watershed during this analysis. The limits set on the cross sections varied from station to station, although they all covered the most secure features of the watershed. The results produced were also made more conservative by restricting the boundaries of the cross sections drawn normal across the profile of Swan Creek.

Table 2.4-219 shows the resulting water levels at the various stations along Swan Creek for the PMF analysis (Alternative II). The maximum flood elevation at the Fermi 3 site, determined under this scenario, is 176.52 m (579.15 ft) NAVD 88. This flood elevation is 3.1 m (10.2 ft) below the Fermi 3 finished grade elevation for sately related structures of 179.6 m (589.3 ft) NAVD 88. Therefore, safety related structures are not susceptible to flooding from a PMF storm event. The Swan Creek water surface profile for this scenario is shown on Figure 2.4-220. Water surface profiles shown along the two cross sections most critical to the Fermi 3 site are shown on Figure 2.4-221 and Figure 2.4-222.

Table 2.4-220 shows the resulting water levels at the various stations along Swan Creek for the 500-year flood analysis (Alternative I). The maximum flood elevation at the Fermi 3 site, determined under this scenario, is 176.59 m (579.39 ft) NAVD 88. This flood elevation is 3.0 m (9.9 ft) below the Fermi 3 finished grade elevation of 179.6 m (589.3 ft) NAVD 88. Therefore, safety related structures

are not susceptible to flooding from a 500-year storm event. The Swan Creek water surface profile for this scenario is shown on Figure 2.4-223. Water surface profiles shown along the two cross sections most critical to the Fermi 3 site are shown on Figure 2.4-224 and Figure 2.4-225.

Table 2.4-221 shows the resulting water levels at the various stations along Swan Creek for the Probable Maximum Surge and Seiche analysis (Alternative III). The maximum Swan Creek flood elevation at the Fermi 3 site, determined under this scenario, is 178.4 m (585.4 ft) NAVD 88. This flood elevation is 1.2 m (3.9 ft) below the Fermi 3 finished grade. Therefore, safety related structures are not susceptible to flooding from a Probable Maximum Surge and Seiche Flooding event. The Swan Creek water surface profile for this scenario is shown on Figure 2.4-226. Water surface profiles shown along the two cross sections most critical to the Fermi 3 site are shown on Figure 2.4-227 and Figure 2.4-228.

2.4.3.6 Coincident Wind Wave Activity

Subsection 2.4.5 analyzes the wave run-up of Lake Erie induced by Probable Maximum Windstorm (PMWS) winds. Wave run-up and potential overtopping rates were calculated with the Automated Coastal Engineering System (ACES) model (Reference 2.4-256). Wave run-up on the slope to the Fermi 3 finished grade was analyzed, and it was determined that waves will break on the berm that is between the onshore flat area and the Fermi 3 finished grade. Therefore, waves will not overtop the slope and will not directly impact Fermi 3. See Subsection 2.4.5 for details.

2.4.4 Potential Dam Failures

The water supply for Fermi 3 is from Lake Erie. The outflow from Lake Erie is not regulated. The outflow from Lake Erie is controlled exclusively by the hydraulic characteristics of the outlet rivers (Reference 2.4-247). Thus, there are no dam failures that could impact the water supply for Fermi 3.

Fermi 3 is located within the Swan Creek watershed. The Swan Creek watershed contains no dams upstream or downstream within the vicinity of Fermi 3. Thus, there are no dam failures that could result in flooding to the Fermi 3 site. Additionally, there are no water control structures erected on the Fermi site whose failure would cause potential flooding. (Reference 2.4-295)

Therefore, there are no potential dam failures that could affect Fermi 3 safety-related structures or components.

2.4.5 Probable Maximum Surge and Seiche Flooding

This section discusses the development of the hydrometeorological design basis to ensure that any potential hazard to the safety-related facilities due to the effects of probable maximum surge and seiche are considered in the plant design. The analyses discussed in this section are based on ANSI/ANS-2.8-1992 (Reference 2.4-248). ANSI/ANS-2.8-1992, Section 9.2.3, describes the combined events criteria for an enclosed body of water, which is appropriate for analyzing postulated flooding at the Fermi 3 power reactor site due to wind and wave conditions in Lake Erie.

Specifically, ANSI/ANS-2.8-1992, Section 9.2.3.1, states that the following combination of flood causing events provides an adequate design base for shore locations.

1. Probable maximum surge and seiche with wind-wave activity.
2. 100-year or maximum controlled level in water body, whichever is less.

These event combinations are addressed in the following discussion.

2.4.5.1 Probable Maximum Winds and Associated Meteorological Parameters

According to Section 7.2.2.1 of ANSI/ANS-2.8-1992, for the area of the Great Lakes in the vicinity of the site, the probable maximum surge and seiche is calculated from the PMWS (Reference 2.4-248). Section 7.2.2.3.1 of ANSI/ANS-2.8-1992 further indicates that parameters of the PMWS should be determined by a meteorological study, and in lieu of a study, the following may be used:

1. Set maximum over-water wind speed at ~ 160 km/hr (100 mph).
2. Set lowest pressure within the PMWS to ~950 mbar.
3. Apply a most critical, constant translational speed during the life of the PMWS. This may require several trials.
4. Assume that wind speeds over water vary diurnally from 1.3 (day) to 1.6 (night) times the overland speed (This assumption is based on work by Lemire from ANSI/ANS-2.8-1992 with some modifications).
5. Assume that winds blow 10 degrees across the isobars over the water body. Decreased friction over the water will cause the wind to approach the isobars, but gradient flow will not be reached because of the imbalance of forces.

2.4.5.2 Surge and Seiche

2.4.5.2.1 Surge & Seiche History

2.4.5.2.1.1 Maximum Historical Lake Levels

Historical Lake Erie water levels are discussed in Subsection 2.4.2.1. The discussion in Subsection 2.4.2.1 includes flooding events due to wind storms on Lake Erie.

2.4.5.2.2 Surge and Seiche Water Levels in Lake Erie

In order to determine the maximum postulated still-water level at the site, the predicted storm surge is combined with the Lake Erie 100-year lake water level. The sections that follow discuss the determination of the 100-year water level, the storm surge, and the subsequent postulated maximum still-water level.

2.4.5.2.2.1 Lake Erie 100-Year Water Level

In order to establish the 100-year lake level for Lake Erie, data was incorporated in a statistical frequency analysis using the Log Pearson Type 3 distribution. Historical lake level data was obtained for 14 water level gauging stations that exist along the shore of the lake (Figure 2.4-229). Eight gauging stations are maintained by the National Oceanic and Atmospheric Administration (NOAA) of the U.S. Department of Commerce; the other six gauging stations are maintained by the Department of Fisheries and Oceans (DFO) in Canada.

Historical lake level data consists of available digital records. Records for the U.S. gauges were obtained from the NOAA Tides and Currents Website (Reference 2.4-255). Records from the Canadian gauges were obtained from the Tide and Water Level Inventory of the Integrated Science Data Management branch of the DFO (Reference 2.4-254). Data for the majority of U.S. gauges are readily available for the period from January 1, 1970 to present. Data for the Canadian gauges are available for the period from June 1, 1966 to present. The period of record for one of the Canadian gauges (Port Stanley, Ontario – 12400) extends back to June 1, 1926 with a gap in the record between December 31, 1940 to November 1, 1961. For this analysis, data from 1970 through 2007 was used to provide a homogenous data set.

The recorded data includes the effects of surges and seiches that may have occurred in the lake. To eliminate this effect, the historical lake levels have been determined by calculating a weighted average of the hourly lake levels of the individual gauges. The weight is based on the area of influence of the individual gauges.

Based on the above data, the 100-year lake level was calculated to be 1.72 m (5.64 ft) above the low water level. The chart datum is 173.5 m (569.2 ft) IGLD 85 or 173.6 m (569.5 ft) NAVD 88. The chart datum is based on low water lake levels; therefore, the depths have to be adjusted to account for the 100- year level in the lake. Therefore, the 100-year lake level is 175.2 m (574.8 ft) IGLD 85, corresponding to 175.3 m (575.1 ft) NAVD 88.

2.4.5.2.2.2 Surge

ANSI/ANS-2.8-1992 recommends using the U.S. Army Corps of Engineers Shore Protection Manual (Reference 2.4-249) for analyzing wave action. Reference 2.4-249, however, has been superseded by the U.S. Army Corps of Engineers Coastal Engineering Manual (CEM) (Reference 2.4-250). Thus, for the purpose of this analysis, the CEM was used.

Wave action includes deep and shallow water wave generation. The CEM recommends that, except for areas with very simple bathymetry, a numerical model should be used for nearshore wave studies. For the Fermi site, the numerical methods used are contained in computer code STWAVE. STWAVE is a steady-state finite-difference model. It includes the simulation of depth-induced wave refraction and shoaling, diffraction, wind-wave growth and wave-wave interaction and whitecapping; these factors redistribute and dissipate energy in a growing wave field. (Reference 2.4-251)

For the analyses, a constant 160 km/hour (100 mph) wind-speed is used for the purpose of wind-wave generation in STWAVE. This is based on the guidelines for the Great Lakes Region which allows use of a maximum over-water wind speed of 160 km/hr (100 mph) in lieu of a more detailed meteorological study (Reference 2.4-248). Time variations in wind speed and direction were not considered because STWAVE is a steady state model.

Wave heights and frequency are dependent on water depth. Bathymetric data was used to define the water depths in the model. Bathymetric soundings were downloaded from the Electronic Navigational Charts (ENC) Direct website of the National Oceanic and Atmospheric Administration (NOAA) (Reference 2.4-252). The data was downloaded in digital form using the ESRI Arc/Info Point Coverage format in the Lambert Conformal NAD 83 projection. The data downloaded corresponded to the entire Lake Erie. Data was then converted to an ESRI point-shapefile format.

The bathymetric soundings were complemented with bathymetric contours downloaded from the Great Lakes Information Network (GLIN) (Reference 2.4-253). These were downloaded in digital form using the ESRI point-shapefile format in the World Geodetic Coordinate System (WGS 84). The originator of the data is the Great Lakes Environmental Research Laboratory and NOAA's National Geophysical Data Center (NGDC). The shapefile was projected to the Lambert Conformal NAD 83 projection to match the soundings coordinate system. Contours with depths equal to zero were selected to define the shore of the lake and the islands.

For wind set-up, the Bretschneider methods (Reference 2.4-257) were used to calculate wind stress. Wind stress was then used for wind set-up and storm surge. The Coastal Engineering Manual (Reference 2.4-250) does not recommend any specific methods for calculating storm surge. The Bretschneider method was selected because it was considered to be the most appropriate method for this location. Two other methods were considered for the analysis. The Zeider Zee formula was not used in the analysis because it was developed for fjords which are long, narrow and deeper than Lake Erie. The Sibul method was considered but not used because the wind set-up predicted by the Sibul method was significantly smaller than that of the Bretschneider method and therefore the Bretschneider method was more conservative.

The Bretschneider method is appropriate for lakes and reservoirs that are regular in shape and somewhat irregular in shape. The method can be improved for lakes with varying depths by segmenting the lake and making calculations for each segment, which was done in the analysis. The key parameters that affect storm surge are the fetch length, water depth, wind speed, and coefficients used to calculate wind stress, and bottom stress. The Bretschneider method uses straight line fetches and therefore the longest straight line fetch distance was used in the calculations. This distance was calculated to be 154,781 m. The fetch length was divided into 10 segments and the average depth within each segment was calculated. The average depths ranged from 8.7 m, closest to shore, to 23.2 m with an overall average depth of 16.2 m.

STWAVE was used to simulate wave generation and ultimately the wave height and period to be used in the ACES modeling software (Reference 2.4-256). The ACES model is an integrated collection of coastal engineering design and analysis software. It provides a comprehensive environment for applying a broad spectrum of coastal engineering technologies. These technologies include functional areas such as wave prediction, wave theory, wave transformation, structural processes, wave run-up, littoral processes, inlet processes and harbor design. The Linear Wave Theory application provides a simple estimate for wave shoaling and refraction using Snell's law with wave properties predicted by linear wave theory. The wave run-up application estimates wave run-up and overtopping on rough and smooth slope structures that are assumed to be impermeable.

Based on this methodology, the storm surge is calculated to be 3.14 m (10.3 ft). To verify that the wind set-up predicted by the Bretschneider method was conservative and reasonable, the predicted value was compared to measured storm surges in Lake Erie. According to the Corps of Engineers Detroit District, the 100-yr storm surge for December at the Fermi site is 3.9 ft (Reference 2.4-245). In addition, according to the NOAA web site, (Reference 2.4-248) the maximum water level during the period of record was 576.22 (IGLD 85) or 576.48 (NAVD 88). This was recorded on April 9, 1998 at 1400. This value was 3 ft above the average monthly water level for April 1998. The maximum recorded water level is also 9 ft below the water level used in the flood calculations.

As discussed in Subsection 2.4.5.2.2.1, the 100-year lake level is 175.2 m (574.8 ft) IGLD 85, corresponding to 175.3 m (575.1 ft) NAVD 88. The calculated still-water level for the storm surge in addition to the 100-year level is 178.4 m (585.4 ft) NAVD 88, corresponding to 178.8 m (586.6 ft) plant grade datum. The plant grade elevation for the safety-related structures of Fermi 3 is 180.0 m (590.5 ft) plant grade datum. Thus, the still-water elevation is 1.3 m (3.9 ft) below plant grade. Table 2.0-1 specifies that the maximum flood level is at least 0.3 m (1 ft) below plant grade. Therefore, the Fermi 3 design satisfies the enveloping site parameter in the DCD.

2.4.5.2.2.3 Seiche

Seiches are standing waves of relatively long periods that occur in lakes and other water bodies. Lake Erie is subject to occasional seiches of irregular amount and duration, which sometimes result from a sudden change, or a series of intermittent periodic changes, in atmospheric pressure or wind velocity. The maximum deviations from mean lake levels at Toledo were reported in the U.S. Army Corps of Engineers Shore Protection Manual (Reference 2.4-249). The maximum recorded rise was 1.9 m (6.3 ft) and the maximum recorded fall was 2.7 m (8.9 ft) for the period from 1941 to 1981. The value of the rise is significantly less than the storm surge calculated using the Bretschneider methods, noted above.

Seiche events can also result in minimum lake water levels at the site. The Ultimate Heat Sink (UHS) for Fermi 3 is described in Subsection 9.2.5. The Isolation Condenser/Passive Containment Cooling System (IC/PCCS) pools contain a separate water supply in place during Fermi 3 operation

for safety-related cooling in the event that use of the UHS is required. Lake Erie is not used for safety-related water withdrawal for Fermi 3. Therefore, a seiche event will not affect a safety-related water supply for Fermi 3.

2.4.5.2.2.4 Surge Due to Moving Squall Line

According to the ANSI/ANS-2.8-1992 standards, Section 7.2.3.1, “A moving squall line should be considered for the locations along Lake Michigan where significant surges have been observed because of such a meteorological event. The possible region of occurrence includes others of the Great Lakes”. The standard further defines the conditions to be used in the analysis which include a pressure jump of 8 mbar within a 10 nautical mile width of the squall lines with a 65 knot wind. In addition, the squall line should move at the resonant speed of the surge.

In the Great Lakes area, most of the analyses of storm surges due to moving squall lines have been in Lake Michigan. As reported by Platzman (1965) (Reference 2.4-314) most of the moving squall lines in this region move in a northwest to southeast direction. The effect of the pressure gradient and wind stress acting on the water surface produces a surface disturbance that can cause surges at the shoreline. The effect is greatest when the propagation of the squall line is approximately equal to the speed of waves in the lake. The speed of waves in the lake is dependent on the water depth.

Fast moving squall lines have on several occasions produced storm surges in the range of 6 to 8 ft in Lake Michigan. These same storms would not produce significant storm surges in Lake Erie because the storm would move over the water surface too quickly. Reference 2.4-315 reported on storm surges that affected Lake Huron and Lake Erie in 1952 that were associated with a moving squall line. The storm traveled in a southeasterly direction over Lake Erie with a propagation speed of about 27 mph, approximately the resonant speed of the surge. A storm surge of less than 2 ft was observed in Cleveland. For a pressure jump of 8 mbar, the storm surge would have been about 4 ft.

The Fermi site is sheltered from the predominant direction of squalls moving through this region of the Great Lakes. To generate the greatest storm surge the squall line would have to move in a southeast to northwest direction, opposite to the direction in which they are observed to travel. Based on historical data and analyses of storm surges conducted for Great Lakes areas it can be concluded that a storm surge from the prescribed conditions could produce a water level rise of up to a few feet. As discussed previously in Subsection 2.4.5.2.2.2, the surge used in the flood analysis is 10.3 feet. Therefore, the surge from a moving squall line would be much less than the condition used in the analysis.

2.4.5.3 Wave Action

Wave run-up is evaluated to determine the wind-induced wave run-up under PMWS winds. Wave run-up and potential overtopping rates were calculated using the ACES model (Reference 2.4-256).

Results of the STWAVE model were used to define wave characteristics (wave height and period) necessary as inputs to the ACES model. Other required inputs are characteristics of the shoreline protection, including slopes and material used (e.g., rip-rap, rubble, tetrapods). Calculations were made assuming irregular waves. In calculating overtopping rates, the relative heights of the embankment to the still-water level were important. For these calculations, it was assumed the still-water level was a combination of the 100-year water level plus increases in water level due to surge and seiche.

The potential for wave action to cause flooding of the safety related features was considered for all alternatives. The approach was to first examine the effects of waves for the worst case scenario which was Alternative III. This alternative includes the 100 year level of the waterbody and probable maximum surge with wind wave activity.

2.4.5.3.1 Wave Run-Up Analysis Approach

The wave run-up models were used to calculate the run-up that occurs when waves encounter a shoreline or embankment. Overtopping rates were also calculated in this determination. The required inputs include wave type, breaking criteria, wave height, wave period, structure slope, structure height, slope type, and roughness coefficient. The cases modeled were for a flooded berm. Roughness coefficients consistent with rip-rap were used for the cases with rough surfaces.

Wave transmission and wave run-up modules in the ACES model were derived from physical model studies originally conducted for specific structures and wave climates (Reference 2.4-256). General assumptions for the wave run-up on an impermeable embankment are:

- Waves are monochromatic, normally incident to the structure, and unbroken in the vicinity of the structure toe.
- Waves are specified at the structure location.
- All structure types are considered to be impermeable.
- For sloped structures the crest of the structure must be above the still-water level.
- For vertical and composite structures, partial and complete submersion for the structure is considered.
- Run-up estimates on sloped structures require the assumption of infinite structure height and a simple plane slope.
- The expressions for the transmission by overtopping use the actual finite structure height.

2.4.5.3.2 Wave Run-Up Results

2.4.5.3.2.1 Description of Nearshore and Shallow Onshore Areas

Profiles have been developed to describe the nearshore and shallow onshore areas. For purposes of the wave transmission and wave run-up analysis the following areas were defined. Slopes are reported as Horizontal: Vertical (H: V). These areas are shown on Figure 2.4-263.

- Nearshore – the area from 1.0 m (3.3 ft) depth Mean Low Water (MLW) to 0 m (0 ft) depth MLW. This area is between the point used to describe the waves at the shore (from STWAVE model) to the base of the seawall. The area is about 660 m (2,160 ft) to 1,000 m (3,280 ft) wide with a slope of about 200 H: 1 V.
- Seawall – the area of onshore protection from an elevation of 174 m (571 ft) to 178 m (583 ft) plant grade datum, with a slope of 3H: 1V to 2H: 1V.
- Onshore - the area immediately behind the seawall. This area is approximately flat with a width of about 300 m (1,000 ft) at elevation 178 m (583 ft) plant grade datum.
- Berm – area between the onshore flat area, at elevation 178 m (583 ft) plant grade datum, and the project site, at elevation 180.0 m (590.5 ft) plant grade datum or 179.6 m (589.3 ft) NAVD 88. This berm area has a slope of about 12.5 H: 1V with smooth slopes.

2.4.5.3.2.2 Results from the STWAVE Model

Wave characteristics were obtained from the STWAVE model. Several points that were closest to shore were examined to determine the highest waves generated. The point used to represent the waves reaching the shore was located about 61.0 m (200 ft) from shore at a depth of 1.0 m (3.3 ft) MLW. The result of the modeling showed that the highest waves generated (H_{mo}) were 3.77 m (12.37 ft) high with a peak spectral period (Tp) of 11.1 seconds. Figure 2.4-264 provides the contours of the wave height distribution overlain on the bathymetric map of Lake Erie from NOAA (Reference 2.4-316). The wave height contours were prepared using the results from the STWAVE analysis. Wave heights are in meters and the contours have 0.1 meter accuracy.

As waves move across the nearshore area they will shoal resulting in slightly higher waves. At the end of this area the wave height would be 3.92 m (12.86 ft). This wave height was determined using the wave transmission module of the ACES model. The ACES model also showed that soon after reaching the seawall the wave would break.

It is possible that the wave period would be reduced; however, according to the Coastal Engineering Manual (Reference 2.4-250) there are no widely accepted theoretical methods for determining changes in wave period. Therefore, for this analysis the wave period was assumed to remain unchanged at 11.1 seconds.

2.4.5.3.2.3 Breaking Wave Characteristics

Maximum wave heights are constrained by the relative depth (ratio of wave height to water depth) and by wave steepness (ratio of wave height to wave length). Breaking wave heights were calculated according to procedures in Reference 2.4-250. Specifically equation II-4-11, Equation 4, was used to calculate the zero-moment wave height ($H_{mo,b}$) at the time of breaking, using the modified 1951 Miche criterion, which is the same equation used by the STWAVE model. This equation represents both depth and steepness-induced wave breaking. Although not exactly equivalent in definition, the zero-moment wave height is generally considered to be equivalent to the significant wave height. The equation used is:

$$H_{mo,b} = 0.1\ L \tanh(kd) \qquad \text{[Eq. 4]}$$

where:

k = wave number defined as $2\pi/L$
d = water depth

As waves move onshore, the wavelength decreases; thus, the first step is to calculate the appropriate wave length according to Equation 5:

$$L = g/2\pi * T^2 \tanh(2\pi d/L) \qquad \text{[Eq. 5]}$$

Because L is on both sides of the equation, this equation must be solved through an iterative process.

Wavelengths associated with various points in the lake are shown in Table 2.4-223. Breaking wave heights at the toe of the seawall and at the toe of the berm are shown in Table 2.4-224.

2.4.5.3.2.4 Wave Run-up and Overtopping Rates

Wave run-up on the slope to the Fermi 3 grade elevation of 180.0 m (590.5 ft) plant grade datum or 179.6 m (589.3 ft) NAVD 88 was analyzed to determine if waves could impact the unit. The wave characteristics calculated for the toe of the berm were used as inputs to the ACES model to calculate wave run-up and overtopping rates on the berm. Because the berm is onshore, it was simulated as a smooth slope. An example of the inputs and calculated outputs for the on site configuration are shown in Figure 2.4-230. The analysis of wave run-up determined that waves could not directly impact Fermi 3.

Wave runup for Alternative III is predicted to be 3.0 ft, or approximately 0.85 feet below the elevation of the Fermi 3 safety related structures. Wave runup is shown on Figure 2.4-265. The vertical exaggeration on Figure 2.4-265 is approximately 5 to 1. For Alternative II the still water level at the site was calculated to be 578.6 ft NAVD88 or 579.8 ft PD. This elevation is about 3.2 ft below

the elevation of the top of the seawall at the site. For this alternative, there would be water from the waves splashing up onto the onshore area behind the seawall. The still water level for Alternative 1A would be 581.7 ft NAVD88 or 582.9 ft PD which is just below the top of the seawall. A significant amount of water would wash onto the onshore area. The elevation of the safety related structures is 7.5 ft above the onshore area. Based on this information it was concluded that wave activity would not have any impact on the safety related structures for any of the Alternatives considered.

2.4.5.4 Resonance

Resonance generated by waves can cause problems in enclosed water bodies, such as harbors and bays, when the period of oscillation of the water body is equal to the period of the incoming waves. However, the Fermi site is not located in an enclosed embayment. The full exposure to Lake Erie during PMWS conditions, plus the flat slopes surrounding the site area, results in a natural period of oscillation of the flooded area that is much greater than that of the incident shallow-water storm waves. Consequently, resonance is not a problem at the site during PMWS occurrence.

2.4.5.5 Sedimentation and Erosion

Fermi 3 does not rely on Lake Erie for a safety-related water source. Therefore, the loss of functionality of a safety-related water supply to Fermi 3 caused by blockages due to sediment deposition or erosion during a storm surge or seiche event is not a concern. The slope to Fermi 3 is appropriately designed to preclude significant erosion during the postulated storm surge. Erosion protection from wave impacts are described in Subsection 2.4.2.3.

2.4.5.6 Protective Structures

The storm surge and wave run-up results in waves that will break on the berm that is between the onshore flat area and the Fermi 3 elevation of 179.5 m (589.0 ft) IGLD 85 or 179.6 m (589.3 ft) NAVD 88. The analyses of the wave run-up indicate that the waves will not overtop the slope and impact Fermi 3. Therefore, additional protection is not needed.

2.4.6 Probable Maximum Tsunami Flooding

The National Oceanographic and Atmospheric Administration (NOAA) National Geophysical Data Center (NGDC) maintains a historical tsunami database which catalogs tsunami events (Reference 2.4-310). The data in the NGDC database was filtered to exclude invalid events. Based on this filtering, no tsunami events were identified in the Great Lakes.

Furthermore, valid tsunami events in Lake Erie are considered unlikely based on the absence of historical large earthquakes in the Lake Erie region, a low probability of vertical displacement of the lake bed during a seismic event, the relatively shallow depth of Lake Erie, and the very gentle bottom profile of Lake Erie (particularly in the western and central basins). Observed Similar phenomena have been low-amplitude seiches resulting from sudden barometric pressure differences. These events are further discussed in Subsection 2.4.5.

Therefore, there are no potential tsunamis which could affect safety-related structures or components at Fermi 3.

2.4.7 Ice Effects

The emergency cooling system for Fermi 3 is provided by the Ultimate Heat Sink (UHS) which does not rely on water sources external to the plant and is not affected by ice conditions. This is further described in Subsection 9.2.5. Therefore, there are no safety-related systems, structures, or components impacted by ice formations.

Based on information in Reference 2.4-296, there is no evidence to indicate ice/snow blockage along the surrounding areas of Fermi 3. From Reference 2.4-296, the closest documented ice jams are along the Raisin River, which is approximately 10 miles south and does not intersect waterways affecting the Fermi 3 site. Therefore, flooding due to ice jam blockage is not anticipated to impact Fermi 3.

2.4.8 Cooling Water Canals and Reservoirs

As described in Subsection 2.4.1, Fermi 3 uses a natural draft cooling tower for rejecting heat from the CIRC. The Plant Service Water System (PSWS) rejects heat from station heat loads via the CIRC or the two Auxiliary Heat Sink (AHS) mechanical draft cooling towers. Make-up water for the CIRC and PSWS cooling towers are supplied from Lake Erie. Blowdown discharge from the CIRC is returned to Lake Erie via a discharge pipe outfall into the lake.

The Ultimate Heat Sink (UHS) for Fermi 3 is described in Subsection 9.2.5. The IC/PCCS pools contain a separate water supply in place during Fermi 3 operation for safety-related cooling in the event that use of the UHS is required. Lake Erie is not used for safety-related water withdrawal for Fermi 3.

Discussion of the probable maximum flood (PMF) level at the site is provided in Subsection 2.4.3. The effects of probable maximum surge and seiche flooding and ice effect flooding are addressed in Subsection 2.4.5 and Subsection 2.4.7, respectively.

As described above, cooling water canals and reservoirs are not used for safety related functions by Fermi 3. Therefore, the water level effects due to failures of such structures are not applicable to Fermi 3.

2.4.9 Channel Diversions

Fermi 3 site and facilities are discussed in Subsection 2.4.1. No safety-related systems, structures, or components are impacted. The water supply for Fermi 3 is not obtained from channels; therefore, this subsection is not applicable from a water supply perspective.

The topography surrounding Swan Creek slopes gently toward the creek, with the creek sloped to drain in a well established channel into Lake Erie. As identified in UFSAR Subsection 2.5.1 and Subsection 2.5.4, the natural geology consists of lacustrine deposits overlying stronger glacial till

(see UFSAR Subsection 2.5.4, Table 2.5.4-202), which overlies bedrock. The increase of strength with depth of the subsurface soil and bedrock minimizes the possibility of a block-type failure of a stronger layer on a shallow failure plane in a weaker underlying layer; therefore, shallow large area landslides into Swan Creek are not envisioned as a plausible scenario. The shallow slope of the land surface toward the creek combined with the lack of a weak soil layer at depth also reduces the potential for the occurrence of a large area landslide into the creek. Along the incised banks of Swan Creek, local slope failures of the creek bank are part of the natural creek erosion process, however the size of these slope failures would be limited to near bank events which would not result in diversion of Swan Creek.

Refer to Subsection 2.4.7 for discussion on ice jams. Ice jams are not expected to cause a diversion of Swan Creek.

Detroit Edison has managed the Fermi site from 1957 to the present and has no record or knowledge of any human induced or natural diversions of Swan Creek occurring during that time or prior to 1957. The lack of past events suggests that it is unlikely Swan Creek would be diverted by a future event.

As the area surrounding Swan Creek is relatively well established, it is anticipated that future human-induced diversions of Swan Creek that would impact the Fermi 3 site are unlikely.

The Fermi 3 site is not expected to be impacted by channel diversions.

2.4.10 Flooding Protection Requirements

The maximum design basis Lake Erie flood elevation, presented in Subsection 2.4.5, is 178.4 m (585.4 ft) NAVD 88, corresponding to 178.8 m (586.6 ft) plant grade datum. This elevation is below the Fermi 3 site grade elevation of 179.6 m (589.3 ft) NAVD 88 that meets the site parameters required in Table 2.0-1. Furthermore, the maximum Swan Creek flood elevation at the Fermi 3 site is also calculated to be 178.4 m (585.4 ft) NAVD 88 in Subsection 2.4.3.5. The Fermi 3 site grade is above all flood water levels that can possibly occur from the probable maximum storm events within the Swan Creek watershed, which encompasses the safety-related structures, systems, and components of Fermi 3. Rip-rap protection of the slope embankment at the make-up water intake location on Lake Erie will prevent wave activity from eroding the embankment near the on-shore structure.

The effects of intense local precipitation are considered in the design of drainage structures for Fermi 3, as mentioned in Subsection 2.4.2. These facilities are designed such that the peak discharge from the local PMP will not produce flood elevations that pose a flooding hazard to any safety-related structure, system, and component of Fermi 3. Additionally, the design of the drainage facilities incorporate measures to ensure that Fermi 2 safety-related facilities are not subject to flooding during the construction or operation of Fermi 3. Applicable NRC, Federal, State, and local storm water management regulations are followed in the design of all drainage facilities for both the existing and the proposed site.

All safety-related components and structures are designed to withstand combinations of flood conditions as discussed in Subsection 2.4.2, Subsection 2.4.3, and Subsection 2.4.5. Flood protection of safety-related structures, systems, and components, at an elevation of 179.6 m (589.3 ft) NAVD 88, are not necessary since the probable maximum surge still-water elevation only reaches 178.4 m (585.4 ft) NAVD 88.

2.4.11 Low Water Consideration

2.4.11.1 Low Flow in Rivers and Streams

Water from rivers and streams is not used for the operation of Fermi 3; therefore, low water levels in rivers and streams will have no direct effects or safety-risks to Fermi 3. The extent to which rivers and streams impact the water level in Lake Erie is the only effect potentially observed at the plant.

Lake Erie currently provides make-up cooling water for Fermi 2 and will also provide make-up cooling water for Fermi 3. For Fermi 3, the historical minimum lake level for operation is elevation 171.79 m (563.64 ft) IGLD 85, which corresponds to 171.9 m (563.9 ft) NAVD 88. The historic low water levels in Lake Erie are presented in Subsection 2.4.11.3.

The elevation of the base of the intake bay at the location of the pump suction is 169 m (553 ft) IGLD 85. This is more than 3 m (10 ft) below the record low water level for the lake; therefore, pump suction should not be a concern in periods of low lake levels.

The UHS does not rely on water sources external to the plant; therefore, there are no safety-related systems, structures, or components impacted by low water levels of Lake Erie. Consequently, low water levels do not pose a safety-related risk to Fermi 3.

2.4.11.2 Low Water Resulting from Surges, Seiches, or Tsunami

In accordance with RG 1.206, low water resulting from surges, seiches, or tsunami only needs to be considered when these conditions would affect the function of safety-related facilities. Because the UHS does not rely on water sources external to the plant, low water effects resulting from surges, seiches, or tsunami are not considered in Lake Erie. The historical maximum recorded fall in water level due to surge and seiches are discussed in Subsection 2.4.5.

2.4.11.3 Historical Low Water

Table 2.4-225 shows the most significant historical low water levels of Lake Erie, occurring from 1967 through 2007 at the Fermi site (Station No. 9063090) as measured by the NOAA Great Lakes Environmental Research Laboratory (GLERL), which conducts high quality research and provides scientific leadership on important issues in both Great Lakes and marine coastal environments. The lowest water level during this time period was recorded on February 16, 1967 at elevation 171.79 m (563.64 ft) IGLD 85, corresponding to 171.9 m (563.9 ft) NAVD 88. The second lowest water level during this time period was recorded on November 11, 2003 at elevation 171.96 m (564.19 ft) IGLD 85, corresponding to 172.04 m (564.45 ft) NAVD 88. (Reference 2.4-259, Reference 2.4-260)

From the period of record of 1860 through 1973, the lowest observed monthly mean elevation of Lake Erie was during February of 1936, when an elevation of -0.37 m (-1.2 ft) (Low Water Datum) was recorded. For Lake Erie, low lake levels are generally recorded during the month of February. (Reference 2.4-258)

2.4.11.4 Future Controls

There are no future controls anticipated for Lake Erie.

2.4.11.5 Plant Requirements

Lake Erie does not provide water for safety-related cooling; therefore, there are no safety-related plant requirements based on Lake Erie water levels.

2.4.11.6 Heat Sink Dependability Requirements

The Fermi 3 UHS is described in Section 9.2.5. Lake Erie is not relied on as a safety-related source of water withdrawals for emergency cooling.

2.4.12 Groundwater

This section describes the regional, and onsite hydrogeologic conditions present at Fermi 3. For the purposes of this subsection, regional refers to the area of Monroe County, Michigan, and five counties adjacent to Monroe County, and onsite refers to the physical boundaries of the Fermi site. Regional and local groundwater resources that may be affected by the construction and operation of Fermi 3 are discussed. The regional and site-specific data on the physical and hydrologic characteristics of these groundwater resources are summarized in order to provide basic data for an evaluation of impacts on the aquifers of the area.

2.4.12.1 Description and Onsite Use

This section describes the following:

- Regional and onsite groundwater aquifers and associated geologic formations.
- Regional and onsite groundwater sources (areas of recharge) and sinks (areas of discharge). and
- Regional and onsite use of groundwater.

The Fermi site covers an area of approximately 510 hectares (1260 acres) and is located on the glacial plain on the western shoreline of Lake Erie in Monroe County, Michigan. The site is approximately 48 km (30 mi) southwest of Detroit, Michigan, and 39 km (24 mi) northeast of Toledo, Ohio. The existing Fermi 2 plant buildings date from the 1970's. They are located south of the two cooling towers and the circulating water basin, used for cooling water supply. Fermi 3 lies immediately southwest of Fermi 2 and east of the overflow canal (Figure 2.4-231).

Historically, the site vicinity was characterized by surface wetlands. These wetlands were drained through the installation of drainage tiles in the 1800s to accommodate the development of local agriculture. There still exist many drainage ditches and tile systems in the area (Reference 2.4-261). The Fermi site has virtually no relief, since the site lies entirely on imported fill material placed and graded after excavating significant volumes of native material, which was wetland in nature. (Reference 2.4-262) Swan Creek flows into an estuary on the northern edge of the site, which ultimately feeds into Lake Erie. The undeveloped area between the Fermi plant and Fisher Street to the west exhibits seasonally variable surface water and wetland vegetation.

Regional and local surface water features are described in Subsection 2.4.1 and a detailed description of regional and local geology is presented in Subsection 2.5.1.

2.4.12.1.1 Regional Aquifers, Formations, Sources, and Sinks

The site is located in Monroe County, Michigan, and lies in the Eastern Lake Section of the Central Lowlands Physiographic Province (Reference 2.4-263). Physiographic provinces are described in detail in Subsection 2.5.1.1.1. Land surface in this area is characterized by relatively flat topography with some rolling hills. The geologic materials underlying the Central Lowlands Physiographic Province consist of Quaternary sediments of glacial and lake origin atop a sequence of Paleozoic carbonate units (Subsection 2.5.1.1.3).

Regionally, the Surficial Aquifer System is the uppermost and most widespread aquifer in the area (Reference 2.4-264). This aquifer system consists primarily of glacial sediments deposited during multiple glaciations in the Paleo-Pleistocene epochs. In areas where significant quantities of sand and gravel have been deposited, the aquifer may provide water supply for local wells. Glacial deposits thicken northwest of the site. In areas of northern mainland Michigan near Lake Michigan, glacially-derived sand and gravel deposits may be up to 305 m (1000 ft) thick. In the site vicinity, however, these deposits are mapped as being less than 15 m (50 ft) thick, which is confirmed by data collected during the Fermi 3 hydrogeology and geotechnical subsurface investigation, and are comprised almost entirely of clay and other fine-grained sediments (Subsection 2.5.1.2.3). The native glacial materials at the site are not, for the purposes of this document, considered to be an aquifer, since they consist almost entirely of clay and silt, and wells completed in these materials have not generally demonstrated the ability to produce water in economically beneficial quantities. However, regionally, these sediments are hydrologically significant due to the water they transmit over large areas to the underlying bedrock formations.

The unconsolidated deposits that make up the shallow zone vary in thickness in Monroe County from approximately 43 m (140 ft) thick in the northwestern part of Monroe County to zero thickness at some streams. The typical thickness in Monroe County is no more than 15 m (50 ft) (Reference 2.4-264). The unconsolidated deposits are made up primarily of glacial till and lacustrine deposits (Subsection 2.5.1.2.3).

The primary source of recharge for the Surficial Aquifer System is from direct precipitation onto the aquifer surface where it is exposed. During times of elevated water surface elevations in Lake Erie, the shallow aquifer along the coast may be directly recharged from surface water features. Regional sinks, or areas of discharge, from the Surficial Aquifer System include discharge to wells, and discharge to streams, lakes, and other surface water features.

The glacial deposits are underlain by a series of Silurian-Devonian bedrock formations consisting primarily of limestone and dolomite, with some small sandstone layers locally (Figure 2.4-232). These formations reach thicknesses of thousands of feet and contain groundwater that ranges from fresh to brackish. Significant amounts of groundwater are withdrawn from the bedrock aquifer for industrial, municipal, and irrigation purposes (Reference 2.4-264). As part of the U.S. Geological Survey's Regional Aquifer-System Analysis (RASA) program (Reference 2.4-265), the bedrock aquifer, which is composed of Silurian-Devonian aged carbonates, was subdivided into five permeable zones, vertically adjacent and bounded on the top and bottom of this sequence by non-aquifer shales. The units are from bottom to top (oldest to youngest):

- Salina Group.
- Bass Islands Group.
- Sylvania Sandstone.
- Detroit River Dolomite.
- Dundee Formation.

The hydraulic properties of these strata differ. However, there are no significant continuous confining units between them, leading to their consideration regionally as a single undifferentiated bedrock aquifer, in which groundwater occurs under artesian conditions beneath the surficial aquifer. Figure 2.4-233 presents a conceptual cross section of the aquifers trending NW-SE beneath Monroe County (Reference 2.4-261).

Regionally, the Antrim and Coldwater shales overlie the Dundee Formation and generally are not considered to be aquifers, and prevent significant recharge from overlying glacial deposits where present. Thus, where present, these shale units act as a confining unit above the Silurian-Devonian aquifer. The Coldwater Shale was used as the lateral hydraulic boundary in the Michigan Basin RASA. (Reference 2.4-266)

Regionally, the Ordovician or lower Silurian shales comprise the lower boundary to the bedrock aquifer system. The base of the Michigan Basin bedrock aquifer considered here is assumed to be the Salina Group Unit C Shale. The boundary to groundwater flow west of the regional study area is saline water. The density difference between saline and fresh water retards freshwater flow and creates a boundary to regional movement. Lake Erie constitutes a hydraulic boundary to the east. Under pre-development conditions, the lake represented a discharge area for groundwater flow from the bedrock aquifer. In recent decades, however, bedrock water levels in Monroe County have

declined to the point that in places they are tens of meters below lake level in the county, thereby inducing flow from beneath the lake to local discharge areas. It is assumed that water levels in the bedrock aquifer approach lake level at some point eastward beneath Lake Erie (Reference 2.4-267).

The primary source of recharge for the bedrock aquifer is areally extensive downward vertical groundwater flow from the overlying glacial sediments to the bedrock formations, where confining shales are not present. Regional sinks, or areas of discharge, include flow to wells and downward flow from upper bedrock units to those underlying.

2.4.12.1.1.1 Sole Source Aquifers

A Sole Source Aquifer (SSA), as defined by U.S. Environmental Protection Agency (EPA), is an aquifer which is the sole or principal source that supplies at least fifty percent of the drinking water consumed by the area overlying the aquifer. The SSA program was created by the United States Congress in the Safe Drinking Water Act. The Act allows for the protection of these resources.

The Fermi site is located in EPA Region 5, which covers Minnesota, Wisconsin, Illinois, Michigan, Indiana, and Ohio. The EPA has designated seven aquifers in the Region as a SSA (Reference 2.4-268), with one additional aquifer pending designation (Reference 2.4-269). None of these SSAs are located in the state of Michigan. The closest SSA is the Bass Islands aquifer on Catawba Island in eastern Ottawa County, Ohio, about 56 km (35 mi) southeast across Lake Erie.

A map of SSAs in EPA Region 5 is presented on Figure 2.4-234. A summary of SSAs is presented as Table 2.4-226.

2.4.12.1.2 Site Aquifers, Formations, Sources, and Sinks

The zone of shallow overburden characterized by unconsolidated deposits at Fermi 3 average 9 m (28 ft) in thickness (Subsection 2.5.1.2.3.2), which is consistent with conditions in much of Monroe County (Reference 2.4-264). The local bedrock formation subcropping beneath the overburden is the Bass Islands Group. As previously stated, this unit is part of the bedrock aquifer that exists throughout Monroe County. The Salina Group underlies the Bass Islands aquifer at the site. Geologic cross sections based on the Fermi 3 subsurface investigation data are presented in Subsection 2.5.1 and on Figure 2.5.1-228 through Figure 2.5.1-240.

The uppermost hydrogeologic unit present at the site is the shallow overburden. This layer is collectively comprised of rock fill imported for plant construction (0-3 m [0-16 ft]), lacustrine deposits consisting of peaty silt and clay (2-9 m [0-9 ft]), and two distinct units of glacial till composed primarily of clay (1.8-5.8 m [6-19 ft]) (Subsection 2.5.1.2.3.2.1 and Subsection 2.5.1.2.3.2.2). The Fermi site in its undeveloped state was underlain by approximately 9 m (30 ft) of glacial till and lacustrine deposits. Approximately 0-6 m (0-20 ft) of this native material was excavated and removed from some areas during Fermi 2 construction, and replaced with fill material more suitable to geotechnical requirements during construction of Fermi 1 and 2. The fill for Fermi 2 was primarily

rock removed from the onsite quarry southwest of the plant which is now identified as Fermi 2 Quarry Lakes (Figure 2.4-231). Some clay material was used as fill at Fermi 1. The overburden is not considered an aquifer for the purpose of this document, because, with the exception of the quarried rock fill, the earth materials are characterized by low hydraulic conductivity such that water cannot be extracted from a well in significant quantities. As part of the Fermi 3 subsurface investigation, 17 monitoring wells and piezometers were installed into this layer. Hydraulic parameters and groundwater movement within and from this layer are discussed later in this section.

As with the Regional Surficial Aquifer System, the primary source of recharge for the groundwater within the overburden on site is direct precipitation onto the land surface. The portion of precipitation that does not run off, evaporate, or get consumed by plant transpiration ultimately percolates downward through the unsaturated zone to replenish the water table. During times of elevated water surface elevations in Lake Erie, the shallow zone may be directly recharged from surface water features. Additionally, groundwater inflow from the west flows onto the site, as discussed in the water level section in Subsection 2.4.12.2.3 Local sinks in the shallow zone include discharge to surface water features, and to the atmosphere via evapotranspiration losses.

The Bass Islands aquifer lies beneath the overburden at the site. As previously described, this is a bedrock dolomite aquifer in which the primary flow is in the fracture system present in the formation. For the purposes of this discussion, the entire thickness of the Bass Islands Group is considered to be an aquifer. Eleven monitoring wells and/or piezometers were installed into the Bass Islands aquifer as part of the hydrogeologic field program. The primary recharge source for the Bass Islands aquifer at the Fermi site under pre-development conditions is downward vertical flow from the overlying shallow zone and lateral inflow from the west. Surface water features may recharge the Bass Islands aquifer locally as discussed in Subsection 2.4.12.2.3.2.2 and Subsection 2.4.12.2.3.2.4.

The Salina Group underlies the Bass Islands Group at the site. The Salina Group is also a bedrock aquifer with observed joints and fracture systems with multiple orientations, vuggy zones, and paleokarst features, all of which contribute to the hydraulic conductivity. One piezometer (P-398 D) is screened in the Salina Group Unit F. Another piezometer (P-399D) that targeted the Bass Islands Group penetrated the upper few meters of the Salina Group.

2.4.12.1.3 Onsite Use

The plant potable water supply is furnished by Frenchtown Township, Michigan, which uses a water intake in Lake Erie for its source water. The Station Water source for Fermi 3 operations is a new intake structure on Lake Erie.

No permanent dewatering systems are required for Fermi 3. Fermi 3 does not use groundwater for any plant operating requirements or permanent needs.

2.4.12.2 Sources

This section describes:

- Current and projected groundwater use in the region.
- Regional and local groundwater levels and movement.
- Hydrogeologic properties of subsurface materials.
- Potential for reversibility of groundwater flow.
- Effects of groundwater use on gradients beneath the site.

2.4.12.2.1 Present Groundwater Use

Although Lake Erie is the largest regional water supply source, and many communities in the region are supplied by various water supply entities tapping this source, some water user groups in the area rely on groundwater for their supply.

The largest withdrawals of groundwater in Monroe County are at quarries (Reference 2.4-261 and Reference 2.4-270). There are seven quarries in Monroe County that are presently active on at least a seasonal basis. In addition, there are two active quarries in Wayne County. These quarries are shown on Figure 2.4-235.

Some local households are domestically self-sufficient for water. Groundwater is the largest source of water for self-sufficient households according to the year 2000 USGS Water Use estimates (Reference 2.4-270).

Groundwater is used to a lesser extent for public water supply systems as classified by the Michigan Department of Environmental Quality (MDEQ). This information is reported to the EPA which displays the information through the Safe Drinking Water Information System (SDWIS). SDWIS shows that only three community water systems in Monroe County use groundwater as their primary water source (Reference 2.4-271).

- The closest community water system that uses groundwater is the Flat Rock Village Mobile Home Park. The Flat Rock Village Mobile Home Park is located approximately 10.5 km (6.5 mi) to the northwest of the site and serves 830 people.
- The next closest is the Bennett Mobile Home Park located approximately 37 km (23 mi) to the southwest of the site and serves 70 people, and
- The farthest is the Bedford Meadows Apartments also known as Stoney Trail Apartments that serves 140 people and is located approximately 40 km (25 mi) to the southwest of the site.

Monroe County also has 15 non-community, non-transient water systems (a public water system that regularly supplies water to at least 25 of the same people at least six months per year, but not year-round), along with 102 transient, non-community water systems (a public water system that provides water in a place such as a gas station or campground where people do not remain for long periods of time) (Reference 2.4-272) that use groundwater. Wayne County, Michigan, whose

southern boundary is located about 9.7 km (6 mi) north-northeast of the site, has no community water systems using groundwater and only one non-transient, non-community water system using groundwater which is located 56 km (35 mi) north-northwest of the site at Maybury Child Care.

Washtenaw County, Michigan, whose boundary is located approximately 25 km (16 mi) northwest of the site, has 21 community water systems that use groundwater, however, only one is located within 40 km (25 mi) of the site: the City of Milan. The city has four water wells that are located between 24 and 30 m (80 and 100 ft) deep. (Reference 2.4-273)

Groundwater is used for irrigation of crops at many locations throughout Monroe and Washtenaw Counties.

Figure 2.4-236, Figure 2.4-237, and Figure 2.4-238 display all wells in the state databases that lie within 3.2 km, 8 km, and 40 km (2 mi, 5 mi, and 25 mi) of the Fermi site. Because there is no groundwater use at Fermi 3, it is considered that the 40 km (25-mi) radius circle lies well beyond any potential influence from plant operations. Information regarding wells within 40 km (25 mi) of the Fermi site is presented by county in Appendix 2.4AA (Reference 2.4-274, Reference 2.4-275).

2.4.12.2.2 Projected Future Groundwater Use

Year 2000 water use data documented in USGS Circular 1268 (Reference 2.4-270) is supplemented with the State of Michigan water use data for Thermoelectric Power Generation for the year 2000 (Reference 2.4-276), and data presented in USGS Investigations Report 03-4312 (Reference 2.4-261) for a combined estimate of year 2000 water use by water user group. Water user groups include Public Supply, Self-Supplied Domestic, Industrial (including quarries), Irrigation, and Thermoelectric Power Generation.

Using population projection data and the year 2000 water use data, estimates were developed of future water use by user group through the year 2060. A direct linear relationship was assumed between population and water usage for water user groups Public Supply, Self-Supplied Domestic Users, and Industrial Users. The projected water use was increased or decreased by the percentage change in population for both Monroe and Wayne counties. For the user groups Irrigation, Livestock, and Thermoelectric Power Generation, no direct linear relation with population was assumed. Projected use estimates for these categories were maintained at the level of usage reported in the year 2000.

Projected water use by user group for Monroe County and Wayne County, Michigan, is presented in Table 2.4-227 and Table 2.4-228, respectively.

2.4.12.2.3 Ground Water Levels and Movement

This subsection presents regional and local data describing the movement of groundwater at and near Fermi 3. Data was gathered from public sources and collected onsite during the Fermi 3 subsurface investigation in 2007. The details of the subsurface investigations are described in Subsection 2.5.4.2.2.1.

2.4.12.2.3.1 Regional Groundwater Levels and Movement

Prior to the development of agriculture in the state and the associated draining of wetland areas, groundwater elevations along the Lake Erie shoreline in both the surficial aquifer system and the bedrock aquifer were above the lake level, and artesian flow conditions in wells was common (Reference 2.4-261). As part of a regional modeling report, the USGS presents simulated regional groundwater flow in the bedrock aquifer under pre-development conditions (Figure 2.4-239). This figure displays the understanding that under pre-development conditions, regional flow in the bedrock aquifer in the Michigan-Ohio region was generally from the southwest to the northeast, with Lake Erie being an area of regional discharge. These results correspond with regional patterns and pre-development conditions described by Nicholas et al (Reference 2.4-277).

Groundwater conditions in Monroe County were evaluated using data from a series of USGS monitoring wells installed in the county in the early 1990's. There are a total of 40 wells that have some records for the depth to groundwater. As part of the investigation for IR 94-4161 (Reference 2.4-277) the USGS drilled 33 observation wells into the bedrock aquifers and one into the unconsolidated glacial deposits. The USGS also has two long-term observation wells located approximately 3.2 km (2 mi) southeast of Petersburg, Michigan (about 37 km [23 mi] to the west southwest of the site). Ash Township installed four observation wells in early 2006.

Potentiometric surface maps for the bedrock aquifer in Monroe County for the years 1993 and the initial period beginning in 2008 are presented on Figure 2.4-240 and Figure 2.4-241. Most of the wells used in these maps are completed in the Bass Islands Group, although some wells in the northwest portion of Monroe County are completed in younger strata of the Silurian-Devonian bedrock aquifer. These figures reinforce the observation of the southwest to northeast flow direction evident in the regional water levels. Groundwater flow enters beneath Monroe County from the southwest, and the primary flow direction is to the northeast. The 1993 water level map displays a cone of depression along the northeastern county line associated with quarrying operations located there. The 2008 potentiometric surface map displays a significant new groundwater depression centered just southwest of the City of Monroe, Michigan. This is apparently associated with a new quarrying operation that was not active in 1993. The contour maps demonstrate that dewatering of quarries can significantly impact the bedrock groundwater flow.

2.4.12.2.3.2 Site Groundwater Levels and Movement

As part of the Fermi 3 subsurface investigation, 28 groundwater piezometers and monitoring wells were installed and developed at the site. Using the information on the soil and bedrock stratigraphy, monitoring wells were installed in the overburden, and the Bass Islands and Salina Groups. Water levels in these wells were measured on a monthly basis from June 2007 to May 2008. In addition to wells installed for the Fermi 3 program, water levels in some existing Fermi site wells installed as part of other projects were also measured and recorded. The water level elevation data presented in this section is referenced to North American Vertical Datum 1988 (NAVD 88). Table 2.4-229

presents construction details of wells considered in this analysis. The elevation of water recorded in each well is presented in Table 2.4-231.

Five surface water gauging stations (GS-1 through GS-5) were also installed as part of the Fermi 3 subsurface investigation. The surface water gauges installed as part of Fermi 3 were not readable from November 2007 to March 2008 due to ice buildup at the stations. Gauges GS-1 through GS-3, and GS-5, were re-established in April 2008. GS-4 was not re-established since its data was redundant to the other wells. Surface water gauge elevation data is presented on Table 2.4-230. Surface water elevations at GS-1 through GS-4 were used to help develop groundwater contours in the shallow zone. It should be noted, however, that the surface water elevation data are considered somewhat less precise than measured groundwater elevations due to the effects of wind and tides on water at the gauges. For this reason, if small discrepancies between surface water and groundwater elevations were observed, they may not be reflected in the contours if the data was judged to be anomalous with respect to the rest of the data. This circumstance was most prevalent at Gauge GS-3, located in the shallow water of the lagoon south of Fermi Drive, which is in direct hydraulic connection with Lake Erie. Gauge GS-5 is not used for contouring because the quarry in which it is located is hydraulically connected to both the Bass Islands aquifer and the overburden. Surface water elevations from the National Oceanic and Atmospheric Administration (NOAA) Fermi Gauge Station were used. The circulating water basin located to the north of the Fermi 2 Protected Area had a surface water gauge at which data was collected only from June through August 2007. However, this data was not used in developing contours because Fermi 2 construction drawings indicate that the pond is encircled by a clay dike keyed into the underlying glacial till, thereby minimizing the hydraulic connection between the pond and the surrounding rock fill. The surface water features in the undeveloped wetland area west of the overflow canal were used to help shape contours.

2.4.12.2.3.2.1 **Overburden**

The following issues were considered in the interpretation of onsite water level data from wells screened in the overburden.

Seventeen monitor wells/piezometers were installed into the overburden at the site to document hydrogeologic conditions. Additionally, five wells previously installed as part of other projects were included in the overburden data collection (EFT-1 S, EFT-1I, EFT-2 S, MW-5d, and GW-02).

Several man-made features at the site affect groundwater levels in the overburden. The site contains a series of clay-filled construction dikes that were built as part of the construction effort for Fermi 2 (Figure 2.4-231). A former muck disposal site is located in the southwest area of the site. Monitoring wells MW-383 S and MW-384 S are located in this area, and were installed into material that was dredged from the site and/or Lake Erie during and after the construction of Fermi 2. The area of Fermi 1 occupied by EFT-1 S and EFT-2 S consists of clay fill, and these wells are screened

in this material. These issues were considered during the development of overburden water table contours.

Five of the 16 wells installed to date as part of the Fermi 1 License termination were considered for use with this COL Application. These five wells are split into two well groups by location, which are EFT-1 and EFT-2. The EFT-1 well group consists of three wells, a shallow, intermediate, and deep. The EFT-2 well group consists of two wells, a shallow and a deep well. The shallow wells monitor the clay fill installed during construction of Fermi 1, the intermediate well monitors the native glacial till, and the deep wells monitor the upper part of the Bass Islands Group.

Water levels collected in June and July 2007 for monitoring well MW-388S were not used because the recorded water levels at or below well screen at this location.

Water level data were collected at monthly intervals for 12 months from June 2007 to May 2008. Only quarterly maps are presented as part of this discussion, displaying conditions that varied seasonally and with the construction activities on site. The remainder of the monthly water level maps is presented in Appendix 2.4BB.

June 2007: The overburden water table map contoured from data collected on June 29, 2007 is presented on Figure 2.4-242.

Two distinct patterns of groundwater flow are evident in this map; one in the active plant area, and one in the undeveloped area west of the plant. The active plant area is defined for the purpose of this document as the area bounded by the overflow canal, Fermi Drive, and Lake Erie. The undeveloped area is defined as the area between the overflow canal and Fisher Street.

The water table surface in the active plant area is characterized by radial flow outward from a local maximum near the center of the plant area (well MW-5d in Fermi 2) toward the construction dikes previously discussed, and ultimately to the surface water features of Lake Erie, the overflow canal, and the lagoons north and south of the active plant area. It is assumed that the construction dikes control the location of the contours due to the low permeability of clay as compared to the adjacent rock fill. There are local minima in the water table surface apparent at P-397 S and MW-386 S. These may reflect variations in the overburden and/or bedrock.

Wells MW-387 S, P-385 S, and MW-386 S have groundwater elevations lower than the surface water elevations at all five of the surface water gauge stations considered. This indicates that there may be local flow from the surface water features onto the Fermi 3 site during this monitoring event. Local perched groundwater in the southern part of the active area near wells MW-383 S and MW-384 S, and near wells EFT-1 S and EFT-2 S, is likely associated with clay fill placed there during previous construction.

The undeveloped area west of the overflow canal displays contours that indicate flow approximately northwestward from the overflow canal to the offsite area beyond Fisher Street. There are local minima in the water table surface apparent at P-382 S and P-389 S, with water table elevations

lower than the nearby surface water elevations in the overflow canal. These features may reflect variations in underlying bedrock topography or hydraulic conductivity. At P-382 S, there is a sandy silt layer logged at the bottom of the boring that may provide a preferential path for drainage from the overburden to the underlying bedrock, possibly causing this local water table depression.

September 2007: The overburden water table map generated from data collected on September 28-29, 2007 is presented on Figure 2.4-243.

For the active plant area, the groundwater flow patterns are similar to those observed in the June monitoring event. In the Fermi 2 area, groundwater appears to flow radially outward from a local maximum near MW-5d toward the construction dikes and encircling surface water features. Local perched groundwater is apparent near Fermi 1 and in the former muck disposal area in the southwest part of the active area. The water level in the area of Fermi 3 is now higher than the surrounding surface water, indicating groundwater flow discharging to the surface water bodies.

The contours in the undeveloped area west of the plant, by contrast, display a marked change in flow pattern from the June event. Although there is still a small component of flow directed offsite to the northwest, as defined by the low elevation at MW-388 S, the primary flow direction of this area has reversed from the June event. The primary flow direction is now eastward toward the overflow canal. The cause of this change may reflect seasonally variable hydrologic conditions associated with the wetlands present on the surface. Piezometers P-382 S and P-389 S again display groundwater elevations lower than the nearby surface water elevations, defining local minima in the water table.

December 2007: The overburden water table map generated from data collected on December 30, 2007 is presented on Figure 2.4-244.

For the active plant area, the groundwater flow patterns in December are similar to those observed in the June and September monitoring events. In the Fermi 2 area, groundwater still appears to flow radially outward from a local maximum near MW-5d toward the construction dikes and encircling surface water features. Local perched groundwater is apparent near Fermi 1 and in the former muck disposal area in the southwest part of the active area. Groundwater elevations at Fermi 3 are marginally higher than the surface water elevation recorded at the NOAA gauge.

The contours in the undeveloped area west of the plant have changed slightly from the flow pattern displayed in the September event. There is now an unambiguous gradient from the corners of the site toward the surface water features. From MW-381 S, the primary direction of flow is east/northeast toward the wetland surface water feature north of Fermi Drive and the overflow canal. From MW-393 S, flow is southeast toward the same features, indicative of the surface water features being discharge areas for the overburden groundwater flow at the time of data collection. There is no longer any component of flow evident from the contours that indicate offsite flow to the west, as there was in the June and September monitoring events. Piezometer P-389 S displays an

elevation that is a local minimum, lower than the nearby surface water elevations. P-382 S is no longer a minimum as it was in September and June.

March 2008: The shallow zone water table map generated from data collected on March 29, 2008 is presented on Figure 2.4-245.

For the active plant area, the groundwater flow patterns in March are similar to those observed in the previous monitoring events. In the Fermi 2 area, groundwater still appears to flow radially outward from a local maximum near MW-5d toward the construction dikes and encircling surface water features. Local perched groundwater is apparent near Fermi 1 and in the former muck disposal area in the southwest part of the active area. The area near MW-386 S is a local minimum in the water table surface.

The contours in the undeveloped area west of the plant are similar to those displayed in the December event. There is a clear gradient from the corners of the site converging toward the surface water features. From MW-381 S, the primary direction of flow is east/northeast toward the wetland surface water feature north of Fermi Drive and the overflow canal. From MW-393 S, flow is southeast toward the same features, indicative of the surface water features being discharge areas for the shallow zone groundwater flow at the time of data collection. Piezometer P-389 S still displays an elevation that is a local minimum, lower than the nearby surface water elevations.

2.4.12.2.3.2.2 **Bass Islands Aquifer**

The following issues were considered in the interpretation of onsite water level data from wells screened in the Bass Islands aquifer.

Water levels from four wells were omitted from the analysis due to issues regarding their construction details. It was observed that filter packs in wells MW-387 D and GW-01 extended slightly up into the overlying glacial till. Due to this circumstance, it was judged that the water levels measured in these wells were not effectively isolated from the hydraulic influence of groundwater conditions in the overburden, and these data were not contoured. Similarly, wells EFT-1 D and EFT-2 D have approximately one foot of bentonite seal between the top of the well screen and the bottom of the glacial till. For the purpose of water level map development, this seal was not considered adequate between the till and bedrock well screen as compared to other wells included in this data analysis. The comparatively elevated water levels in EFT-1 D and EFT-2 D compared to those nearby suggest that the short bentonite well seal may not effectively isolate the water levels expressed in these bedrock wells from the influence of the groundwater in the overburden, which has a higher head than the groundwater in the bedrock aquifer.

Apart from well construction issues, the heterogeneous conditions of a fracture flow system, coupled with the variety of well screened intervals, introduce a measure of ambiguity into the interpretation of the water level data. Monitoring wells and piezometers screened in the Bass Islands aquifer were installed under both the hydrogeology and the geotechnical subsurface investigations. Under the hydrogeology investigation, screen interval selections were based on the

location of the most fractured and permeable zones identified at each boring location during the packer testing program. Under the geotechnical investigation, boring depths and screen interval selections were based on anticipated excavation depths during plant construction. This results in well completions at varying depths within the Bass Islands aquifer. Some monitoring wells and piezometers are screened near the top of the aquifer, some midway, and others near the bottom. Figure 2.4-257 displays the effective intervals of each well completed in the Bass Islands aquifer. The Bass Islands aquifer is a distinct hydrogeologic unit; however, the varied zones monitored within the Bass Islands aquifer, coupled with the irregular nature of the fracture system introduce considerable local complexity to the data, including evidence of downward vertical flow (discussed in Subsection 2.4.12.2.3.2.4). However, the contours were developed in adherence to the data collected, and reflect the overall trends of groundwater flow within the Bass Islands aquifer.

One piezometer, P-399 D, straddles the Bass Islands Group-Salina Group contact. Inspection of the downhole natural gamma log for this boring indicates that the bottom 1.5 m (5 ft) of the screen penetrates the extreme upper portion of the Salina Group Unit F. This could potentially have the effect of lowering water level measurements in this piezometer due to downward flow from the Bass Islands Group into the Salina Group (discussed in detail in Subsection 2.4.12.2.3.2.4). Because this is an important southern control point, and because the effect of the screen placement on water levels is ambiguous, data from this well were used in the development of potentiometric surface contours.

All bedrock wells have water levels that reflect artesian conditions except for MW-381 D. Water levels measured in MW-381 D are consistently below the top of the Bass Islands Group.

Data from surface water Gauge GS-5 was not used to develop contours. This gauge is located in a lake formed by a quarry that penetrates into the bedrock; therefore, the lake level is hydraulically associated with both the bedrock aquifer and the overburden. It is assumed that the Bass Islands aquifer is effectively hydraulically separated from other surface water features.

June 2007: The Bass Islands aquifer potentiometric surface map generated from data collected on June 29, 2007 is presented on Figure 2.4-246.

The contours developed for June through August 2007 indicate a significantly different flow pattern than the contours developed for the ensuing months. This is likely due to effects from the geotechnical field program, which was being carried out simultaneously with the water level data collection for the summer month monitoring events. Several geotechnical borings in the Fermi 3 area were open during this time period, providing a hydraulic connection between the Bass Islands Group and the underlying Salina Group. Because the vertical gradient between these two units is downward, this provided a temporary local sink for groundwater flow in the Bass Islands aquifer.

The flow pattern indicates that the groundwater appears to be flowing onto the active site area from the north, and converging towards the area of the geotechnical investigation at Fermi 3. The closed contours at Fermi 3 indicate that groundwater is converging on the area from all directions.

Groundwater entering this sink in the Bass Islands aquifer is likely being conveyed downward into the Salina Group through the open geotechnical borings.

More distant from the Fermi 3 area, beneath the undeveloped area west of the overflow canal, flow direction is south by southwest. In the area south of Fermi Drive, the flow direction is approximately northward. The southern and northern flow regimes converge along an axis parallel with the location of Fermi Drive, moving toward a local minimum defined at MW-381 D. This flow direction is counter to the regional flow direction, which is approximately toward Lake Erie, but may be impacted by off-site quarry dewatering activities, as previously discussed.

September 2007: The Bass Islands aquifer potentiometric surface map generated from water level data collected on September 28-29, 2007 is presented on Figure 2.4-247.

All the geotechnical borings that had provided vertical hydraulic connection had been abandoned and backfilled at least seven days prior to this monitoring event. This appears to have had a marked effect on the groundwater flow patterns. There are no longer any closed contours or a groundwater sink evident in the potentiometric surface at Fermi 3. The gradient across the Fermi 3 site is comparatively steep, but flow continues to the southwest and west, and appears to flow offsite to the west.

September is the first month in which water level data was collected from piezometer EB/TSC-C2. Water levels in this piezometer are over 1.2 m (4 ft) higher than those recorded in nearby piezometers P-385 D and CB-C5. The groundwater contour interpretation presented in Figure 2.4-247 displays an elongated lobe of slightly elevated water levels (groundwater mound) over the western half of Fermi 2. The screened interval for piezometer EB/TSC-C2 is considerably shallower than those of P-385 D and CB-C5, creating some complexity in the contour analysis due to the downward gradient in the bedrock (Subsection 2.4.12.2.3.2.4). However, even with the complexities, the contours indicate that the primary flow direction beneath the site is still to the south. The presence of the mound associated with EB/TSC-C2 has the effect of creating a local area of flow beneath Fermi 2 that is directed eastward towards Lake Erie. There is a very small eastward component of flow near MW-391 D in the June potentiometric surface map (Figure 2.4-246), but the inclusion of the elevation data for EB/TSC-C2 accentuates the eastward flow direction in this area.

Flow from the south converges with flow from the north to flow offsite to the west/northwest in the vicinity of MW-381 D.

December 2007: The Bass Islands aquifer potentiometric surface map generated from water level data collected on December 30, 2007 is presented on Figure 2.4-248.

The flow patterns displayed in the potentiometric surface are similar to those observed during the September monitoring event. Flow enters the site from the north and south, and converges to leave the site to the west in the vicinity of MW-381D. There remains a mound in the potentiometric surface associated with EB/TSC-2, and local flow to the east beneath Fermi 2 is toward Lake Erie.

However, the gradient of the flow entering the site from the south appears to be somewhat flatter than was evident in the September map.

March 2008: The Bass Islands aquifer potentiometric surface map generated from water level data collected on March 29, 2008 is presented on Figure 2.4-249.

The flow patterns are similar to those displayed in September and December 2007. Flow enters from the north and south, and exits to the west/northwest in the vicinity of MW-381 D. Mounding is still evident at EB/TSC-2. Locally, flow leaves eastward toward Lake Erie near MW-391 D. The flow gradient of groundwater entering the site from the south continues to flatten.

2.4.12.2.3.2.3 **Salina Group – Unit F Aquifer**

One piezometer intended to be screened in the Bass Islands aquifer is completed within the Salina Group (P-398 D). Since only one well is screened in this unit, contours can not be generated for this aquifer. However, water levels at this well were lower than the surrounding water levels from wells screened in the Bass Islands aquifer.

2.4.12.2.3.2.4 **Vertical Flow**

The USGS indicated that regionally, the vertical gradient of groundwater flow was downward from the surficial aquifer system to the Silurian-Devonian bedrock aquifer (Reference 2.4-261). Local site data confirm this conceptual understanding. Beneath the site, the vertical component of groundwater flow is predominantly downward from the overburden to the Bass Islands aquifer. This is generally evidenced by the paired hydrographs displayed on Figure 2.4-250.

These hydrographs display monthly water level time series for well pairs in which one well is completed in the overburden, and the immediately adjacent well is completed in the bedrock aquifer. The well pairs in the southern half of the site (MW-381, MW-383, MW-384, MW-386, P-385) display strong downward gradients from the overburden to the bedrock aquifer, with head differences of over 4.6 m (15 ft) in some cases (MW-381).

To the north at site MW-395 located along the overflow canal, there is only a very slight difference in head between the two zones, indicating that they are nearly in equilibrium with one another. This is an indication that the Bass Islands aquifer may be receiving more recharge in this area than further south at Fermi 3. Well pairs MW-388/GW-04 and MW-393 S/D, located along the western site boundary in the undeveloped portion of the site, display hydrograph lines that cross, indicating that the direction of vertical flow, though predominantly downward, may reverse locally with seasonal conditions.

The effect of the open geotechnical boreholes during the summer months is also reflected on the hydrographs of the wells located at Fermi 3. Hydrographs for MW-387 D and P-385 D, located within the geotechnical subsurface investigation area, display lower water levels for the months of June through August that recover significantly in September after the geotechnical borings were

properly abandoned and the hydraulic connection between the Bass Islands Group and the Salina Group was removed. This is additional evidence of a downward vertical gradient.

As previously discussed, the Fermi 3 water level patterns for the Bass Islands aquifer for June, July, and August 2007 reflect the presence of a groundwater sink in the area of the geotechnical borings.(July and August maps are included in Appendix 2.4BB). These borings were left open into the Salina Group during this time, and the presence of the closed contour in these maps indicates that water flowed from the Bass Islands Group downward into the Salina Group via the open boreholes, indicating a downward vertical gradient.

Evidence that flow is downward from the Bass Islands aquifer to the Salina Group is also reflected in water levels collected at P-398 D. Although this is the only well completed in the Salina Group, the groundwater elevations here are consistently and significantly lower than those recorded in the nearest Bass Islands wells (MW-391 D and MW-395 D), providing further evidence of a downward gradient between the units.

Downward vertical flow is also evident in the bedrock based on water level data from monitoring wells and piezometers screened in different zones within the Bass Islands aquifer in the immediate area of Fermi 3. The water levels were higher in shallow wells and lower in deeper wells. As noted previously in Subsection 2.4.12.2.3.2.2, water level elevations in piezometer EB/TSC-C2 (where the effective interval monitored is centered at approximately elevation 166.5 m [543 ft] NAVD 88) were over 1.2 m (4 ft) higher than elevations in nearby piezometers CB-C5 and P-385D (where the effective interval monitored is centered at approximately elevation 153.9 m [505 ft] NAVD 88), providing evidence of downward gradient within the Bass Islands aquifer. For reference, Figure 2.4-257 displays monitored intervals for the monitoring wells and piezometers. The figure also provides the locations of the monitored interval relative to the Bass Islands Group and Salina Group – Unit F.

In addition, heat pulse data was collected during geophysical logging of geotechnical borings RB-C8 and TB-C5, and hydrogeologic borings MW-384 D, P-385 D, P-398 D, and P-399 D. Heat pulse data in P-384 D and P-385 D indicate downward flow *within* the Bass Islands aquifer. Data from the other borings where heat pulse readings were recorded indicate downward flow from the Bass Islands aquifer into the Salina Group.

2.4.12.2.3.2.5 **Temporal Groundwater Trends**

Reeves documented the water level declines in Monroe County from 1991-2001. The USGS well database was queried for well data that provides up to date water level data in Monroe County. Water level maps for 1991 and 2008 are described in Subsection 2.4.12.2.3.1. This section presents temporal groundwater trends in Monroe County.

Figure 2.4-251 (Reference 2.4-278) displays hydrographs for selected Monroe County monitoring wells for the years 1991 through 2008. Several different temporal trends are evident across the county from these hydrographs.

Well G-28, located in the area of regional inflow in the southwest corner of the county, displays no long-term decline evident in the water level hydrograph. This well displays large seasonal fluctuations in water level (up to 12 m [40 ft] in some years), but displays no long-term declines since 1991.

Well G-33, located in the southeast corner of the county in an area of groundwater discharge to Lake Erie, also shows stable water levels over the period, indicating no water level declines with time. Seasonal fluctuations in this well are small by comparison, only about 1.2 m (4 ft).

Wells G-8 and G-12 hydrographs display a declining trend from 1991 to 2003, then rebounding water levels from 2003 until 2008. This pattern appears to be evidence of the operation of nearby quarrying for the first part of the hydrograph, reflected by the declining water levels associated with dewatering. The rising water levels in the second half of these hydrographs reflect rising water levels resulting from the closing of the quarry and cessation of dewatering. London Quarry ceased operations in 2003.

Well G-4, located in the northeast part of the county within the influence of the several quarries, displays a declining trend with no water level recovery evident to date. Operations at quarries in this area continue to the present day.

Well G-17, located just southwest of the City of Monroe, displays the largest water level decline through this time period, with levels dropping nearly 27 m (90 ft) between 1994 and 2002. This well is within the influence of the Dennison Quarry (formerly known as the Hanson Quarry), which is currently operating.

Wells G-14, G-15, and G-16, located west of the Fermi site, all show moderate declines of about 3 to 5 m (10 to 15 ft) since 1991, with no recovery apparent to date. These wells are located approximately midway between the cones of depression associated with the quarries to the north and the Dennison Quarry to the south. The moderate declines in this area may be a combined result from both operations.

2.4.12.2.4 Hydrogeologic Properties of Subsurface Materials

This section presents data on the hydrogeologic properties of the overburden and the bedrock aquifer subsurface materials beneath the site.

2.4.12.2.4.1 Overburden

Hydraulic conductivity in the overburden is highly variable. In order to estimate hydraulic conductivities in the overburden, seventeen slug tests (Reference 2.4-279) were performed on thirteen shallow wells or piezometers as part of the site hydrogeologic investigation. Slug tests were performed in the field in June 2007 using electronic transducers to record water levels.

Assumptions for slug test analysis of unconfined strata were as follows:

- Aquifer thickness is equivalent to saturated thickness in the unconfined zone.
- Saturated thickness is equivalent to well depth minus depth to water.
- Screen length from field well completion diagrams and tables were used.
- No “skin effects” due to drilling mud cake on the borehole wall were present.
- Well filter pack porosity was assumed to be 0.3.
- Horizontal to vertical anisotropy ratio was assumed to be 1.

Eleven tests yielded slug test data typical of a damped response to initial displacement, and were analyzed using traditional methods. Slug test data was analyzed using the software Aqtesolv© Version 3.0 and Version 4.5 (Reference 2.4-280), using the assumptions described previously. Analyses on wells with damped response to initial displacement were performed using two methods for which the fundamental assumptions are valid: the Hvorslev method for unconfined aquifers and the Bouwer-Rice method for unconfined aquifers. The average of these two values was calculated and reported as a representative hydraulic conductivity in the immediate vicinity of the monitoring well/piezometer.

Six of the slug tests were performed on monitoring wells/piezometers screened in the rock fill. Inspection of data for these wells (P-385 S, MW-387 S, MW-390 S, MW-391 S, P-392 S, and P-396 S) indicate that initial displacement was small (on the order of one to several inches) and response nearly instantaneous (one to three seconds). The oscillatory pattern of these data indicate conditions of high hydraulic conductivity, wherein inertial forces of water movement and well bore storage effects may be greater than the forces governing flow in porous media. The Butler solution method for unconfined aquifers of high hydraulic conductivity was used to analyze these data (Reference 2.4-280).

The primary mechanism for producing water from storage in a confined aquifer is through compression of the aquifer mineral skeleton or expansion of water due to changes in the pressure field associated with removal of water from the system. However, this behavior is not restricted to confined aquifers only. Any aquifer that is being stressed during the first few seconds to a minute or so produces water through this mechanism, even unconfined aquifers (Reference 2.4-311, Reference 2.4-312, Reference 2.4-313, Reference 2.4-279). The Butler solution method for confined aquifers and the Springer-Gelhar solution method for unconfined aquifers were selected to evaluate the slug test data for monitoring wells/piezometers screened in the quarry rock fill. These methods are intended for aquifers with a high hydraulic conductivity.

Calculated hydraulic conductivity values for the overburden ranged from 0.028 to 16.5 ft/day in the quaternary and clay fill materials, and 251 to 1,776 ft/day in the rock fill (to be conservative, the maximum values calculated using the Butler and Springer-Gelhar methods for the wells in the rock fill are reported). Table 2.4-232 provides hydraulic conductivity estimates for the wells screened in

the overburden. Figure 2.4-252 displays the locations of overburden hydraulic conductivity results on the site map. Slug test data are included in UFSAR Appendix 2.4CC.

2.4.12.2.4.2 Bass Islands Aquifer

Estimates of hydraulic conductivity (or the associated parameter transmissivity, which is hydraulic conductivity multiplied by aquifer thickness) within the Bass Islands Group may vary widely with location. In Monroe County, USGS monitoring wells G-29 and G-30 are located in the southern part of the county just over 1.6 km (1 mi) from each other. Their reported transmissivities are 316 and 0.93 m^2/day (3400 and 10 ft^2/day), respectively, a difference of over two orders of magnitude (Reference 2.4-261).

Reeves used an estimate of 1.54 m/day (5.0 ft/day) as representative of the Bass Islands Group hydraulic conductivity in the USGS regional groundwater model (Reference 2.4-261).

A pump test performed south of the site near Stony Point in 1959 yielded hydraulic conductivity estimates of 3.2 and 11 m/day (10.6 and 36.1 ft/day) for two different zones in the bedrock aquifer. One of these zones may have been at least partially in the Salina Group. Estimates for the storage coefficient of the aquifer from these aquifer tests ranged from 4.1×10^{-5} to 2.5×10^{-4}. These storativity values are typical of confined aquifer conditions. (Reference 2.4-281)

To estimate the hydraulic conductivity in the local bedrock aquifer beneath the site, packer tests were performed in boreholes advanced into the Bass Islands Group. Tests were performed at multiple depths in each borehole in zones which were identified from boring logs or geophysical logs as being fractured. Transducers were placed in the target test zone, and also in the zones directly above and below the packers to record piezometric heads and determine if there were any packer leaks or hydraulic connection with zones outside the target zone. Injected water into the test zone of the aquifer was also recorded with time. Packer test analyses are performed using the equation reported in Royle (Reference 2.4-282):

$$T = \frac{Q \ln\left(\frac{R}{r_b}\right)}{2\pi P_i} \qquad \text{[Eq. 6]}$$

where:

T = Transmissivity (ft^2/day)
Q = Injection flow rate (ft^3/day)
R = Radius of influence (ft)
r_b = Radius of borehole (ft)
P_i = Net pressure injection (ft)

and

$$K = T/b \qquad \text{[Eq. 7]}$$

where:

K = Hydraulic conductivity (ft/day)
T = Transmissivity (ft^2/day)
b = Length of interval tested

Hydraulic conductivity in the Bass Islands Group is highly variable. In general, hydraulic conductivity decreases with depth in this unit. Some packer test data indicated hydraulic connection with zones above or below the zone being tested, thereby violating the assumptions of the analysis. However, these data are included in the presentation of results for the purpose of completeness. If these data are not considered, the average hydraulic conductivity calculated for the Bass Islands zone is 1 m/day (3.28 ft/day). If these data are considered, the average is 2.1 m/day (6.93 ft/day).

A summary table of hydraulic conductivity estimates calculated from packer test analysis results for the boreholes advanced into the Bass Islands Group is presented on Figure 2.4-253 and in Table 2.4-233. Packer test data is included in Appendix 2.4DD.

2.4.12.2.5 Potential Reversibility of Ground Water Flow

On a regional level, the potential exists for reversal of groundwater flow due to the large impact of quarry dewatering on the water levels in Monroe County and surrounding counties. Presently, multiple quarries are operating that significantly impact water levels in the county. Water levels have declined nearly 27 m (90 ft) southwest of the site, and nearly 12 m (40 ft) to the north of the site. These regional cones of depression may be affecting the current local flow direction, at the site. In other words, the present flow pattern is reversed from the pre-development flow pattern. If the quarries were to stop operating, water levels in the county could potentially recover to the point that the flow direction beneath the site might revert to the natural pre-development patterns.

As stated previously, Fermi 3 operations do not rely on groundwater and therefore have no impact on reversibility.

On a local scale, however, construction of Fermi 3 includes excavation into the Bass Islands Group to build foundations. This activity will require temporary dewatering of the excavation site to levels approximately 14-15 m (45-50 ft) below the present groundwater elevation. This will alter groundwater flow locally near the site. A groundwater model is utilized to estimate the off-site area in the Bass Islands aquifer to experience drawdown resulting from excavation dewatering activities during construction of Fermi 3.

2.4.12.2.5.1 Groundwater Modeling for Excavation Dewatering

A published 2003 USGS MODFLOW (Reference 2.4-283, Reference 2.4-284) regional model was used for this analysis. The original regional model was a steady-state model, and this application is also steady-state. The proprietary software package Groundwater Modeling System Version 6.0 (Reference 2.4-285) was used for pre- and post-processing.

The active area of the model includes all of Monroe County and parts of six other counties in Michigan and Ohio (Figure 2.4-239). The purpose of the original regional USGS MODFLOW groundwater model is to simulate regional water level declines associated with the increased dewatering activities by the quarrying industry in Monroe County. The purpose of this model application is to evaluate off-site effects of excavation dewatering, including drawdown and flow changes.

The original regional model grid was re-discretized vertically and laterally to provide a finer grid in the excavation area. The original grid is 297 rows x 194 columns x 10 layers. The refined grid consists of 349 rows x 235 columns x 11 layers (Figure 2.4-254). All physical and hydrogeologic parameters are retained from the regional model. Quarry dewatering in the original regional model was represented using MODFLOW's drain package. This conceptual approach was maintained for the excavation dewatering analysis. The target groundwater elevations during dewatering, represented by the assigned MODFLOW drain elevation, are 1.5 m (5 ft) lower than the excavation bottom elevation. The overlying glacial material will be stripped away.

Two simulations were performed as follows representing two possible approaches to the excavation system combining excavation support and seepage control:

- A reinforced diaphragm concrete wall surrounding the excavation with the interior bedrock below the excavation grouted.
- A grout curtain or freeze wall surrounding the excavation with the interior bedrock below the excavation grouted.

The effects of a pressure grouting program are represented by reducing the hydraulic conductivity of the rock below the excavation from the native value of 1.54 m/day to 0.29 m/day, based on reported results from the Fermi 2 grouting program (Reference 2.4-286). Diaphragm concrete wall cells are assigned a hydraulic conductivity of 1.0×10^{-7} cm/sec (8.64×10^{-5} m/day), a value representative of a hydraulic barrier wall.

Figure 2.4-255 and Figure 2.4-256 display the 0.305-m (1-ft) drawdown contour for each of the two simulations described, along with the location of registered wells in the Michigan state database. On Figure 2.4-255, which represents the diaphragm concrete wall simulation, the 0.305-m (1-ft) drawdown contour is entirely within the site. On Figure 2.4-256, which represents the grout curtain or freeze wall, the 0.305-m (1-ft) drawdown contour is approximately 2,591 m (8500 ft) from due west of the reactor. These results reflect the fact that the second simulation represents less

restrictive barrier conditions (grout curtain or freeze wall) than the first simulation (with perimeter diaphragm concrete wall).

Drawdown of this magnitude in the bedrock aquifer should not impact water levels in the onsite wetlands. The wetlands are hydraulically connected to Lake Erie via culverts, so the lake level will control wetland water levels at the site.

2.4.12.2.6 Potential Recharge Areas Within Influence of Plant

As discussed during presentation of the site water level data in Subsection 2.4.12.2.3.2.2, it appears that the Bass Islands aquifer may be receiving recharge from the overlying overflow canal through the glacial till. However, there is no onsite use of Bass Islands aquifer groundwater, so there is no significant consequence should this local recharge feature be temporarily affected.

2.4.12.3 Subsurface Groundwater Pathways

This subsection presents an evaluation of subsurface groundwater pathways for Fermi 3 to potential groundwater discharge locations.

2.4.12.3.1 Potential Groundwater Pathways

As discussed in Subsection 2.4.12.1.1, the geology beneath the site consists of native glacial deposits and imported fill, overlying Bass Islands Group dolomite. This subsection discusses possible subsurface pathways of groundwater through the overburden and bedrock. The center of the Reactor Building is used as a representative point of reference to estimate the lengths of the groundwater flow pathways to potential discharge locations. The center of the Reactor Building is selected, as it is a central location within the power block, which results in groundwater flow pathways that are indicative of what can be expected for flow from Fermi 3 to potential groundwater discharge locations. For other locations within the Fermi 3 site, travel distances may be different than estimated herein.

For groundwater within the overburden, the potential discharge locations are considered to be Lake Erie or other contiguous surface water features such as the overflow canal. The distance from the center of the Reactor Building to the overflow canal is the shortest pathway for groundwater discharge. The gradient in the vicinity of Fermi 3 is very low, and as a result may actually display changes in direction during different months. A westward gradient toward the overflow canal is observed during several months, so this pathway is possible. The distance is about 250 m (820 ft).

For groundwater in the Bass Islands aquifer, potential pathways are considered for the following two conditions:

- The documented present day condition, in which the groundwater flow direction in the Bass Islands aquifer is westward off-site.
- A possible future condition in which the flow direction has returned to flow toward Lake Erie.

The documented groundwater flow direction beneath the Reactor Building is consistently south by southwest, with the flow direction changing to west by northwest as the groundwater flows offsite (Figure 2.4-248). The nearest discharge point offsite along this flow path is household well 58000002901, listed in the state database as a bedrock well with a depth of 22.6 m (74 ft) and use type of household. The well is located immediately west of the corner of Fermi Drive and Toll Road (Figure 2.4-236). The distance from the Reactor Building to this well is approximately 1,450 m (4,756 ft) along the flowpath. (Reference 2.4-274)

As discussed in Subsection 2.4.12.2.5, the possibility exists for a return to flow toward Lake Erie in the Bass Islands aquifer should all quarry dewatering in the county come to a halt. In this case, the most direct pathway is to Lake Erie, approximately 450 m (1476 ft) to the east. This assumes that Lake Erie and the Bass Islands aquifer are in hydraulic communication at the shoreline, which is a conservative assumption.

2.4.12.3.2 Groundwater Travel Times to Discharge Locations

The travel time of groundwater from the center of the Reactor Building to the potential discharge location is dependent of the flow path length and the groundwater flow velocity. The groundwater flow velocity (or seepage velocity) is calculated from the following equation (Reference 2.4-287):

$$V = Ki/ n_e \qquad \text{[Eq. 8]}$$

where:

V = Average linear velocity (ft/day)
K = Hydraulic Conductivity (ft/day)
i = Hydraulic gradient (ft/ft)
n_e = Effective porosity (dimensionless)

The travel time to a discharge location is calculated by:

$$T = D/V \qquad \text{[Eq. 9]}$$

where:

T = Travel time (days)
D = Distance from center of Reactor Building to discharge location (ft).
V = Average linear groundwater velocity (ft/day)

- Groundwater velocity is locally dependent on hydraulic conductivity, hydraulic gradient, and porosity. Hydraulic conductivity is estimated from slug test and packer test data collected during the Fermi 3 subsurface investigation, and is discussed in Subsection 2.4.12.2.4.1 and

Subsection 2.4.12.2.4.2. Hydraulic gradient is estimated from Fermi 3 potentiometric surface maps (November water level maps were selected as being representative of site conditions).

Total porosity for the rock fill was estimated to be 25 percent, which is typical of coarse gravel (Reference 2.4-287 and Reference 2.4-288). For the Bass Islands dolomite, effective and total porosity estimates were located in literature. In Otsego County, Michigan, the total porosity of the Bass Islands is estimated to range from 13 to 21 percent (Reference 2.4-294). In the Milwaukee, Wisconsin area, the effective porosity of dolomite overlain by glacial till was estimated to be 1 percent (Reference 2.4-291). In addition, for the Bass Islands formation, as described in UFSARSubsection 2.4.13.2.2, site specific estimates for effective porosity were developed based on site measured parameters for hydraulic conductivity and Rock Quality Designation (RQD). The estimates for effective porosity range from 0.1% to 0.8%. For the purposes of this evaluation, a conservative value for effective porosity of 0.1% is used. These site specific estimates for effective porosity are conservative (less than) relative to the literature values for similar materials.

For flow in the rock fill overburden at Fermi 3, the following conditions are assumed:

- Hydraulic conductivity is 357 m/day (1,170 ft/day) based on the P-385S slug test.
- The gradient is 0.0007, based on the November water table map (Appendix 2.4BB).
- Porosity is 25 percent of the rock fill.

This results in a calculated flow velocity of 0.996 m/day (3.27 ft/day). Appling this velocity to the pathway distance of 250 m (820ft) to the overflow canal, the groundwater travel time is calculated to be 0.69 years (250 days).

For flow in the Bass Islands aquifer under present day potentiometric surface conditions, the following conditions are assumed:

- The average gradient along the flowpath from Fermi 3 to the point that it leaves the site to the west is 0.002.
- Effective porosity is assumed to be 0.1 percent.

The highest hydraulic conductivity estimate for a packer test that did not indicate vertical leakage to adjacent zones was 5.4 m/day (17.57 ft/day) (MW-395D at 11 m (37 ft): it should be noted that this boring is near the cooling towers, not along the flowpath). The lowest hydraulic conductivity for a valid packer test is 0.034 m/day (0.11 ft/day) (MW-383D at 20 m [67 ft]). Based on the maximum hydraulic conductivity estimate, the calculated velocity is 11 m/day (35 ft/day). Based on the minimum hydraulic conductivity estimate, the calculated velocity is 0.06 m/day (0.2 ft/day). Based on a pathway distance of 1,450 m (4,756 ft), the two velocity estimates yield groundwater travel time estimates along this pathway to the offsite well west of the site ranging from 0.37 years to 65 years.

To evaluate the pre-development groundwater flow gradient, Figure 2.4-239 was reviewed and an eastward gradient of 0.001 was estimated near the Fermi plant. Under pre-development conditions,

with this gradient and the range of hydraulic conductivities discussed in the previous paragraph, calculated groundwater velocities range from 0.03 to 5 m/day (0.1 to 17.6 ft/day). Based on this range of velocities, the estimated groundwater travel time for the (1,476 ft) pathway east to Lake Erie ranges from 0.23 to 40 years.

2.4.12.4 Groundwater Monitoring

A limited groundwater level monitoring program at Fermi 2 is currently performed as part of the Radiological Environmental Monitoring Program (REMP). Fermi 2 has four groundwater wells included in its REMP which are monitored monthly for water levels and sampled quarterly for the radionuclides and sensitivities specified in the Offsite Dose Calculation Manual (ODCM) (Reference 2.4-289).

In addition, 16 groundwater monitoring wells have been installed around Fermi 1 in support of decommissioning activities. These are also sampled on a quarterly basis with samples assayed for tritium and gamma emitters for the sensitivities specified in the Fermi 2 ODCM.

Some of the existing Fermi 3 piezometers will be abandoned prior to construction activities due to anticipated earth work and heavy construction requirements. It is not anticipated that this will affect any future groundwater monitoring program. **[START COM 2.4-12-001]** However, prior to the commencement of construction activities, the monitoring well network will be evaluated to determine if any significant data gaps are created by the abandonment of existing wells.

As part of the detailed design for Fermi 3, the present groundwater monitoring programs will be evaluated with respect to the addition of Fermi 3 to determine if any modification of the existing programs is required to adequately monitor plant effects on the groundwater. **[END COM 2.4-12-001]** As mentioned previously, several wells exist on-site from previous projects and investigations. It may be possible to integrate some of these wells into future monitoring activities. Any revised integrated monitoring plan will adhere to the guidance outlined in “Integrated Ground-Water Monitoring Strategy for NRC-Licensed Facilities and Sites: Logic, Strategic Approach and Discussion” (Reference 2.4-290) and NEI 08-08A, "Generic FSAR Template Guidance for Life Cycle Minimization of Contamination.". Possible components of monitoring plans to be evaluated may include the following for both the overburden and the Bass Islands aquifer.

- Construction Groundwater Monitoring
- During construction dewatering, piezometers are monitored as needed to evaluate drawdown of overburden and bedrock groundwater levels associated with dewatering. Detroit Edison will use Fermi 3 wells or piezometers, as appropriate. Monitoring is performed at frequent intervals when construction dewatering begins, in order to document water level declines. Monitoring frequency is reduced after dewatering levels have stabilized.

- Post construction dewatering: Monitor shallow and bedrock piezometers and monitoring wells monthly to establish groundwater flow patterns with Fermi 3 in-place. Use dewatering piezometers and Fermi 3 monitoring wells and piezometers, as appropriate.
- Pre-operational Groundwater Monitoring:
- Two monitoring well nests, one upgradient and one downgradient of Fermi 3, are established. The monitoring well nest locations are based on the post dewatering flow patterns. If existing wells are insufficient, new wells will be installed.
- One set of groundwater samples is collected from each of the Fermi 3 upgradient and downgradient locations. The water samples are analyzed for radionuclides and sensitivities specified in the ODCM. These results are used to characterize background water quality.
- Measure groundwater levels monthly. Use dewatering piezometers and Fermi 3 piezometers, as appropriate.
- Operational Groundwater Monitoring:
- The on-site groundwater monitoring program will be developed consistent with NEI 08-08A, "Generic FSAR Template Guidance for Life Cycle Minimization of Contamination."
- Operational Groundwater Accident Monitoring.
- This is triggered in the event of an accidental liquid release from Fermi 3, and includes monthly groundwater sampling of the upgradient well and selected wells located downgradient from the point of release. Wells are selected based on flow directions documented in the most recent water level maps available for the site. The water samples are analyzed for radionuclides and sensitivities specified in the ODCM.

Safeguards will be implemented to minimize the possibility of adverse impacts to groundwater due to construction and operation of Fermi 3. Such safeguards would include typical Best Management Practices (BMPs) for storage, handling, and conveyance of hazardous materials, such as appropriate containment areas around storage tanks, emergency cleanup procedures in the event of surface contaminant spills, secure hazardous materials storage areas, etc.

2.4.12.5 Design Basis for Subsurface Hydrostatic Loadings

The DCD requires the groundwater level to be 0.6 m (2 ft) below plant grade, as specified in Table 2.0-1. A detailed discussion of the geotechnical aspects of hydrostatic loading is presented in Subsection 2.5.4.10.3.

The maximum historical high groundwater level under non-flood conditions applicable to calculate subsurface hydrostatic loadings for Fermi 3 structures is 175.6 m (576.11 ft) NAVD 88, recorded at well MW-7 at the site of the Fermi 2 Combustion Turbine Peaking Units on January 17, 2001. This is greater than 0.6 m (2 ft) below the present site grade of approximately 176.9 m (580.3 ft) NAVD

88 and the Fermi 3 plant grade of 179.6 m (589.3 ft) NAVD 88, and therefore meets the DCD requirements.

During the Probable Maximum Flood (PMF), the flood level onsite is 178.4 m (585.4 ft) NAVD 88. Rock fill used to establish the existing and future site grade is characterized by a high hydraulic conductivity, as documented in Subsection 2.4.12.2.4.1, and thus groundwater elevations are capable of being raised during the design basis PMF due to the infiltration of surface water. Therefore, the Fermi 3 design groundwater level for hydrostatic loading is equal to the design basis PMF elevation (Subsection 2.4.5.2.2.2). The plant grade is at elevation 179.6 m (589.3 ft) NAVD 88, almost 1.2 m (4 ft) higher than the 178.4 m (585.4 ft) elevation. Seismic events will not affect the design groundwater level.

2.4.13 Accidental Releases of Liquid Effluents to Ground and Surface Waters

2.4.13.1 Mitigating Design Features

Mitigating design features specified in NUREG 0800 Branch Technical Position (BTP) 11-6 are incorporated into the design of Fermi 3 to preclude an accidental release of liquid effluents. Descriptions of these features are provided below.

Below-grade tanks containing radioactivity are located on levels B1F and B2F of the Radwaste Building. The Radwaste Building is designed to seismic requirements as specified in Table 3.6-2. In addition, as described in Subsection 11.2.2.3, compartments containing high level liquid radwaste are steel lined up to a height capable of containing the release of all liquid radwaste in the compartment. Leaks as a result of major cracks in tanks result in confinement of the liquid radwaste in the compartment and the building sump system for containment in other tanks or emergency tanks. Because of these design capabilities, it is not considered feasible that any major event involving the release of liquid radwaste into these volumes results in the release of these liquids to the groundwater environment via the liquid pathway.

The Condensate Storage Tank (CST), part of the Condensate Storage and Transfer System (CS&TS), is the only above-grade tank that potentially could contain radioactivity outside of containment, the reactor building, or the radwaste building. The CS&TS, described in Section 9.2.6, meets GDC 60 by compliance with RG 1.143, Position C.1.2 for design features provided to control the release of liquid effluents containing radioactive material. The basin surrounding the tank is designed to prevent uncontrolled runoff in the event of a tank failure. The basin volume is sized to contain the total tank capacity. Tank overflow is also collected in this basin. A sump located inside the retention basin has provisions for sampling collected liquids prior to routing them to the Liquid Waste Management System (LWMS) or the storm sewer as per sampling and release requirements. These design features are intended to preclude the release of liquids from the CST to either the ground or surface water environment via the liquid pathway.

The mitigating design features described above demonstrate that the radioactive waste management systems, structures, and components for Fermi 3, as defined in RG 1.143, include features to preclude accidental releases of radionuclides into potential liquid pathways. Nevertheless, an analysis of accidental releases of radioactive liquid effluents in groundwater is performed. Descriptions and results of these analyses are provided below.

2.4.13.2 Groundwater Analysis

The discussion in Subsection 2.4.13.1 demonstrates that the Fermi 3 LWMS design will preclude accidental release of radioactive liquid effluents to the environment. Nevertheless, in accordance with SRP 11.2, analyses of the bounding release of radioactive liquid effluents to the groundwater and consequently to the nearest sources of potable water in an unrestricted area are performed.

This section provides a conservative analysis of a postulated, accidental release of radioactive liquid effluents to the groundwater. The accident scenario is described, and the model used to evaluate radionuclide transport is presented, along with potential pathways of contamination to water users. The radionuclide transport analysis is described, and the results are summarized. The radionuclide concentrations are compared against the regulatory limits.

2.4.13.2.1 Accident Scenario

A liquid radwaste tank outside of containment is postulated to fail, coincident with the non-mechanistic failure of the above described mitigating design features, thus allowing the tank contents to be released to groundwater. The volume of the liquid assumed released and the associated radionuclide concentrations were selected to produce an accident scenario that leads to the most adverse contamination of groundwater.

Radwaste tanks outside of containment are located on levels B1F and B2F of the radwaste building as shown on Figure 1.2-25. The radwaste tanks having the largest volumes include the three equipment drain collection tanks and the two equipment drain sample tanks, all in the lowest level, B2F. Each of these tanks has a volume of approximately 37,000 gallons (140 m^3) per Table 11.2-2a.

Activity concentrations in various liquid radwaste tanks are provided in Tables 12.2-13a through 12.2-13g. Of these tanks, the limiting tank in terms of radionuclide activity is the equipment drain collection tank; whose activity is provided in Table 12.2-13a (Table 2.0-2 for Subsection 2.4.13 identifies Table 12.2-13a as the source term for this analysis).

The scenario assumes that one of the equipment drain collection tanks fails and its contents are released to the groundwater. Note that this accident scenario is extremely conservative because the radwaste building is seismically designed in accordance with RG 1.143, Class RW-IIa, as described in Subsection 12.2.1.4. Also, each tank cubicle is provided with a steel liner, as described in Subsection 11.2.2.3, to preclude any potential liquid releases to the environment.

2.4.13.2.2 Transport Model

Based on the COL stage investigations of the Fermi 3 power block and surrounding area documented in Section 2.4.12, specific site characteristics related to groundwater and transport pathway through the underlying material were developed.

The conceptual transport model is used to evaluate the accidental release of radioactive liquid effluent to groundwater. Key elements and assumptions embodied in this evaluation are described and discussed below.

As indicated earlier, one of the equipment drain collection tanks is assumed to be the source of the release, with each tank having a capacity of 140 m^3 (37,000 gal) and radionuclide concentrations as given in Table 12.2-13a. These tanks are located on the lowest level of the radwaste building (level B2F), which has a floor elevation of approximately 540 feet NAVD 88 (Figure 2.5.4-204). One of the tanks is postulated to rupture and the contents released to the room.

The assumption of release to the groundwater following tank rupture is conservative because it requires failure of the floor drain system, plus it ignores the barriers presented by the basemat concrete and the steel liners incorporated into the tank cubicles of the radwaste building, which is seismically designed. It should also be recognized that level B2F of the radwaste building is well below the water table. Piezometric head contour maps presented in Figure 2.4-246 through Figure 2.4-249 indicate that the ambient water table in the vicinity of the radwaste building is about 567 feet NAVD 88, or 27 ft above the radwaste building floor elevation. If the basemat or exterior walls of the radwaste building and associated steel liners were to fail simultaneously, groundwater would flow into the radwaste building, precluding the release of liquid effluents out of the building. Only if the interior of the radwaste building was flooded to a level higher than the surrounding groundwater would there be a pathway for liquid effluents to be released out of the building and to the groundwater. As described later, this water head is credited for dilution in the equipment drain collection tank room prior to release; however, this head is not credited with precluding or delaying the release. Hence, the assumption of an accidental release of liquid effluents from the radwaste building to groundwater is extremely conservative, given the design features of the radwaste building intended to prevent an accidental release and the hydrogeologic conditions at the site.

In the worst-case postulated accidental release scenario, radionuclides are released directly to the Bass Islands aquifer and migrate with the groundwater in the direction of decreasing hydraulic head. Subsection 2.4.12.3.1 describes potential pathways in the bedrock (Bass Islands aquifer). As described in Subsection 2.4.12.3.1 there are two potential pathways for groundwater:

- The documented present day condition, in which the groundwater flow direction in the Bass Islands aquifer is westward off-site.
- A possible future condition in which the flow direction has returned to the east toward Lake Erie.

The present day condition is attributed to dewatering associated with quarrying operations westward of the site. The possible future condition is intended to account for the case where the

quarrying operations were to cease. For the purposes of this evaluation, both potential flow paths are considered. To the west off-site, the assumed receptor is a well located at the west corner of Enrico Fermi Drive and Toll Road as shown on Figure 2.4-236. To the east, the receptor is the closest potable water intake in Lake Erie. The distances from the source to each receptor are conservatively selected. For the path from the radwaste building to the well off-site to the west, the source location is assumed to be the closest western side of the radwaste building. For the path from the radwaste building to the potable water intake in Lake Erie, the source is assumed to be the closest eastern side of the radwaste building. Figure 2.4-266 provides a schematic of the conceptual model used for this analysis.

The analysis allows for radionuclide decay during transport by groundwater, and considers this decay in the analysis. Radionuclide transport by groundwater is affected by adsorption by the surrounding soils.

Parameters such as hydraulic conductivity, effective porosity, and hydraulic gradient used in the analysis are provided in Table 2.4-234. All radioisotope constituents of the source term in Table 12.2-13a are included in the analysis.

Effective porosity was estimated using Reference 2.4-317 and Reference 2.4-318, using site measured parameters for hydraulic conductivity and Rock Quality Designation (RQD) for the corresponding location. Hydraulic conductivity was determined based on Packer Testing (Subsection 2.4.12.2.4.2). Using this method and site specific inputs, effective porosity was estimated at several on site locations with results ranging from 0.1% to 0.8%. For the purposes of the radionuclide transport analysis, a conservative value for effective porosity of 0.1% is used.

Dilution of the radionuclide source term released from the equipment drain collection tank inside the radwaste building is credited in the analysis. As described above, the ambient water table in the vicinity of the radwaste building is approximately 27 feet above the radwaste building floor elevation. If the basemat or exterior walls of the radwaste building and associated steel liners were to fail simultaneously, groundwater would flow into the radwaste building. Based on the available volume in an equipment drain collection tank room and the entire volume of the tank (140 m^3), the dilution factor would be more than three. For the analysis, a dilution factor of three is credited. The entire diluted volume is then assumed to be released instantaneously outside the radwaste building and available for transport.

Aquifer parameters were established for the Bass Island aquifer (see Subsection 2.4.12). For this accidental release groundwater transport model, the hydraulic conductivity and hydraulic gradient measured at the site were selected to ensure conservative results.

2.4.13.2.3 Radionuclide Transport Analysis

The radionuclide transport analysis is conducted to estimate the radionuclide concentrations in drinking water based on an instantaneous release of the equipment drain collection tank to the equipment drain collection tank room and an instantaneous release of the equipment drain

collection tank room contents (diluted as described above) to the Bass Islands aquifer. Release pathways to the nearest offsite well and to the nearest potable water source in Lake Erie are considered.

Analysis of liquid effluent release begins with the simplest of screening models, using demonstratively conservative assumptions and coefficients. Radionuclide concentrations resulting from the screening analysis are then compared against the maximum permissible concentrations, stated as the effluent concentration limits (ECLs) identified in 10 CFR 20, Appendix B, Table 2, Column 2, to determine acceptability. 10 CFR 20, Appendix B, Table 2 imposes additional requirements when the identity and concentration of each radionuclide in a mixture are known. In this case, the ratio present in the mixture and the concentration otherwise established in 10 CFR 20 for the specified radionuclides not in a mixture must be determined. The sum of such ratios for all of the radionuclides in the mixture may not exceed “1” (i.e., “unity”). The sum of fractions approach is applied to the radionuclide concentrations for both pathways. Further analysis, using progressively more realistic and less conservative assumptions and modeling techniques, is conducted when results using conservative assumptions and coefficients cause the radionuclide concentrations to exceed either more than one percent of the associated ECL (i.e.,, the one percent is used as a screening value) or the sum of fractions unity limit. The analysis results are considered to be acceptable when the radionuclide concentrations are all less than the associated ECL and the sum of fractions is less than unity.

This analysis accounts for the parent radionuclides expected to be present in the equipment drain collection tank plus progeny radionuclides that would be generated subsequently during transport. The analysis considered progeny radionuclides in the decay chain sequences. Reference 2.4-319 was used to identify the half lives and decay chain sequences. The derivation of the equations governing the transport of the parent and progeny radionuclides follows.

One-dimensional transport of the parent radionuclide along a groundwater pathline is governed by the advection-dispersionreaction equation (Reference 2.4-320), which is given as

$$R\frac{\partial C}{\partial t} = D\frac{\partial^2 C}{\partial x^2} - v\frac{\partial C}{\partial x} - \lambda RC \qquad \text{[Eq. 1]}$$

where:
C = radionuclide concentration;
R = retardation factor;
D = coefficient of longitudinal hydrodynamic dispersion;
v = average linear velocity;
t = groundwater travel time,
x = travel distance, and

λ = radioactive decay constant.

The retardation factor is defined from the relationship

$$R = 1 + \frac{\rho_b K_d}{n_e} \qquad \text{[Eq. 2]}$$

where:
ρ_b = bulk density;
K_d = distribution coefficient; and
n_e = effective porosity.

The average linear velocity is determined using Darcy's law, which is

$$v = -\frac{K}{n_e}\frac{dh}{dx} \qquad \text{[Eq. 3]}$$

where:
K = hydraulic conductivity; and
dh/dx = hydraulic gradient.

The radioactive decay constant can be written as

$$\lambda = \frac{\ln 2}{t_{1/2}} \qquad \text{[Eq. 4]}$$

where:
$t_{1/2}$ = radionuclide half-life.

Using the method of characteristics approach described in Reference 2.4-321, the material derivative of concentration can be written as

$$\frac{dC}{\mathrm{dt}} = \frac{\partial C}{\partial t} + \frac{dx}{dt}\frac{\partial C}{\partial x} \qquad \text{[Eq. 5]}$$

According to Reference 2.4-320 the coefficient of longitudinal hydrodynamic dispersion (D) is determined from the relationship:

$$D = \alpha_l v \qquad \text{[Eq. 6]}$$

The longitudinal dispersivity (α_l) is estimated from Reference 2.4-293, which is based on Reference 2.4-294:

$$a_l = 0.2(x)^{0.56632} \qquad \text{[Eq. 7]}$$

where:
α_l = longitudinal dispersivity in meters and
x = the distance down gradient from the contaminant source in meters.

From the same references, the average transverse horizontal dispersivity is estimated as

$$\alpha_{th} = 0.28\alpha_l \qquad \text{[Eq. 8]}$$

where:
α_{th} = average transverse horizontal dispersivity in meters

Using site-specific values for x and v, the longitudinal dispersivity and the longitudinal coefficient of hydrodynamic dispersion are obtained. The average transverse horizontal dispersivity is obtained from Equation (8).

To estimate the radionuclide concentrations in groundwater, the following sections describe the equations that are applied as appropriate along the groundwater transport pathways originating at the radwaste building.

2.4.13.2.3.1 Transport Considering Radioactive Decay

The initial screening analysis was performed considering radioactive decay only. The Lake Erie pathway is the shortest pathway with the shortest travel time, thus having the least radioactive decay. The offsite well pathway and travel time are longer, allowing more decay time.

This analysis assumed that all radionuclides migrate at the same rate as groundwater and considered no adsorption, retardation or dispersion, which could otherwise result in changes in plume concentrations over distance. Under these assumptions, the radionuclide concentration along a groundwater pathline can be expressed as a function of the groundwater travel time using the Bateman equations as given in Appendix B of Reference 2.4-320. The expressions for the parent, first progeny, and second progeny are as follows:

$$C_1(t) = C_{10}\exp(-\lambda t) \qquad \text{[Eq. 9]}$$

$$C_2(t) = \left(\frac{d_{12}\lambda_2 C_{10}}{\lambda_2 - \lambda_1}\right)\exp(-\lambda_1 t) + \left(C_{20} - \frac{d_{12}\lambda_2 C_{10}}{\lambda_2 - \lambda_1}\right)\exp(-\lambda_1 t) \qquad \text{[Eq. 10]}$$

$$C_3(t) = \left[\frac{d_{13}\lambda_3 C_{10}}{\lambda_3-\lambda_1} + \frac{d_{23}\lambda_2 d_{12}\lambda_3 C_{10}}{(\lambda_3-\lambda_1)(\lambda_2-\lambda_1)}\right]\exp(-\lambda_1 t) \qquad \text{[Eq. 11]}$$

$$+\left[\frac{d_{23}\lambda_3 C_{20}}{\lambda_3-\lambda_2} - \frac{d_{23}\lambda_2 d_{12}\lambda_3 C_{10}}{(\lambda_3-\lambda_2)(\lambda_2-\lambda_1)}\right]\exp(-\lambda_2 t)$$

$$+\left[C_{30} - \frac{d_{13}\lambda_3 C_{10}}{\lambda_3-\lambda_1} - \frac{d_{23}\lambda_3 C_{20}}{\lambda_3-\lambda_2} + \frac{d_{23}\lambda_2 d_{12}\lambda_3 C_{10}}{(\lambda_3-\lambda_1)(\lambda_3-\lambda_2)}\right]\exp(-\lambda_3 t)$$

where:
C_1 = concentration of the parent radionuclide
C_2 = concentration of the first progeny radionuclide
C_3 = concentration of the second progeny radionuclide
C_{10} = initial concentration of the parent radionuclide
C_{20} = initial concentration of the first progeny radionuclide
C_{30} = initial concentration of the second progeny radionuclide
λ_1 = radioactive decay constant for the parent radionuclide
λ_2 = radioactive decay constant for the first progeny radionuclide
λ_3 = radioactive decay constant for the second progeny radionuclide
d_{12} = fraction of parent radionuclide transitions resulting in first progeny production
d_{13} = fraction of parent radionuclide transitions resulting in second progeny
d_{23} = fraction of first progeny transitions that result in production of second progeny
t = groundwater travel time

The radioactive decay constant expressed in Equation (4) is related to the radionuclide half-life.

The two pathways are screened only crediting radioactive decay using the relevant physical inputs. The results of the screening analysis for each path are presented in Table 2.4-235 and Table 2.4-236.

The computed concentrations were compared with the 10 CFR 20, Appendix B, Table 2, ECLs. The ratio of the groundwater concentration to the ECL was used as the screening indicator. Ratios that were greater than or equal to 0.01, which means that the groundwater concentration is predicted to be greater than or equal to one percent of the ECL, were selected for further evaluation using adsorption, advection, and dispersion. The results for Lake Erie where the ratio exceeds 0.01 are highlighted in Table 2.4-235. The results for the nearest offsite well where the ratio exceeds 0.01 are highlighted in Table 2.4-236.

2.4.13.2.3.2 Transport Considering Radioactive Decay and Adsorption

Radionuclides retained from the radioactive decay screening analysis were further evaluated and screened considering adsorption and retardation in addition to radioactive decay.

Distribution (adsorption) coefficients (Kd values) were determined based on laboratory testing of rock samples from the Bass Islands formation. Samples for the laboratory testing were taken from nine different locations on site. The locations for the laboratory testing samples were selected based on the postulated groundwater flow path either to the west to the off site water well or to the east to Lake Erie. Water samples from on-site monitoring wells screened in the Bass Islands aquifer approximately along the flow paths were used during the laboratory testing. Based on the use of site water samples for the laboratory testing, impacts due to potential contaminants in the groundwater at the site that could affect the transport and adsorption are accounted for. In order to simulate the fractured nature of the Bass Islands formation, the samples were broken into pieces for the laboratory testing. The material was not crushed or pulverized as this may not conservatively represent the sub-surface conditions.

Distribution coefficient measurements were obtained for cerium, cesium, cobalt, iron, manganese, ruthenium, silver, strontium, yttrium, and zinc. Selection of radionuclides for determination of distribution coefficients was based on the activity of the equipment drain collection tank source term and screening evaluations. The screening evaluations determined concentrations for the various radionuclides present in the equipment drain collection tank, including the associated progeny(s) considering only the decay of the radionuclides during the transport to the nearest off site water well and surface water body. The results from the screening evaluation were then compared to the 10 CFR Part 20, Appendix B, Table 2, limits. Radionuclides were selected for the laboratory analysis where the concentration predicted, crediting decay only, exceeded the limit.

In the transport analysis, the minimum distribution coefficient values were used for each element analyzed irrespective of their sample location. Distribution coefficients for other elements in the analysis were assigned a value of zero, which is conservative since it assumes no retardation during transport. Using the minimum distribution coefficient values ensures that the transport analysis results are conservative. The values for the distribution coefficients used in the analysis are shown in Table 2.4-234.

Conservatively neglecting hydrodynamic dispersion and using the material derivative of concentration from Equation (5), the characteristic equations for Equation (1) can be expressed as follows:

$$\frac{\partial C}{\partial t} = -\lambda C \qquad \text{[Eq. 12]}$$

$$\frac{\partial x}{\partial t} = \frac{v}{R} \qquad \text{[Eq. 13]}$$

The solutions of the system of equations comprising Equation (12) and Equation (13) can be obtained by integration to yield the characteristic curves of Equation (1). For the parent radionuclide, the equations representing the characteristic curves can be obtained as:

$$C_1(t) = C_{10}\exp(-\lambda t) \qquad \text{[Eq. 14]}$$

where:
$t = R_1L/v$;
C_1 = concentration of the parent radionuclide;
C_{10} = initial concentration of the parent radionuclide;
λ_1 = radioactive decay constant for the parent radionuclide;
R_1 = retardation factor for the parent radionuclide; and
L = groundwater pathline length.

Similar relationships exist for progeny radionuclides. For the first progeny in the decay chain, the advection-dispersion-reaction equation is:

$$R_2\frac{\partial C_2}{\partial t} = D\frac{\partial^2 C_2}{\partial x^2} - v\frac{\partial C_2}{\partial x} + d_{12}\lambda_1 R_1 C_1 - \lambda_2 R_2 C_2 \qquad \text{[Eq. 15]}$$

where:
subscript 2 denotes the first progeny radionuclide; and
d_{12} = fraction of parent radionuclide transitions that result in production of the progeny radionuclide.

The characteristic equations for Equation (15), again conservatively neglecting hydrodynamic dispersion can be derived as:

$$\frac{\partial C_2}{\partial t} = d_{12}\lambda'_1 C_1 - \lambda_2 C_2 \qquad \text{[Eq. 16]}$$

$$\frac{\partial x}{\partial t} = \frac{v}{R_2} \qquad \text{[Eq. 17]}$$

where:
$\lambda'_1=\lambda_1R_1/R_2$.

These equations can be integrated to yield:

$$C_2(t) = K_1\exp(-\lambda'_1 t) + K_2\exp(-\lambda t) \qquad \text{[Eq. 18]}$$

where: $t = R_2L/\mathrm{v}$ and for which

$$K_1 = \frac{d_{12}\lambda_2 C_{10}}{\lambda_2 - \lambda'_1}$$

$$K_2 = C_{20} - \frac{d_{12}\lambda_2 C_{10}}{\lambda_2 - \lambda'_1}$$

The advection-dispersion-reaction equation for the second progeny in the decay chain is:

$$R_3 \frac{\partial C_3}{\partial t} = D\frac{\partial^2 C_3}{\partial x^2} - v\frac{\partial C_3}{\partial x} + d_{13}\lambda_1 R_1 C_1 + d_{23}\lambda_2 R_2 C_2 - \lambda_3 R_3 C_3 \text{ [Eq. 19]}$$

where:
subscript 3 denotes the second progeny radionuclide;
d_{13} = fraction of parent radionuclide transitions that result in production of the second progeny radionuclide; and
d_{23} = fraction of the first progeny radionuclide transitions that result in production of the second progeny radionuclide.

The characteristic equations for Equation (19), again conservatively neglecting hydrodynamic dispersion can be derived as:

$$\frac{\partial C_3}{\partial t} = d_{13}\lambda'_1 C_1 + d_{23}\lambda'_2 C_2 - \lambda_3 C_3 \text{ [Eq. 20]}$$

$$\frac{\partial x}{\partial t} = \frac{v}{R_3} \qquad \text{[Eq. 21]}$$

where:
$\lambda'_1 = \lambda_1 R_1/R_3$ and
$\lambda'_2 = \lambda_2 R_2/R_3$.

These equations can be integrated to yield:

$$C_3(t) = K_1 \exp(-\lambda'_1 t) + K_2 \exp(-\lambda'_2 t) + K_3 \exp(-\lambda_3 t) \text{ [Eq. 22]}$$

where: $t = R_3 L/\mathrm{v}$ and for which

$$K_1 = \frac{d_{13}\lambda_3 C_{10}}{\lambda_3 - \lambda'_1} + \frac{d_{23}\lambda'_2 d_{12}\lambda_3 C_{10}}{(\lambda_3 - \lambda'_1)(\lambda'_2 - \lambda'_1)}$$

$$K_2 = \frac{d_{23}\lambda_3 C_{20}}{\lambda_3 - \lambda'_2} + \frac{d_{23}\lambda'_2 d_{12}\lambda_3 C_{10}}{(\lambda_3 - \lambda'_2)(\lambda'_2 - \lambda'_1)}$$

$$K_3 = C_{30} - \frac{d_{13}\lambda_3 C_{10}}{\lambda_3 - \lambda'_1} - \frac{d_{23}\lambda_3 C_{20}}{\lambda_3 - \lambda'_2} + \frac{d_{23}\lambda'_2 d_{12}\lambda_3 C_{10}}{(\lambda_3 - \lambda'_1)(\lambda_3 - \lambda'_2)}$$

Retardation factors were calculated using Equation (2) with the minimum site-specific distribution coefficients, an effective porosity of 0.001 and a bulk density of 2.4 g/cm^3.

The results of the screening analysis for each path are presented in Table 2.4-238 and Table 2.4-239.

The computed concentrations were compared with the 10 CFR 20, Appendix B, Table 2, ECLs. The ratio of the groundwater concentration to the ECL was used as the screening indicator. Ratios that were greater than or equal to 0.01, which means that the groundwater concentration is predicted to be greater than or equal to one percent of the ECL, were selected for further evaluation using adsorption, advection, and dispersion. The results for Lake Erie where the ratio exceeds 0.01 are highlighted in Table 2.4-238. The results for the nearest offsite well where the ratio exceeds 0.01 are highlighted in Table 2.4-239.

2.4.13.2.3.3 Transport Considering Radioactive Decay, Adsorption and Dilution in Lake Erie

Dilution between where the contaminated groundwater enters Lake Erie and the closest potable water source was considered. The nearest potable water intake for Lake Erie is approximately 1600 meters from the point where contaminated groundwater is expected to enter the lake. The lake depth varies, near the vicinity of the shoreline; a representative water depth of 2.2 meters is used. The nearest potable water intake is the Wilfred L. LePage Pumping Station 30” intake which is 474 meters offshore. These parameters give a lake volume between where the groundwater enters the lake and nearest potable water intake of more than 1,600,000 m^3. This volume would provide a dilution factor of approximately 3500. However, to be conservative, a dilution factor of 10 is applied for the nearest potable water intake in Lake Erie.

The results for Lake Erie applying the conservative dilution factor are provided in Table 2.4-240. The results show the predicted concentration of each of the radionuclides is less than the associated maximum permissible concentration and that the sum of fractions of all of the radionuclides is a maximum of 0.29 at 0.65 years; i.e., less than 1.0. Therefore, further evaluation for the release to the lake is not necessary.

2.4.13.2.3.4 Transport to the Closest Offsite Well Considering Radioactive Decay, Adsorption, Advection and Longitudinal Dispersion

The three radionuclides with the largest ECL fractions are considered to disperse in this analysis; i.e., H-3, Ni-63 and Pu-239.

The representative average linear velocity is considered to best represent subsurface site conditions in the one dimensional (longitudinal) sense along a groundwater pathline for each aquifer. The radionuclides of concern identified by the prior analyses are further evaluated in the next step, considering radioactive decay, adsorption, retardation, advection and dispersion using the pathway specific travel times.

Assuming a constant input concentration for a period of time t0, the concentration along a groundwater pathline may be given by (Reference 2.4-320):

$$\frac{C(x,t)}{C_0} = A(x,t) \quad 0 < t \le t_0 \qquad \text{[Eq. 23]}$$

$$\frac{C(x,t)}{C_0} = A(x,t) - A(x,t-t) \quad t > t_0$$

where:

$$A(x,t) = \frac{v}{v+U}\exp\left[\frac{x(v-U)}{2D}\right]erfc\left[\frac{Rx-Ut}{2(DRt)^{1/2}}\right] \qquad \text{[Eq. 24]}$$

$$+\frac{v}{v-U}\exp\left[\frac{x(v+U)}{2D}\right]erfc\left[\frac{Rx+Ut}{2(DRt)^{1/2}}\right]$$

$$+\frac{v^2}{2DR\lambda}\exp\left[\frac{xv}{D}-\lambda t\right]erfc\left[\frac{Rx+vt}{2(DRt)^{1/2}}\right]$$

with

$$U = (v^2 + 4DR\lambda)^{1/2} \qquad \text{[Eq. 25]}$$

Definitions for the parameters in the above equations are as follows:

C = radionuclide concentration (μCi/cm^3)

C_0 = radionuclide input concentration (μCi/cm^3)

t_0 = period of time a radionuclide is input at C_0 (y)

v = average pore water velocity (ft/y)

D = longitudinal coefficient of hydrodynamic dispersion (ft^2/y)

R = retardation factor

λ = radioactive decay constant (y^{-1})

The parameters to be specified in Equations (23) and (24) include C_0, t_0, v, D, R, and λ. The basis for assigning these parameters is described below.

The radionuclide input concentration C_0 is assumed to be the concentration in the equipment drain collection tank room. The input concentration of Pu-239 (a daughter product of Np-239) is estimated by assuming all source Np-239 decays instantaneously to Pu-239. This is a reasonable assumption considering the half-life of Np-239 is small relative to the transport time scales of interest. The input concentration for Pu-239 was calculated using the relationship between the activity concentration and atom density.

$$C = \lambda N \qquad \text{[Eq. 26]}$$

where N is the atom density ($atoms/cm^3$).

The input time period t_0 is taken to be the operating life of the plant or 60 years (40 years initial operating license plus 20 years license renewal). This assumption is conservative in that the equipment drain collection tank room is taken to provide a constant concentration source term continuously for the entire plant operating life. At the end of plant operation, it is assumed that the tank is drained and that the continuous constant source ceases at that point in time.

The predicted concentrations of the radionuclides from the analysis of the closest offsite well pathway using site-specific input conditions and one-dimensional dispersion are summarized in Table 2.4-241. Note that dispersion is only considered for H-3, Ni-63 and Pu-239, while decay and adsorption (where applicable) are considered for the other radionuclides. Although no radionuclides exceed their ECLs, the sum of the fractions of all radionuclides slightly exceeds unity (i.e., 1.029) at 3 years.

2.4.13.2.3.5 Transport to the Closest Offsite Well Considering Radioactive Decay, Adsorption, Advection Including Longitudinal and Transverse Horizontal Dispersion

The three radionuclides with the largest ECL fractions are considered to disperse in this step of the analysis; i.e., H-3, Ni-63 and Pu-239.

From Reference 2.4-320 if a homogeneous, isotropic porous medium having a unidirectional steady state flow with seepage velocity v is considered and if a Cartesian coordinate system is chosen with the x axis oriented along the direction of flow and if the magnitude of the dispersion coefficients in that direction and orthogonal to it are defined by DL and DT, respectively, then the two dimensional (longitudinal and transverse horizontal) advection-dispersion equation, as follows, can be used:

$$D_L \frac{\partial^2 C}{\partial x^2} + D_T \frac{\partial^2 C}{\partial y^2} - v\frac{\partial C}{\partial x} - \lambda RC = R\frac{\partial C}{\partial t} \quad \text{[Eq. 27]}$$

where R is the retardation factor for the given type solute.

If the medium is assumed to be initially free of a particular solute species and at a certain time a strip type source with length 2a, orthogonal to the groundwater flow direction, is introduced along the y axis and if the concentration of the solute diminishes exponentially with time, the initial and boundary conditions of this mathematical model may be written as

$$C(0, y, t) = C_0 e^{-at} \quad -a \le y \le a \qquad \text{[Eq. 28]}$$

$$C(0, y, t) = 0 \quad \text{other values of y}$$

$$\lim_{x \to \pm\infty} \frac{\partial C}{\partial y} = 0 \qquad \text{[Eq. 29]}$$

$$\lim_{x \to \pm\infty} \frac{\partial C}{\partial x} = 0$$

An analytical solution (Reference 2.4-323) to the above model may be presented as:

$$C(x, y, t) = \frac{C_0 x}{4(\pi D_L)^{1/2}} \exp\left(\frac{vx}{2D_L} - \alpha t\right) \quad \text{[Eq. 30]}$$

$$* \int_0^{(t/R)} \exp\left[-\left(\lambda R - \alpha R + \frac{v^2}{4D_L}\right)\tau - \frac{x^2}{4D_L \tau}\right] \tau^{-3/2}$$

$$* \left[erf\left(\frac{a-y}{2\left(D_T \tau\right)^{1/2}}\right) + erf\left(\frac{a+y}{2\left(D_T \tau\right)^{1/2}}\right)\right] d\tau$$

The integral is determined by numerical methods.

The predicted concentrations of the radionuclides from the analysis of the closest offsite well pathway using site-specific input conditions and two-dimensional dispersion are summarized in Table 2.4-242. Note that dispersion is only considered for H-3, Ni-63 and Pu-239, while decay and adsorption (where applicable) are considered for the other radionuclides. No radionuclides exceed their ECLs and the sum of the fractions of all radionuclides is less than unity at all time points.

2.4.13.2.4 Compliance with 10 CFR 20

As described above, the concentrations of the radionuclides predicted at both the potable water intake in Lake Erie and the closest off site well are less than the limits in 10 CFR 20, Appendix B, Table 2, Column 2. Meeting 10 CFR 20 limits at the closest off site well demonstrates that the radiological consequences of a postulated failure of one of the equipment drain collection tanks are also acceptable for larger distances from the radwaste building.

10 CFR 20, Appendix B, Table 2 imposes additional requirements when the identity and concentration of each radionuclide in a mixture are known. In this case, the ratio present in the mixture and the concentration otherwise established in 10 CFR 20 for the specified radionuclides not in a mixture must be determined. The sum of such ratios for all of the radionuclides in the mixture may not exceed “1” (i.e., “unity”). The sum of fractions approach has been applied to the radionuclide concentrations for both pathways. As described above, the sum of fractions for the mixtures at the closest off site well and at the potable water intake in Lake Erie are less than unity.

10 CFR 20, Appendix B states, 'The columns in Table 2 of this appendix captioned “Effluents,” “Air,” and “Water,” are applicable to the assessment and control of dose to the public, particularly in the implementation of the provisions of §20.1302. The concentration values given in Columns 1 and 2 of Table 2 are equivalent to the radionuclide concentrations which, if inhaled or ingested continuously over the course of a year, would produce a total effective dose equivalent of 0.05 rem (50 millirem or 0.5 millisieverts).” Thus, meeting the concentration limits of 10 CFR 20, Appendix B, Table 2, Column 2 results in a dose of less than 0.05 rem and therefore demonstrates that the requirements of 10 CFR 20.1301 and 10 CFR 20.1302 are met.

2.4.14 Technical Specifications and Emergency Operation Requirements

The design plant grade elevation for safety-related SSCs is located above the design basis flood level, as stated in Subsection 2.4.2, and above the maximum groundwater elevation, as stated in Subsection 2.4.12. Safety-related SSCs for the plant are protected from external floods as discussed in Section 3.4. The elevation of exterior access openings, which are above the PMF and local PMP flood levels, and the design of exterior penetrations below design flood and groundwater levels, which are appropriately sealed, result in a design and site combination that do not necessitate emergency procedures or meet the criteria for Technical Specification LCOs to ensure safety-related functions at the plant.

The plant elevation is also above flood and groundwater elevations for Regulatory Treatment of Non-Safety Systems (RTNSS) SSCs used to provide the makeup water to the UHS (IC/PCCS pools) from 72 hours to 7 days after an accident. The Seismic Category I FWSC SSCs are also protected from external floods. Therefore, no technical specifications or emergency procedures are required to prevent hydrological phenomena from degrading the UHS.

2.4.15 References

2.4-201 The Great Lakes: An Environmental Atlas and Resource Book. “State of the Great Lakes 2005.” November 2005, http://binational.net/solec/English/SOLEC%202004/Tagged%20PDFs/SOGL%202005%20Report/English%20Version/Lake%20Sections/Lake%20Erie%20-%20tagged.pdf, accessed 7 February 2007.

2.4-202 Great Lakes Information Network. 1 November 2006, http://www.great-lakes.net/envt/flora-fauna/people.html, accessed 8 October 2007.

2.4-203 National Geophysical Data Center. 7 November, 2007. http://www.ngdc.noaa.gov/mgg/greatlakes/greatlakes.html, accessed 26 November 2007.

2.4-204 Great Lakes Environmental Research Laboratory. “Subbasins around Lake Erie, 1948-2005.” 5 October 2005, http://www.glerl.noaa.gov/ifyle/data/Model/LBRM/runoff.html, accessed 26 November 2007.

2.4-205 Environment Canada and U.S. Environmental Protection Agency. “Lake Erie Management Plan (LaMP) Update 2003.” http://www.binational.net, accessed 13 December 2007.

2.4-206 Morreale, D.J. “A Survey of Current Great Lakes Research.” July 2002, http://www.eng.buffalo.edu/glp/articles/review.htm, accessed 2 May 2008.

2.4-207 U.S. Army Corps of Engineers. 16 February 2007, http://www.lre.usace.army.mil/greatlakes/hh/outflows/current_regulated_outflows, accessed 13 November 2007.

2.4-208 The Mackinac Center Report Groundwater Regulation: An Assessment by Russ Harding. April 2005.

2.4-209 Great Lakes Commission. “2004 Annual Report of Great Lakes Regional Water Use Database Repository.” 13 November 2006, http://www.michigan.gov/deq/0,1607,7-135-3313_3677_3704-72931--,00.html, accessed 21 April 2008.

2.4-210 Great Lakes Commission. “2003 Annual Report of Great Lakes Regional Water Use Database Repository.” 4 October 2006, http://www.michigan.gov/deq/0,1607,7-135-3313_3677_3704-72931--,00.html, accessed 21 April 2008.

2.4-211 Great Lakes Commission. “2002 Annual Report of Great Lakes Regional Water Use Database Repository.” 14 July 2005,

http://www.michigan.gov/deq/0,1607,7-135-3313_3677_3704-72931--,00.html, accessed 21 April 2008.

2.4-212 Great Lakes Commission. “2001 Annual Report of Great Lakes Regional Water Use Database Repository.” 12 July 2005, http://www.michigan.gov/deq/0,1607,7-135-3313_3677_3704-72931--,00.html, accessed 21 April 2008.

2.4-213 Great Lakes Commission. “2000 Annual Report of Great Lakes Regional Water Use Database Repository.” 30 July 2004, http://www.michigan.gov/deq/0,1607,7-135-3313_3677_3704-72931--,00.html, accessed 21 April 2008.

2.4-214 Great Lakes Commission. “1999 Annual Report of Great Lakes Regional Water Use Database Repository.” 13 August 2004, http://www.michigan.gov/deq/0,1607,7-135-3313_3677_3704-72931--,00.html, accessed 21 April 2008.

2.4-215 Great Lakes Commission. “1998 Annual Report of Great Lakes Regional Water Use Database Repository.” 16 August 2002, http://www.michigan.gov/deq/0,1607,7-135-3313_3677_3704-72931--,00.html, accessed 21 April 2008.

2.4-216 The Michigan Department of Environmental Quality. http://www.michigan.gov/deq/0,1607,7-135-3313_3677_3704-72931--,00.html, accessed 21 April 2008.

2.4-217 U.S. Army Corps of Engineers, Detroit District Corps of Engineers. “Monthly Bulletin of Lake Levels For The Great Lakes.” December 2006 through November 2007.

2.4-218 U.S. Environmental Protection Agency. “The Great Lakes - An Environmental Atlas and Resource Book.” 8 March 2006, Chapter 2, http://www.epa.gov/glnpo/atlas/glat-ch2.html, accessed 13 December 2007.

2.4-219 Environment Canada and U.S. Environmental Protection Agency. “Lake Erie Management Plan (LaMP) Updated 2005.” http://www.binational.net, accessed 13 December 2007.

2.4-220 Kovacik, T.L. “Information on the Velocity and Flow Pattern of Detroit River Water in Western Lake Erie Revealed by an Accidental Salt Spill.” The Ohio Journal of Science, 28 June 1972.

2.4-221 The Michigan Department of Environmental Quality. “Monroe Water Use 2005.” The Michigan Water Use Program.

2.4-222 The Michigan Department of Environmental Quality. “Monroe Water Use 2006.” The Michigan Water Use Program.

2.4-223 Environmental Systems Research Institute (ESRI), ArcGIS Data DVD, Version 9.2, USA and Canada Map Data, 2007.

2.4-224 Michigan Department of Environmental Quality. Hydraulic Data Collection and Analysis, Flood Discharge Database, Raisin Watershed, River Raisin (Mouth), 20 December 2007, http://www.deq.state.mi.us/flow/hflow.asp?FileNumber=20070540-3, accessed 3 June 2007.

2.4-225 GE- Hitachi Nuclear Energy ESBWR Design Control Document Tier 2, Revision 4, September 2007.

2.4-226 American National Standard ANSI/ANS-2.8-1992. "Determining Design Basis flooding at Power Reactor Sites." American Nuclear Society, 1992.

2.4-227 NOAA National Weather Service. "Hydrometeorological Reports 51, 52, 53, and 54." http://www.nws.noaa.gov/oh/hdsc/studies/pmp.html, accessed 10 March 2008.

2.4-228 NOAA Tides and Currents. "Historic Great Lakes Water Level Data." Fermi Power Plant, MI, Extremes, 23 November 2005, http://tidesandcurrents.noaa.gov/data_menu.shtml?stn=9063090%20Fermi%20Power%20Plant,%20MI&type=Extremes, accessed 13 June 2008.

2.4-229 Hydrology Water Quantity and Quality Control. 2nd Edition, John Wiley & Sons, Inc, 1997.

2.4-230 Lindburg, M.R. Civil Engineering Reference Manual for PE Exam - 9th Edition. "Mannings Rougness Coefficient." PE Professional Publications, Inc, Belmont CA, 2003.

2.4-231 Lindburg, M.R. Civil Engineering Reference Manual for PE Exam - 9th Edition. "Rational Method Run-off C-Coefficient." PE Professional Publications, Inc, Belmont CA, 2003.

2.4-232 Michigan Department of Environmental Quality. Hydraulic Data Collection and Analysis, Flood Discharge Database, Huron (Lake) Watershed, Swan Creek (Mouth), 20 December 2007, http://www.deq.state.mi.us/flow/hflow.asp?FileNumber=20070540-1, accessed 3 June 2007.

2.4-233 Michigan Department of Environmental Quality. Hydraulic Data Collection and Analysis, Flood Discharge Database, Stony Creek Watershed, Stony Creek (Mouth), 20 December 2007, http://www.deq.state.mi.us/flow/hflow.asp?FileNumber=20070540-2, accessed 12 June 2007.

2.4-234 NOAA Tides and Currents. "Historic Great Lakes Water Level Data." Fermi Power Plant, MI, 23 November 2005, http://tidesandcurrents.noaa.gov/data_menu.shtml?stn=9063090%20Fermi%20Power%20Plant,%20MI&type=Historic+Great+Lakes+Water+Level+Data, accessed 13 June 2008.

2.4-235 American National Standard ANSI/ANS-2.8-1992. “Determining Design Basis flooding at Power Reactor Sites.” American Nuclear Society, 1992.

2.4-236 NOAA National Weather Service. “Hydrometeorological Reports 51, 52, and 53.” http://www.nws.noaa.gov/oh/hdsc/studies/pmp.html, accessed 10 March 2008.

2.4-237 Lindburg, M.R. Civil Engineering Reference Manual for PE Exam - 9th Edition. “NRCS Synthetic Unit Hydrograph.” PE Professional Publications, Inc, Belmont CA, 2003.

2.4-238 Viessman, W. and G. Lewis. Introduction to Hydrology. “Synthetic Unit Hydrographs” 5th edition, Harper Collins College Publishers Hydrology, 1997.

2.4-239 Iowa Stormwater Management Manual. “Runoff Hydrograph Determination.” Version 1, Section 2C-7, 19 February 2007.

2.4-240 Environmental Systems Research Institute (ESRI), ArcGIS Data DVD, Version 9.2, USA and Canada Map Data, 2007.

2.4-241 U.S. Army Corp of Engineers Hydrologic Engineering Center. “HEC-GeoRAS Software.” Version 4, approved for public release on September 2005.

2.4-242 U.S. Army Corp of Engineers. “HEC-RAS 4.0 Beta Software.” 2008.

2.4-243 Fang, X., D.B. Thompson, et al. “Time of Concentration Estimated Using Watershed Parameters by Automated and Manual Methods.” Document planned to be published by June 2008.

2.4-244 Michigan Department of Environmental Quality. Hydraulic Data Collection and Analysis, Flood Discharge Database, Huron (Lake) Watershed, Swan Creek (Mouth), 20 December 2007, http://www.deq.state.mi.us/flow/hflow.asp?FileNumber=20070540-1, accessed 3 June 2007.

2.4-245 U.S. Army Corps of Engineers, Detroit District, Engineering and Technical Services. 3 May 2006, http://www.lre.usace.army.mil/greatlakes/hh/greatlakeswaterlevels/historicdata/stormprobabilitytables/, accessed 2 October 2007.

2.4-246 Michigan Department of Environmental Quality. Hydraulic Data Collection and Analysis, Low Flow Discharge Database, Huron (Lake) Watershed, File No. 6690, Swan Creek, 8 January 2008, http://www.deq.state.mi.us/flow/lflow.asp?FileNumber=6690, accessed 3 June 2007.

2.4-247 United States Army Corp Of Engineers, “Current Regulated Outflows, http://www.lre.usace.army.mil/greatlakes/hh/outflows/current_regulated_outflows, accessed 16 February 2008.

2.4-248 American Nuclear Society. “Determining Design Basis Flooding at Power Reactor Sites.” ANSI/ANS-2.8-1992.

2.4-249 U.S. Army Corps of Engineers. “Shore Protection Manual”. Coastal Engineering Research Center, Waterways Experiment Station, Vicksburg, Mississippi, Fourth Edition, 1984.

2.4-250 U.S. Army Corps of Engineers. “Coastal Engineering Manual”. Engineer Manual 1110-2-1100, 2002.

2.4-251 Smith, J.M.; Sherlock A.R. and Resio D.T. “STWAVE: Steady-State Spectral Wave Model User’s Manual for STWAVE, Version 3.0. February 2001.

2.4-252 NOAA ENC Direct to GIS. http://ocs-spatial.ncd.noaa.gov/website/encdirect/viewer.htm, accessed 20 May 2007.

2.4-253 Great Lakes Information Network (GLIN). Regional GIS Data by Topic – Elevation, Lake Erie Bathymetry. http://gis.glin.net/ogc/services.php#lake_erie_bathymetry, accessed 20 May 2007.

2.4-254 Fisheries and Oceans Canada. Integrated Science Data Management - Tide and Water Level Inventory. http://www.meds-sdmm.dfo-mpo.gc.ca/meds/Databases/TWL/TWL_inventory_e.htm, accessed 20 May 2007.

2.4-255 NOAA Tides and Currents. http://Tidesandcurrents.noaa.gov/olddata, accessed 20 May 2007.

2.4-256 Leenknecht, D.A., A. Szuwalski, and A.R. Sherlock. “Automated Coastal Engineering System: Technical Reference.” September 1992, Coastal Engineering Research Center, Department of the Army, Vicksburg, MS.

2.4-257 Ippen Phd, Arthur T. “Estuary & Coastline Hydrodynamics.” Engineering Societies Monographs, 1966.

2.4-258 Enrico Fermi, Unit 2 Updated Final Safety Analysis Report, Amendment 14 (November 2006).

2.4-259 NOAA Tides and Currents. “Historic Great Lakes Water Level Data.” Fermi Power Plant, MI, Extremes, 23 November 2005, http://tidesandcurrents.noaa.gov/data_menu.shtml?stn=9063090%20Fermi%20Power%20Plant,%20MI&type=Extremes, accessed 13 June 2008.

2.4-260 NOAA Tides and Currents. “Historic Great Lakes Water Level Data.” Fermi Power Plant, MI, 23 November 2005, http://tidesandcurrents.noaa.gov/data_menu.shtml?stn=9063090%20Fermi%20Power

%20Plant,%20MI&type=Historic+Great+Lakes+Water+Level+Data, accessed 13 June 2008.

2.4-261 Reeves, H.W, K.V. Wright, and J.R. Nicholas, “Hydrogeology and Simulation of Regional Ground-Water-Level Declines in Monroe County, Michigan,” U.S. Geological Survey Water-Resources Investigations Report 03-4312, 2004.

2.4-262 Detroit Edison, “Fermi Unit 2, Environmental Report,” Supplement 5, January 1979.

2.4-263 Fenneman, N.M., and D.W. Johnson, “Physical Divisions of the United States [Physiography],” U.S. Department of the Interior, Geological Survey, scale 1:7,000,000, 1946, http://water.usgs.gov/GIS/dsdl/physio.e00.gz, accessed 3 December 2007.

2.4-264 U.S. Geological Survey, “Groundwater Atlas of the United States,” Segment 9, Iowa, Michigan, Minnesota, Wisconsin. Hydrologic Investigations Atlas 730-J, Reston, VA, 1992.

2.4-265 Casey, G.D., "Hydrogeologic Framework of the Midwestern Basins and Arches Region in Parts of Indiana, Ohio, Michigan, and Illinois", U.S. Geological survey Professional paper 1423-B, 1996.

2.4-266 Bugliosi, E.F., "The Midwestern Basins and Arches Regional Aquifer System in Parts of Indiana, Ohio, Michigan, and Illinois; Summary", USGS Professional Paper 1423-A, 1999.

2.4-267 "Regional Ground-Water Flow and Geochemistry in the Midwest Basins and Arches Aquifer System in Parts of Indiana, Ohio, Michigan and Illinois", USGS Professional Paper 1423-C, 2000.

2.4-268 U.S. Environmental Protection Agency, “Designated Sole Source Aquifers in EPA Region 5,” http://www.epa.gov/safewater/sourcewater/pubs/qrg_ssamap_reg5.pdf, accessed 20 September 2007.

2.4-269 Bryan Municipal Utilities, City of Bryan, “City Submits Petition for Aquifer Protection,” (22 October 2007), http://www.cityofbryan.net/PR20071022.asp, accessed 16 November 2007.

2.4-270 United States Geological Survey, “Estimated Use of Water in the United States in 2000,” USGS Circular 1268, 2005.

2.4-271 U.S. Environmental Protection Agency, "Safe Drinking Water Information System," database last updated April 15, 2008, http://www.epa.gov/enviro/html/sdwis/sdwis_query.html, accessed 22 July 2008.

2.4-272 U.S. Environmental Protection Agency, “EPA Public Drink Water Systems: Facts and Figures,” 28 April 2006, http://www.epa.gov/safewater/pws/factoids.html, accessed 29 May 2008.

2.4-273 City of Milan, Michigan, “2006 City of Milan Annual Water Quality Report,” http://www.ci.milan.mi.us/public_works/Milan_Water_Quality_Report_2006.pdf, accessed 20 February 2008.

2.4-274 Department of Information Technology, Center for Geographic Information, “Michigan Geographic Data Library,”, Michigan Department of Environment Quality , State of Michigan (Well data generated 8 October 2007), http://www.mcgi.state.mi.us/mgdl/, accessed 11 October 2007.

2.4-275 Ohio Department of Natural Resources, “Water Well Log,” Ground Water Mapping and Technical Services, Division of Water, http://www.dnr.state.oh.us/water/maptechs/wellogs/appNEW/custom.aspx, accessed 20 September 2007.

2.4-276 Michigan Department of Environmental Quality, “Thermoelectric Power Generation Water Use Year 2000,” http://www.deq.state.mi.us/documents/deq-wd-wurp-TE2000.pdf, accessed 7 February 2008.

2.4-277 Nicholas, J. R.; G.L. Rowe, and J. R. Brannen, “Hydrology, Water Quality, and Effects of Drought in Monroe County, Michigan,” Water-Resources Investigations Report 94-4161, 1996.

2.4-278 U.S. Geological Survey, “National Water Information System - Groundwater Levels for Michigan,” http://nwis.waterdata.usgs.gov/mi/nwis/gwlevels, accessed 17 April 2008.

2.4-279 Weight, W.D., and J.L. Sonderegger, “Manual of Applied Field Hydrogeology,” Slug Testing, Chapter 11, McGraw-Hill, 2001.

2.4-280 HydroSOLVE, Inc., “Aqtesolv for Windows User’s Guide,” Reston, VA, July 24, 2000.

2.4-281 Zumberge, J.H., "Report on Pumping Test Analysis, PRDC Property, Monroe, Michigan,” unpublished, July 25, 1959.

2.4-282 Royle, M., “Standard Operating Procedures for Borehole Packer Testing.”

2.4-283 McDonald, M., and A. Harbaugh, “A Modular Three-Dimensional Finite-Difference Ground-Water Flow Model,” Techniques of Water-Resources Investigations of the United States Geological Survey, Book 6, Chapter A1, 1988.

2.4-284 Harbaugh, A.W., E.R. Banta, M.C. Hill, and M.G. McDonald, “MODFLOW-2000, The U.S. Geological Survey Modular Ground-Water Model – User Guide to Modularization Concepts and the Ground-Water Flow Processes,” U.S. Geological Survey Open-File Report 00-92, Reston, Virginia, 2000.

2.4-285 Brigham Young University Environmental Modeling Research Laboratory, “Groundwater Modeling System Tutorials,” Version 6.0, Vols. I, II, and III, October 20, 2005.

2.4-286 Dames & Moore, “Rock Foundation Treatment Residual Heat Removal Complex Fermi II Nuclear Power Plant for the Detroit Edison Company,” July 3, 1974.

2.4-287 Fetter, C.W., “Applied Hydrogeology,” Bell & Howell Co., Columbus, OH, 1980.

2.4-288 Driscoll F.G., “Groundwater and Wells,” 2nd Edition, Johnson (Well Screen) Division, St. Paul Minnesota, 1986.

2.4-289 Detroit Edison, “Fermi 2, Offsite Dose Calculation Manual,” Revision 14, 1999.

2.4-290 U.S. Nuclear Regulatory Commission, “Integrated Ground-Water Monitoring Strategy for NRC-Licensed Facilities and Sites: Logic, Strategic Approach and Discussion,” Advanced Environmental Solutions LLC for Division of Fuel, Engineering, and Radiological Research, Office of Nuclear Regulatory Research, NUREG/CR-6948, November 2007.

2.4-291 USGS Scientific Investigations Report 2004-5031,“Simulation of Ground-Water Flow, Surface Water Flow, and a Deep Sewer Tunnel System in the Menomonee Valley, Milwaukee, Wisconsin.”

2.4-292 Boulding, J.R. and Ginn, J.S., “Practical Handbook of Soil, Vadose Zone, and Ground-Water Contamination, Assessment and Prevention,” CRC Press, Boca Raton, Florida, 2004.

2.4-293 Electric Power Research Institute (EPRI), Estimation of Hydrodynamic Dispersivity in Selected Subsurface Materials, EPRI RP2485-05, EPRI, Palo Alto, California, 1994.

2.4-294 Midwest Regional Carbon Sequestration Partnership (MRCSP), Fact Sheet for Partnership Field Validation Test, Submitted by Battelle, dated November 2007. http://www.netl.doe.gov/publications/proceedings/07/rcsp/fac tsheets/17-MRCSP_Michigan%20Basin%20Geologic%20Test.pdf

2.4-295 CorpsMap, National Inventory of Dams, https://nid.usace.army.mil, accessed September 2, 2009.

2.4-296 Corps of Engineers Ice Jam Database https://rgis.crrel.usace.army.mil/apex/f?p=273:3:1818914186479561, accessed September 2, 2009.

2.4-297 US Department of Commerce Weather Bureau, “TP 25 Rainfall Intensity – Duration – Frequency Curves for Selected Stations in the United States, Alaska, Hawaiian Islands, and Puerto Rico.”

2.4-298 US Department of Agriculture, “Urban Hydrology for Small Watersheds,” Technical Release 55, June 1986.

2.4-299 Michigan DEQ Surface Water Quality Division. “Guidebook of Best Management Practices for Michigan Watersheds,” Reprinted October 1, 1998.

2.4-300 Federal Emergency Management Agency. Flood Insurance Study Monroe County, Michigan. April 20, 2000.

2.4-301 NOAA, “Application of Probable Maximum Precipitation Estimates-United States East of the 105th Meridian” Hydrometeorological Report No. 52, August 1982.

2.4-302 US Army Corps of Engineers Hydrologic Engineering Standard, “Probable Maximum Storm, HMR 52 User’s Manual” March 1984.

2.4-303 U.S. Army Corps of Engineers, “Runoff from Snowmelt. EM 1110-2-1406” March 1998.

2.4-304 NOAA, “Probable Maximum Precipitation Estimates, United States East of the 105th Meridian” Hydrometeorological Report No. 51, June 1978

2.4-305 US Army Corps of Engineers Hydrologic Engineering Standard, “Probable Maximum Storm, HMR 51 User’s Manual” March 1984.

2.4-306 US Department of Commerce Weather Bureau, Technical Paper No. 40, Rainfall Frequency Atlas of the United States for Duration from 30 minutes to 24 hours and return periods from 1 to 100 years. May 1961.

2.4-307 Corps of Engineers Ice Jam Database https://rgis.crrel.usace.army.mil/apex/f?p=273:3:1818914186479561, accessed September 2, 2009.

2.4-308 Federal Emergency Management Agency. Flood Insurance Study Monroe County, Michigan. April 20, 2000.

2.4-309 CorpsMap, National Inventory of Dams, https://nid.usace.army.mil, accessed September 2, 2009.

2.4-310 National Geophysical Data Center Historical Tsunami Record, National Oceanic and Atmospheric Administration, Website: http:www.ngdc.noaa.gov/hazard/hazards.shtml

2.4-311 Prickett, T. A., 1965. Type-Curve solution to Aquifer Tests Under Water-Table Conditions. Ground Water, Vol. 3, No. 3, pp. 5-14.

2.4-312 Neuman, S. P., 1979. Perspective on “Delayed Yield”. Water Resources Research, Vol. 15, pp. 899-908.

2.4-313 Moench, A. F., 1993. Computation of Type Curves for Flow to Partially Penetrating Wells in Water-Table Aquifers. Ground Water, Vol. 31, No. 6, pp. 966-971.

2.4-314 Platzman, G.W. “The Prediction of Surges in the Southern Basin of Lake Michigan. Part I. “The Dynamical Basis for Prediction,” Monthly Weather Review, vol 93, No. 5, May 1965, pp. 275-281.

2.4-315 Donn, W.L., “The Great Lakes Storm Surge of May 5, 1952,” Journal of Geophysical Research, vol 64, No. 2 Feb. 1959, pp. 191-198.

2.4-316 NOAA Great Lakes Environmental Research Laboratory, http://www.glerl.noaa.gov/data/char/bathymetry.html, accessed 21 January 2010.

2.4-317 International Journal of Rock Mechanics and Mining Sciences 36 (1999) 581-596, Liu, J.; et al., “Linking stress-Dependent Effective Porosity and Hydraulic Conductivity Fields to RMR,” Accepted March 13, 1999.

2.4-318 2.4-316 Rock Mechanics and Rock Engineering, (2000) 33 (2), 75-92, Liu, J.; et al., “Strain-dependent Fluid Flow Defined Through Rock Mass Classification Schemes.”

2.4-319 2.4-317 Federal Guidance Report No. 12 (FGR 12), “External Exposure to Radionuclides in Air, Water and Soil,” 1993.

2.4-320 2.4-318 “Groundwater Transport: Handbook of Mathematical Models, Water Resources Monograph 10,” Javandel, I., Doughty, C. and Tsang, C.F., American Geophysical Union, 1984.

2.4-321 2.4-319 “Computer Model of Two-Dimensional Solute Transport and Dispersion in Ground Water,” Chapter C2, Book 7, Techniques of Water-Resources Investigations of the United States Geological Survey, Konikow, L. F., and Bredehoeft, J. D., 1978.

2.4-322 2.4-320 “Residual Radioactive Contamination from Decommissioning,” NUREG/CR-5512, Volume 1, Kennedy, W.E and Strenge, D.L., Pacific Northwest Laboratory, October, 1992.

2.4-323 2.4-321 Cleary, R.W., and M.J. Ungs, Groundwater Pollution and Hydrology, Mathematical Models and Computer Programs, Report 78-WR-15, Water Resources Program, Princeton University, Princeton, NJ, 1978.

Table 2.4-201 2004 Water Usage - Withdrawal and Consumptive Uses for Lake Erie

Units: Mgal (US)/d

BASIN REPORT – Lake Erie **Basin Total** **Year of Data: 2004**

Total Report – All Facilities

Category	Withdrawls				Diversions		Consumptive Use
	GLSW	OSW	GW	TOTAL	Intrabasin	Interbasin	
Public Supply	1105.82	263.00	152.30	1521.12	0.00	-1.41	200.22
Domestic Supply	12.33	0.00	96.41	108.74	0.00	0.00	15.02
Irrigation	1.42	38.41	32.16	71.99	0.00	0.00	36.14
Livestock	1.56	5.06	27.60	34.23	0.00	0.00	17.23
Industrial	698.31	123.05	61.05	882.42	0.00	0.00	107.41
Fossil Fuel Power	7147.98	831.49	0.43	7979.90	0.00	0.00	94.49
Nuclear Power	202.90	0.00	0.00	202.90	0.00	0.00	16.02
Hydroelectric Power	47,372.00	0.00	0.00	47,372.00	0.00	0.00	0.00
Other	0.68	9.11	0.50	10.29	5816.39	-10.10	0.00

The totals represent withdrawals and consumption for the state of Indiana, Michigan, New York, Ohio, Pennsylvania, and the province of Ontario, Canada

Consumptive use: that portion of water withdrawn or withheld from the Great Lakes basin and assumed to be lost or otherwise not returned to the Great Lakes basin due to evapotranspiration, incorporation into products, or other processes

Great Lakes surface water (GLSW): the Great Lakes, their connecting channels(the St. Clair River, the Detroit River, the Niagara River and the St. Marys River), and the St. Lawrence River

Groundwater (GW): all subsurface water

Other surface water (OSW): tributary streams, lakes, ponds, and reservoirs within the Great Lakes basin

Interbasin diversion (positive): water transferred from the Great Lakes basin into another watershed

Interbasin diversion (negative): water transferred from another watershed into the Great Lakes basin

Intrabasin diversion (positive): water transferred out of one Great Lakes watershed into another

Intrabasin diversion (negative): water transferred into of one Great Lakes watershed into from another

Source: Reference 2.4-209

Table 2.4-202 2003 Summary Report and 2002 Basin Report for Lake Erie Water Usage

Units: Mgal (US)/d

SUMMARY REPORT – GREAT LAKES BASIN Year of Data: 2003

Water-Use by Basin – All Facilities

Basin	Withdrawls				Diversions		Consumptive Use
	GLSW	OSW	GW	TOTAL	Intrabasin	Interbasin	
Lake Superior	1145.13	41,942.74	30.87	43,118.74	0.00	-4007.75	78.32
Lake Michigan	9822.82	2241.64	691.47	12,755.92	0.00	1230.62	651.13
Lake Huron	25,958.52	13731.15	94.10	39,783.77	47.97	0.00	141.48
Lake Erie	49,440.31	1105.33	376.11	50,921.74	5816.39	-14.41	495.47
Lake Ontario	42,645.22	89,483.54	188.37	13,2317.13	-5802.39	40.77	351.51
St. Lawrence River	32,1257.25	232,485.48	141.16	553,883.88	0.00	0.00	194.83
Total:	450,269.24	380,989.88	1522.08	832,781.19	61.97	-2750.78	1912.74

Units: Mgal (US)/d

BASIN REPORT – Lake Erie Basin Total Year of Data: 2002

Total Report – All Facilities

Category	Withdrawls				Diversions		Consumptive Use
	GLSW	OSW	GW	TOTAL	Intrabasin	Interbasin	
Public Supply	1204.70	264.38	167.26	1636.34	0.00	-0.53	215.25
Domestic Supply	12.33	0.00	95.93	108.26	0.00	0.00	14.97
Irrigation	1.80	42.98	37.20	81.98	0.00	0.00	45.15
Livestock	1.56	2.87	26.41	30.84	0.00	0.00	14.52
Industrial	726.22	107.01	62.81	896.03	0.00	0.00	108.55
Fossil Fuel Power	7312.13	702.15	0.41	8014.69	0.00	0.00	94.00
Nuclear Power	156.70	0.00	0.00	156.70	0.00	0.00	11.30
Hydroelectric Power	44,522.00	0.00	0.00	44,522.00	0.00	0.00	0.00
Other	0.80	4.08	0.30	5.18	5105.39	-11.35	0.00

Source: Reference 2.4-210, Reference 2.4-211

Table 2.4-203 2001 and 2000 Basin Water Usage Report for Lake Erie

BASIN REPORT – Lake Erie	Basin Total	Units: Mgal (US)/d Year of Data: 2001

Total Report – All Facilities

Category	Withdrawls				Diversions		Consumptive Use
	GLSW	OSW	GW	TOTAL	Intrabasin	Interbasin	
Public Supply	1227.57	293.80	153.31	1674.67	0.00	-0.64	219.57
Domestic Supply	12.33	0.00	96.40	108.73	0.00	0.00	15.03
Irrigation	1.61	39.75	33.25	74.61	0.00	0.00	38.58
Livestock	1.56	2.80	26.59	30.95	0.00	0.00	14.62
Industrial	805.54	134.39	66.86	1006.78	0.00	0.00	130.93
Fossil Fuel Power	7149.60	670.89	0.42	7820.91	0.00	0.00	92.53
Nuclear Power	180.11	0.00	0.00	180.11	0.00	0.00	13.83
Hydroelectric Power	38407.00	0.00	0.00	38407.00	0.00	0.00	0.00
Other	0.82	9.10	2.72	12.64	5105.39	-9.61	0.00

BASIN REPORT – Lake Erie	Basin Total	Units: Mgal (US)/d Year of Data: 2000

Total Report – All Facilities

Category	Withdrawls				Diversions		Consumptive Use
	GLSW	OSW	GW	TOTAL	Intrabasin	Interbasin	
Public Supply	1188.85	286.18	150.11	1625.13	0.00	-0.57	213.87
Domestic Supply	12.70	2.39	96.74	111.83	0.00	0.00	15.51
Irrigation	1.09	32.73	32.52	66.34	0.00	0.00	31.04
Livestock	1.56	3.83	27.62	33.01	0.00	0.00	16.27
Industrial	802.04	139.65	79.08	1020.77	0.00	0.00	135.01
Fossil Fuel Power	7883.59	6.37	0.34	7890.30	0.00	0.00	94.10
Nuclear Power	178.96	0.00	0.00	178.96	0.00	0.00	20.64
Hydroelectric Power	40386.00	0.00	0.00	40386.00	0.00	0.00	0.00
Other	0.04	2.98	0.10	3.12	5105.39	-9.88	0.00

Source: Reference 2.4-212, Reference 2.4-213

Table 2.4-204 1999 and 1998 Basin Water Usage Report for Lake Erie

BASIN REPORT – Lake Erie **Basin Totals** **Units: Mgal (US)/d** **Year of Data: 1999**

Total Report – All Facilities

Category	Withdr	Diver	Consum	GLSW	OSW	GW	Intrabasin	Interbasin
Public Supply	1687.85	-0.56	221.87	1263.22	277.15	147.48	0.00	-0.56
Domestic Supply	111.22	0.00	15.42	12.70	2.41	96.11	0.00	0.00
Irrigation	76.72	0.00	65.44	1.42	42.11	33.19	0.00	0.00
Livestock	32.73	0.00	27.72	1.56	3.88	27.28	0.00	0.00
Industrial	1001.25	0.00	135.73	806.34	136.39	58.52	0.00	0.00
Fossil Fuel Power	9912.83	0.00	115.73	9906.74	5.75	0.34	0.00	0.00
Nuclear Power	178.31	0.00	20.50	178.31	0.00	0.00	0.00	0.00
Hydroelectric Power	43369.00	0.00	0.00	43369.00	0.00	0.00	0.00	0.00
Other	3.79	-10.05	0.00	0.12	3.58	0.09	4252.88	-10.05

BASIN REPORT – Lake Erie **Basin Totals** **Units: Mgal (US)/d** **Year of Data: 1998**

Total Report – All Facilities

Category	Withdr	Diver	Consum	GLSW	OSW	GW	Intrabasin	Interbasin
Public Supply	1781.16	-38.63	236.15	1354.45	258.73	167.97	-38.07	-0.56
Domestic Supply	104.81	0.00	14.48	12.33	0.00	92.48	0.00	0.00
Irrigation	64.13	0.00	54.77	0.68	49.10	14.35	0.00	0.00
Livestock	31.71	0.00	25.79	1.54	2.08	28.09	0.00	0.00
Industrial	1055.56	0.00	140.37	827.46	157.96	70.14	0.00	0.00
Fossil Fuel Power	9990.54	0.00	97.73	9983.79	6.46	0.29	0.00	0.00
Nuclear Power	172.36	0.00	21.91	172.36	0.00	0.00	0.00	0.00
Hydroelectric Power	57849.00	0.00	0.00	57849.00	0.00	0.00	0.00	0.00
Other	5.12	5702.07	0.00	1.16	3.41	0.55	5711.25	-9.18

Source: Reference 2.4-214, Reference 2.4-215

Table 2.4-205 Monroe County Water Usage (2000 – 2006) (Sheet 1 of 2)

Monroe County Water Use	2006	Water Withdrawn (MGD)		
	Great Lakes	Surface-Water	Groundwater	Total
Thermoelectric Power	1752.55	0.00	0.11	1752.66
Public Water Supply	13.02	0.72	0.12	13.86
Agricultural Irrigation	0.00	2.51	0.88	3.40
Monroe County Water Use	**2005**	**Water Withdrawn (MGD)**		
	Great Lakes	**Surface-Water**	**Groundwater**	**Total**
Thermoelectric Power	1808.34	0.00	0.09	1808.43
Public Water Supply	13.90	0.00	0.87	14.77
Agricultural Irrigation	0.00	2.45	0.86	3.31
Monroe County Water Use	**2004**	**Water Withdrawn (MGD)**		
	Great Lakes	**Surface-Water**	**Groundwater**	**Total**
Thermoelectric Power	1755.42	0.00	0.08	1755.49
Public Water Supply	12.64	0.65	0.17	13.46
Agricultural Irrigation	0.00	2.46	0.86	3.33
Self-Supply Industrial	0.00	1.36	8.63	9.99
Golf Course Irrigation	0.00	0.03	0.72	0.75
Monroe County Water Use	**2003**	**Water Withdrawn (MGD)**		
	Great Lakes	**Surface-Water**	**Groundwater**	**Total**
Thermoelectric Power	1750.36	0.00	0.08	1750.44
Public Water Supply	12.04	0.57	0.20	12.81
Agricultural Irrigation	0.00	2.21	0.77	2.98
Self-Supply Industrial	0.00	1.86	7.73	9.59
Golf Course Irrigation	0.00	0.13	0.59	0.71
Monroe County Water Use	**2002**	**Water Withdrawn (MGD)**		
	Great Lakes	**Surface-Water**	**Groundwater**	**Total**
Thermoelectric Power	1701.42	0.00	0.09	1701.51
Public Water Supply	11.96	0.64	0.21	12.81
Agricultural Irrigation	0.00	3.22	1.13	4.35
Self-Supply Industrial	0.00	1.31	15.69	17.00
Golf Course Irrigation	0.00	0.37	0.37	0.74

Table 2.4-205 Monroe County Water Usage (2000 – 2006) (Sheet 2 of 2)

Monroe County Water Use	2001	Water Withdrawn (MGD)		
	Great Lakes	Surface-Water	Groundwater	Total
Thermoelectric Power	1711.61	0.00	0.09	1711.70
Public Water Supply	11.65	0.71	0.23	12.59
Agricultural Irrigation	0.00	2.51	0.88	3.40
Self-Supply Industrial	0.00	1.67	14.33	16.00
Golf Course Irrigation	0.00	0.35	0.37	0.72

Monroe County Water Use	2000	Water Withdrawn (MGD)		
	Great Lakes	Surface-Water	Groundwater	Total
Thermoelectric Power	1697.08	0.00	0.07	1697.16
Public Water Supply	11.81	0.68	0.23	12.73
Agricultural Irrigation	0.00	1.58	0.55	2.13
Self-Supply Industrial	0.00	1.78	15.65	17.42
Golf Course Irrigation	0.00	0.40	0.29	0.69

MGD = million gallons per day

Source: Reference 2.4-216

Table 2.4-206 2005 Monroe County Report

Industrial	Facility Name	Groundwater Use (Mgal)	Surface-Water Use (Mgal)	Great Lakes Use (Mgal)
Holcim (US) Inc.	Dundee Plant		286.7	
Stoneco	Denniston Quarry	155.58		
Sylvania Minerals		3073.88		

Golf Course Irrigation	Facility Name	Groundwater Use (Mgal)	Surface-Water Use (Mgal)	Great Lakes Use (Mgal)
Carleton Glen Golf Club			21	
Wyndridge Oaks Golf Course		8.091841		

Thermoelectric Power Generation	Facility Name	Groundwater Use (Mgal)	Surface-Water Use (Mgal)	Great Lakes Use (Mgal)
Consumers Energy Company	J R Whiting	32.29		77,440
Detroit Edison Company	Monroe			572,846
Detroit Edison Company	Fermi 2			18,756

Mgal = million gallons

Source: Reference 2.4-221

Table 2.4-207 2006 Monroe County Report

Industrial	Facility Name	Groundwater Use (Mgal)	Surface-Water Use (Mgal)	Great Lakes Use (Mgal)
Holcim (US) Inc.	Dundee Plant		286.9	
Stoneco	Maybee Quarry	442.66		
Stoneco	Newport Quarry	222.65		
Stoneco	Ottawa Lake Quarry	1024.78		
Stoneco	Denniston Quarry	109.13		
Sylvania Minerals		4131.64		
Tenneco Inc.		17		

Golf Course Irrigation	Facility Name	Groundwater Use (Mgal)	Surface-Water Use (Mgal)	Great Lakes Use (Mgal)
Carleton Glen Golf Club			30.412	
Deme Acres Golf Course		6.55017		
Green Meadows Golf Course Inc.		13.187718		
Maple Grove Golf Course		25.037445		
Monroe Golf & Country Club		12.688		
Raisin River Golf Club		15.69		
Sandy Creek Golf Course		33.9		
Whiteford Valley Golf Course		43.55		

Thermoelectric Power Generation	Facility Name	Groundwater Use (Mgal)	Surface-Water Use (Mgal)	Great Lakes Use (Mgal)
Consumers Energy Company	J R Whiting	39.02		81,490
Detroit Edison Company	Monroe			540,283
Detroit Edison Company	Fermi 2			17,906

Mgal = million gallons

Source: Reference 2.4-222

Table 2.4-208 2006 Monroe County Water Capacity Report

Industrial	Facility Name	Groundwater Capacity	Units	Surface-Water Capacity	Units	Great Lakes Capacity	Units
Holcim (US) Inc.	Dundee Plant			0.585	MGD		
Stoneco	Maybee Quarry	11.52	MGD				
Stoneco	Newport Quarry	9.36	MGD				
Stoneco	Ottawa Lake Quarry	23.88	MGD				
Stoneco	Denniston Quarry	16.74	MGD				
Sylvania Minerals		30.53	MGD				
Tenneco Inc.		200	GPM				
Golf Course Irrigation	**Facility Name**	**Groundwater Capacity**	**Units**	**Surface-Water Capacity**	**Units**	**Great Lakes Capacity**	**Units**
Carleton Glen Golf Club				275	GPM		
Deme Acres Golf Course		155	GPM				
Green Meadows Golf Course Inc.		850	GPM				
Maple Grove Golf Course		600	GPM				
Monroe Golf & Country Club		800	GPM				
Raisin River Golf Club		875	GPM				
Sandy Creek Golf Course		600	GPM				
Whiteford Valley Golf Course		750	GPM				
Thermoelectric Power Generation	**Facility Name**	**Groundwater Capacity**	**Units**	**Surface-Water Capacity**	**Units**	**Great Lakes Capacity**	**Units**
Consumers Energy Company	J R Whiting	0.864	MGD			325	MGD
Detroit Edison Company	Monroe					2,056	MGD
Detroit Edison Company	Fermi 2					45	MGD

MGD = million gallons per day

GPM = gallons per minute

Source: Reference 2.4-222

Table 2.4-209 Net Basin Supply for Lake Erie

Yearly Lake Erie Net Basin Supply Averaged from 1948-2005

Component Method using overland precipitation depth (precipitation + runoff - evaporation) (m^3/sec)

Jan	Feb	Mar	Apr	May	Jun	Jul	Aug	Sep	Oct	Nov	Dec
1053	1366	1885	1962	1360	994	418	-92	-516	-755	-78	560
								Mean Total per year (m^3/sec)			676
								Total Volume per year (m^3)			2.13E+10
								Total Volume per year(ft^3)			7.53E+11
					(Bgal) = Billion gallons			Total Volume per year(Bgal)			5631

Yearly Lake Erie Net Basin Supply Averaged from 1948-2005

Component Method using overlake precipitation depth (precipitation + runoff - evaporation) (m^3/sec)

Jan	Feb	Mar	Apr	May	Jun	Jul	Aug	Sep	Oct	Nov	Dec
1080	1380	1900	1954	1293	926	322	-86	-460	-706	-18	607
								Mean Total per year (m^3/sec)			678
								Total Volume per year (m^3)			2.13E+10
								Total Volume per year(ft^3)			7.55E+11
					(Bgal) = Billion gallons			Total Volume per year(Bgal)			5648

Yearly Inflow for Lake Erie for 2005(Detroit River via Upper Great Lakes and Tributaries) (expressed as m^3/sec)

Jan	Feb	Mar	Apr	May	Jun	Jul	Aug	Sep	Oct	Nov	Dec
4730	4800	4900	5090	5010	5050	5080	5000	4920	4900	4810	4810
								Mean Total per year (m^3/sec)			4925
								Total Volume per year (m^3)			1.55E+11
								Total Volume per year(ft^3)			5.48E+12
					(Bgal) = Billion gallons			Total Volume per year(Bgal)			41030

Net Total Supply (Bgal) = Net Basin Supply + Inflow	46661

Source: Reference 2.4-204

Table 2.4-210 Extreme Lake Levels for the Western Basin of Lake Erie at the Fermi Site (ID 9063090) (Sheet 1 of 2)

	NAVD 88		IGLD 85	
Year	Max (ft)	Min (ft)	Max (ft)	Min (ft)
*1967		563.90		563.64
1970	574.04	567.63	573.78	567.37
1971	574.15	565.98	573.89	565.72
1972	575.80	565.96	575.54	565.70
1973	576.73	569.18	576.47	568.92
1974	576.60	569.38	576.34	569.12
1975	576.21	567.23	575.95	566.97
1976	575.74	569.52	575.48	569.26
1977	575.06	567.24	574.80	566.98
1978	574.71	567.05	574.45	566.79
1979	574.87	564.26	574.61	564.00
1980	576.13	567.66	575.87	567.40
1981	574.31	568.47	574.05	568.21
1982	575.62	566.66	575.36	566.40
1983	575.50	569.50	575.24	569.24
1984	575.50	569.39	575.24	569.13
1985	576.73	567.64	576.47	567.38
1986	576.61	570.42	576.35	570.16
1987	576.30	566.83	576.04	566.57
1988	574.23	568.19	573.97	567.93
1989	574.29	567.15	574.03	566.89
1990	575.60	567.37	575.34	567.11
1991	574.90	565.96	574.64	565.70
1992	574.65	567.89	574.39	567.63
1993	575.13	568.81	574.87	568.55
1994	574.45	567.37	574.19	567.11
1995	574.67	567.75	574.41	567.49
1996	574.61	566.56	574.35	566.30
1997	575.59	569.33	575.33	569.07
1998	576.48	566.62	576.22	566.36
1999	574.45	567.63	574.19	567.37

Table 2.4-210 Extreme Lake Levels for the Western Basin of Lake Erie at the Fermi Site (ID 9063090) (Sheet 2 of 2)

	NAVD 88		IGLD 85	
Year	Max (ft)	Min (ft)	Max (ft)	Min (ft)
2000	573.58	565.99	573.32	565.73
2001	572.85	565.86	572.59	565.60
2002	573.41	564.92	573.15	564.66
2003	573.70	564.45	573.44	564.19
2004	573.47	567.43	573.21	567.17
2005	574.07	566.80	573.81	566.54
2006	573.89	565.75	573.63	565.49
2007	573.73	566.56	573.47	566.30

* The lowest elevation recorded was noted on a Nuclear Generation Memorandum NP-00-0064 dated August 16, 2000. Elevation has been confirmed by NOAA on 02/07/2008

Source: Reference 2.4-228, Reference 2.4-234

Table 2.4-211 Local Intense PMP Depth Duration

Duration (minutes)	1-Hour Multiplier	PMP Depth (inches)
60	1.000	17.3
30	0.762	13.2
15	0.530	9.2
5	0.337	5.8

Table 2.4-212 Discharge (Q) from Existing Locations Calculated with the Rational Method

DRAINAGE TO POND 1 (OVER LAND)				
Drainage Areas	**Q_{10}**	**Q_{25}**	**Q_{50}**	**Q_{100}**
Area 1	0.45	0.60	0.64	0.74
Area 2	5.76	6.62	7.56	8.50
Area 3	4.95	6.12	6.88	7.56
Area 4	1.51	1.84	1.99	2.38
Area 5	1.53	1.84	2.06	2.26
Area 6	5.06	5.98	6.67	7.36
Area 10	2.13	2.73	3.07	3.41
Area 11	2.20	2.58	2.95	3.33
Total Q =	**23.59**	**28.30**	**31.82**	**35.54**
DRAINAGE TO STAGNANT POND (OVER LAND)				
Drainage Areas	**Q_{10}**	**Q_{25}**	**Q_{50}**	**Q_{100}**
Area 7	10.47	12.08	12.88	14.49
Area 12	1.62	1.90	2.17	2.45
Area 21	3.62	4.18	4.46	5.02
Area 23	5.65	6.78	7.80	8.36
Total Q =	**21.36**	**24.93**	**27.31**	**30.32**
DRAINAGE THROUGH INLETS				
Drainage Areas	**Q_{10}**	**Q_{25}**	**Q_{50}**	**Q_{100}**
Area 8	28.73	34.88	38.48	42.32
Area 9	10.77	12.66	14.18	15.12
Area 13	4.80	5.63	6.08	6.83
Area 14	4.86	5.70	6.16	6.92
Area 15	2.62	3.08	3.32	3.73
Area 16	3.52	4.13	4.46	5.01
Area 17	6.66	7.80	8.42	9.46
Area 18	5.59	6.45	6.88	7.74
Area 19	2.50	2.93	3.16	3.55
Area 20	6.78	7.95	8.59	9.65
Area 22	9.33	11.02	12.72	13.57
Total Q =	**86.16**	**102.22**	**112.43**	**123.89**

Note: Inlets discharge through main outfall, existing underground 96-inch overflow canal and north to pond.
Q is storm runoff flow-rate with values are listed in cfs

Table 2.4-213 Discharge (Q) from Final Grade Locations Calculated with the Rational Method

From Detroit, Michigan Rainfall-Intensity Curves

C = Dimensionless coefficient of discharge

A (acres) = Area

T_t (min) = Time of concentration

I_{10} (in/hr) = 10-year storm intensity

I_{25} (in/hr) = 25-year storm intensity

I_{50} (in/hr) = 50-year storm intensity

I_{100} (in/hr) = 100-year storm intensity

Q (cfs) = Storm runoff flow

Section	C	A	T_t	I_{10}	I_{25}	I_{50}	I_{100}	Q_{10}	Q_{25}	Q_{50}	Q_{100}
S1	1	4.48	6.50	6.00	7.00	8.00	8.90	26.88	31.36	35.84	39.84
S2	1	4.60	9	5.40	6.50	7.10	8.00	24.87	29.93	32.69	36.84
S3	1	4.38	8.33	5.50	6.60	7.50	8.00	24.08	28.89	32.83	35.02
N1	1	3.98	7.7	5.60	6.80	7.50	8.25	22.29	27.06	29.85	32.84
N2	1	1.32	5.49	6.50	7.50	8.00	9.00	8.58	9.90	10.56	11.88
N3	1	25.96	20.22	3.75	4.50	5.00	5.50	97.35	116.82	129.80	142.78

Source: Reference 2.4-297

Total Discharges

Destination	Q_{10}	Q_{25}	Q_{50}	Q_{100}
North Outfall (S1, S2, S3, N1, N2)	106.70	127.14	141.77	156.45
NW Sump (N3)	97.35	116.82	129.80	142.78
Total	204.05	243.96	271.57	299.23

Table 2.4-214 Existing Site and Final Grade Runoff Comparison

	Total Discharges			
	Q_{10}	Q_{25}	Q_{50}	Q_{100}
Existing	131.11	155.45	171.56	189.75
Final Grade	204.05	243.96	271.57	299.23
Additional Runoff	72.94 (55.6%)	88.51 (56.9%)	100.01 (58.3%)	109.48 (57.7%)

Q is storm runoff flow-rate with values of cubic feet per second (cfs)

Table 2.4-215 Swan Creek Flow Characteristics

Month	50% Exceedence Flow (cfs)	95% Exceedence Flow (cfs)	Mean Monthly Flow (cfs)
Jan	12	2.8	30
Feb	19	2.7	65
Mar	82	18	140
Apr	70	20	120
May	32	6.1	72
Jun	11	2.4	27
Jul	2.8	0	16
Aug	3.2	0	6
Sep	3.2	0	6.6
Oct	8.6	1	20
Nov	13	2.9	32
Dec	17	2.8	46

Source: Reference 2.4-266

Table 2.4-216 Swan Creek Watershed Incremental PMP Depths for the 72-Hour Storm

6 Hour Time Increment	Incremental PMP Depth (inches)
1	21.41
2	3.4
3	1.19
4	1.21
5	0.61
6	0.63
7	0.63
8	0.58
9	0.47
10	0.43
11	0.43
12	0.38

Storm Duration (hours)	Total PMP Depth (inches)
6	21.41
12	24.81
18	26.00
24	27.21
30	27.82
36	28.45
42	29.08
48	29.66
54	30.13
60	30.56
66	30.99
72	31.37

Source: Reference 2.4-235, Reference 2.4-236

Table 2.4-217 PMP Temporal Distribution

Time (hours)	6 Hour Time Increment	Incremental PMP Depth (inches)
0 to 6	12	0.4
6 to 12	10	0.4
12 to 18	11	0.4
18 to 24	9	0.5
24 to 30	4	1.2
30 to 36	2	3.4
36 to 42	1	21.4
42 to 48	3	1.2
48 to 54	6	0.6
54 to 60	7	0.6
60 to 66	5	0.6
66 to 72	8	0.6

Table 2.4-218 NRCS Dimensionless Unit Hydrograph Ordinates

Time ratio, t/t_p	Discharge ratio, q/q_p	Mass curve ratio, Q_a/Q
0	0.000	0.000
0.1	0.030	0.001
0.2	0.100	0.006
0.3	0.190	0.012
0.4	0.310	0.035
0.5	0.470	0.065
0.6	0.660	0.107
0.7	0.820	0.163
0.8	0.930	0.228
0.9	0.990	0.300
1.0	1.000	0.375
1.1	0.990	0.450
1.2	0.930	0.522
1.3	0.860	0.589
1.4	0.780	0.650
1.5	0.680	0.700
1.6	0.560	0.751
1.7	0.460	0.790
1.8	0.390	0.822
1.9	0.330	0.849
2.0	0.280	0.871
2.2	0.207	0.908
2.4	0.147	0.934
2.6	0.107	0.953
2.8	0.077	0.967
3.0	0.055	0.977
3.2	0.040	0.984
3.4	0.029	0.989
3.6	0.021	0.993
3.8	0.015	0.995
4.0	0.011	0.997
4.5	0.005	0.999

Source: Reference 2.4-238

Table 2.4-219 Summary of Results for Alternative II - PMF

Reach	River Station	Profile	Q Total (cfs)	Min Ch El (ft)	W.S. Elev (ft)	Crit W.S. (ft)	E.G. Elev (ft)	E.G. Slope (ft/ft)	Vel Ch (ft/s)	Flow Area (sq ft)	Top Width (ft)	Froude # Chl
Lower	11183.750	PMF	113200	571.44	584.92		585.21	0.00109	4.01	26629.2	5354.7	0.21
Lower	10494.990	PMF	113200	571.44	583.70		584.21	0.00218	5.57	19960.0	4908.8	0.30
Lower	7638.755	PMF	113200	571.44	581.16		581.37	0.00061	2.57	33040.8	7411.7	0.15
Lower	6964.589	PMF	113200	571.44	580.80		581.00	0.00058	2.53	33456.9	6896.7	0.15
Lower	5464.923	PMF	113200	571.43	580.02		580.19	0.00046	2.16	36615.4	7411.9	0.13
Lower	3964.480	PMF	113200	571.44	579.68		579.75	0.00016	1.26	54248.9	9514.8	0.08
Lower	1936.913	PMF	113200	570.86	579.15		579.30	0.00028	1.58	43181.5	6524.5	0.10
Lower	530.7749	PMF	113200	571.41	578.59	574.9	578.73	0.00070	2.24	42550.6	7550.4	0.16

Table 2.4-220 Summary of Results for Alternative I – 500-Year Flood

Reach	River Station	Profile	Q Total (cfs)	Min Ch El (ft)	W.S. Elev (ft)	Crit W.S. (ft)	E.G. Elev (ft)	E.G. Slope (ft/ft)	Vel Ch (ft/s)	Flow Area (sq ft)	Top Width (ft)	Froude # Ch
Lower	11183.750	Q500	5000	571.44	579.50		579.51	0.000076	0.75	6686.1	1040.3	0.05
Lower	10494.990	Q500	5000	571.44	579.42		579.44	0.000147	1.03	4901.3	890.8	0.07
Lower	7638.755	Q500	5000	571.44	579.40		579.40	0.000005	0.19	20424.8	5378.9	0.01
Lower	6964.589	Q500	5000	571.44	579.40		579.40	0.000003	0.17	23787.7	6196.8	0.01
Lower	5464.923	Q500	5000	571.43	579.39		579.39	0.000001	0.11	31970.0	7333.5	0.01
Lower	3964.480	Q500	5000	571.44	579.39		579.39	0	0.06	51528.2	9514.8	0
Lower	1936.913	Q500	5000	570.86	579.39		579.39	0	0.07	44727.1	6525.6	0
Lower	530.7749	Q500	5000	571.41	579.39	572.54	579.39	0.000001	0.08	48592.0	7553.2	0.01

Table 2.4-221 Summary of Results for Alternative III – Probable Maximum Surge and Seiche

Reach	River Station	Profile	Q Total (cfs)	Min Ch El (ft)	W.S. Elev (ft)	Crit W.S. (ft)	E.G. Elev (ft)	E.G. Slope (ft/ft)	Vel Ch (ft/s)	Flow Area (sq ft)	Top Width (ft)	Froude # Ch
Lower	11183.750	Surge	3100	571.44	585.43		585.43	0.000001	0.10	29400.1	5486.5	0.01
Lower	10494.990	Surge	3100	571.44	585.43		585.43	0.000001	0.09	28865.1	5264.0	0
Lower	7638.755	Surge	3100	571.44	585.43		585.43	0	0.03	64710.1	7411.7	0
Lower	6964.589	Surge	3100	571.44	585.43		585.43	0	0.03	65374.9	6896.7	0
Lower	5464.923	Surge	3100	571.43	585.43		585.43	0	0.02	76715.0	7411.9	0
Lower	3964.480	Surge	3100	571.44	585.43		585.43	0	0.02	108980.7	9514.8	0
Lower	1936.913	Surge	3100	570.86	585.43		585.43	0	0.02	96091.8	9641.7	0
Lower	530.7749	Surge	3100	571.41	585.43	572.21	585.43	0	0.02	101365.3	9418.9	0

Table 2.4-222 Lake Erie - Possible Storm Induced Lake Level Increases (Ft)

Month	20%	10%	3%	2%	1%
January	2.20	2.50	3.00	3.30	3.60
February	1.90	2.20	2.70	3.00	3.30
March	2.20	2.50	2.80	3.00	3.20
April	2.10	2.50	3.00	3.30	3.70
May	1.40	1.70	2.00	2.30	2.50
June	1.30	1.50	1.90	2.10	2.40
July	1.10	1.30	1.50	1.60	1.80
August	1.10	1.30	1.40	1.50	1.60
September	1.40	1.70	2.00	2.20	2.40
October	1.80	2.10	2.40	2.70	2.90
November	2.00	2.30	2.60	2.80	3.00
December	2.30	2.70	3.20	3.60	4.00

Source: Reference 2.4-245

Table 2.4-223 Wavelengths for Various Points in the Lake

Location	Depth		Wave Length	
	(m)	(ft)	(m)	(ft)
Deepwater			192	630
STWAVE point	5.85	19.2	81.4	267
Seawall	4.85	15.9	74.6	245
Onshore	1.11	3.65	36.2	119

Table 2.4-224 Breaking Wave Heights

Location	Depth		Wave Height	
	(m)	(ft)	(m)	(ft)
Seawall	4.85	15.9	2.89	9.5
Berm	1.11	3.65	0.68	2.2

Table 2.4-225 Lake Erie Extreme Low Water Elevations from 1967-2007 at the Fermi Site (Station No. 9063090)

Rank	Elevation (ft, IGLD 85)	Date
1[1]	563.64	February 16, 1967
2	564.19	November 13, 2003
3	564.66	March 10, 2002
4	565.49	December 1, 2006
5	565.60	October 26, 2001
6	565.73	December 17, 2000
7	566.30	November 6, 2007
8	566.36	November 11, 1998
9	566.40	December 23, 2007
10	566.49	February 1, 2002
11	566.54	November 6, 2005

Note:

1. This elevation was noted on Nuclear Generation Memorandum NP-00-0064, dated August 16, 2000. This elevation has also been confirmed by NOAA on February 7, 2008.

Source: Reference 2.4-259, Reference 2.4-260

Table 2.4-226 EPA Region 5 Sole Source Aquifers

State	Sole Source Aquifer Name	Federal Register Cit.	Public. Date	Approximate Distance to Fermi 3
IN	St. Joseph Aquifer System	53 FR 23682	06/23/88	120 mi
MN	Mille Lacs Aquifer	55 FR 43407	10/29/90	570 mi
OH	Pleasant City Aquifer	52 FR 32342	08/27/87	166 mi
OH	Bass Islands Aquifer, Catawba Island	52 FR 37009	10/02/87	34 mi
OH	Miami Valley Buried Aquifer	53 FR 15876	05/04/88	112 mi
OH	OKI extension of the Miami Buried Valley Aquifer	53 FR 25670	07/08/88	112 mi
OH	Allen County Area Combined Aquifer System	57 FR 53111	11/06/92	88 mi
OH/MI/IN	Michindoh Glacial Aquifer	Pending	N/A	43 mi

Source: Reference 2.4-268, Reference 2.4-269

Table 2.4-227 Monroe County, Michigan Projected Groundwater Use Through 2060

Category	2000	2008	2013	2018	2020	2030	2040	2050	2060	Data Source
Total population of county, in thousands	146	158	166	174	177	194	213	234	258	Environmental Report, Section 2.5
Domestic, self-supplied population, in thousands	49.64	53.79	56.38	59.08	60.20	66.12	72.61	79.75	87.59	Reference 2.4-270
Public supply, total population served, in thousands	96.30	104.36	109.37	114.62	116.79	128.27	140.87	154.72	169.92	Reference 2.4-270
Public supply, groundwater withdrawals, fresh, in Mgal/d	0.24	0.26	0.27	0.29	0.29	0.32	0.35	0.39	0.42	Reference 2.4-270
Domestic, groundwater self-supplied withdrawals, fresh, in Mgal/d	4.28	4.64	4.86	5.09	5.19	5.70	6.26	6.88	7.55	Reference 2.4-270
Industrial, groundwater self-supplied withdrawals, fresh, in Mgal/d	23	24.9	26.1	27.4	27.9	30.6	33.6	37.0	40.6	Reference 2.4-261
Irrigation, groundwater withdrawals, fresh, in Mgal/d	0.78	0.78	0.78	0.78	0.78	0.78	0.78	0.78	0.78	Reference 2.4-270
Livestock, groundwater withdrawals, fresh, in Mgal/d	0.05	0.05	0.05	0.05	0.05	0.05	0.05	0.05	0.05	Reference 2.4-270
Thermoelectric, groundwater withdrawals, fresh, in Mgal/d	0.07	0.07	0.07	0.07	0.07	0.07	0.07	0.07	0.07	Reference 2.4-276
Total groundwater withdrawals, fresh, in Mgal/d	28.42	30.72	32.15	33.65	34.27	37.55	41.16	45.11	49.46	

Table 2.4-228 Wayne County, Michigan Projected Groundwater Use Through 2060

Category	2000	2008	2013	2018	2020	2030	2040	2050	2060	Data Source
Total population of county, in thousands	2061.16	1967.62	1929.38	1891.88	1877.08	1804.82	1735.35	1668.54	1604.31	Environmental Report, Section 2.5
Domestic, self-supplied population, in thousands	0.67	0.64	0.63	0.61	0.61	0.59	0.56	0.54	0.52	Reference 2.4-270
Public supply, total population served, in thousands	1360.08	1298.36	1273.12	1248.38	1238.61	1190.93	1145.09	1101.00	1058.62	Reference 2.4-270
Public supply, groundwater withdrawals, fresh, in Mgal/d	0.00	0.00	0.00	0.00	0.00	0.00	0.00	0.00	0.00	Reference 2.4-270
Domestic, groundwater self-supplied withdrawals, fresh, in Mgal/d	0.06	0.06	0.06	0.06	0.05	0.05	0.05	0.05	0.05	Reference 2.4-270
Industrial, groundwater self-supplied withdrawals, fresh, in Mgal/d	0.08	0.08	0.08	0.08	0.08	0.08	0.08	0.08	0.08	Reference 2.4-261
Irrigation, groundwater withdrawals, fresh, in Mgal/d	0.58	0.58	0.58	0.58	0.58	0.58	0.58	0.58	0.58	Reference 2.4-270
Livestock, groundwater withdrawals, fresh, in Mgal/d	0.00	0.00	0.00	0.00	0.00	0.00	0.00	0.00	0.00	Reference 2.4-270
Thermoelectric, groundwater withdrawals, fresh, in Mgal/d	0.00	0.00	0.00	0.00	0.00	0.00	0.00	0.00	0.00	Reference 2.4-276
Total groundwater withdrawals, fresh, in Mgal/d	0.72	0.72	0.72	0.72	0.71	0.71	0.71	0.71	0.71	

Table 2.4-229 Monitoring Well/Piezometer Construction Data (Sheet 1 of 2)

Boring Number	Coordinates		Ground Surface Elevation (NAVD 88)	Top of Casing Elevation (NAVD 88)	Top of Filter Elevation (NAVD 88)	Top of Screen Elevation (NAVD 88)	Bottom of Screen Elevation (NAVD 88)	Bottom of Filter Elevation (NAVD 88)	Bottom of Boring Elevation (NAVD 88)
	Plant North	Plant East							
MW-381 D	5304.6	1843	579.78	582.35	544.78	543.28	533.28	530.78	480.78
MW-381 S	5306.7	1838.4	579.88	582.52	573.88	572.08	571.08	570.38	570.38
MW-383 D	5805.4	3435.7	582.28	585.16	553.58	551.28	541.28	539.18	481.28
MW-383 S	5809.1	3432.7	582.38	584.15	576.38	574.28	569.28	568.38	565.88
MW-384 D	5537.6	4402.8	581.28	583.98	541.28	539.18	529.18	526.28	480.28
MW-384 S	5532.6	4403.9	581.38	583.66	576.78	575.28	565.28	564.38	564.38
MW-386 D	6336.7	5203.8	582.28	583.91	531.78	529.48	519.48	516.28	490.78
MW-386 S	6343.9	5203.6	582.38	584.18	569.88	565.98	560.98	560.38	560.38
MW-387 D	6660.2	4150.1	579.68	582.29	549.68	547.08	537.08	534.68	476.18
MW-387 S	6665.8	4148.2	579.28	582.16	573.48	571.28	566.28	565.28	563.08
MW-388 S	8082.4	2168.8	574.78	577.6	571.28	569.43	568.43	568.28	568.28
MW-390 S	7960.1	4245.7	578.88	582.09	573.88	571.88	566.88	566.38	562.38
MW-391 D	8240.3	5237.2	578.68	581.17	537.68	535.88	525.88	523.68	477.68
MW-391 S	8242.9	5232.9	578.58	581.39	575.58	570.58	560.58	559.6	559.58
MW-393 D	9367.4	2922.8	576.58	578.33	550.58	548.88	538.88	536.23	426.58
MW-393 S	9360	2918.2	576.48	579.35	572.38	570.28	567.28	566.68	566.68
MW-395 D	8900	4600.1	577.28	579.83	547.28	545.28	535.28	533.28	476.28
MW-395 S	8906.2	4599.7	577.28	579.9	570.88	568.78	563.78	562.88	562.88
P-382 S	5730.3	3132.4	576.38	578.46	571.78	569.88	561.98	559.88	559.88
P-385 D	6201.7	4390	580.08	583.13	514.68	511.78	501.78	501.08	477.58
P-385 S	6198.1	4385.6	580.18	583.25	572.18	570.68	565.68	563.18	563.18
P-389 S	7821.4	3889.3	576.88	579.18	572.48	570.38	560.38	559.88	559.88
P-392 S	8088.7	5841.5	580.58	583.19	575.08	572.88	562.88	562.58	562.58

Table 2.4-229 Monitoring Well/Piezometer Construction Data (Sheet 2 of 2)

Boring Number	Coordinates		Ground Surface Elevation (NAVD 88)	Top of Casing Elevation (NAVD 88)	Top of Filter Elevation (NAVD 88)	Top of Screen Elevation (NAVD 88)	Bottom of Screen Elevation (NAVD 88)	Bottom of Filter Elevation (NAVD 88)	Bottom of Boring Elevation (NAVD 88)
	Plant North	Plant East							
P-396 S	8949.8	5248.8	578.38	581.22	572.88	570.88	560.88	560.38	558.88
P-397 S	8901.4	5748.5	575.98	578.95	567.48	564.98	554.98	554.48	554.48
P-398 D	9510.6	5352.1	577.88	580.55	528.88	527.38	517.38	514.98	476.88
P-398 S	9504.3	5350.4	577.98	580.38	572.48	570.48	560.48	559.98	559.98
P-399 D	2565.59	5228.73	574.72	577.46	532.72	531.22	521.22	518.62	470.7
GW-01	5480.8	5881.1	578.98	580.66	551.98	550.98	545.98	545.98	545.98
GW-02	1631.8	4341.6	577.08	578.99	560.08	559.08	554.08	553.08	553.08
GW-03	1791.85	2236.85	577.88	580.65	561.88	560.38	555.38	555.38	555.38
GW-04	8075.4	2165.6	575.78	577.94	563.78	562.78	557.78	557.78	557.78
EFT-01 S	6366.2	5492.6	581.2	583.68	579.2	577.2	572.2	571.2	571.2
EFT-01 I	6366.2	5492.6	581.2	583.69	566.7	564.7	559.7	559.7	559.7
EFT-01 D	6366.2	5492.4	581.2	583.69	553.2	550.7	545.7	545.7	545.7
EFT-02 S	6570.55	5734.62	582.4	582.17	580.4	578.4	573.4	572.4	572.4
EFT-02 D	6570.55	5734.62	582.3	581.88	551.3	549.3	544.3	543.8	543.8
MW-5d	7245.57	4893.81	581.84	581.54	564.84	562.84	560.84	559.84	557.84
CB-C5	6123	4663.4	580.98	580.77	503.88	496.98	491.98	488.78	449.98
EB/TSC-C2	6579.3	4697.2	581.37	581.12	546.57	544.37	539.37	536.87	530.87

Table 2.4-230 Surface Water Gauge Construction Data

Surface Water Gauge	Coordinates		June 29, 2007 - November 29, 2007			April 29, 2008 - May 29, 2008		
	Plant North	Plant East	Elevation @ 6.66' on Gauge (Plant)	Elevation @ 6.66' on Gauge (NAVD 88)	Elevation @ 0.00' on Gauge (NAVD 88)	Elevation @ 6.66' on Gauge (Plant)	Elevation @ 6.66' on Gauge (NAVD 88)	Elevation @ 0.00' on Gauge (NAVD 88)
GS-1	7897	3947.5	576.28	575.06	568.40	576.15	574.93	568.27
GS-2	9647.25	5299.97	576.42	575.20	568.54	575.01	573.79	567.13
GS-3	5447.53	4676.31	576.57	575.35	568.69	576.23	575.01	568.35
GS-4	8714.94	4471.81	576.40	575.18	568.52	Not Restored		
GS-5	3124.72	2345.66	570.68	569.46	562.80	574.49	573.27	566.61

Table 2.4-231 Water Level Data (Sheet 1 of 5)

Well Number	Hydrogeologic Unit Monitored	Piezometeric Water Level in Feet (NAVD 1988)					
		6/29/2007	7/29/2007	8/29/2007	9/28/2007 & 9/29/2007	10/30/2007	11/29/2007
MW-381 D	Bass Islands	560.59	559.22	563.19	559.77	558.20	558.08
MW-383 D	Bass Islands	563.28	561.81	563.05	563.87	563.09	563.11
MW-384 D	Bass Islands	561.68	560.40	561.92	563.80	562.93	562.93
MW-386 D	Bass Islands	566.43	564.19	565.90	567.67	566.96	566.68
MW-387 D	Bass Islands/ Overburden	567.75	565.82	567.19	570.80	570.38	570.59
MW-391 D	Bass Islands	566.80	565.65	567.27	567.28	566.60	566.35
MW-393 D	Bass Islands	570.07	568.10	571.45	569.27	568.78	570.68
MW-395 D	Bass Islands	571.89	571.59	572.51	572.10	571.76	572.06
P-385 D	Bass Islands	559.18	559.24	560.28	565.10	564.28	564.21
GW-03	Bass Islands	566.64	565.97	566.56	566.02	564.98	565.24
GW-04	Bass Islands	570.29	567.76	572.74	569.32	569.86	573.18
EFT-1 D	Bass Islands	570.19	568.83	569.91	570.83	570.35	570.46
EFT-2 D	Bass Islands	570.67	569.43	570.61	571.08	570.57	570.73
CB-C5 (D)	Bass Islands	ND	ND	560.82	565.30	564.41	564.29
EB/TSC-C2 (D)	Bass Islands	ND	ND	ND	569.55	569.08	569.21
GW-01	Bass Islands/ Overburden	ND	ND	ND	567.15	566.40	565.98
P-399 D	Bass Islands/ Salina	563.72	562.73	564.80	563.36	562.45	562.30
P-398 D	Salina	552.74	552.11	553.55	552.48	551.57	551.07
GS-5 A	Overburden/ Bass Islands	566.05	565.43	565.80	565.42	564.95	565.60
GS-5 B	Overburden/ Bass Islands	ND	ND	ND	ND	ND	ND
MW-5d	Overburden	573.03	572.33	573.18	572.76	573.45	572.74
GW-02	Overburden	566.94	565.90	568.18	566.31	565.74	565.60
EFT-1I	Overburden	572.78	573.24	573.49	573.96	573.61	572.80
MW-381 S	Overburden	571.59	572.90	575.05	575.61	575.88	575.98
MW-383 S	Overburden	573.56	572.58	574.23	573.10	572.64	573.17
MW-384 S	Overburden	574.38	573.77	574.83	573.98	573.96	574.03

Table 2.4-231 Water Level Data (Sheet 2 of 5)

Well Number	Hydrogeologic Unit Monitored	Piezometeric Water Level in Feet (NAVD 1988)					
		6/29/2007	7/29/2007	8/29/2007	9/28/2007 & 9/29/2007	10/30/2007	11/29/2007
MW-386 S	Overburden	571.59	571.43	571.31	572.48	572.23	571.73
MW-387 S	Overburden	571.86	571.66	572.04	571.37	571.09	571.05
MW-388 S	Overburden	569.16	569.00	569.86	569.98	569.88	570.24
MW-390 S	Overburden	572.52	572.22	573.08	572.67	572.34	572.64
MW-391 S	Overburden	572.34	572.05	572.91	572.50	572.16	572.47
MW-393 S	Overburden	568.37	570.43	571.05	571.51	572.02	573.53
MW-395 S	Overburden	572.27	571.98	572.84	572.42	572.09	572.40
P-382 S	Overburden	569.53	568.57	572.17	569.31	569.66	571.64
P-385 S	Overburden	571.92	571.71	572.10	571.45	571.14	571.11
P-389 S	Overburden	571.00	570.63	570.75	570.15	569.77	570.00
P-392 S	Overburden	572.51	572.23	573.09	572.66	572.36	572.64
P-396 S	Overburden	572.29	571.99	572.86	572.44	572.11	572.41
P-397 S	Overburden	571.10	570.39	574.30	572.07	570.64	572.23
P-398 S	Overburden	572.23	571.81	572.74	572.21	571.91	572.06
EFT-1 S	Overburden	576.80	577.50	577.75	577.32	576.62	575.71
EFT-2 S	Overburden	577.93	577.66	577.51	577.14	576.62	576.12
GS-1 A	Surface Water	572.05	571.75	571.76	570.86	570.65	570.46
GS-2 A	Surface Water	571.94	571.60	571.56	570.84	570.44	570.38
GS-3 A	Surface Water	571.99	571.75	571.75	571.29	ND	571.13
GS-4 A	Surface Water	572.02	571.69	ND	570.82	570.57	570.42
GS-1 B	Surface Water	ND	ND	ND	ND	ND	ND
GS-2 B	Surface Water	ND	ND	ND	ND	ND	ND
GS-3 B	Surface Water	ND	ND	ND	ND	ND	ND

Table 2.4-231 Water Level Data (Sheet 3 of 5)

Well Number	Hydrogeologic Unit Monitored	Piezometeric Water Level in Feet (NAVD 1988)					
		12/29/2007	1/29/2008	2/28/2008	3/21/2008	4/29/2008	5/29/2008
MW-381 D	Bass Islands	562.74	562.88	563.75	566.51	564.53	561.97
MW-383 D	Bass Islands	565.35	566.41	566.93	568.78	567.43	565.73
MW-384 D	Bass Islands	565.21	565.80	566.34	567.64	566.83	565.46
MW-386 D	Bass Islands	568.24	568.71	569.05	569.80	569.16	568.30
MW-387 D	Bass Islands/ Overburden	571.55	571.81	572.05	572.54	571.96	571.35
MW-391 D	Bass Islands	567.69	568.20	568.45	568.95	568.45	567.69
MW-393 D	Bass Islands	572.53	572.26	572.42	573.85	572.74	571.56
MW-395 D	Bass Islands	572.61	572.72	572.90	573.18	572.66	572.27
P-385 D	Bass Islands	566.29	566.84	567.34	568.48	567.69	566.42
GW-03	Bass Islands	565.68	566.10	567.04	567.97	568.39	568.04
GW-04	Bass Islands	574.64	573.54	573.43	575.06	573.65	572.54
EFT-1 D	Bass Islands	571.39	571.58	571.76	572.62	571.75	571.13
EFT-2 D	Bass Islands	ND	ND	ND	ND	571.90	ND
CB-C5 (D)	Bass Islands	566.33	566.91	ND	ND	567.87	566.65
EB/TSC-C2 (D)	Bass Islands	570.42	570.78	571.01	571.61	571.00	570.26
GW-01	Bass Islands/ Overburden	567.58	568.04	568.40	569.12	568.63	567.73
P-399 D	Bass Islands/ Salina	564.73	565.08	565.80	566.96	566.39	564.98
P-398 D	Salina	553.00	553.83	554.15	554.74	554.67	553.48
GS-5 A	Overburden/ Bass Islands	ND	ND	ND	ND	ND	ND

Table 2.4-231 Water Level Data (Sheet 4 of 5)

Well Number	Hydrogeologic Unit Monitored	Piezometeric Water Level in Feet (NAVD 1988)					
		12/29/2007	1/29/2008	2/28/2008	3/21/2008	4/29/2008	5/29/2008
GS-5 B	Overburden/ Bass Islands	ND	ND	ND	ND	567.94	567.61
MW-5d	Overburden	573.25	573.35	573.34	573.78	573.26	572.91
GW-02	Overburden	568.07	568.69	569.11	570.85	570.81	569.59
EFT-1I	Overburden	572.19	571.96	571.80	571.55	571.92	572.22
MW-381 S	Overburden	576.61	576.87	576.88	577.06	577.17	576.67
MW-383 S	Overburden	575.48	575.93	575.67	576.13	575.93	574.99
MW-384 S	Overburden	575.03	575.39	575.02	575.66	575.20	574.61
MW-386 S	Overburden	571.30	570.68	570.90	570.96	571.53	571.75
MW-387 S	Overburden	571.20	571.03	571.51	572.26	572.30	572.13
MW-388 S	Overburden	572.62	573.17	573.31	574.01	573.47	572.50
MW-390 S	Overburden	573.14	573.24	573.41	573.67	573.15	572.78
MW-391 S	Overburden	572.97	573.07	573.24	573.51	572.98	572.61
MW-393 S	Overburden	575.35	574.18	574.12	576.12	574.95	573.93
MW-395 S	Overburden	572.90	573.00	573.17	573.44	572.91	572.55

Table 2.4-231 Water Level Data (Sheet 5 of 5)

Well Number	Hydrogeologic Unit Monitored	Piezometeric Water Level in Feet (NAVD 1988)					
		6/29/2007	7/29/2007	8/29/2007	9/28/2007 & 9/29/2007	10/30/2007	11/29/2007
P-382 S	Overburden	572.80	572.38	572.56	573.02	572.70	572.04
P-385 S	Overburden	571.26	571.07	571.57	572.32	572.36	572.18
P-389 S	Overburden	570.49	570.37	570.91	571.74	571.42	571.41
P-392 S	Overburden	573.14	573.23	573.41	573.68	573.16	572.79
P-396 S	Overburden	572.91	573.00	573.17	573.43	572.91	572.54
P-397 S	Overburden	573.73	573.37	574.04	574.49	574.06	573.08
P-398 S	Overburden	572.65	573.06	572.99	573.26	573.01	572.61
EFT-1 S	Overburden	576.25	575.95	575.68	575.82	575.54	576.07
EFT-2 S	Overburden	575.36	575.27	574.80	574.87	574.49	576.60
GS-1 A	Surface Water	ND	ND	ND	ND	ND	ND
GS-2 A	Surface Water	ND	ND	ND	ND	ND	ND
GS-3 A	Surface Water	ND	ND	ND	ND	ND	ND
GS-4 A	Surface Water	ND	ND	ND	ND	ND	ND
GS-1 B	Surface Water	ND	ND	ND	ND	571.87	572.17
GS-2 B	Surface Water	ND	ND	ND	ND	571.81	572.03
GS-3 B	Surface Water	ND	ND	ND	ND	571.98	572.25

Note: CB-C5 installed in Aug '07; EB/TSC-C2 installed in Sep '07; GW-01 located in Sep '07; "A" gauge stations are June 2007 to November 2007 & "B" gauge stations are April & May 2008; ND equals No Data

Table 2.4-232 Overburden Hydraulic Conductivity

Monitoring Well/Piezometer	Monitored Strata	K (ft/day)[1]
P-382 S	Quaternary	0.11
P-389 S	Quaternary	0.17
MW-395 S	Quaternary	16.5
P-397 S	Quaternary	0.028
P-398 S	Quaternary	0.56
MW-383 S	Clay Fill	0.036
MW-384 S	Clay Fill	0.046
P-385 S	Rock Fill	1,170
MW-387 S	Rock Fill	1,285
MW-390 S	Rock Fill	977
MW-391 S	Rock Fill	1,776
P-392 S	Rock Fill	251
P-396 S	Rock Fill	505

Notes:

1. K values from Fermi 3 slug test analyses. For Quaternary and clay fill piezometers the average value is reported. For rock fill piezometers the maximum value calculated using the Butler and Springer-Gelhar methods is reported.

Table 2.4-233 Bedrock Aquifer Hydraulic Conductivity (Sheet 1 of 2)

Well #	Avg Depth (ft)	Average K (ft/day)	Comment
MW-381	30	9.03	0
	42	11.53	0
MW-383	36	2.76	0
	50	1.47	0
	67	0.11	0
	91	1.99	1
MW-384 D	48	25.08	1
	61	40.07	2
	64	31.83	2
	77.5	13.47	0
P-385 D	42	0.23	0
	73	2.59	1
	86	1.27	0
MW-386 D	34	3.39	0
	48	2.11	0
	59	4.02	1
	80	1.53	1
MW-387 D	38.8	33.88	2
	58	1.08	0
	72	0.42	0
MW-391 D	58	2.26	0
	74	0.37	0
	86	0.91	1
MW-393 D	33	2.80	1
	56	0.67	1
	73	0.22	0
	109	1.98	1
MW-395D	37	17.57	0
	49	0.26	0
	66	0.15	0
	86	0.30	1

Table 2.4-233 Bedrock Aquifer Hydraulic Conductivity (Sheet 2 of 2)

Well #	Avg Depth (ft)	Average K (ft/day)	Comment
P-398 D	39	0.08	0
	56	0.81	0
	80	0.25	0
P-399 D	38	28.84	1
	49	9.82	2
	73	1.15	1

Notes:

Data collected during Fermi 3 Subsurface Investigation, 2007.

Comments:

0 = No hydraulic connection with adjacent zones observed.

1 = Hydraulic connection with lower zone observed.

2 = Hydraulic connection with upper zone observed.

Table 2.4-234 Site Specific Inputs

Parameter	Description	Value
Cerium Kd (cm^3/g)	Radionuclide-specific distribution coefficient (Off-Site Well/Lake Erie)	4575/5894
Cesium Kd (cm^3/g)	Radionuclide-specific distribution coefficient (Off-Site Well/Lake Erie)	1078/1078
Cobalt Kd (cm^3/g)	Radionuclide-specific distribution coefficient (Off-Site Well/Lake Erie)	640/1513
Iron Kd (cm^3/g)	Radionuclide-specific distribution coefficient (Off-Site Well/Lake Erie)	2.88/4.2
Manganese Kd (cm^3/g)	Radionuclide-specific distribution coefficient (Off-Site Well/Lake Erie)	394/588
Ruthenium Kd (cm^3/g)	Radionuclide-specific distribution coefficient (Off-Site Well/Lake Erie)	42.9/265
Silver Kd (cm^3/g)	Radionuclide-specific distribution coefficient (Off-Site Well/Lake Erie)	0.41/2.12
Strontium Kd (cm^3/g)	Radionuclide-specific distribution coefficient (Off-Site Well/Lake Erie)	0.44/33.1
Yttrium Kd (cm^3/g)	Radionuclide-specific distribution coefficient (Off-Site Well/Lake Erie)	3183/7366
Zinc Kd (cm^3/g)	Radionuclide-specific distribution coefficient (Off-Site Well/Lake Erie)	16.7/16.7
Effective porosity (unitless)	The amount of interconnected pore space through which fluids can pass, expressed as a percent of bulk volume	0.001
Hydraulic conductivity (m/yr(ft/day))	A coefficient of proportionality describing the rate at which water can move through a permeable medium	365.16 (3.28)
Hydraulic gradient to surface water body and off site well (unitless)	Change in groundwater elevation per unit of distance in the direction of groundwater flow to a surface water body or off site well.	0.002
Distance to the nearest off site water well not in a restricted area (ft. (m))	Distance to the nearest off-site water well	4373 (1333)
Distance to the nearest surface water body (Lake Erie) (ft. (m))	Distance to the nearest off-site surface water body that contributes to a potable drinking water source	1554 (474)
Dry bulk density (gm/cm^3)	Mass of (dry) solids in a unit volume of soil. A range of average dry bulk densities was determined based on tests.	1.68 – 2.4

Table 2.4-235 Comparison of Liquid Release Concentrations With 10 CFR 20 Concentrations - Lake Erie (Sheet 1 of 3)

Decay Only Concentrations At Lake (µCi/ml)										Decay Only GW/ECL at Lake						
		Yrs	Yrs	Yrs	Yrs	Yrs	Yrs	Yrs		Yrs	Yrs	Yrs	Yrs	Yrs	Yrs	Yrs
Nuclide	**Progeny**	0.65	1	1.83	2	3	5	6		0.65	1	1.83	2	3	5	6
H-3		8.452E-04	8.766E-04	7.910E-04	7.835E-04	7.407E-04	6.621E-04	6.259E-04		8.452E-01	8.766E-01	7.910E-01	7.835E-01	7.407E-01	6.621E-01	6.259E-01
Na-24																
P-32		1.793E-09	3.651E-12							1.992E-04	4.057E-07					
Cr-51		6.184E-05	2.523E-06	1.281E-09	2.708E-10	2.906E-14				1.237E-01	5.046E-03	2.561E-06	5.415E-07	5.811E-11		
Mn-54		5.235E-04	3.944E-04	2.016E-04	1.757E-04	7.823E-05	1.552E-05	6.911E-06		1.745E+01	1.315E+01	6.718E+00	5.855E+00	2.608E+00	5.172E-01	2.304E-01
Mn-56																
Fe-55		2.348E-02	2.146E-02	1.734E-02	1.660E-02	1.284E-02	7.685E-03	5.945E-03		2.348E+02	2.146E+02	1.734E+02	1.660E+02	1.284E+02	7.685E+01	5.945E+01
Fe-59		8.525E-06	1.164E-06	1.036E-08	3.937E-09	1.331E-11				8.525E-01	1.164E-01	1.036E-03	3.937E-04	1.331E-06		
Co-58		1.551E-04	4.438E-05	2.282E-06	1.242E-06	3.477E-08	2.724E-11	7.626E-13		7.757E+00	2.219E+00	1.141E-01	6.211E-02	1.739E-03	1.362E-06	3.813E-08
Co-60		5.170E-03	4.938E-03	4.429E-03	4.331E-03	3.799E-03	2.922E-03	2.563E-03		1.723E+03	1.646E+03	1.476E+03	1.444E+03	1.266E+03	9.741E+02	8.543E+02
Ni-63		2.905E-05	2.898E-05	2.881E-05	2.877E-05	2.856E-05	2.816E-05	2.795E-05		2.905E-01	2.898E-01	2.881E-01	2.877E-01	2.856E-01	2.816E-01	2.795E-01
Cu-64																
Zn-65		1.216E-02	8.459E-03	3.575E-03	2.997E-03	1.062E-03	1.333E-04	4.723E-05		2.432E+03	1.692E+03	7.150E+02	5.994E+02	2.124E+02	2.666E+01	9.446E+00
Rb-89																
	Sr-89	4.952E-05	8.566E-06	1.335E-07	5.695E-08	3.787E-10	1.674E-14			6.190E+00	1.071E+00	1.669E-02	7.119E-03	4.733E-05	2.093E-09	
Sr-90		1.978E-04	1.962E-04	1.923E-04	1.915E-04	1.870E-04	1.783E-04	1.741E-04		3.956E+02	3.923E+02	3.846E+02	3.831E+02	3.740E+02	3.566E+02	3.482E+02
	Y-90	1.978E-04	1.962E-04	1.923E-04	1.915E-04	1.870E-04	1.783E-04	1.741E-04		2.826E+01	2.802E+01	2.747E+01	2.736E+01	2.672E+01	2.547E+01	2.487E+01
Sr-91																
	Y-91m															
	Y-91	3.417E-05	7.513E-06	2.069E-07	9.915E-08	1.309E-09	2.279E-13	3.008E-15		4.271E+00	9.391E-01	2.587E-02	1.239E-02	1.636E-04	2.849E-08	3.760E-10
Sr-92																
	Y-92															

Table 2.4-235 Comparison of Liquid Release Concentrations With 10 CFR 20 Concentrations - Lake Erie (Sheet 2 of 3)

Decay Only Concentrations At Lake (µCi/ml)										Decay Only GW/ECL at Lake						
		Yrs	Yrs	Yrs	Yrs	Yrs	Yrs	Yrs		Yrs	Yrs	Yrs	Yrs	Yrs	Yrs	Yrs
Nuclide	**Progeny**	0.65	1	1.83	2	3	5	6		0.65	1	1.83	2	3	5	6
Y-93																
Zr-95		9.228E-06	2.311E-06	8.667E-08	4.424E-08	8.469E-10	3.103E-13	5.941E-15		4.614E-01	1.155E-01	4.333E-03	2.212E-03	4.234E-05	1.552E-08	2.970E-10
	Nb-95m	6.845E-08	1.714E-08	6.430E-10	3.282E-10	6.282E-12	2.302E-15			2.282E-03	5.715E-04	2.143E-05	1.094E-05	2.094E-07	7.674E-11	
	Nb-95	1.875E-05	4.995E-06	1.923E-07	9.824E-08	1.883E-09	6.899E-13	1.321E-14		6.249E-01	1.665E-01	6.410E-03	3.275E-03	6.276E-05	2.300E-08	4.403E-10
Mo-99																
	Tc-99m															
Ru-103		3.270E-06	3.430E-07	1.634E-09	5.465E-10	8.707E-13				1.090E-01	1.143E-02	5.446E-05	1.822E-05	2.902E-08		
	Rh-103m	3.263E-06	3.423E-07	1.631E-09	5.454E-10	8.689E-13				5.439E-04	5.706E-05	2.718E-07	9.090E-08	1.448E-10		
Ru-106		4.706E-05	3.699E-05	2.090E-05	1.859E-05	9.345E-06	2.360E-06	1.186E-06		1.569E+01	1.233E+01	6.966E+00	6.198E+00	3.115E+00	7.868E-01	3.955E-01
	Rh-106	4.706E-05	3.699E-05	2.090E-05	1.859E-05	9.345E-06	2.360E-06	1.186E-06								
Ag-110m		1.245E-05	8.737E-06	3.770E-06	3.174E-06	1.153E-06	1.521E-07	5.525E-08		2.076E+00	1.456E+00	6.283E-01	5.290E-01	1.921E-01	2.535E-02	9.209E-03
	Ag-110	1.656E-07	1.162E-07	5.014E-08	4.221E-08	1.533E-08	2.023E-09	7.349E-10								
Te-129m		2.885E-06	2.064E-07	3.969E-10	1.103E-10	5.889E-14				4.121E-01	2.949E-02	5.671E-05	1.575E-05	8.413E-09		
	Te-129	1.878E-06	1.344E-07	2.584E-10	7.177E-11	3.834E-14				4.694E-03	3.359E-04	6.459E-07	1.794E-07	9.584E-11		
Te-131m																
	Te-131															
	I-131	8.029 E-12								8.029E-06						
Te-132																
	I-132															
I-133																

Table 2.4-235 Comparison of Liquid Release Concentrations With 10 CFR 20 Concentrations - Lake Erie (Sheet 3 of 3)

		Decay Only Concentrations At Lake (µCi/ml)								Decay Only GW/ECL at Lake						
		Yrs	Yrs	Yrs	Yrs	Yrs	Yrs	Yrs		Yrs	Yrs	Yrs	Yrs	Yrs	Yrs	Yrs
Nuclide	**Progeny**	0.65	1	1.83	2	3	5	6		0.65	1	1.83	2	3	5	6
	Xe-133m															
	Xe-133															
I-134																
I-135																
	Xe-135m															
	Xe-135															
Cs-134		5.329E-04	4.737E-04	3.584E-04	3.385E-04	2.418E-04	1.234E-04	8.820E-05		5.921E+02	5.264E+02	3.982E+02	3.761E+02	2.687E+02	1.372E+02	9.800E+01
Cs-136		2.288E-10	2.641E-13							3.813E-05	4.402E-08					
Cs-137		1.855E-03	1.840E-03	1.805E-03	1.798E-03	1.757E-03	1.678E-03	1.640E-03		1.855E+03	1.840E+03	1.805E+03	1.798E+03	1.757E+03	1.678E+03	1.640E+03
	Ba-137m	1.755E-03	1.741E-03	1.708E-03	1.701E-03	1.662E-03	1.588E-03	1.551E-03								
Cs-138																
Ba-140		3.718E-09	3.468E-12							4.647E-04	4.336E-07					
	La-140	4.285E-09	3.997E-12							4.761E-04	4.441E-07					
Ce-141		1.692E-06	1.107E-07	1.723E-10	4.584E-11	1.897E-14				5.640E-02	3.691E-03	5.744E-06	1.528E-06	6.324E-10		
Ce-144		3.967E-05	2.904E-05	1.386E-05	1.191E-05	4.883E-06	8.210E-07	3.367E-07		1.322E+01	9.679E+00	4.618E+00	3.969E+00	1.628E+00	2.737E-01	1.122E-01
	Pr-144m	7.061E-07	5.169E-07	2.466E-07	2.119E-07	8.691E-08	1.461E-08	5.993E-09								
	Pr-144	3.967E-05	2.904E-05	1.386E-05	1.191E-05	4.883E-06	8.210E-07	3.367E-07		6.612E-02	4.840E-02	2.309E-02	1.985E-02	8.138E-03	1.368E-03	5.611E-04
W-187																
Np-239																
	Pu-239	1.734E-09	1.734E-09	1.734E-09	1.734E-09	1.734E-09	1.734E-09	1.734E-09		8.671E-02	8.671E-02	8.671E-02	8.671E-02	8.671E-02	8.670E-02	8.670E-02
								Sum of Fractions		7.332E+03	6.382E+03	5.001E+03	4.812E+03	4.042E+03	3.278E+03	3.036E+03

(1) Blank cells (i.e., no numerical results) represent results that are essentially zero.

Table 2.4-236 Comparison of Liquid Release Concentrations With 10 CFR 20 Concentrations - Off Site Water Well (Sheet 1 of 3)

		Decay Only Concentrations At Well (µCi/ml)						Decay Only GW/ECL at Well				
		Yrs	Yrs	Yrs	Yrs	Yrs		Yrs	Yrs	Yrs	Yrs	Yrs
Nuclide	Progeny	1.83	2	3	5	6		1.83	2	3	5	6
H-3		7.910E-04	7.835E-04	7.407E-04	6.621E-04	6.259E-04		7.910E-01	7.835E-01	7.407E-01	6.621E-01	6.259E-01
Na-24												
P-32												
Cr-51		1.281E-09	2.708E-10	2.906E-14				2.561E-06	5.415E-07	5.811E-11		
Mn-54		2.016E-04	1.757E-04	7.823E-05	1.552E-05	6.911E-06		6.718E+00	5.855E+00	2.608E+00	5.172E-01	2.304E-01
Mn-56												
Fe-55		1.734E-02	1.660E-02	1.284E-02	7.685E-03	5.945E-03		1.734E+02	1.660E+02	1.284E+02	7.685E+01	5.945E+01
Fe-59		1.036E-08	3.937E-09	1.331E-11				1.036E-03	3.937E-04	1.331E-06		
Co-58		2.282E-06	1.242E-06	3.477E-08	2.724E-11	7.626E-13		1.141E-01	6.211E-02	1.739E-03	1.362E-06	3.813E-08
Co-60		4.429E-03	4.331E-03	3.799E-03	2.922E-03	2.563E-03		1.476E+03	1.444E+03	1.266E+03	9.741E+02	8.543E+02
Ni-63		2.881E-05	2.877E-05	2.856E-05	2.816E-05	2.795E-05		2.881E-01	2.877E-01	2.856E-01	2.816E-01	2.795E-01
Cu-64												
Zn-65		3.575E-03	2.997E-03	1.062E-03	1.333E-04	4.723E-05		7.150E+02	5.994E+02	2.124E+02	2.666E+01	9.446E+00
Rb-89												
	Sr-89	1.335E-07	5.695E-08	3.787E-10	1.674E-14			1.669E-02	7.119E-03	4.733E-05	2.093E-09	
Sr-90		1.923E-04	1.915E-04	1.870E-04	1.783E-04	1.741E-04		3.846E+02	3.831E+02	3.740E+02	3.566E+02	3.482E+02
	Y-90	1.923E-04	1.915E-04	1.870E-04	1.783E-04	1.741E-04		2.747E+01	2.736E+01	2.672E+01	2.547E+01	2.487E+01
Sr-91												
	Y-91m											
	Y-91	2.069E-07	9.915E-08	1.309E-09	2.279E-13	3.008E-15		2.587E-02	1.239E-02	1.636E-04	2.849E-08	3.760E-10
Sr-92												
	Y-92											

Table 2.4-236 Comparison of Liquid Release Concentrations With 10 CFR 20 Concentrations - Off Site Water Well (Sheet 2 of 3)

		Decay Only Concentrations At Well (µCi/ml)						Decay Only GW/ECL at Well				
		Yrs	Yrs	Yrs	Yrs	Yrs		Yrs	Yrs	Yrs	Yrs	Yrs
Nuclide	Progeny	1.83	2	3	5	6		1.83	2	3	5	6
Y-93												
Zr-95		8.667E-08	4.424E-08	8.469E-10	3.103E-13	5.941E-15		4.333E-03	2.212E-03	4.234E-05	1.552E-08	2.970E-10
	Nb-95m	6.430E-10	3.282E-10	6.282E-12	2.302E-15			2.143E-05	1.094E-05	2.094E-07	7.674E-11	
	Nb-95	1.923E-07	9.824E-08	1.883E-09	6.899E-13	1.321E-14		6.410E-03	3.275E-03	6.276E-05	2.300E-08	4.403E-10
Mo-99												
	Tc-99m											
Ru-103		1.634E-09	5.465E-10	8.707E-13				5.446E-05	1.822E-05	2.902E-08		
	Rh-103m	1.631E-09	5.454E-10	8.689E-13				2.718E-07	9.090E-08	1.448E-10		
Ru-106		2.090E-05	1.859E-05	9.345E-06	2.360E-06	1.186E-06		6.966E+00	6.198E+00	3.115E+00	7.868E-01	3.955E-01
	Rh-106	2.090E-05	1.859E-05	9.345E-06	2.360E-06	1.186E-06						
Ag-110m		3.770E-06	3.174E-06	1.153E-06	1.521E-07	5.525E-08		6.283E-01	5.290E-01	1.921E-01	2.535E-02	9.209E-03
	Ag-110	5.014E-08	4.221E-08	1.533E-08	2.023E-09	7.349E-10						
Te-129m		3.969E-10	1.103E-10	5.889E-14				5.671E-05	1.575E-05	8.413E-09		
	Te-129	2.584E-10	7.177E-11	3.834E-14				6.459E-07	1.794E-07	9.584E-11		
Te-131m												
	Te-131											
	I-131											
Te-132												
	I-132											
I-133												
	Xe-133m											
	Xe-133											

Table 2.4-236 Comparison of Liquid Release Concentrations With 10 CFR 20 Concentrations - Off Site Water Well (Sheet 3 of 3)

		Decay Only Concentrations At Well (µCi/ml)						Decay Only GW/ECL at Well				
		Yrs	Yrs	Yrs	Yrs	Yrs		Yrs	Yrs	Yrs	Yrs	Yrs
Nuclide	Progeny	1.83	2	3	5	6		1.83	2	3	5	6
I-134												
I-135												
	Xe-135m											
	Xe-135											
Cs-134		3.584E-04	3.385E-04	2.418E-04	1.234E-04	8.820E-05		3.982E+02	3.761E+02	2.687E+02	1.372E+02	9.800E+01
Cs-136												
Cs-137		1.805E-03	1.798E-03	1.757E-03	1.678E-03	1.640E-03		1.805E+03	1.798E+03	1.757E+03	1.678E+03	1.640E+03
	Ba-137m	1.708E-03	1.701E-03	1.662E-03	1.588E-03	1.551E-03						
Cs-138												
Ba-140												
	La-140											
Ce-141		1.723E-10	4.584E-11	1.897E-14				5.744E-06	1.528E-06	6.324E-10		
Ce-144		1.386E-05	1.191E-05	4.883E-06	8.210E-07	3.367E-07		4.618E+00	3.969E+00	1.628E+00	2.737E-01	1.122E-01
	Pr-144m	2.466E-07	2.119E-07	8.691E-08	1.461E-08	5.993E-09						
	Pr-144	1.386E-05	1.191E-05	4.883E-06	8.210E-07	3.367E-07		2.309E-02	1.985E-02	8.138E-03	1.368E-03	5.611E-04
W-187												
Np-239												
	Pu-239	1.734E-09	1.734E-09	1.734E-09	1.734E-09	1.734E-09		8.671E-02	8.671E-02	8.671E-02	8.670E-02	8.670E-02
						Sum of Fractions		5.001E+03	4.812E+03	4.042E+03	3.278E+03	3.036E+03

(1) Blank cells (i.e., no numerical results) represent results that are essentially zero.

Table 2.4-237 Depth-Area-Duration Data

All Season Probable Maximum Precipitaton (inches)

Storm Size (Mi^2)	Storm Duration (hrs)				
	6	12	24	48	72
10	25.4	28.8	31.0	33.9	35.8
200	17.8	21.2	22.7	25.5	27.3
1000	12.9	15.6	17.5	20.0	22.0
5000	7.8	10.6	12.5	15.8	16.6
10000	6.1	8.6	10.0	13.0	14.7
20000	4.4	6.6	8.4	10.9	12.5

Source: Reference 2.4-302

Table 2.4-238 Lake Erie - Decay Plus Retardation (Sheet 1 of 3)

		Decay Plus Retardation Concentrations At Lake (µCi/ml)								Decay Plus Retardation GW/ECL at Lake						
		Yrs	Yrs	Yrs	Yrs	Yrs	Yrs	Yrs		Yrs	Yrs	Yrs	Yrs	Yrs	Yrs	Yrs
Nuclide	**Progeny**	0.65	1	1.83	2	3	5	6		0.65	1	1.83	2	3	5	6
H-3		8.452E-04	8.287E-04	7.910E-04	7.835E-04	7.407E-04	6.621E-04	6.259E-04		8.452E-01	8.287E-01	7.910E-01	7.835E-01	7.407E-01	6.621E-01	6.259E-01
Na-24																
P-32		1.793E-09	3.651E-12							1.992E-04	4.057E-07					
Cr-51		6.184E-05	2.523E-06	1.281E-09	2.708E-10	2.906E-14				1.237E-01	5.046E-03	2.561E-06	5.415E-07	5.811E-11		
Mn-54																
Mn-56																
Fe-55																
Fe-59																
Co-58																
Co-60																
Ni-63		2.905E-05	2.898E-05	2.881E-05	2.877E-05	2.856E-05	2.816E-05	2.795E-05		2.905E-01	2.898E-01	2.881E-01	2.877E-01	2.856E-01	2.816E-01	2.795E-01
Cu-64																
Zn-65																
Rb-89																
	Sr-89															
Sr-90		1.501E-11	2.183E-15							3.002E-05	4.365E-09					
	Y-90	1.501E-11	2.183E-15							2.144E-06	3.118E-10					
Sr-91																
	Y-91m															
	Y-91															
Sr-92																
	Y-92															
Y-93																
Zr-95		9.228E-06	2.311E-06	8.667E-08	4.424E-08	8.469E-10	3.103E-13	5.941E-15		4.614E-01	1.155E-01	4.333E-03	2.212E-03	4.234E-05	1.552E-08	2.970E-10
	Nb-95m	6.845E-08	1.714E-08	6.430E-10	3.282E-10	6.282E-12	2.302E-15			2.282E-03	5.715E-04	2.143E-05	1.094E-05	2.094E-07	7.674E-11	
	Nb-95	1.875E-05	4.995E-06	1.923E-07	9.824E-08	1.883E-09	6.899E-13	1.321E-14		6.249E-01	1.665E-01	6.410E-03	3.275E-03	6.276E-05	2.300E-08	4.403E-10

Table 2.4-238 Lake Erie - Decay Plus Retardation (Sheet 2 of 3)

Decay Plus Retardation Concentrations At Lake (µCi/ml)										Decay Plus Retardation GW/ECL at Lake						
		Yrs	Yrs	Yrs	Yrs	Yrs	Yrs	Yrs		Yrs	Yrs	Yrs	Yrs	Yrs	Yrs	Yrs
Nuclide	**Progeny**	0.65	1	1.83	2	3	5	6		0.65	1	1.83	2	3	5	6
Mo-99																
	Tc-99m															
Ru-103																
	Rh-103 m															
Ru-106																
	Rh-106															
Ag-110m																
	Ag-110															
Te-129m		2.885E-06	2.064E-07	3.969E-10	1.103E-10	5.889E-14				4.121E-01	2.949E-02	5.671E-05	1.575E-05	8.413E-09		
	Te-129	1.878E-06	1.344E-07	2.584E-10	7.177E-11	3.834E-14				4.694E-03	3.359E-04	6.459E-07	1.794E-07	9.584E-11		
Te-131m																
	Te-131															
	I-131	8.029E-12								8.029E-06						
Te-132																
	I-132															
I-133																
	Xe-133 m															
	Xe-133															
I-134																
I-135																
	Xe-135 m															
	Xe-135															
Cs-134																
Cs-136		2.288E-10	2.641E-13							3.813E-05	4.402E-08					

Table 2.4-238 Lake Erie - Decay Plus Retardation (Sheet 3 of 3)

Decay Plus Retardation Concentrations At Lake (µCi/ml)										Decay Plus Retardation GW/ECL at Lake						
		Yrs	Yrs	Yrs	Yrs	Yrs	Yrs	Yrs		Yrs	Yrs	Yrs	Yrs	Yrs	Yrs	Yrs
Nuclide	**Progeny**	0.65	1	1.83	2	3	5	6		0.65	1	1.83	2	3	5	6
Cs-137																
	Ba-137 m															
Cs-138																
Ba-140		3.718E-09	3.468E-12							4.647E-04	4.336E-07					
	La-140	4.285E-09	3.997E-12							4.761E-04	4.441E-07					
Ce-141		1.692E-06	1.107E-07	1.723E-10	4.584E-11	1.897E-14				5.640E-02	3.691E-03	5.744E-06	1.528E-06	6.32E-10		
Ce-144																
	Pr-144m															
	Pr-144															
W-187																
Np-239																
	Pu-239	1.734E-09	1.734E-09	1.734E-09	1.734E-09	1.734E-09	1.734E-09	1.734E-09		8.671E-02	8.671E-02	8.671E-02	8.671E-02	8.671E-02	8.670E-02	8.670E-02
								Sum of Fractions		2.909E+00	1.526E+00	1.177E+00	1.163E+00	1.113E+00	1.030E+00	9.921E-01

(1) Blank cells (i.e., no numerical results) represent results that are essentially zero.

Table 2.4-239 Off Site Well – Decay Plus Retardation (Sheet 1 of 3)

		Decay Plus Retardation Concentrations at Well (µCi/ml)						Decay Plus Retardation GW/ECL at Well				
		Yrs	Yrs	Yrs	Yrs	Yrs		Yrs	Yrs	Yrs	Yrs	Yrs
Nuclide	Progeny	1.83	2	3	5	6		1.83	2	3	5	6
H-3		7.910E-04	7.835E-04	7.407E-04	6.621E-04	6.259E-04		7.910E-01	7.835E-01	7.407E-01	6.621E-01	6.259E-01
Na-24												
P-32												
Cr-51		1.281E-09	2.708E-10	2.906E-14				2.561E-06	5.415E-07	5.811E-11		
Mn-54												
Mn-56												
Fe-55												
Fe-59												
Co-58												
Co-60												
Ni-63		2.881E-05	2.877E-05	2.856E-05	2.816E-05	2.795E-05		2.881E-01	2.877E-01	2.856E-01	2.816E-01	2.795E-01
Cu-64												
Zn-65												
Rb-89												
	Sr-89											
Sr-90												
	Y-90											
Sr-91												
	Y-91m											
	Y-91											
Sr-92												
	Y-92											
Y-93												

Table 2.4-239 Off Site Well – Decay Plus Retardation (Sheet 2 of 3)

		Decay Plus Retardation Concentrations at Well (µCi/ml)						Decay Plus Retardation GW/ECL at Well				
		Yrs	Yrs	Yrs	Yrs	Yrs		Yrs	Yrs	Yrs	Yrs	Yrs
Nuclide	Progeny	1.83	2	3	5	6		1.83	2	3	5	6
Zr-95		8.667E-08	4.424E-08	8.469E-10	3.103E-13	5.941E-15		4.333E-03	2.212E-03	4.234E-05	1.552E-08	2.970E-10
	Nb-95m	6.430E-10	3.282E-10	6.282E-12	2.302E-15			2.143E-05	1.094E-05	2.094E-07	7.674E-11	
	Nb-95	1.923E-07	9.824E-08	1.883E-09	6.899E-13	1.321E-14		6.410E-03	3.275E-03	6.276E-05	2.300E-08	4.403E-10
Mo-99												
	Tc-99m											
Ru-103												
	Rh-103m											
Ru-106												
	Rh-106											
Ag-110m												
	Ag-110											
Te-129m		3.969E-10	1.103E-10	5.889E-14				5.671E-05	1.575E-05	8.413E-09		
	Te-129	2.584E-10	7.177E-11	3.834E-14				6.459E-07	1.794E-07	9.584E-11		
Te-131m												
	Te-131											
	I-131											
Te-132												
	I-132											
I-133												
	Xe-133m											
	Xe-133											
I-134												
I-135												

Table 2.4-239 Off Site Well – Decay Plus Retardation (Sheet 3 of 3)

		Decay Plus Retardation Concentrations at Well (µCi/ml)						Decay Plus Retardation GW/ECL at Well				
		Yrs	Yrs	Yrs	Yrs	Yrs		Yrs	Yrs	Yrs	Yrs	Yrs
Nuclide	Progeny	1.83	2	3	5	6		1.83	2	3	5	6
	Xe-135m											
	Xe-135											
Cs-134												
Cs-136												
Cs-137												
	Ba-137m											
Cs-138												
Ba-140												
	La-140											
Ce-141		1.723E-10	4.584E-11	1.897E-14				5.744E-06	1.528E-06	6.324E-10		
Ce-144												
	Pr-144m											
	Pr-144											
W-187												
Np-239												
	Pu-239	1.734E-09	1.734E-09	1.734E-09	1.734E-09	1.734E-09		8.671E-02	8.671E-02	8.671E-02	8.670E-02	8.670E-02
						Sum of Fractions		1.177E+00	1.163E+00	1.113E+00	1.030E+00	9.921E-01

(1) Blank cells (i.e., no numerical results) represent results that are essentially zero.

Table 2.4-240 Lake Erie - Decay Plus Retardation, Factor of 10 for Dilution (Sheet 1 of 3)

Decay Plus Retardation Plus Dilution Concentrations At Lake (µCi/ml)										Decay Plus Retardation Plus Dilution GW/ECL at Lake						
		Yrs	Yrs	Yrs	Yrs	Yrs	Yrs	Yrs		Yrs	Yrs	Yrs	Yrs	Yrs	Yrs	Yrs
Nuclide	Progeny	0.65	1	1.83	2	3	5	6		0.65	1	1.83	2	3	5	6
H-3		8.452E-05	8.287E-05	7.910E-05	7.835E-05	7.407E-05	6.621E-05	6.259E-05		8.452E-02	8.287E-02	7.910E-02	7.835E-02	7.407E-02	6.621E-02	6.259E-02
Na-24																
P-32		1.793E-10	3.651E-13							1.992E-05	4.057E-08					
Cr-51		6.184E-06	2.523E-07	1.281E-10	2.708E-11	2.906E-15				1.237E-02	5.046E-04	2.561E-07	5.415E-08	5.811E-12		
Mn-54																
Mn-56																
Fe-55																
Fe-59																
Co-58																
Co-60																
Ni-63		2.905E-06	2.898E-06	2.881E-06	2.877E-06	2.856E-06	2.816E-06	2.795E-06		2.905E-02	2.898E-02	2.881E-02	2.877E-02	2.856E-02	2.816E-02	2.795E-02
Cu-64																
Zn-65																
Rb-89																
	Sr-89															
Sr-90		1.501E-12								3.002E-06						
	Y-90	1.501E-12								2.144E-07						
Sr-91																
	Y-91m															
	Y-91															
Sr-92																
	Y-92															
Y-93																

Table 2.4-240 Lake Erie - Decay Plus Retardation, Factor of 10 for Dilution (Sheet 2 of 3)

Decay Plus Retardation Plus Dilution Concentrations At Lake (µCi/ml)										Decay Plus Retardation Plus Dilution GW/ECL at Lake						
		Yrs	Yrs	Yrs	Yrs	Yrs	Yrs	Yrs		Yrs	Yrs	Yrs	Yrs	Yrs	Yrs	Yrs
Nuclide	Progeny	0.65	1	1.83	2	3	5	6		0.65	1	1.83	2	3	5	6
Zr-95		9.228E-07	2.311E-07	8.667E-09	4.424E-09	8.469E-11	3.103E-14			4.614E-02	1.155E-02	4.333E-04	2.212E-04	4.234E-06	1.552E-09	
	Nb-95m	6.845E-09	1.714E-09	6.430E-11	3.282E-11	6.282E-13				2.282E-04	5.715E-05	2.143E-06	1.094E-06	2.094E-08		
	Nb-95	1.875E-06	4.995E-07	1.923E-08	9.824E-09	1.883E-10	6.899E-14	1.321E-15		6.249E-02	1.665E-02	6.410E-04	3.275E-04	6.276E-06	2.300E-09	4.403E-11
Mo-99																
	Tc-99m															
Ru-103																
	Rh-103m															
Ru-106																
	Rh-106															
Ag-110m																
	Ag-110															
Te-129m		2.885E-07	2.064E-08	3.969E-11	1.103E-11	5.889E-15				4.121E-02	2.949E-03	5.671E-06	1.575E-06	8.413E-10		
	Te-129	1.878E-07	1.344E-08	2.584E-11	7.177E-12	3.834E-15				4.694E-04	3.359E-05	6.459E-08	1.794E-08	9.584E-12		
Te-131m																
	Te-131															
	I-131	8.029E-13								8.029E-07						
Te-132																
	I-132															
I-133																
	Xe-133m															
	Xe-133															
I-134																
I-135																
	Xe-135m															
	Xe-135															
Cs-134																

Table 2.4-240 Lake Erie - Decay Plus Retardation, Factor of 10 for Dilution (Sheet 3 of 3)

Decay Plus Retardation Plus Dilution Concentrations At Lake (µCi/ml)										Decay Plus Retardation Plus Dilution GW/ECL at Lake						
		Yrs	Yrs	Yrs	Yrs	Yrs	Yrs	Yrs		Yrs	Yrs	Yrs	Yrs	Yrs	Yrs	Yrs
Nuclide	Progeny	0.65	1	1.83	2	3	5	6		0.65	1	1.83	2	3	5	6
Cs-136		2.288E-11	2.641E-14							3.813E-06	4.402E-09					
Cs-137																
	Ba-137m															
Cs-138																
Ba-140		3.718E-10	3.468E-13							4.647E-05	4.336E-08					
	La-140	4.285E-10	3.997E-13							4.761E-05	4.441E-08					
Ce-141		1.692E-07	1.107E-08	1.723E-11	4.584E-12	1.897E-15				5.640E-03	3.691E-04	5.744E-07	1.528E-07	6.324E-11		
Ce-144																
	Pr-144m															
	Pr-144															
W-187																
Np-239																
	Pu-239	1.734E-10	1.734E-10	1.734E-10	1.734E-10	1.734E-10	1.734E-10	1.734E-10		8.671E-03	8.671E-03	8.671E-03	8.671E-03	8.671E-03	8.670E-03	8.670E-03
								Sum of Fractions		2.909E-01	1.526E-01	1.177E-01	1.163E-01	1.113E-01	1.030E-01	9.921E-02

(1) Blank cells (i.e., no numerical results) represent results that are essentially zero.
(2) The above table shows the results out to six years; which are sufficient to show a decline in the radionuclide concentrations.

Table 2.4-241 Off Site Well - Decay Plus Retardation Plus 1-D Dispersion (H-3, Ni-63, Pu-239 Only) (Sheet 1 of 3)

Decay Plus Retardation Plus 1-D Dispersion Concentrations At Well (µCi/ml)									Decay Plus Retardation Plus 1-D Dispersion GW/ECL at Well					
		Yrs	Yrs	Yrs	Yrs	Yrs	Yrs		Yrs	Yrs	Yrs	Yrs	Yrs	Yrs
Nuclide	Progeny	1.83	2	3	4	5	6		1.83	2	3	4	5	6
H-3		4.023E-04	5.923E-04	7.407E-04	7.003E-04	6.620E-04	6.259E-04		4.023E-01	5.923E-01	7.407E-01	7.003E-01	6.620E-01	6.259E-01
Na-24														
P-32														
Cr-51		1.281E-09	2.708E-10	2.906E-14					2.561E-06	5.415E-07	5.811E-11			
Mn-54														
Mn-56														
Fe-55														
Fe-59														
Co-58														
Co-60														
Ni-63		1.465E-05	2.175E-05	2.856E-05	2.836E-05	2.816E-05	2.795E-05		1.465E-01	2.175E-01	2.856E-01	2.836E-01	2.816E-01	2.795E-01
Cu-64														
Zn-65														
Rb-89														
	Sr-89													
Sr-90														
	Y-90													
Sr-91														
	Y-91m													
	Y-91													
Sr-92														
	Y-92													
Y-93														
Zr-95		8.667E-08	4.424E-08	8.469E-10		3.103E-13	5.941E-15		4.333E-03	2.212E-03	4.234E-05		1.552E-08	2.970E-10

Table 2.4-241 Off Site Well - Decay Plus Retardation Plus 1-D Dispersion (H-3, Ni-63, Pu-239 Only) (Sheet 2 of 3)

Decay Plus Retardation Plus 1-D Dispersion Concentrations At Well (µCi/ml)									Decay Plus Retardation Plus 1-D Dispersion GW/ECL at Well					
		Yrs	Yrs	Yrs	Yrs	Yrs	Yrs		Yrs	Yrs	Yrs	Yrs	Yrs	Yrs
Nuclide	Progeny	1.83	2	3	4	5	6		1.83	2	3	4	5	6
	Nb-95m	6.430E-10	3.282E-10	6.282E-12		2.302E-15			2.143E-05	1.094E-05	2.094E-07		7.674E-11	
	Nb-95	1.923E-07	9.824E-08	1.883E-09		6.899E-13	1.321E-14		6.410E-03	3.275E-03	6.276E-05		2.300E-08	4.403E-10
Mo-99														
	Tc-99m													
Ru-103														
	Rh-103m													
Ru-106														
	Rh-106													
Ag-110m														
	Ag-110													
Te-129m		3.969E-10	1.103E-10	5.889E-14					5.671E-05	1.575E-05	8.413E-09			
	Te-129	2.584E-10	7.177E-11	3.834E-14					6.459E-07	1.794E-07	9.584E-11			
Te-131m														
	Te-131													
	I-131													
Te-132														
	I-132													
I-133														
	Xe-133m													
	Xe-133													
I-134														
I-135														
	Xe-135m													
	Xe-135													

Table 2.4-241 Off Site Well - Decay Plus Retardation Plus 1-D Dispersion (H-3, Ni-63, Pu-239 Only) (Sheet 3 of 3)

Decay Plus Retardation Plus 1-D Dispersion Concentrations At Well (µCi/ml)									Decay Plus Retardation Plus 1-D Dispersion GW/ECL at Well					
		Yrs	Yrs	Yrs	Yrs	Yrs	Yrs		Yrs	Yrs	Yrs	Yrs	Yrs	Yrs
Nuclide	Progeny	1.83	2	3	4	5	6		1.83	2	3	4	5	6
Cs-134														
Cs-136														
Cs-137														
	Ba-137m													
Cs-138														
Ba-140														
	La-140													
Ce-141		1.723E-10	4.584E-11	1.897E-14					5.744E-06	1.528E-06	6.324E-10			
Ce-144														
	Pr-144m													
	Pr-144													
W-187														
Np-239														
	Pu-239	2.940E-11	4.370E-11	5.780E-11	5.780E-11	5.780E-11	5.780E-11		1.470E-03	2.185E-03	2.890E-03	2.890E-03	2.890E-03	2.890E-03
							Sum of Fractions		5.611E-01	8.175E-01	1.029E+00	9.868E-01	9.465E-01	9.083E-01

(1) Blank cells (i.e., no numerical results) are essentially zero.

Table 2.4-242 Off Site Well - Decay Plus Retardation Plus 2-D Dispersion (H-3, Ni-63, Pu-239 Only) (Sheet 1 of 3)

Decay Plus Retardation Plus 2-D Dispersion Concentrations At Well (µCi/ml)									Decay Plus Retardation Plus 2-D Dispersion GW/ECL at Well					
		Yrs	Yrs	Yrs	Yrs	Yrs	Yrs		Yrs	Yrs	Yrs	Yrs	Yrs	Yrs
Nuclide	Progeny	1.83	2	3	4	5	6		1.83	2	3	4	5	6
H-3		3.381E-05	4.797E-05	5.701E-05	5.390E-05	5.096E-05	4.817E-05		3.381E-02	4.797E-02	5.701E-02	5.390E-02	5.096E-02	4.817E-02
Na-24														
P-32														
Cr-51		1.281E-09	2.708E-10	2.906E-14					2.561E-06	5.415E-07	5.811E-11			
Mn-54														
Mn-56														
Fe-55														
Fe-59														
Co-58														
Co-60														
Ni-63		1.231E-06	1.762E-06	2.200E-06	2.185E-06	2.169E-06	2.154E-06		1.231E-02	1.762E-02	2.200E-02	2.185E-02	2.169E-02	2.154E-02
Cu-64														
Zn-65														
Rb-89														
	Sr-89													
Sr-90														
	Y-90													
Sr-91														
	Y-91m													
	Y-91													
Sr-92														
	Y-92													
Y-93														
Zr-95		8.667E-08	4.424E-08	8.469E-10	1.621E-11	3.103E-13	5.941E-15		4.333E-03	2.212E-03	4.234E-05	8.106E-07	1.552E-08	2.970E-10

Table 2.4-242 Off Site Well - Decay Plus Retardation Plus 2-D Dispersion (H-3, Ni-63, Pu-239 Only) (Sheet 2 of 3)

Decay Plus Retardation Plus 2-D Dispersion Concentrations At Well (µCi/ml)									Decay Plus Retardation Plus 2-D Dispersion GW/ECL at Well					
		Yrs	Yrs	Yrs	Yrs	Yrs	Yrs		Yrs	Yrs	Yrs	Yrs	Yrs	Yrs
Nuclide	Progeny	1.83	2	3	4	5	6		1.83	2	3	4	5	6
	Nb-95m	6.430E-10	3.282E-10	6.282E-12	1.203E-13	2.302E-15			2.143E-05	1.094E-05	2.094E-07	4.009E-09	7.674E-11	
	Nb-95	1.923E-07	9.824E-08	1.883E-09	3.604E-11	6.899E-13	1.321E-14		6.410E-03	3.275E-03	6.276E-05	1.201E-06	2.300E-08	4.403E-10
Mo-99														
	Tc-99m													
Ru-103														
	Rh-103m													
Ru-106														
	Rh-106													
Ag-110m														
	Ag-110													
Te-129m		3.969E-10	1.103E-10	5.889E-14					5.671E-05	1.575E-05	8.413E-09			
	Te-129	2.584E-10	7.177E-11	3.834E-14					6.459E-07	1.794E-07	9.584E-11			
Te-131m														
	Te-131													
	I-131													
Te-132														
	I-132													
I-133														
	Xe-133m													
	Xe-133													
I-134														
I-135														
	Xe-135m													
	Xe-135													

Table 2.4-242 Off Site Well - Decay Plus Retardation Plus 2-D Dispersion (H-3, Ni-63, Pu-239 Only) (Sheet 3 of 3)

Decay Plus Retardation Plus 2-D Dispersion Concentrations At Well (µCi/ml)									Decay Plus Retardation Plus 2-D Dispersion GW/ECL at Well					
		Yrs	Yrs	Yrs	Yrs	Yrs	Yrs		Yrs	Yrs	Yrs	Yrs	Yrs	Yrs
Nuclide	Progeny	1.83	2	3	4	5	6		1.83	2	3	4	5	6
Cs-134														
Cs-136														
Cs-137														
	Ba-137m													
Cs-138														
Ba-140														
	La-140													
Ce-141		1.723E-10	4.584E-11	1.897E-14					5.744E-06	1.528E-06	6.324E-10			
Ce-144														
	Pr-144m													
	Pr-144													
W-187														
Np-239														
	Pu-239	2.471E-12	3.540E-12	4.451E-12	4.451E-12	4.451E-12	4.451E-12		1.235E-04	1.770E-04	2.225E-04	2.225E-04	2.225E-04	2.225E-04
							Sum of Fractions		5.708E-02	7.128E-02	7.934E-02	7.597E-02	7.287E-02	6.993E-02

(1) Blank cells (i.e., no numerical results) are essentially zero.
(2) The above table shows the results out to six years; which are sufficient to show a decline in the radionuclide concentrations.

Figure 2.4-201 Central, Eastern and Western Basin Areas of Lake Erie

Lake Saint Clair (Area 1)

The Islands Area (Area 2)

Pelee-Lorain Ridge, Point Pelee Ridge, Point Pelee Fan, and Sandusky Basin (Area 3)

Long Point Spit, Pennsylvania Channel, Clear Creek Ridge, Long Point-Erie Ridge, and Presque Isle Spit (Area 4)

Long Point Escarpment (Area 5)

Northern Shore of Eastern Erie Basin (Areas 6a and 6b)

Western Erie Basin (Area 7)

Central Erie Basin (Area 8)

Eastern Erie Basin (Area 9)

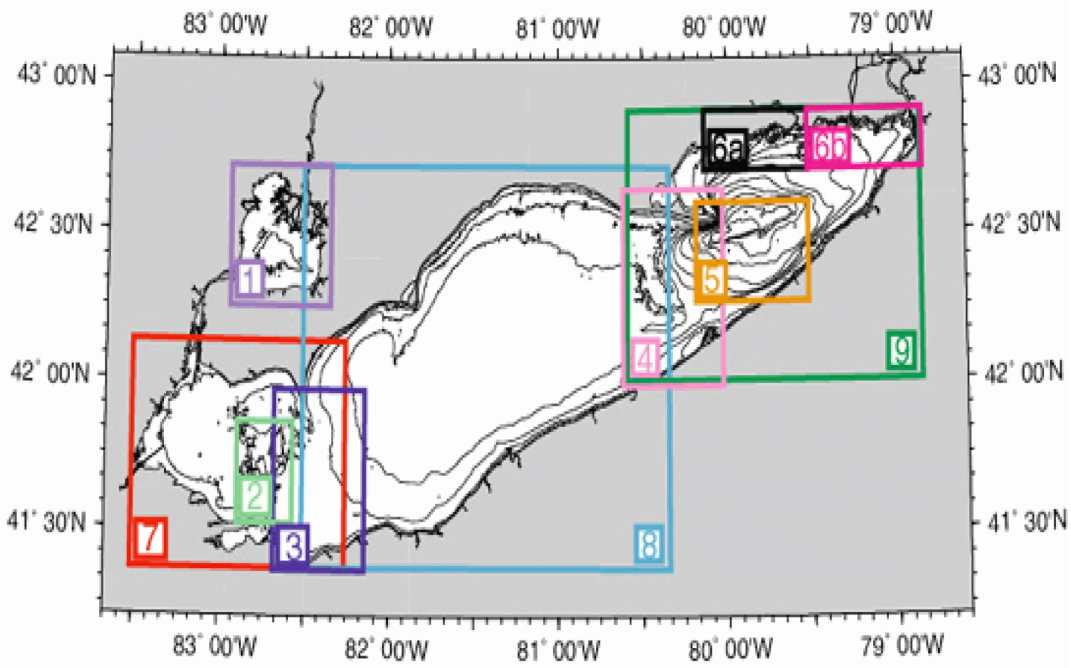

Source: Reference 2.4-203

Figure 2.4-202 Bathymetry of Lake Erie and Lake Saint Clair

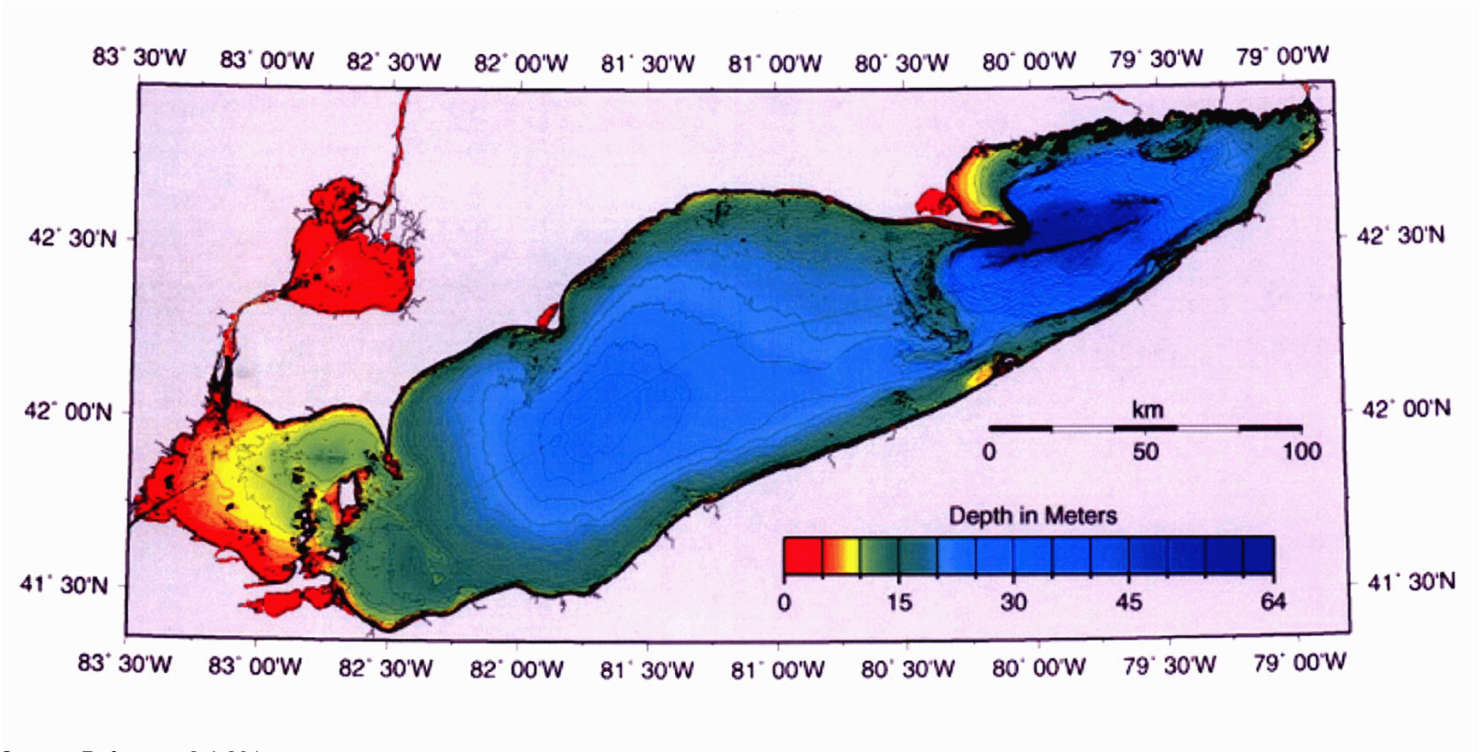

Source: Reference 2.4-201

Figure 2.4-203 Major Tributaries of Lake Erie

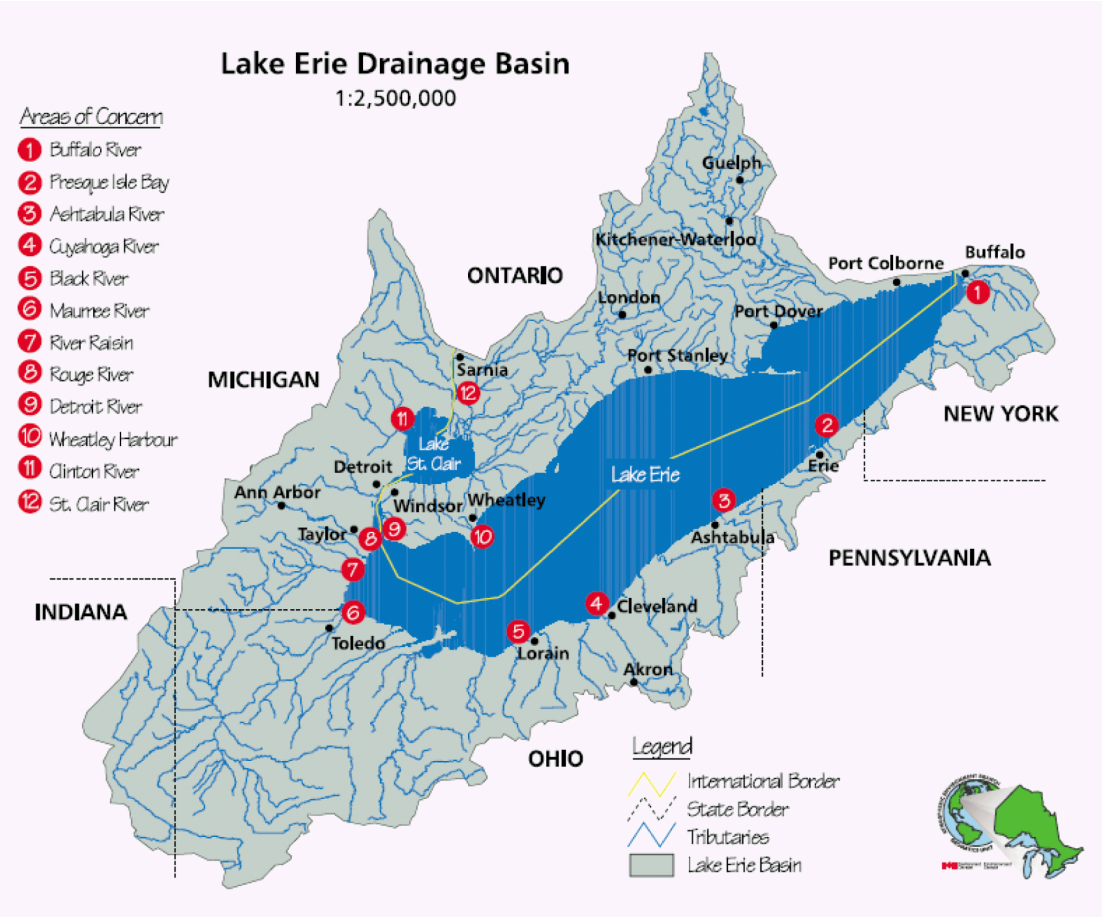

Source: Reference 2.4-205

Figure 2.4-204 The Great Lakes Region

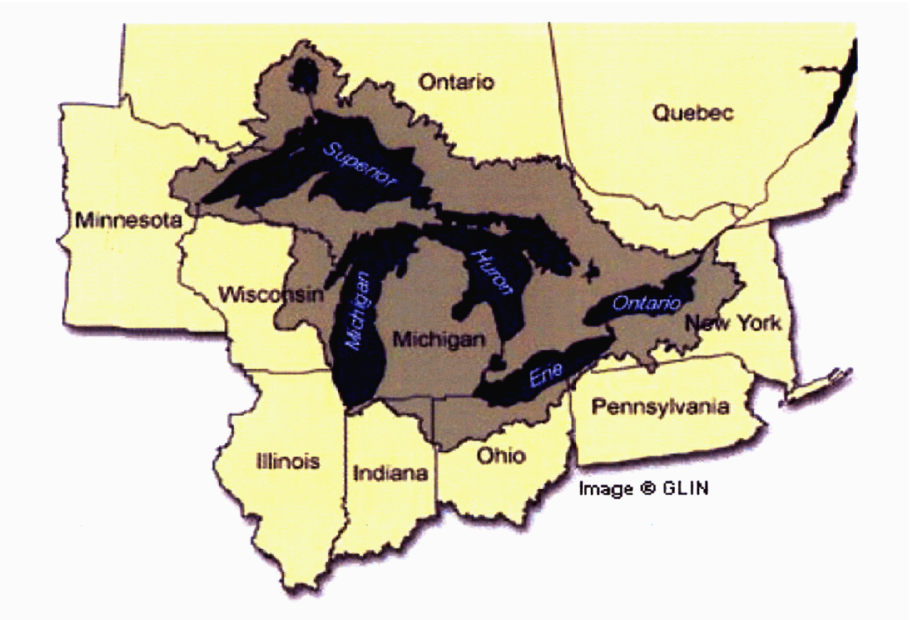

Source: Reference 2.4-206

Figure 2.4-205 Site Location and Vicinity Within 12 Km (7.5 Mi)

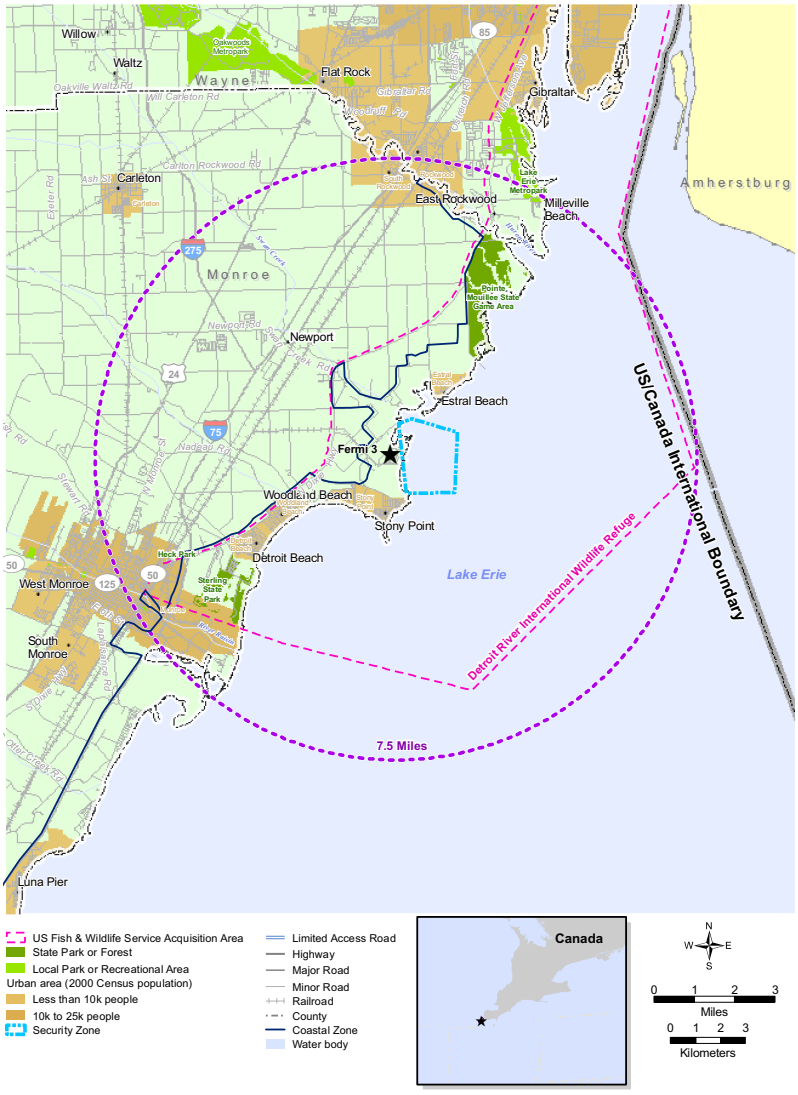

Figure 2.4-206 Hydrology of the Great Lakes Water System

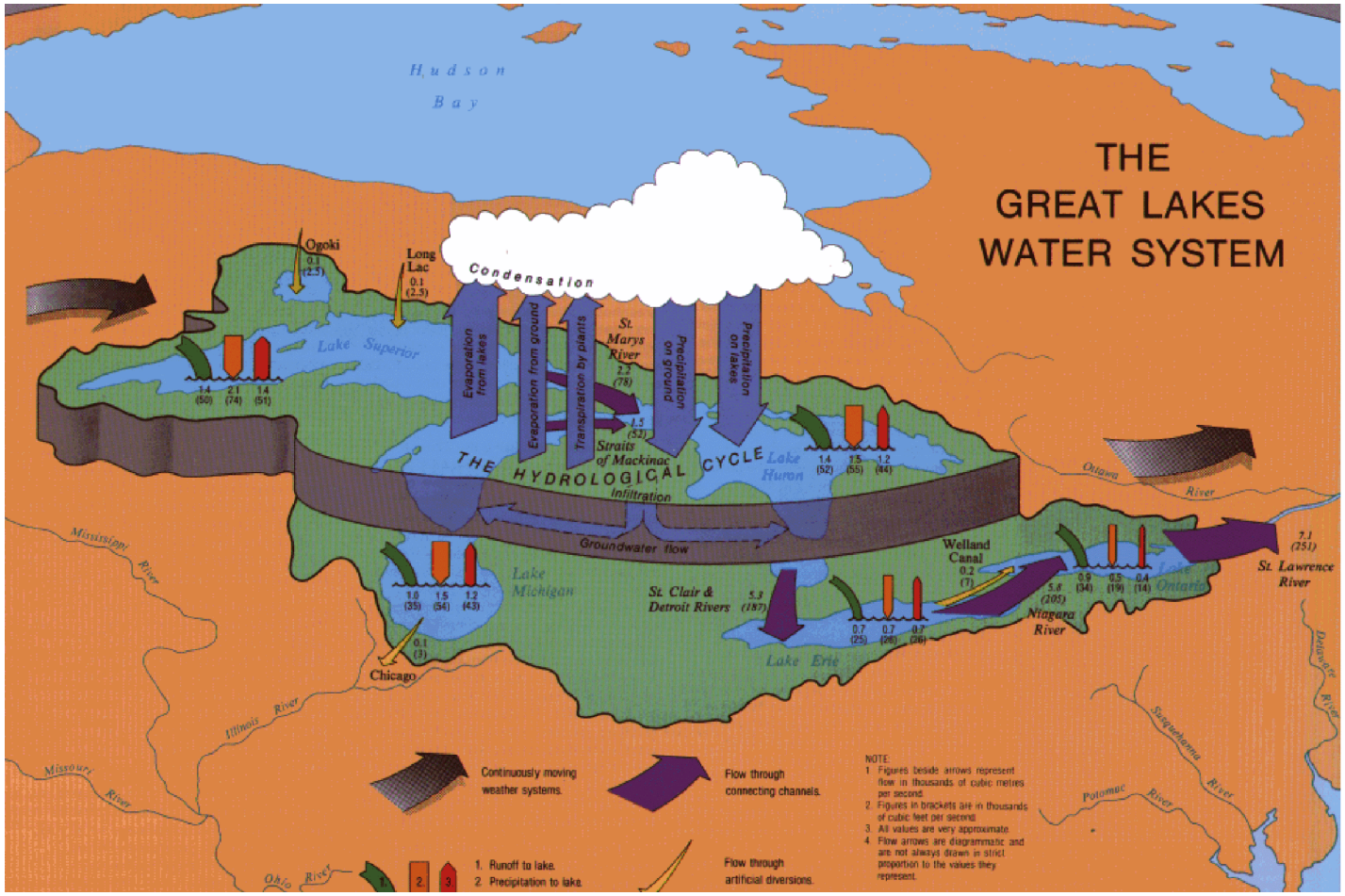

Source: Reference 2.4-218

Figure 2.4-207 Total Water Withdrawals by Sector in Michigan (MGD) 2000-2004

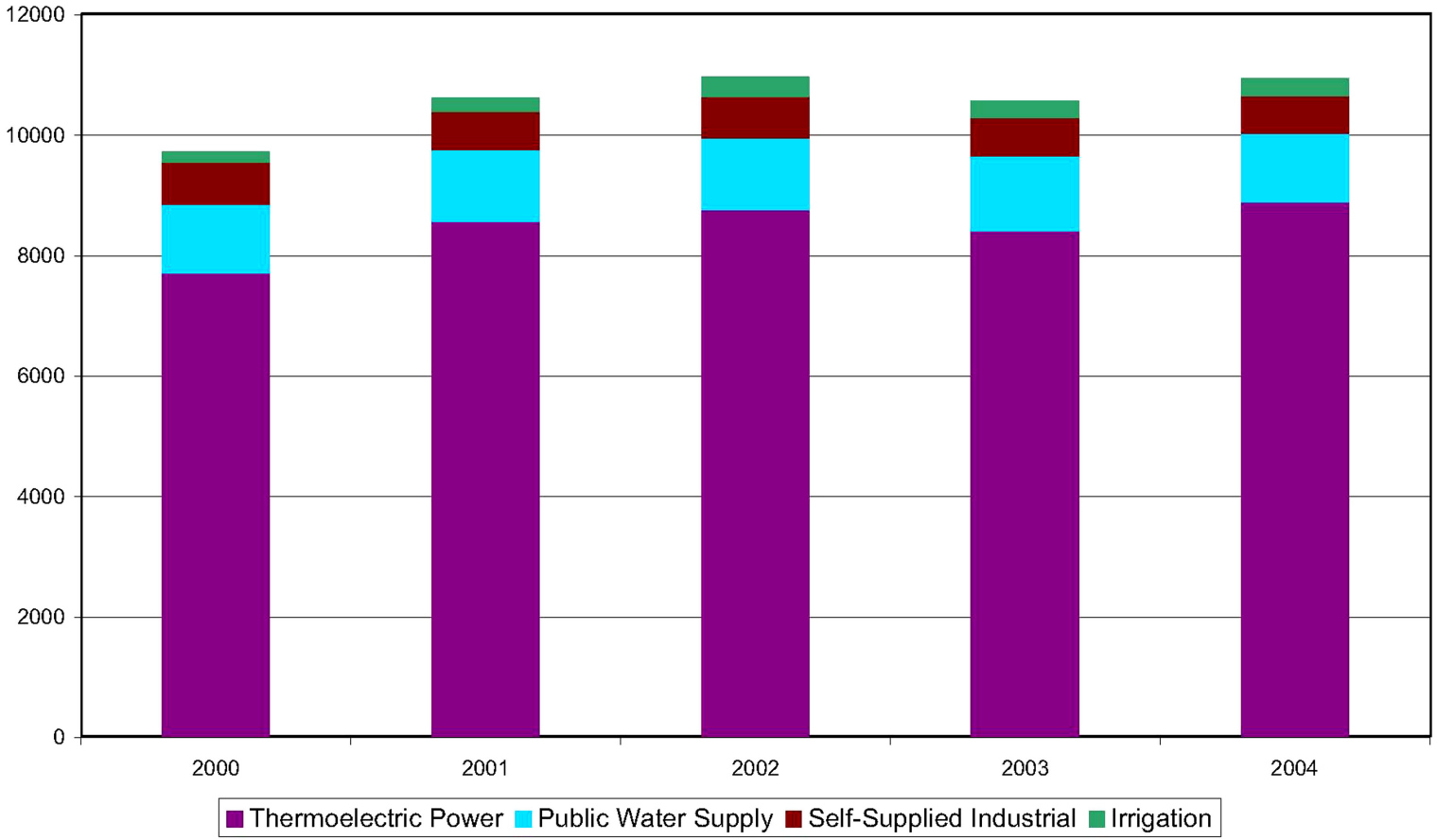

Source: Reference 2.4-216

Figure 2.4-208 Swan Creek and Stony Creek Watershed Basins

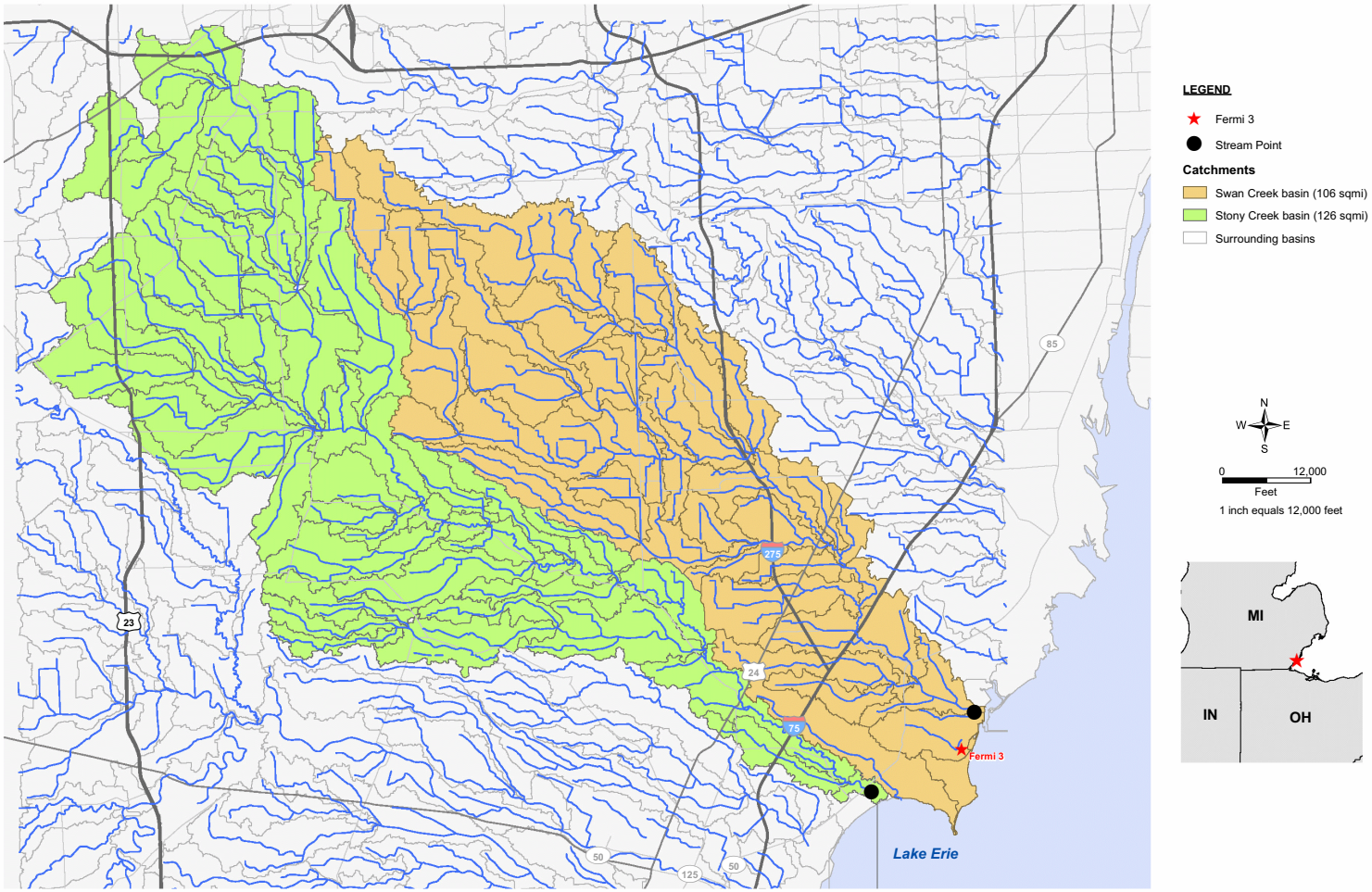

Source: Reference 2.4-240

Figure 2.4-209 Topographic Map for 12 km Vicinity around the Fermi Property (Base map: USGS 1:100,000 Scale Metric Topographic Map Series)

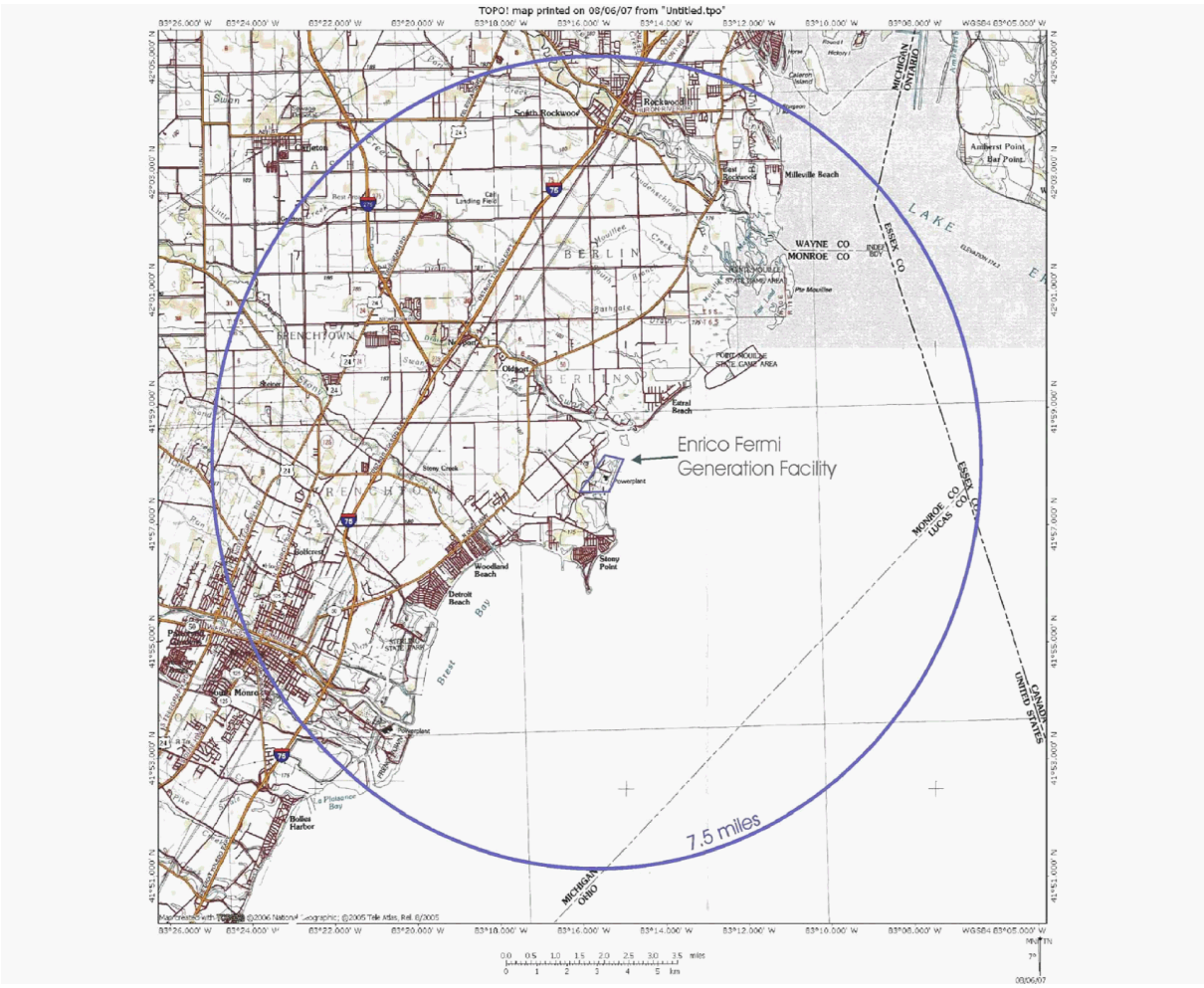
TOPO! map printed on 09/06/07 from "Untitled.tpo"
Enrico Fermi
Generation Facility
7.5 miles
LAKE
E
BERLIN
BRENCHTOWN
WAYNE CO
MONROE CO
ESSEX CO
MONROE CO
LUCAS CO
ESSEX CO
MICHIGAN
ONTARIO
CANADA
UNITED STATES
MICHIGAN
OHIO
Rockwood
South Rockwood
Milleville Beach
Amherst Point
Bar Point
Carleton
Gibraltar
Stony Point
Woodland Beach
Detroit Beach
Bolles Harbor
Monroe
Erie
Bay
Brest
Stony Creek
Swan
Sugar
Bolcover
Oldfield
Extral Beach
Fort Mouillee State Game Area
Pte Mouillee
Sterling State Park
Cal Landing Field
Bates
Mouillee Creek
Little Lake Erie
Elevation 174.3
Elevation 174.3
Elevation 174.3

Figure 2.4-210 Topographic Map Showing Fermi Property Boundary (Base map: USGS 1:24,000 7.5 Minute Topographic Series)

Figure 2.4-211 Fermi 3 Site Plan

Figure 2.4-212 Lake Erie Extreme Water Levels (1970-2007) NAVD 88

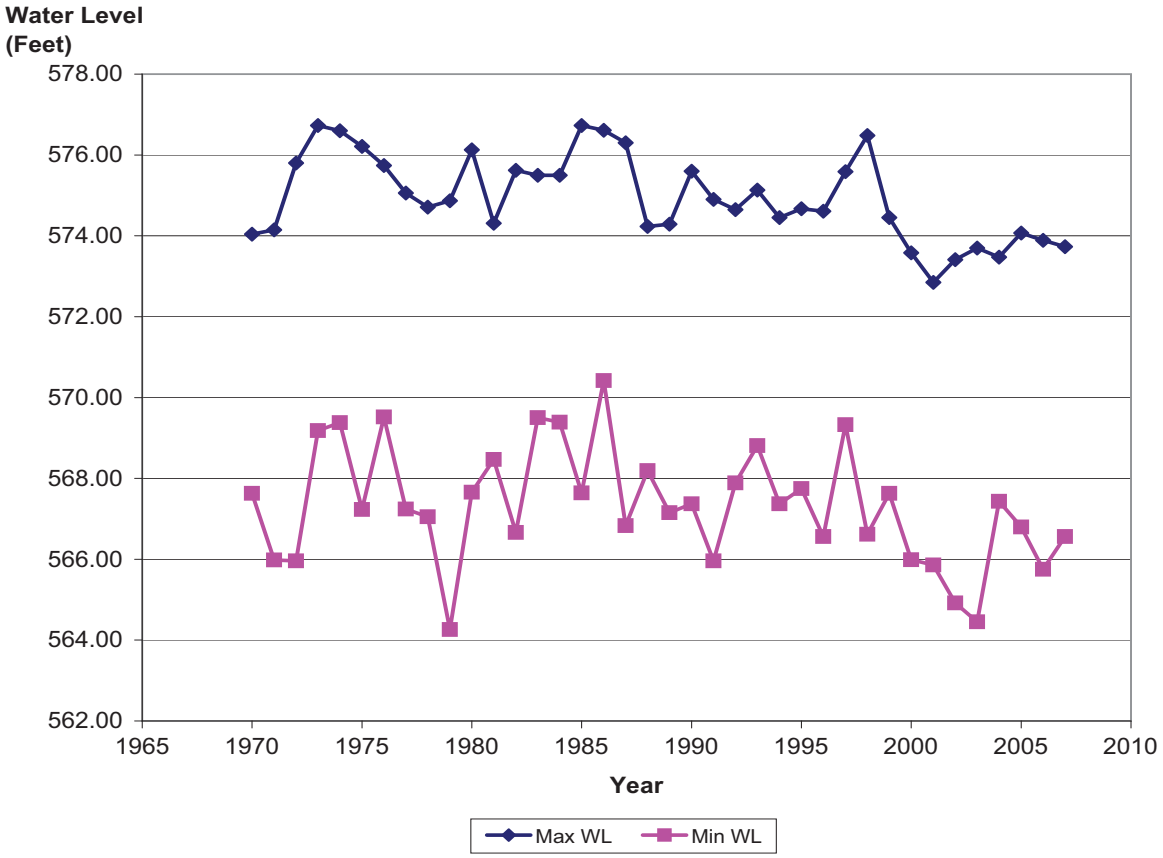

Source: Reference 2.4-228, Reference 2.4-234

Figure 2.4-213 Fermi 3 Site PMP Duration-Intensity Curve

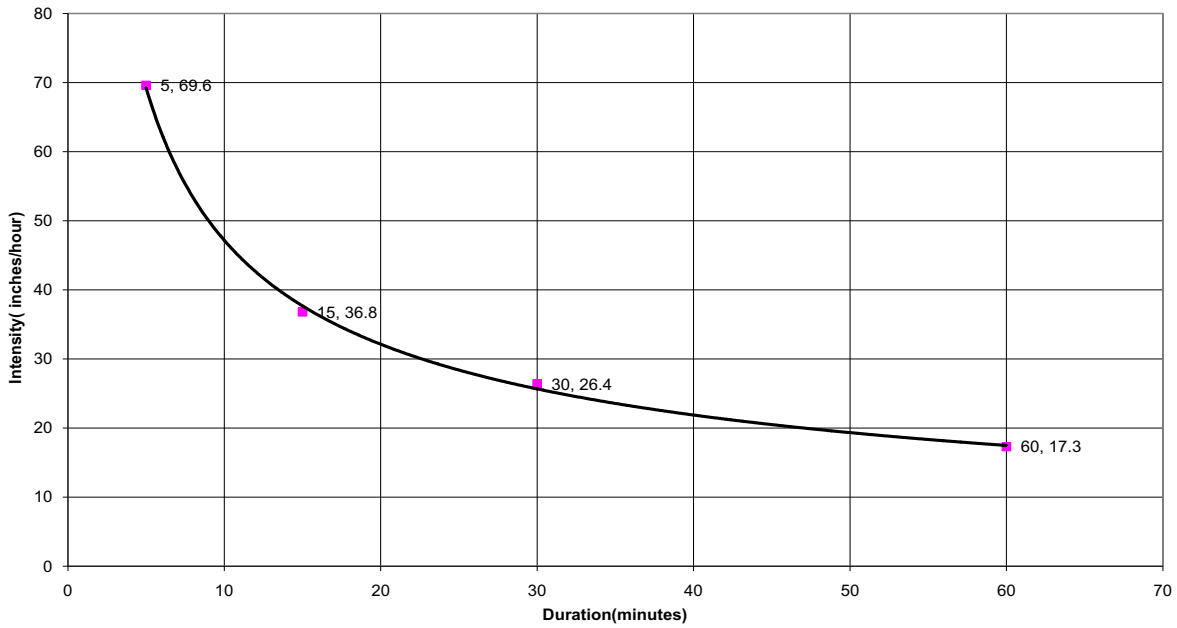

Figure 2.4-214 Existing Sub-Basin Drainage Areas

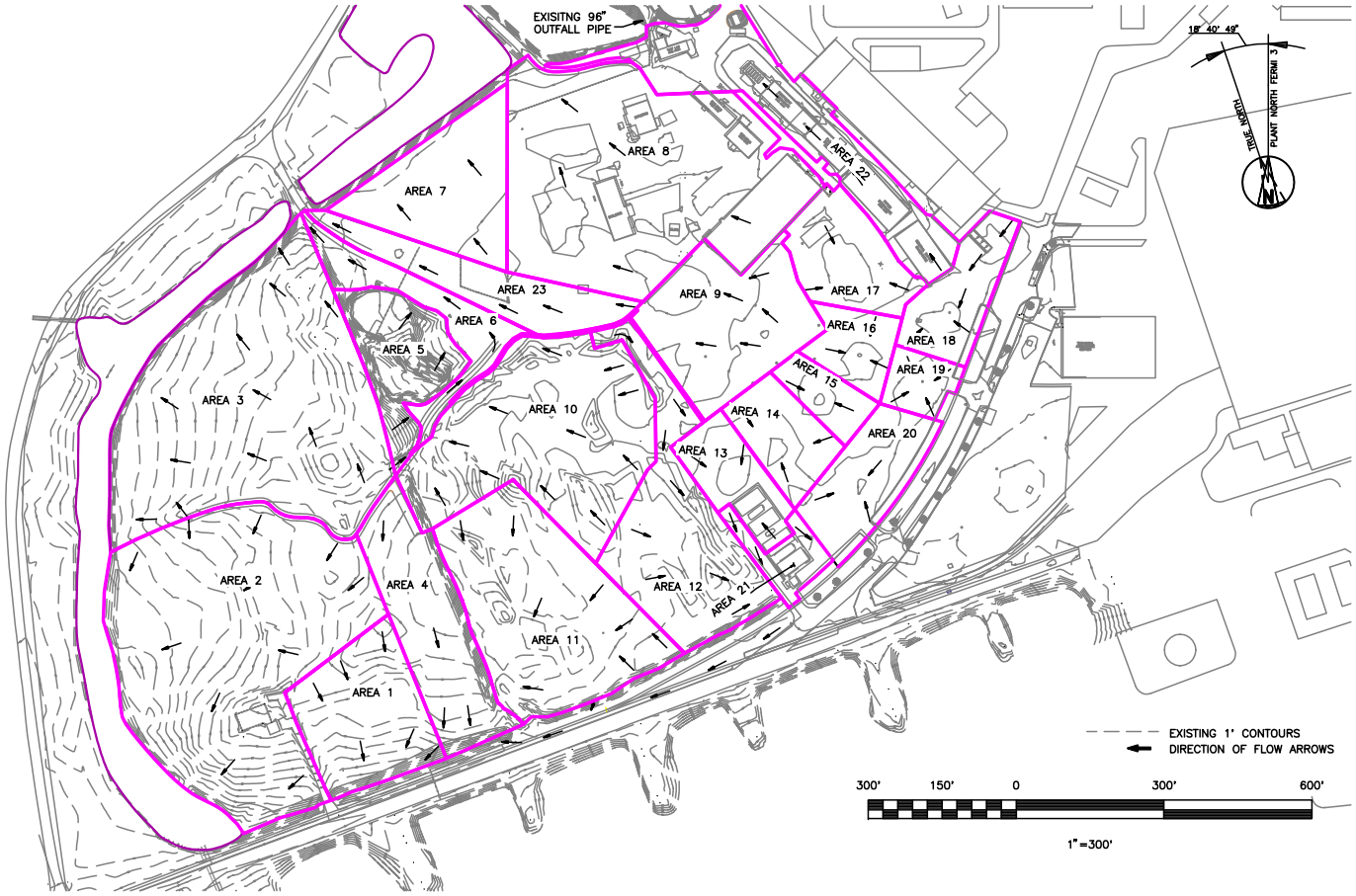

Figure 2.4-215 Final Grade Drainage Areas

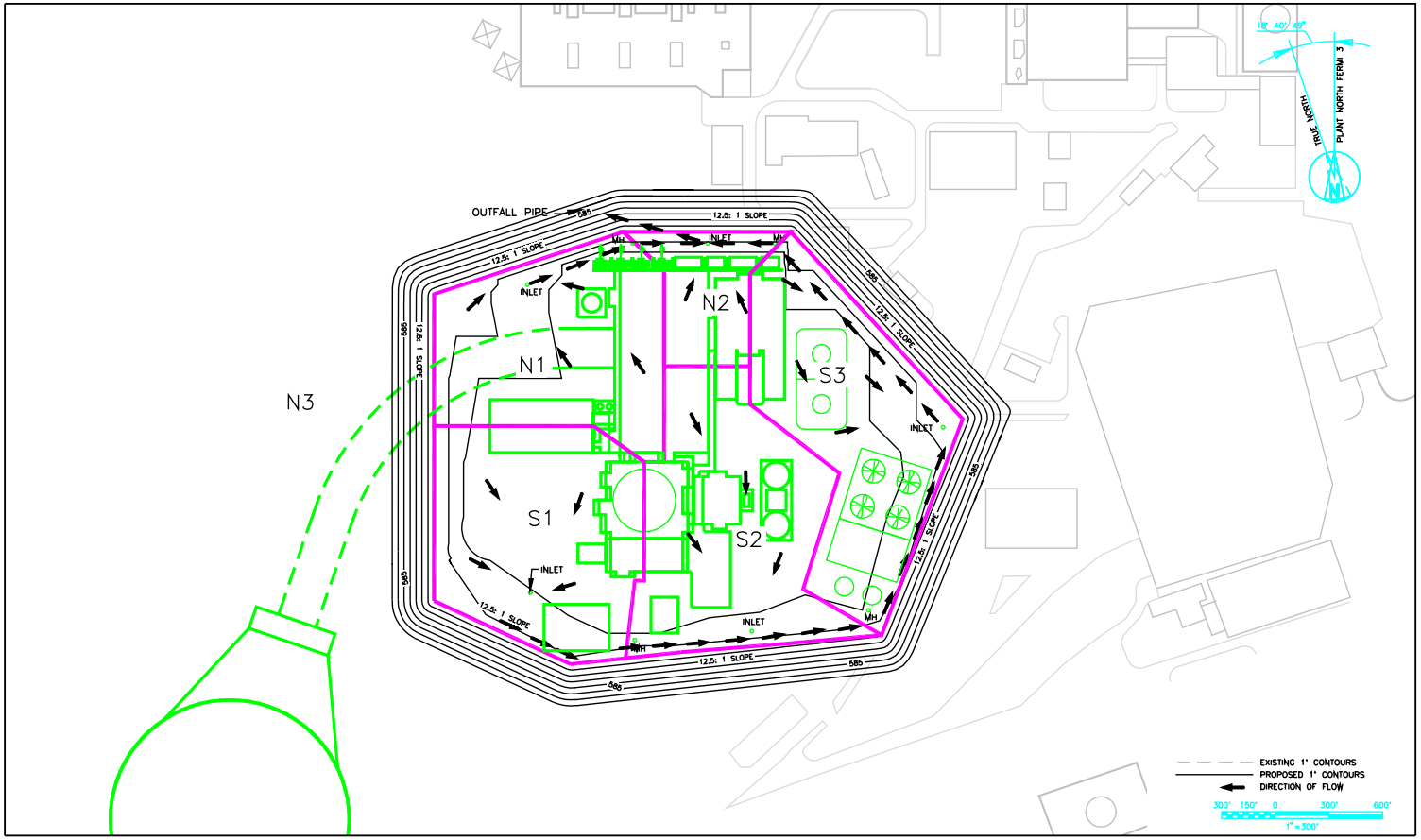

Figure 2.4-216 NRCS Dimensional Unit Hydrograph Q Results for One Square Mi PMF of Fermi 3

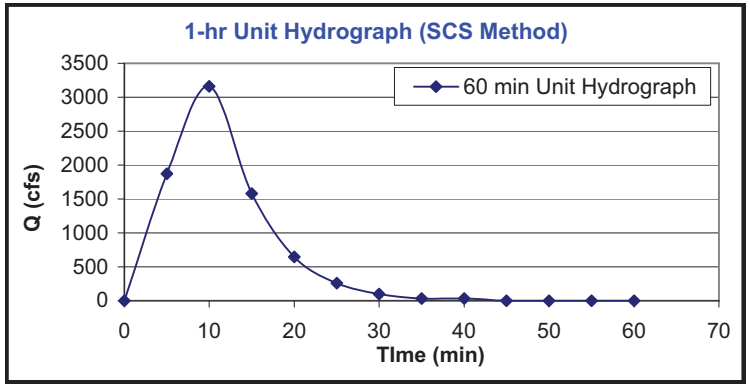

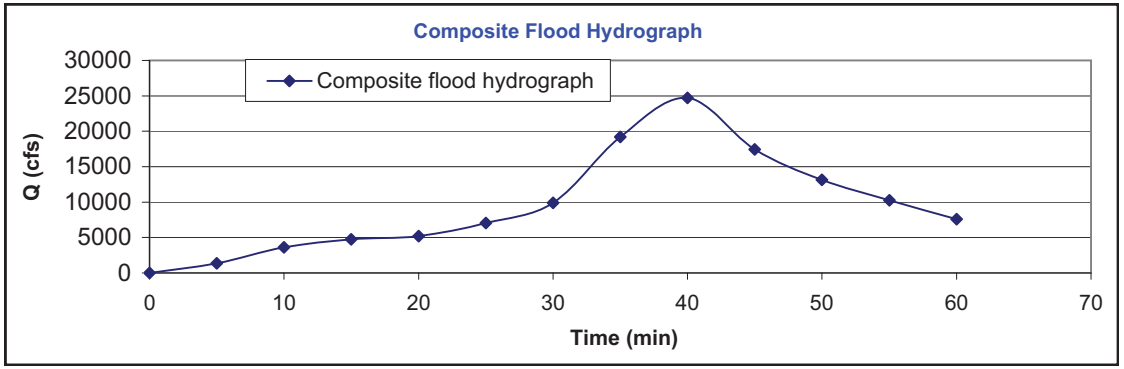

Figure 2.4-217 Final Grade Drainage Areas Assuming Clogged Underground Storm Drains and Culverts

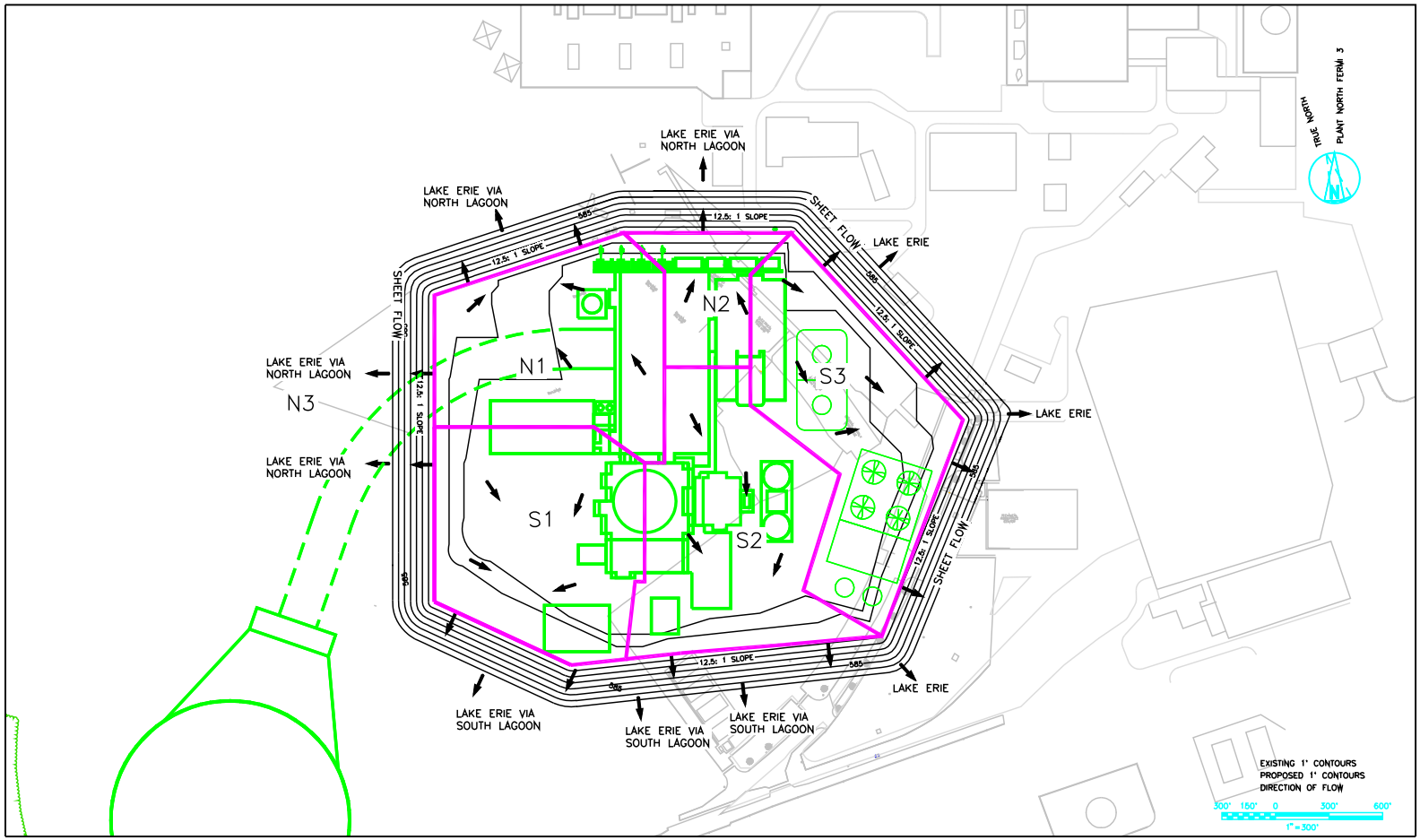

Figure 2.4-218 Swan Creek Cross-Sections

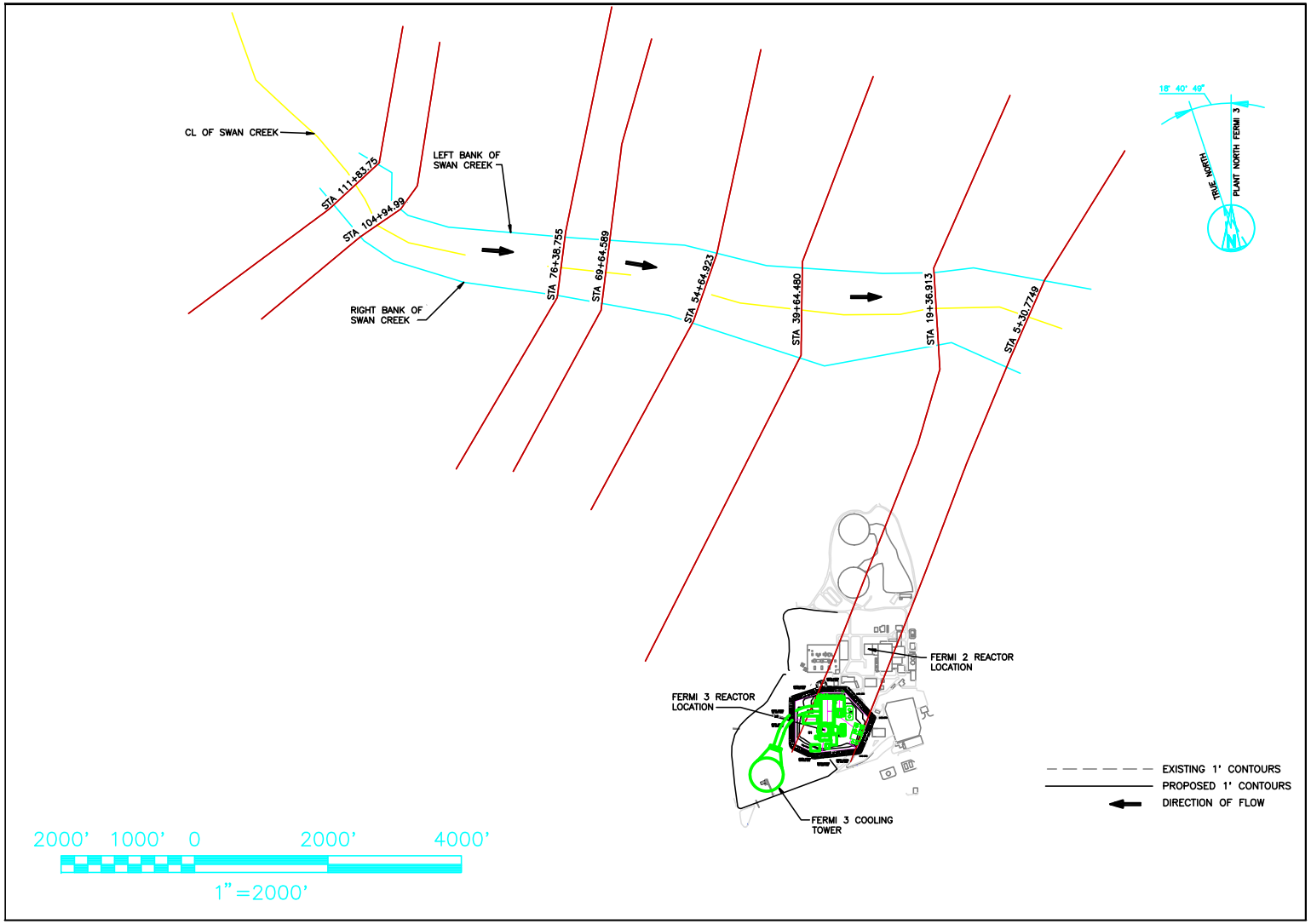

Figure 2.4-219 Hydrograph Results

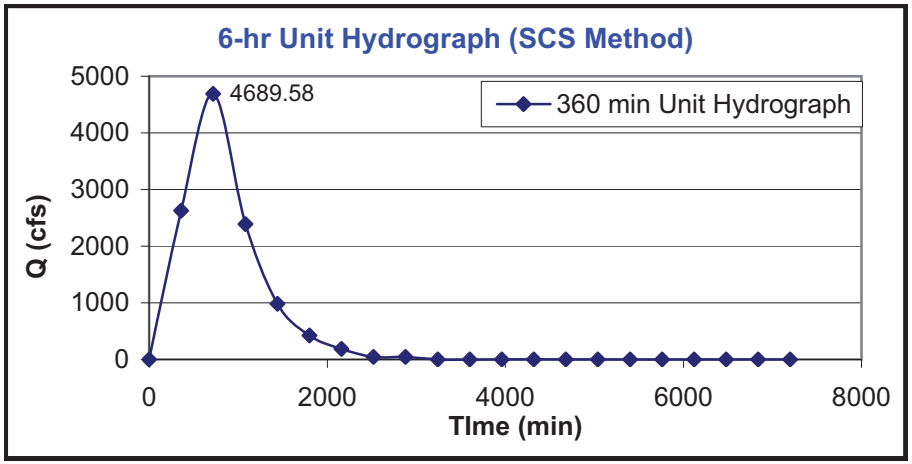

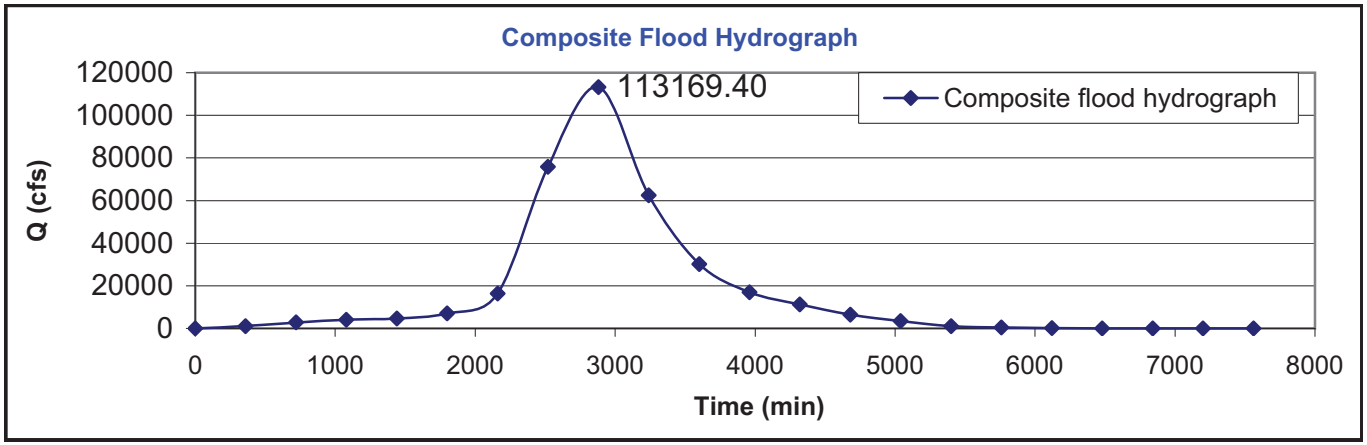

Figure 2.4-220 Alternative II - Swan Creek Profile from Station 0+00.00 to 111+39.77

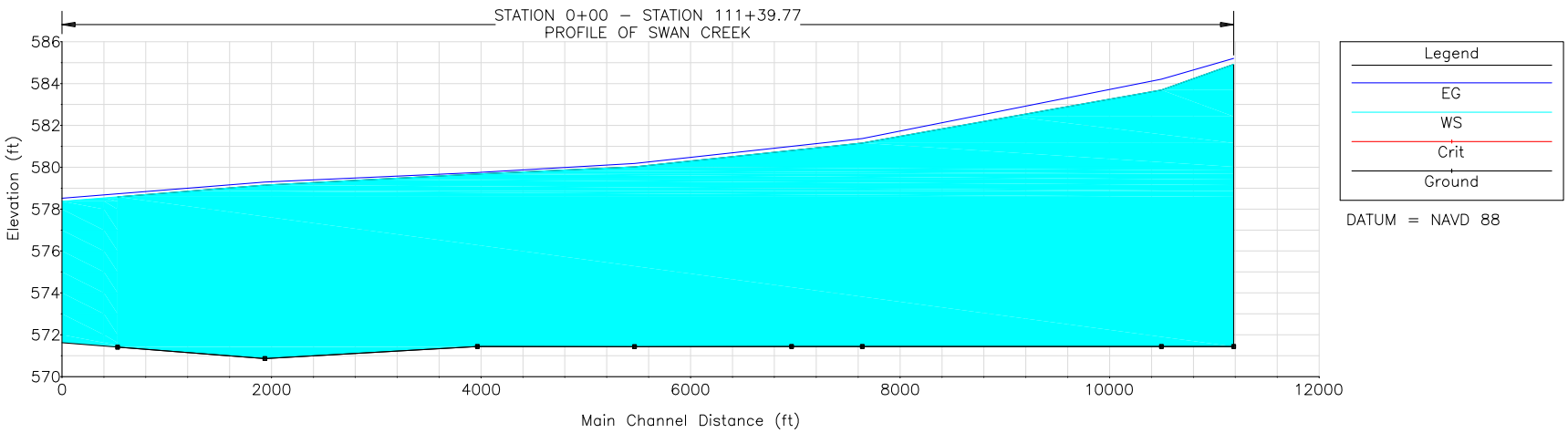

Figure 2.4-221 Alternative II - Swan Creek Profile at Station 5+30.7749 (East Side of Fermi Site)

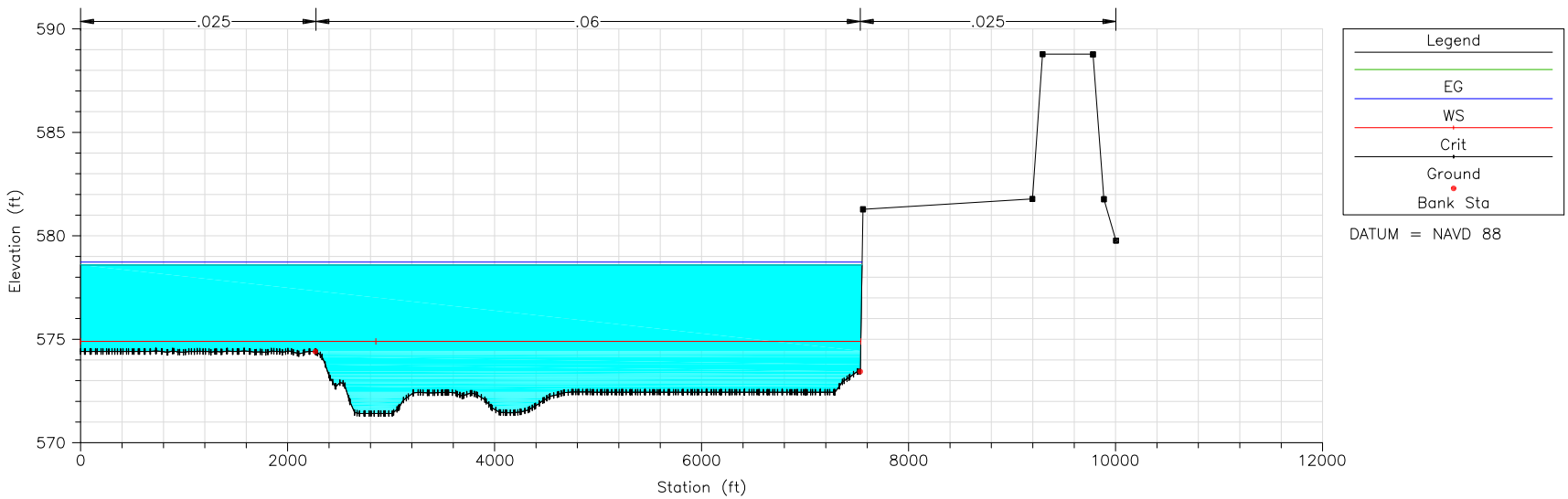

Figure 2.4-222 Alternative II - Swan Creek Profile at Station 19+36.913 (West Side of Fermi Site)

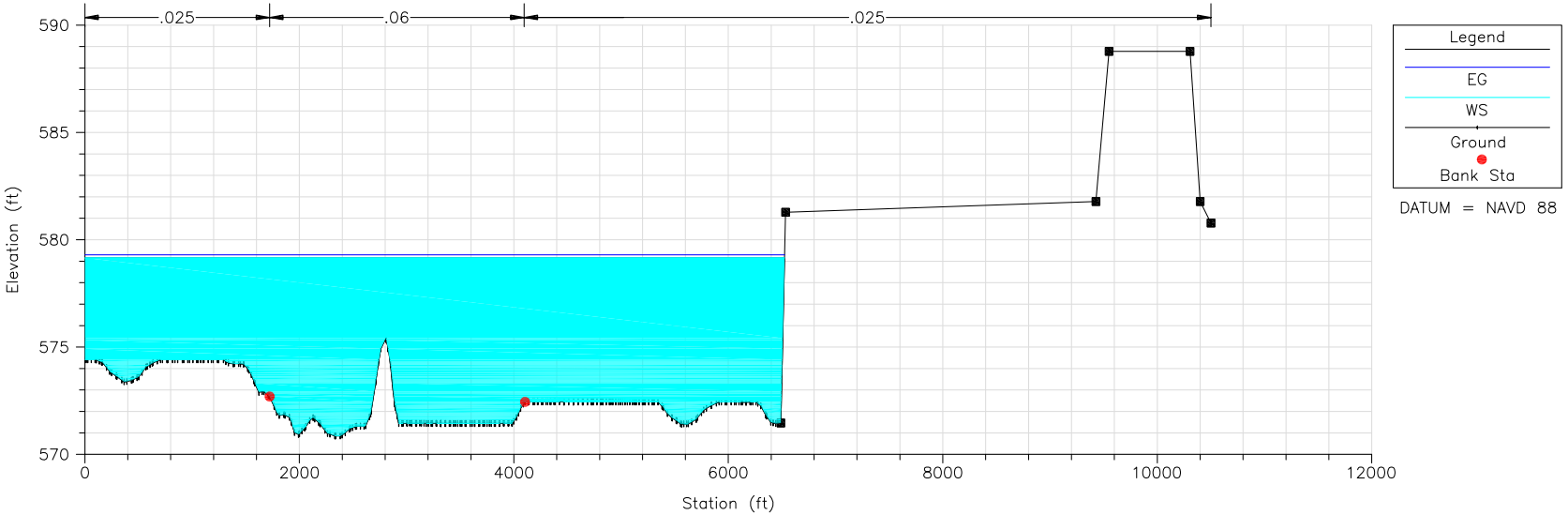

Figure 2.4-223 Profile of Swan Creek for Alternative I from Station 0+00.00 to 111+39.77

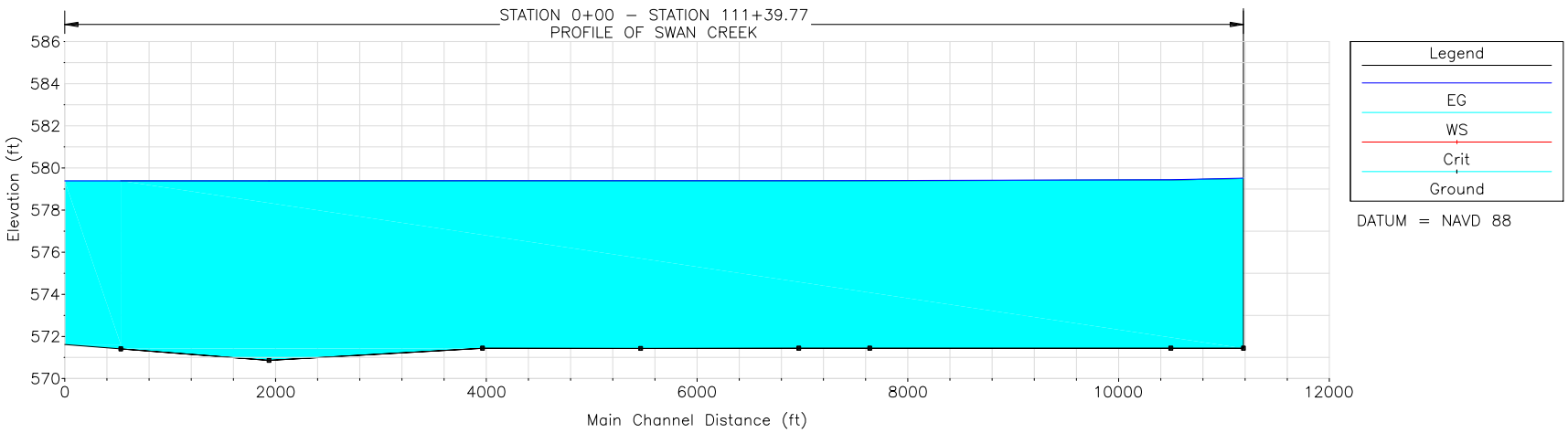

Figure 2.4-224 Alternative I - Swan Creek Profile at Station 5+30.7749 (East Side of Fermi Site)

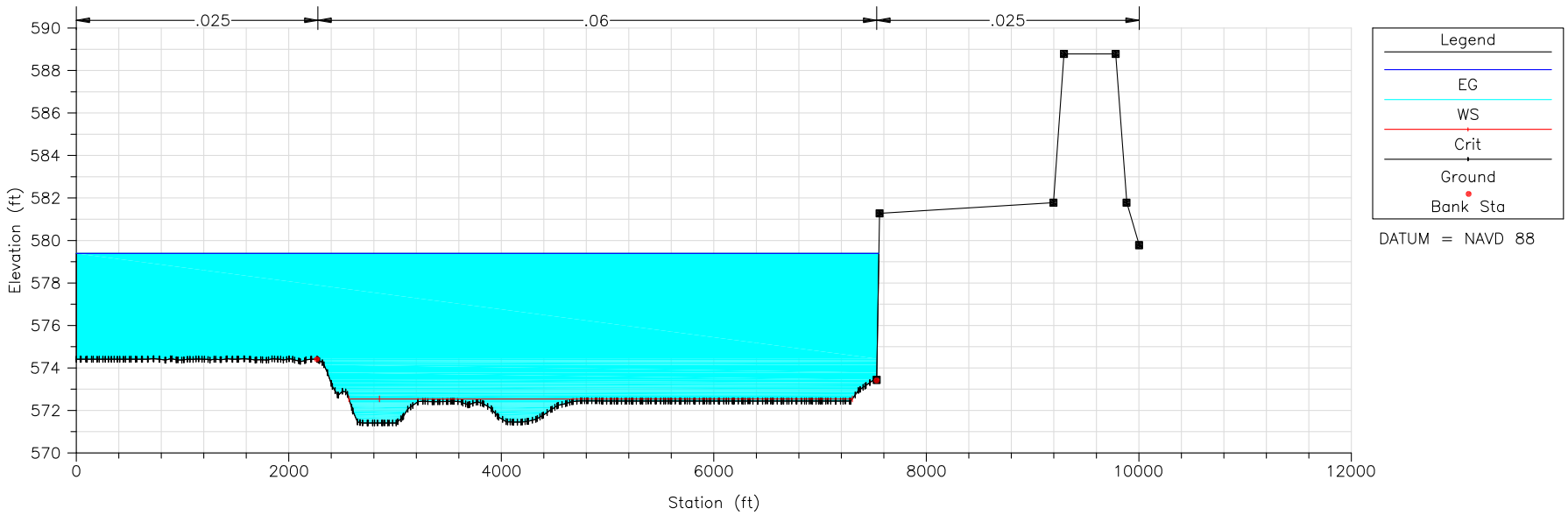

Figure 2.4-225 Alternative I - Swan Creek Profile at Station 19+36.913 (West Side of Fermi Site)

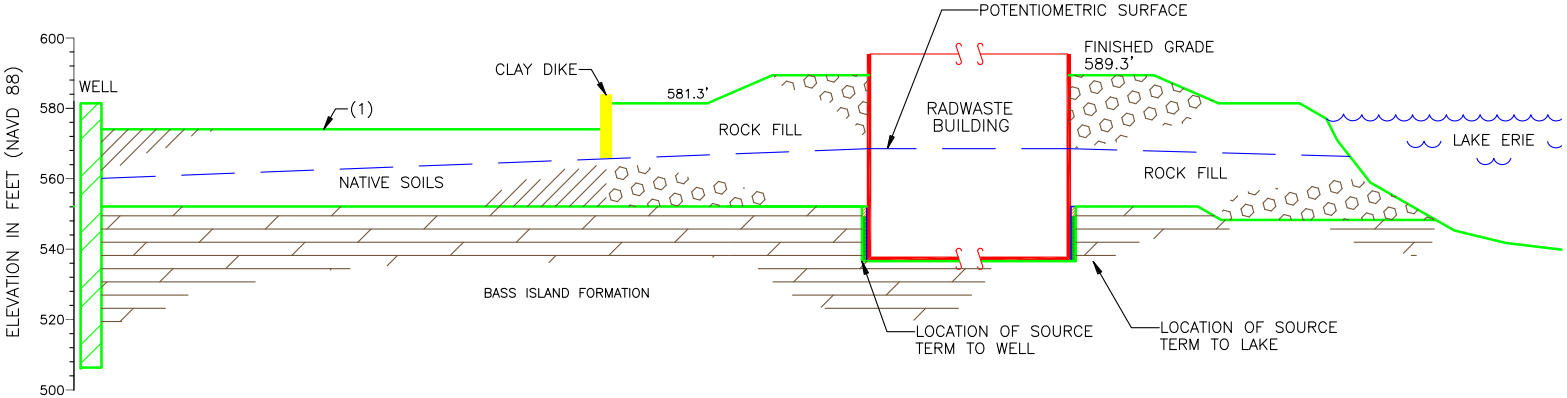

(1) ELEVATION OF NATIVE SOILS NOT PER SCALE.
(2) HYDRAULIC GRADIENT NOT PER SCALE

Figure 2.4-226 Profile of Swan Creek for Alternative III from Station 0+00.00 to 111+39.77

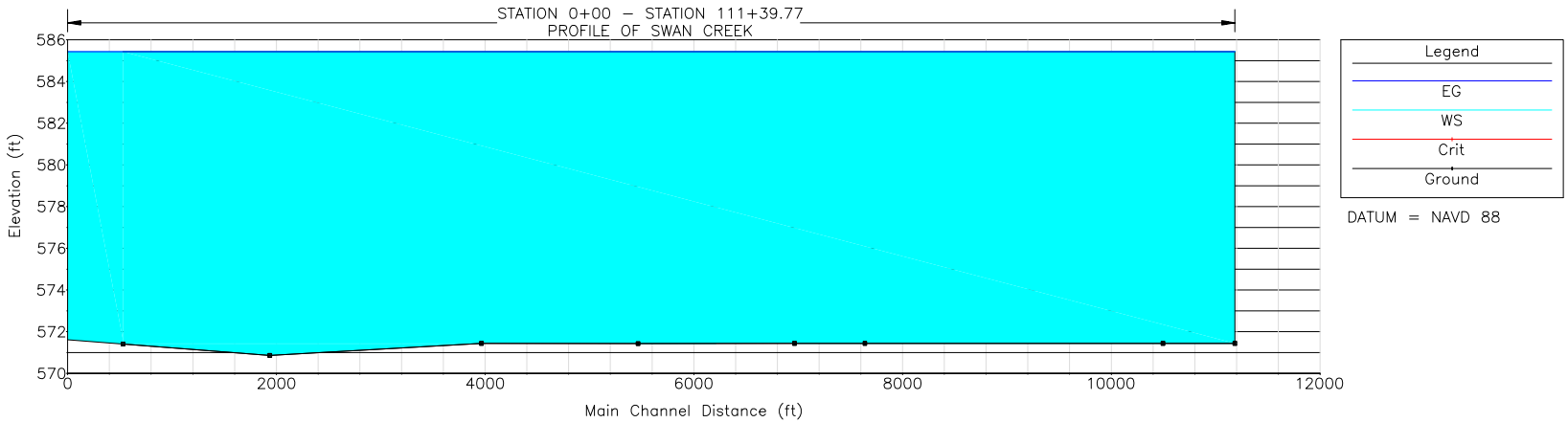

Figure 2.4-227 Alternative III - Swan Creek Profile at Station 5+30.7749 (East Side of Fermi Site)

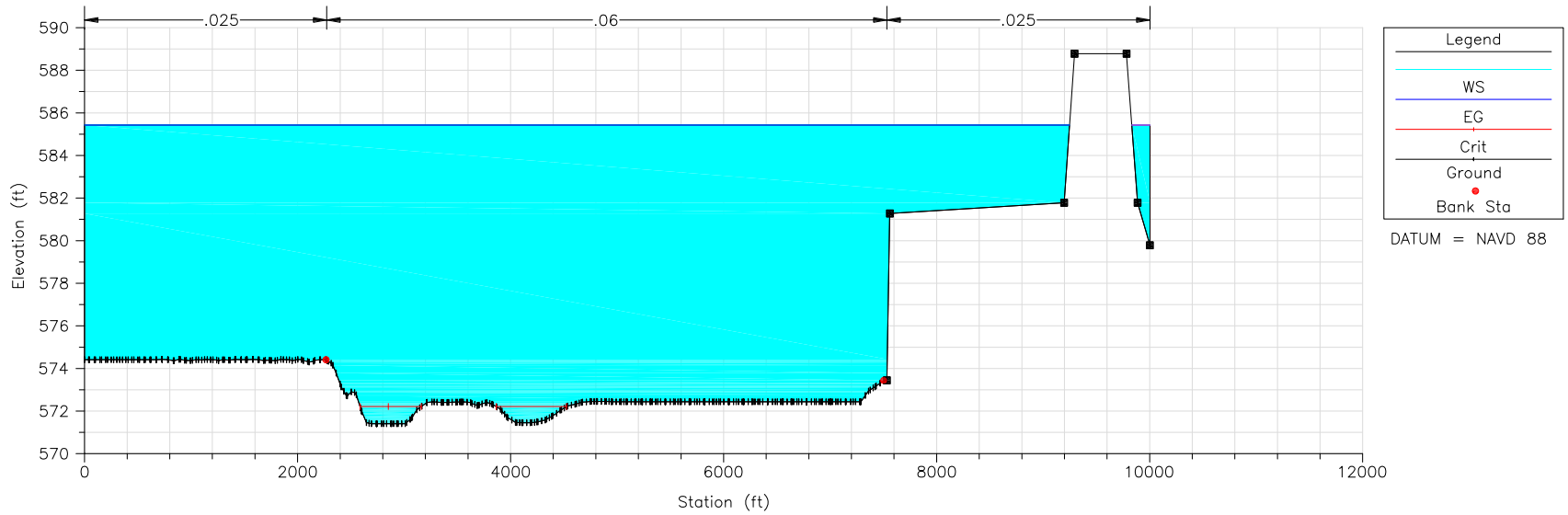

Figure 2.4-228 Alternative III - Swan Creek Profile at Station 19+36.913 (West Side of Fermi Site)

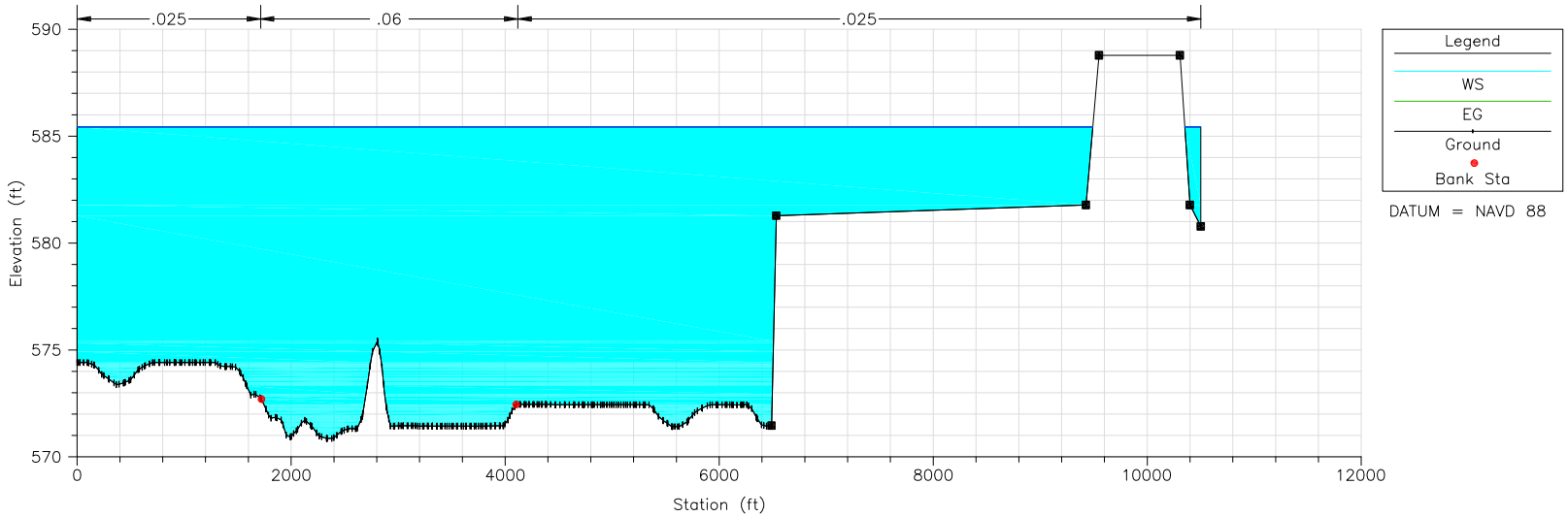

Figure 2.4-229 Water Level Gauging Stations in Lake Erie

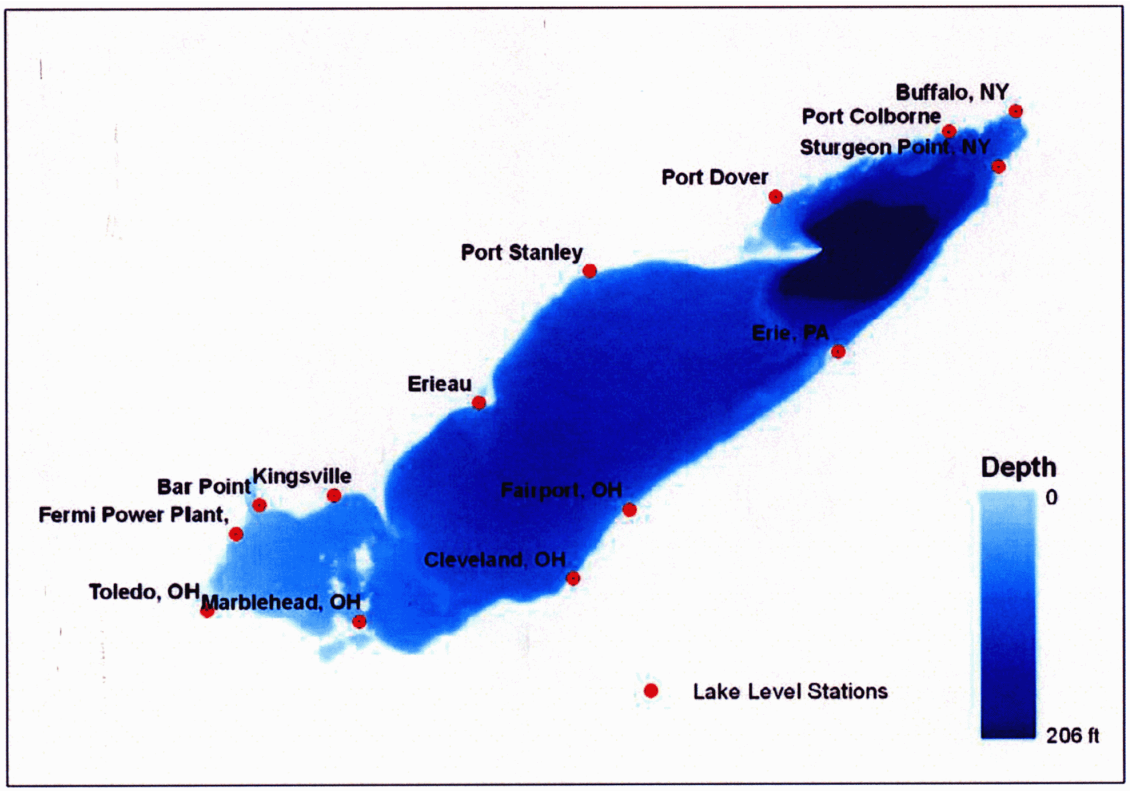

Figure 2.4-230 Wave Run-up and Overtopping on Impermeable Structures (Example)

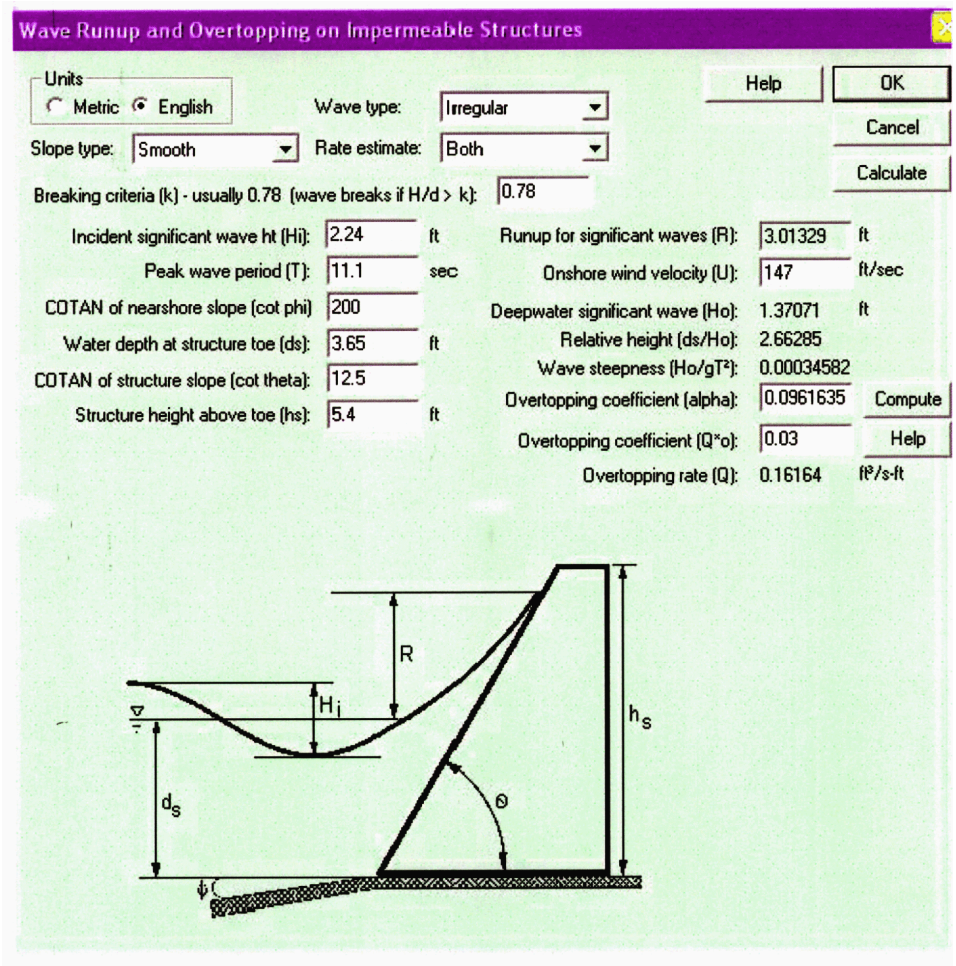

Figure 2.4-231 Site Map

Figure 2.4-232 Regional Aquifer System

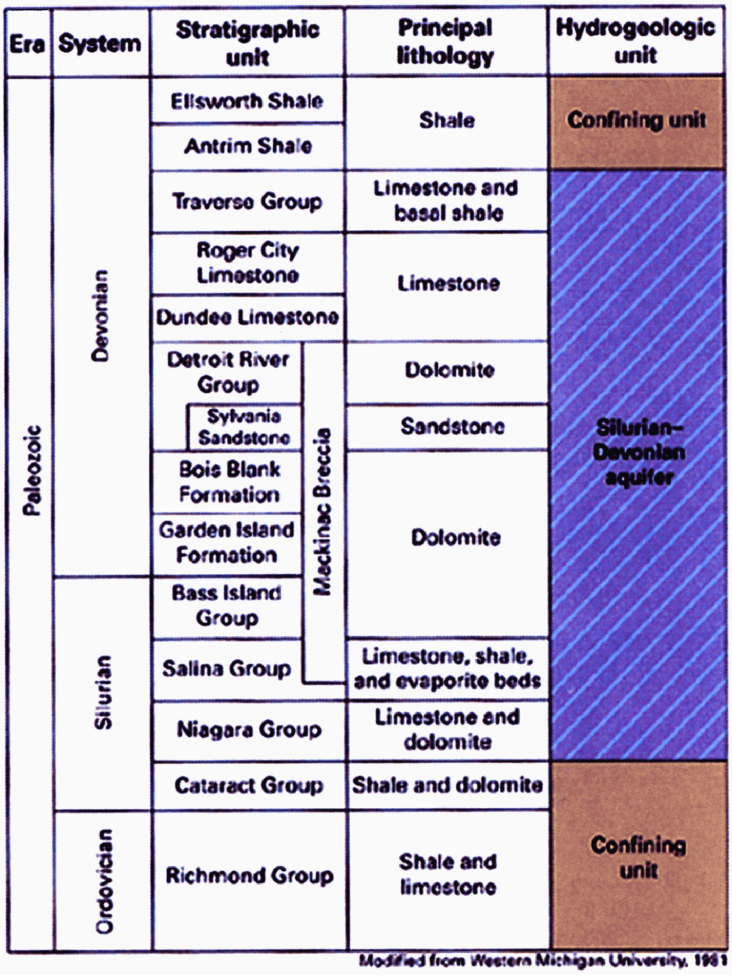

Figure 76. *The Silurian–Devonian aquifer in Michigan consists primarily of dolomite and limestone with interbedded sandstone, shale, and evaporite beds. The Mackinac Breccia results from collapse of Devonian rocks after dissolution of some of the underlying Silurian evaporite beds.*

Source: Reference 2.4-264

Figure 2.4-233 Conceptual Cross-Section of Regional Aquifer System

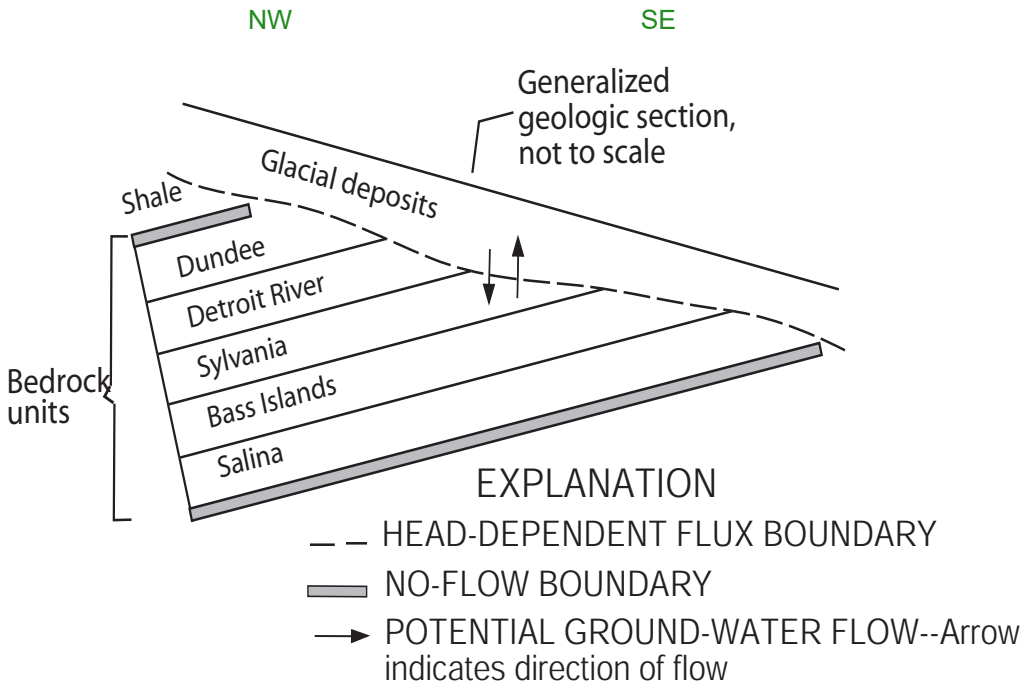

Source: Reference 2.4-261

Figure 2.4-234 Sole Source Aquifers

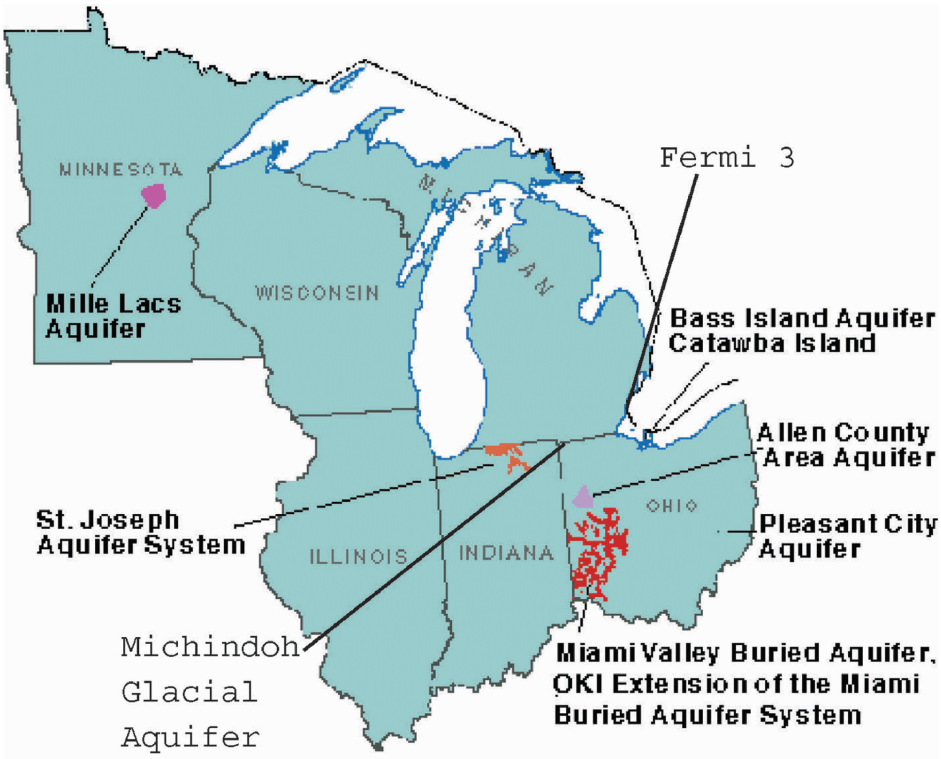

Source: Reference 2.4-268, Reference 2.4-269

Figure 2.4-235 Quarries of Monroe County, Michigan

Figure 2.4-236 All Wells Within 2 Mi

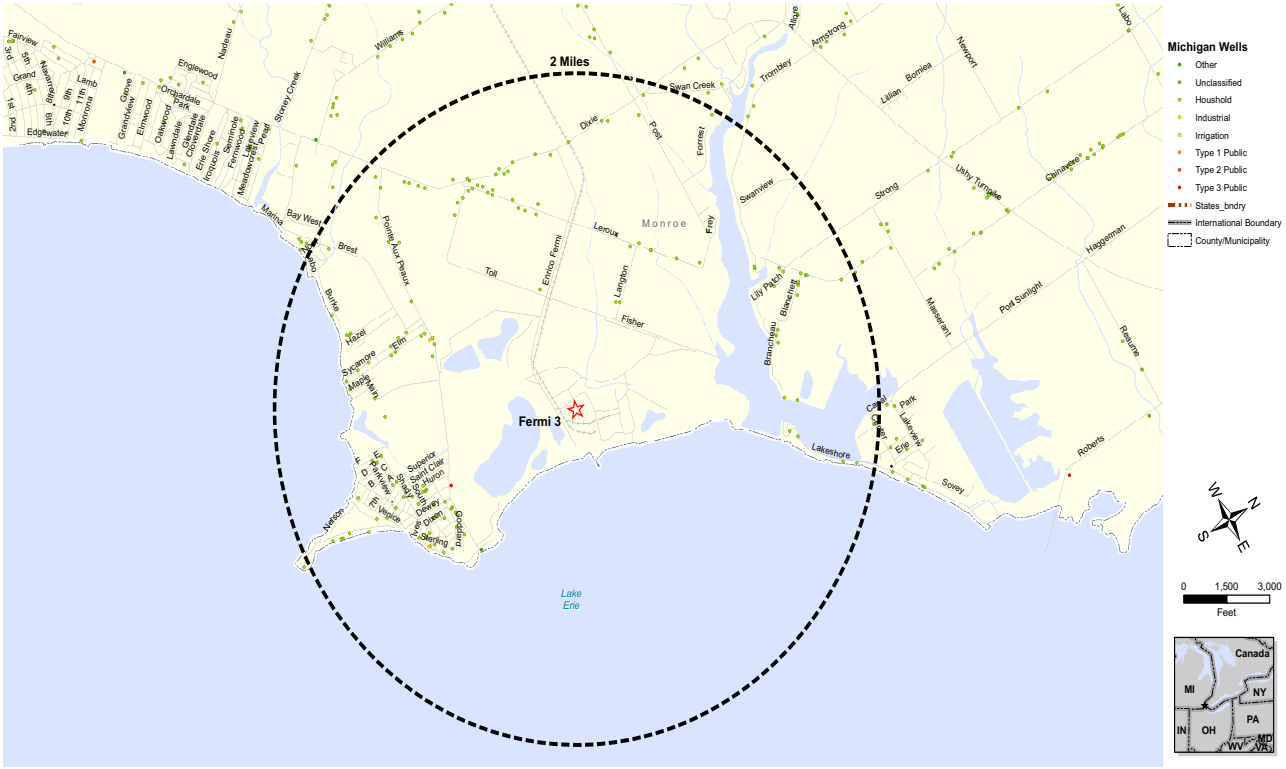

Source: Reference 2.4-274

Figure 2.4-237 All Wells Within 5 Mi

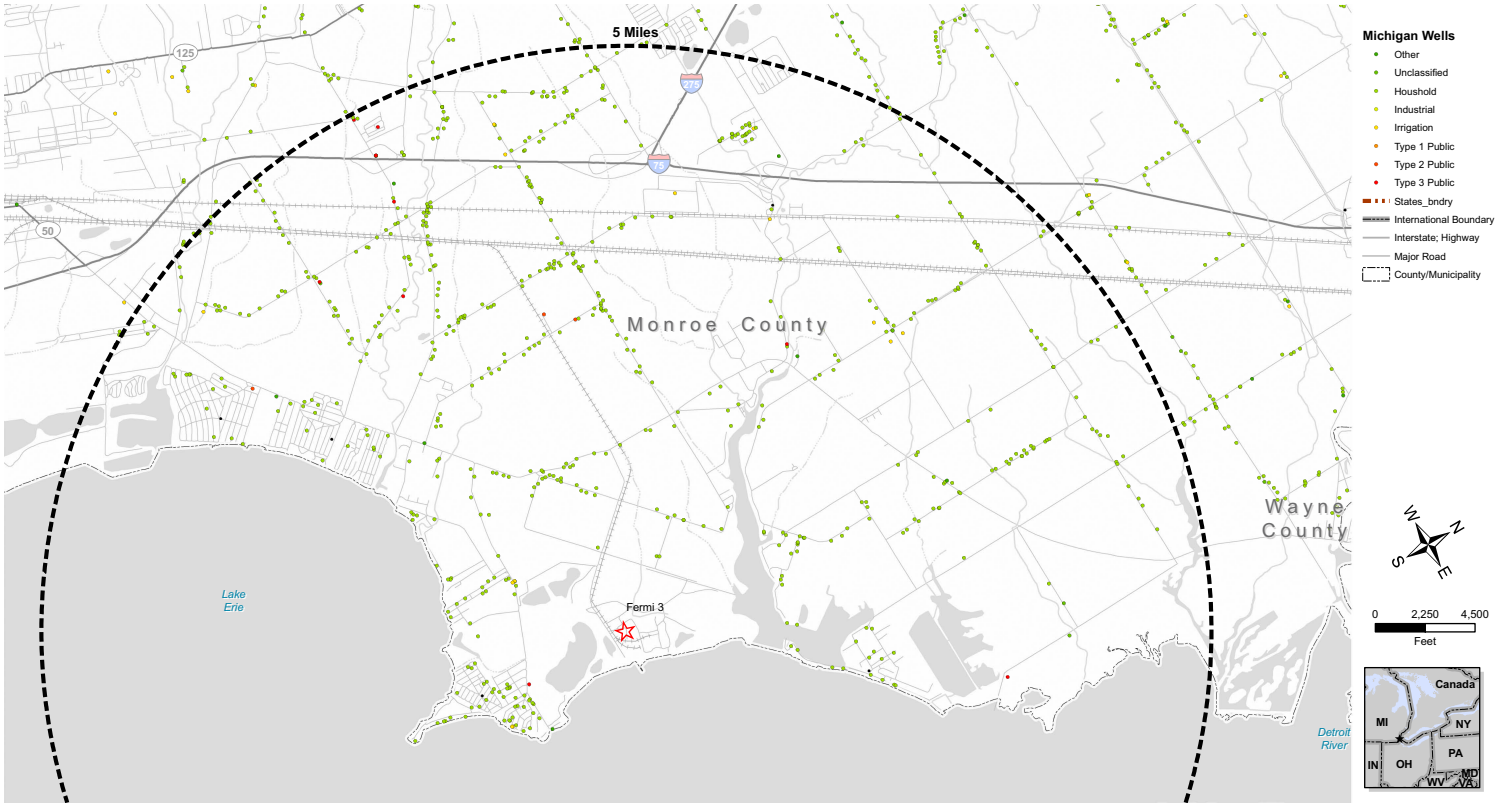

Source: Reference 2.4-274

Figure 2.4-238 All Wells Within 25 Mi

Source: Reference 2.4-274, Reference 2.4-275

Figure 2.4-239 Simulated Pre-Development Water Levels in Bedrock Aquifer

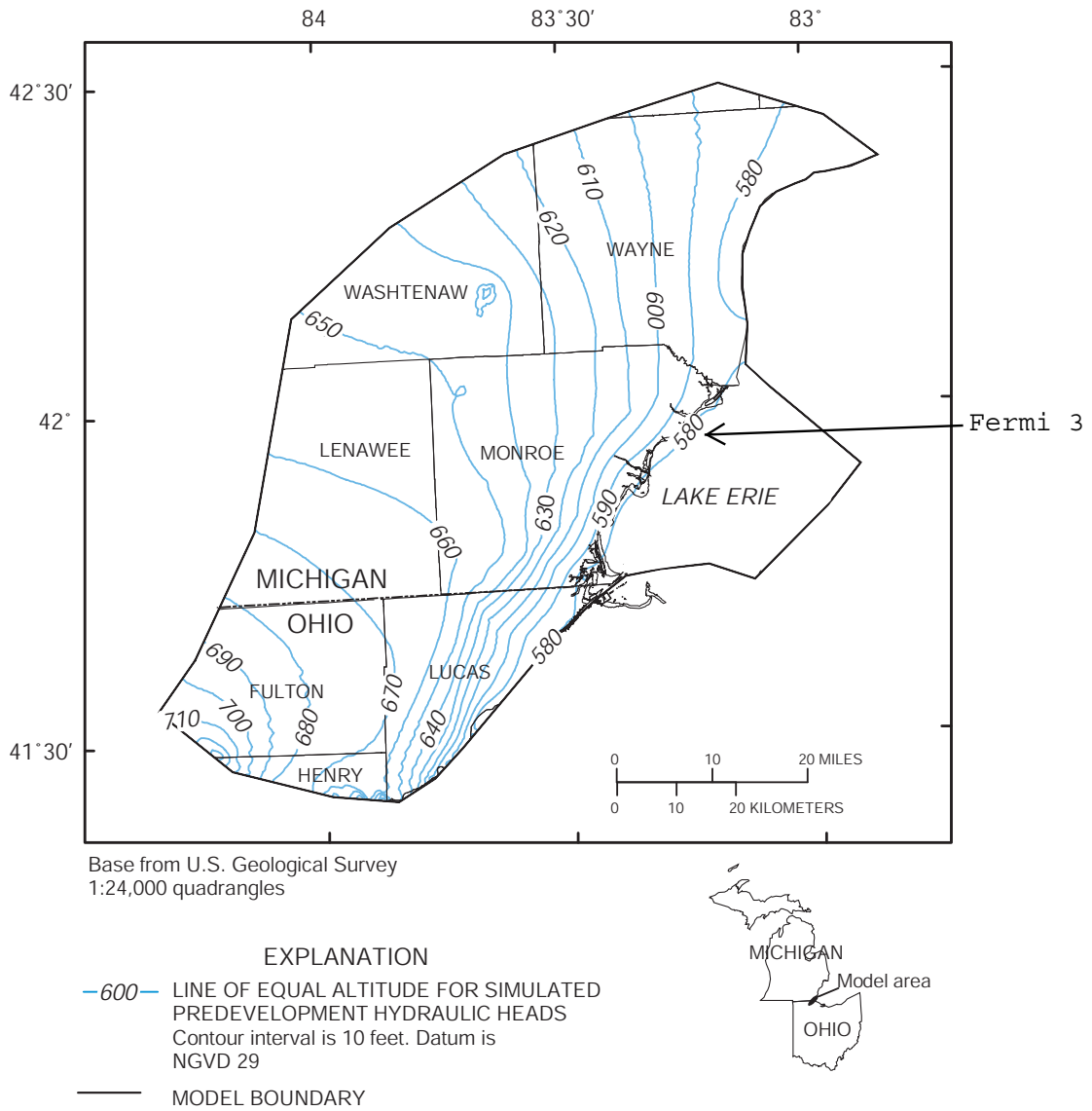

Source: Reference 2.4-261

Figure 2.4-240 1993 Bedrock Aquifer Potentiometric Surface in Monroe County, MI

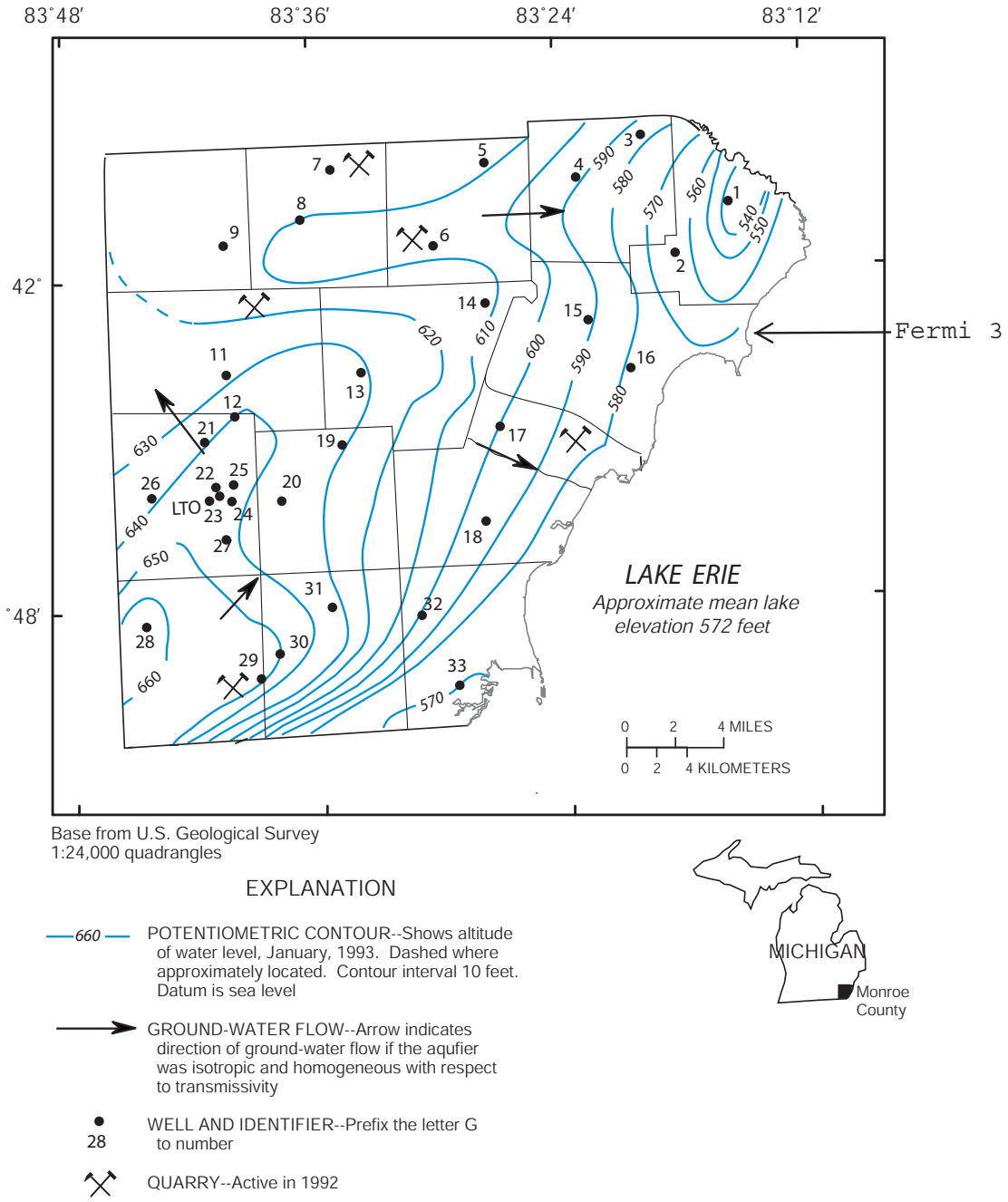

Source: Reference 2.4-261

Figure 2.4-241 2008 Bedrock Aquifer Potentiometric Surface in Monroe County, MI

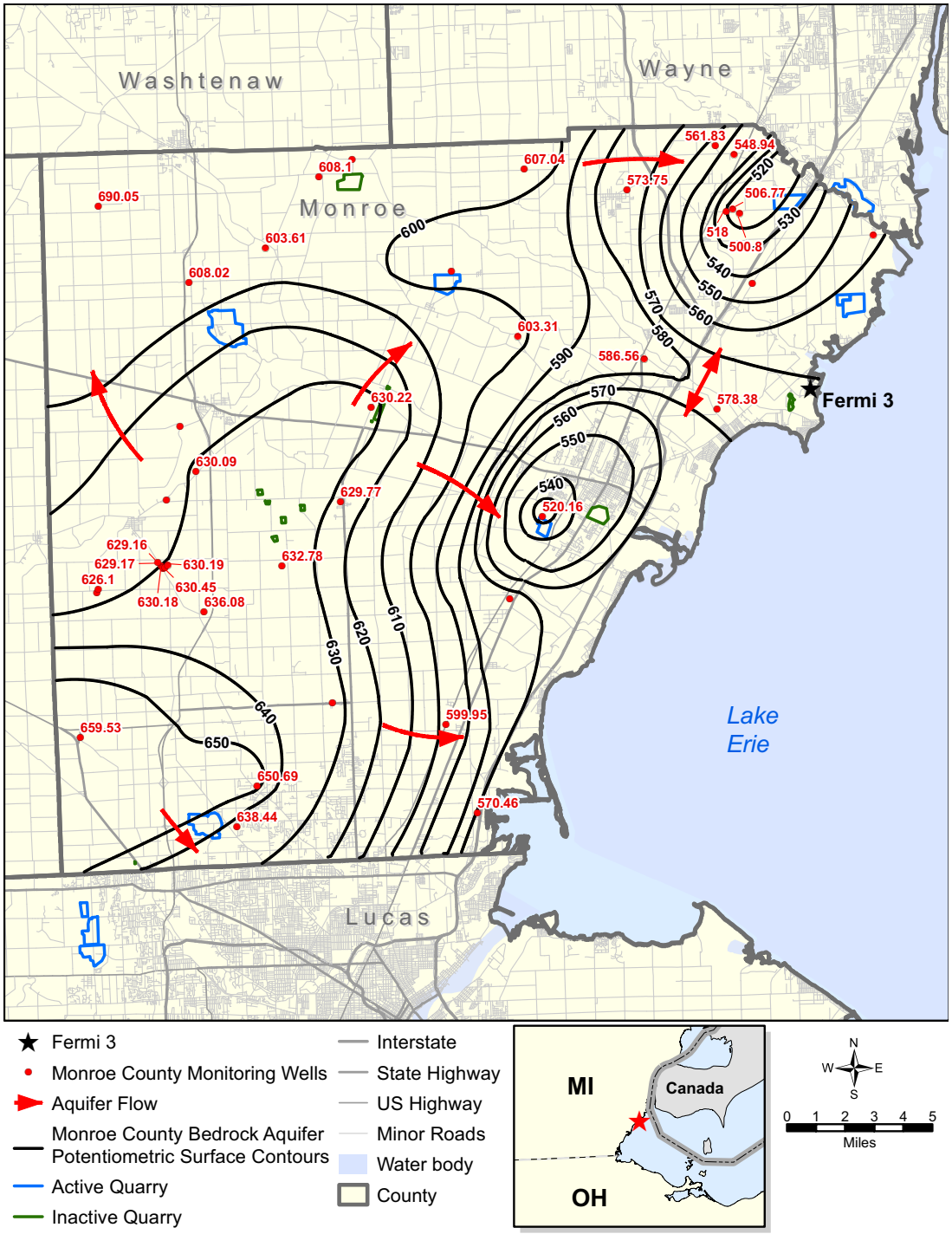

Source: Reference 2.4-278

Figure 2.4-242 Overburden Water Table Map 06/29/2007

Figure 2.4-243 Overburden Water Table Map 09/28/2007-09/29/2007

Figure 2.4-244 Overburden Water Table Map 12/29/2007

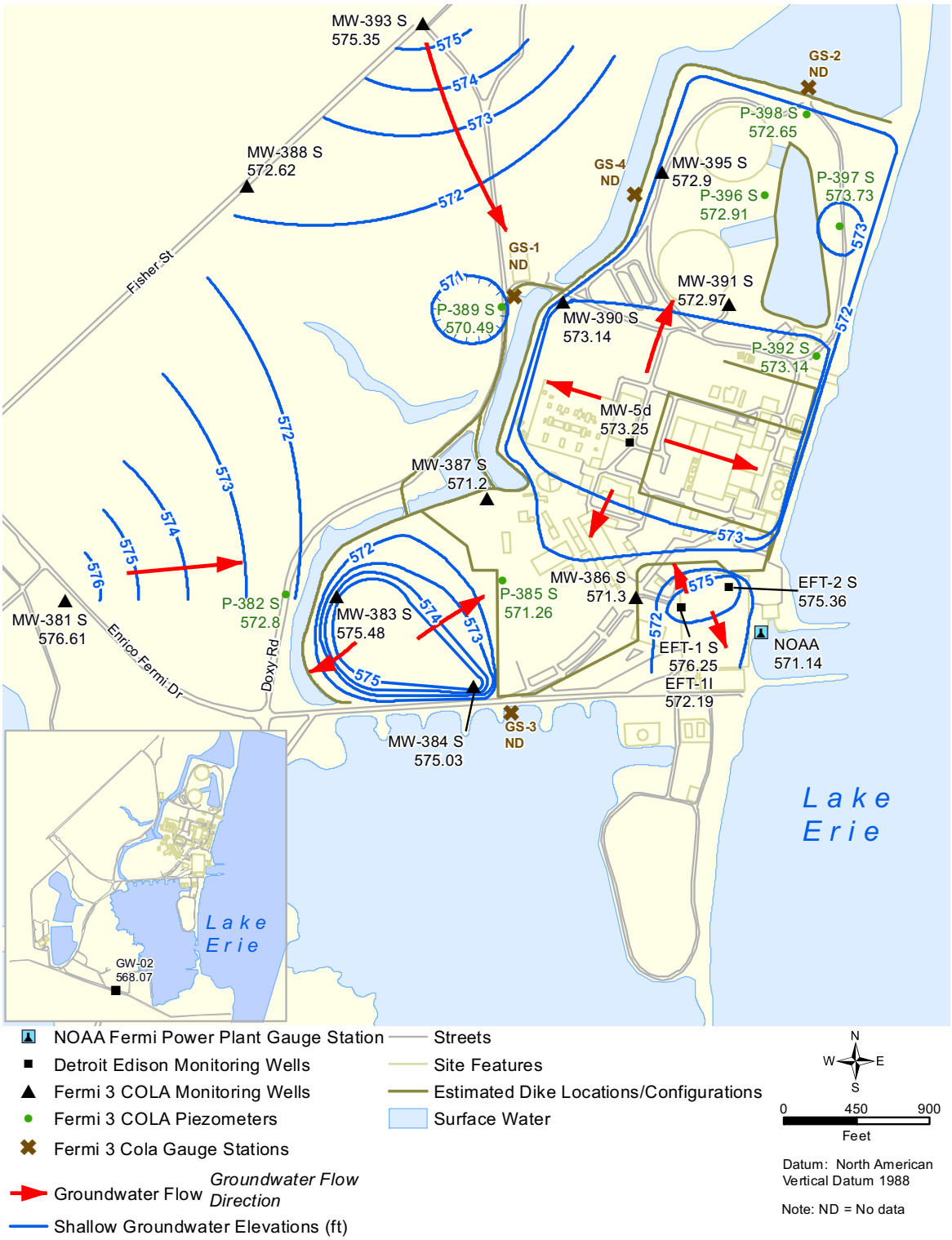

Figure 2.4-245 Overburden Water Table Map 03/21/2008

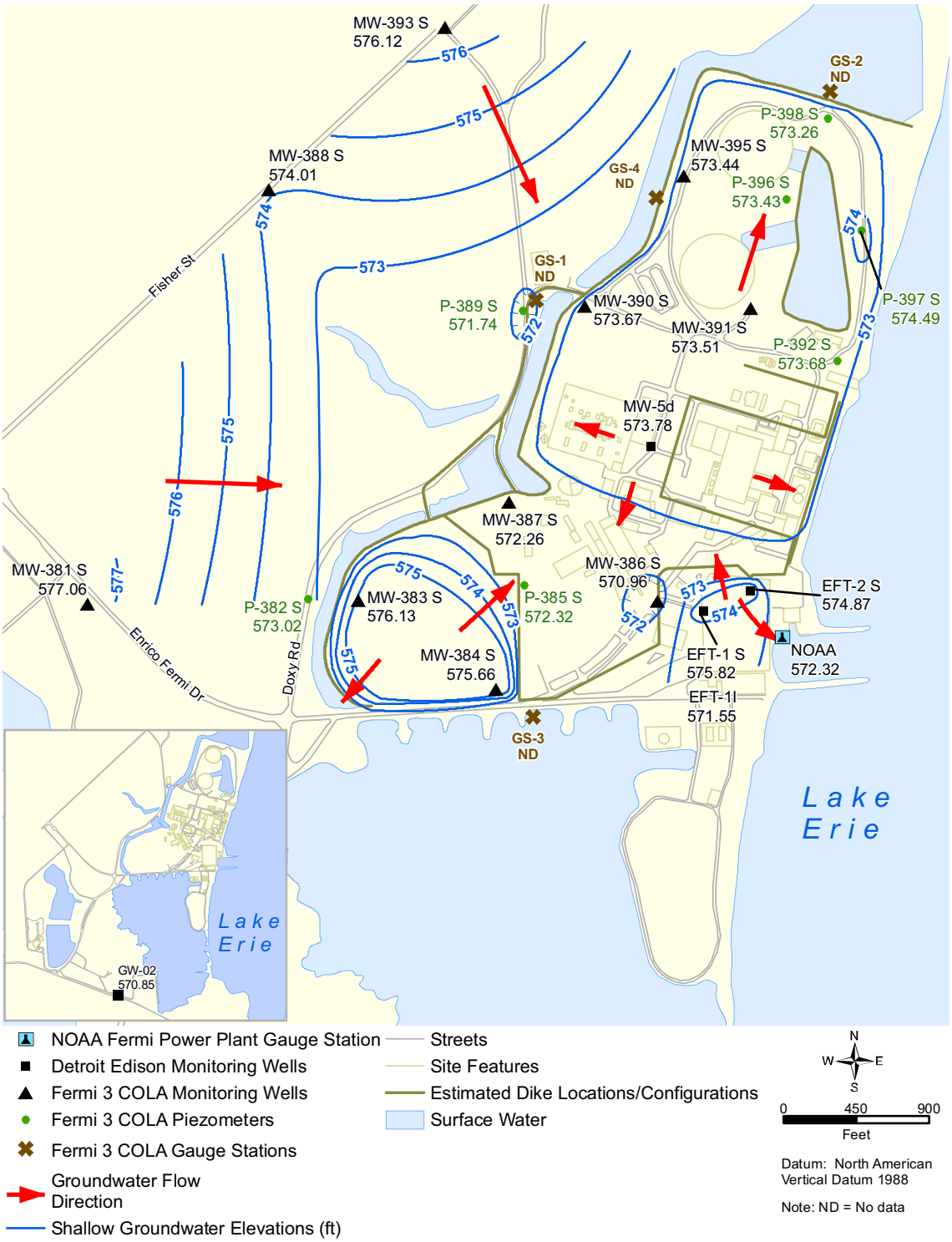

Figure 2.4-246 Bass Islands Aquifer Potentiometric Surface Map 06/29/2007

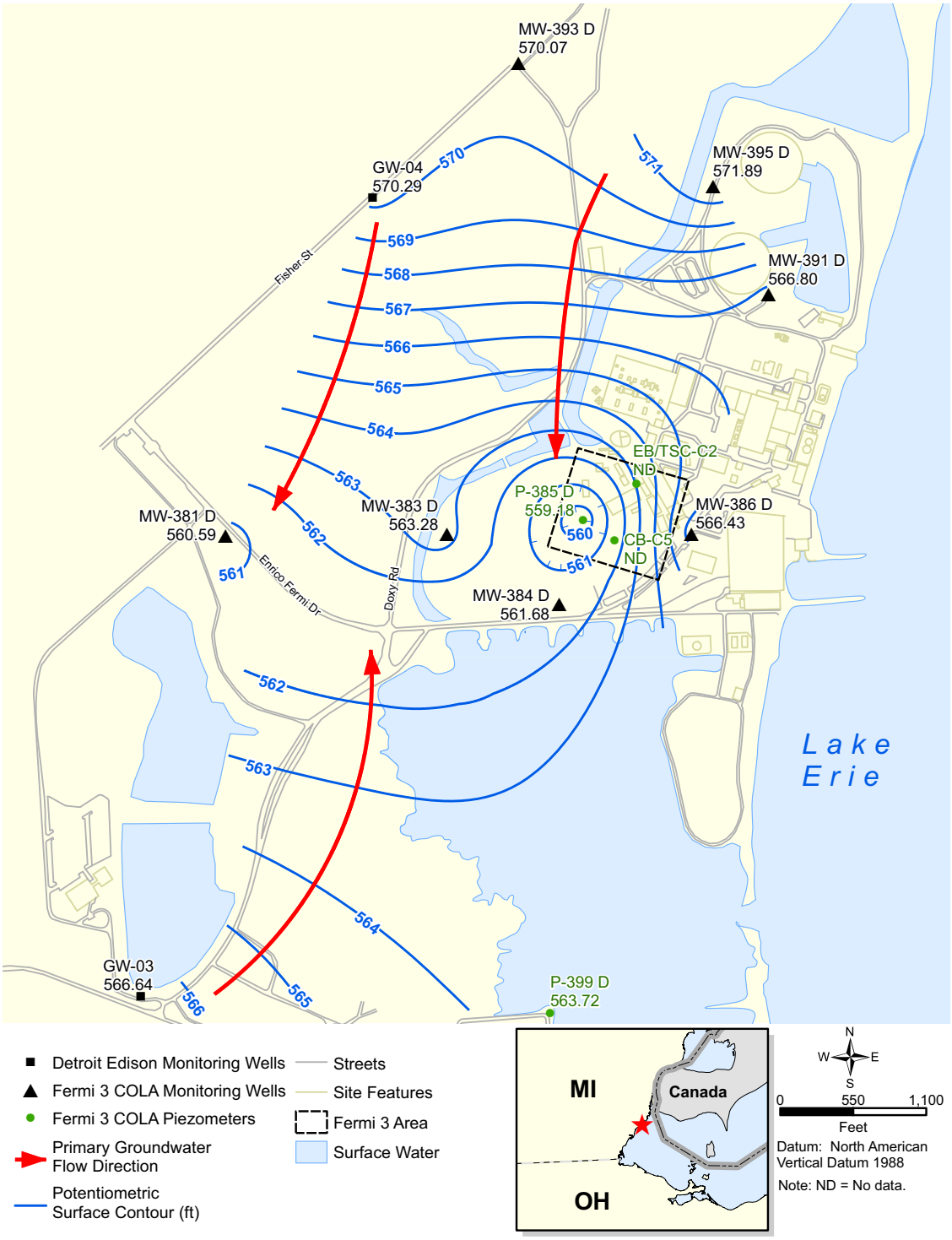

Figure 2.4-247 Bass Islands Aquifer Potentiometric Surface Map 09/28/2007-09/29/2007

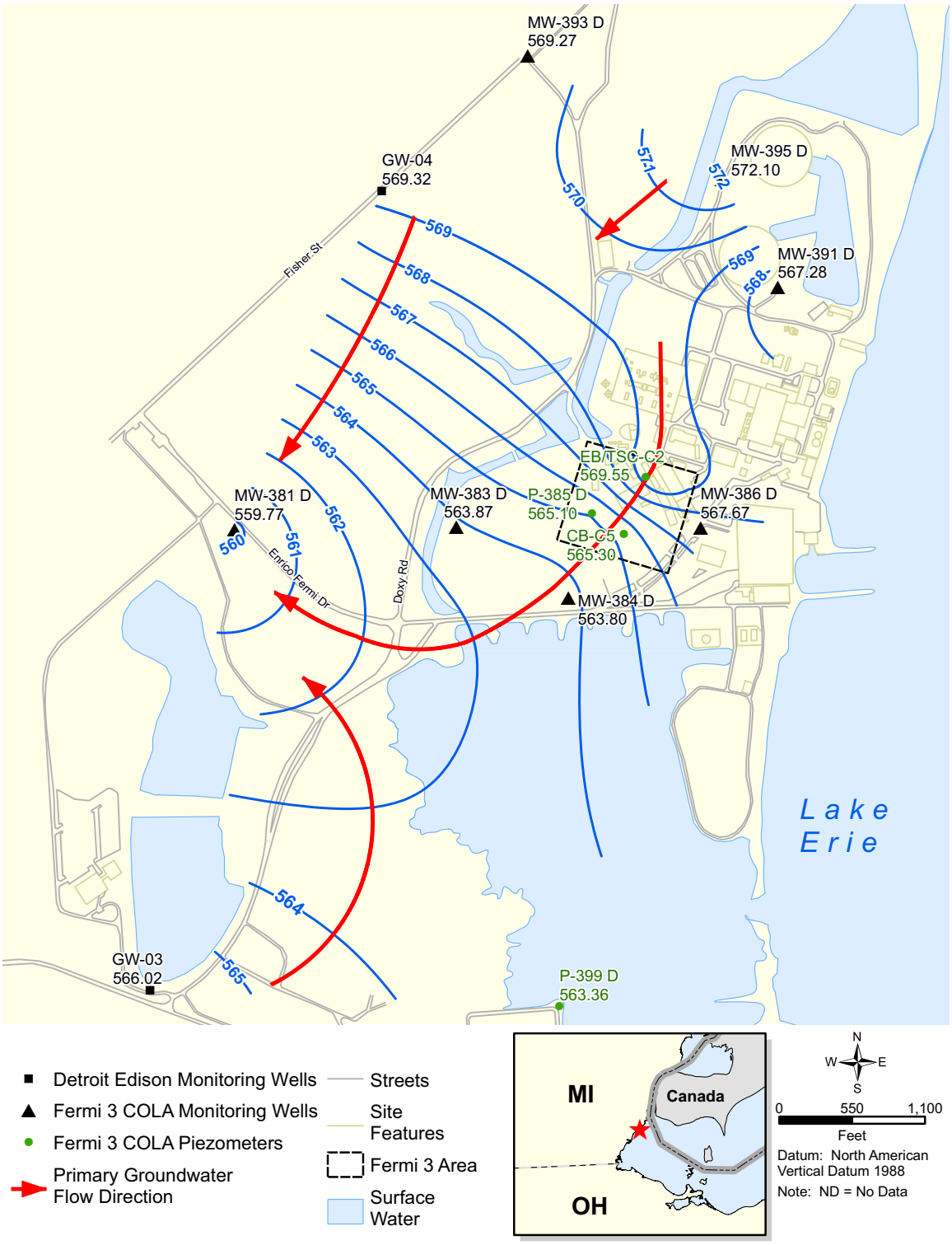

Figure 2.4-248 Bass Islands Aquifer Potentiometric Surface Map 12/29/2007

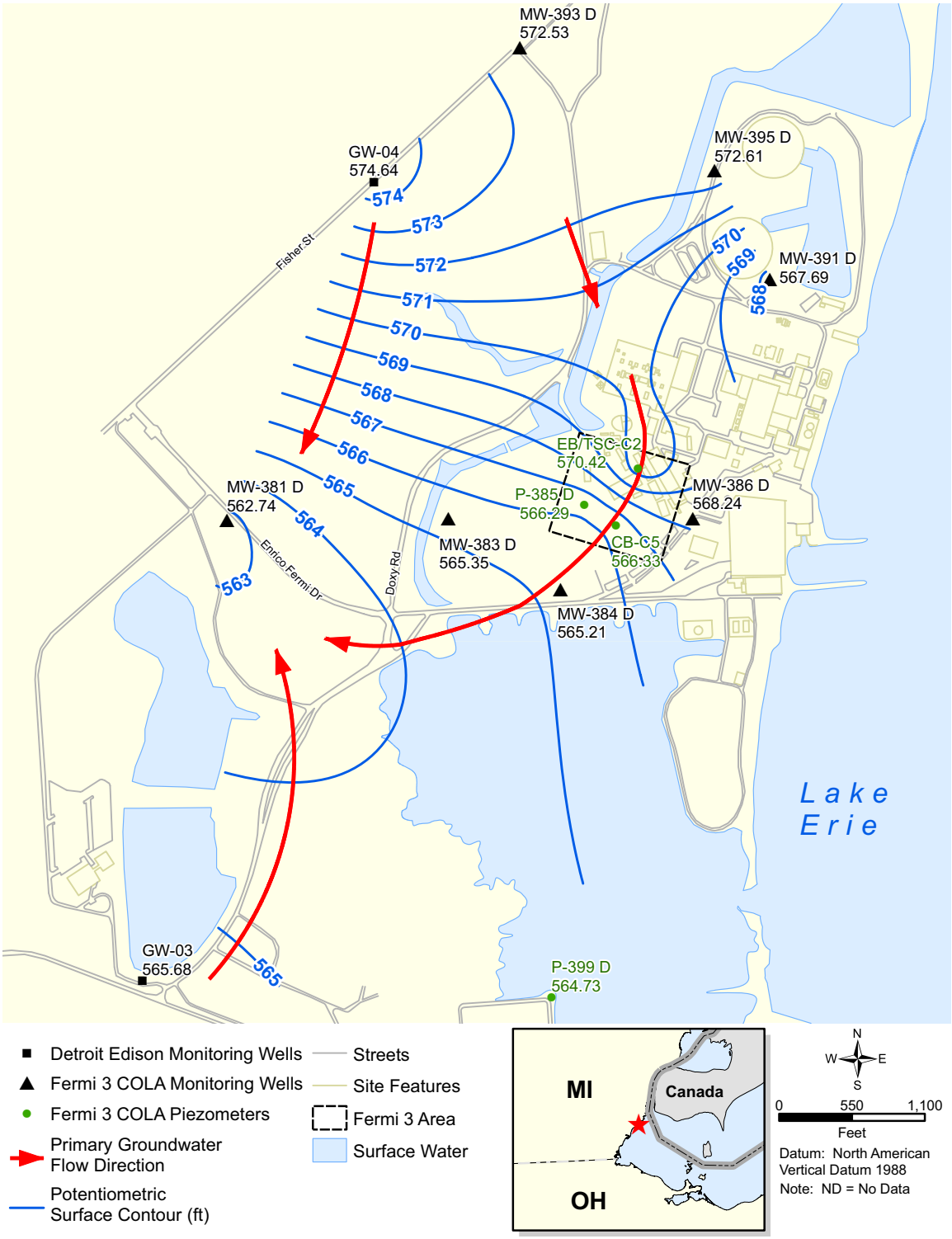

Figure 2.4-249 Bass Islands Aquifer Potentiometric Surface Map 03/29/2008

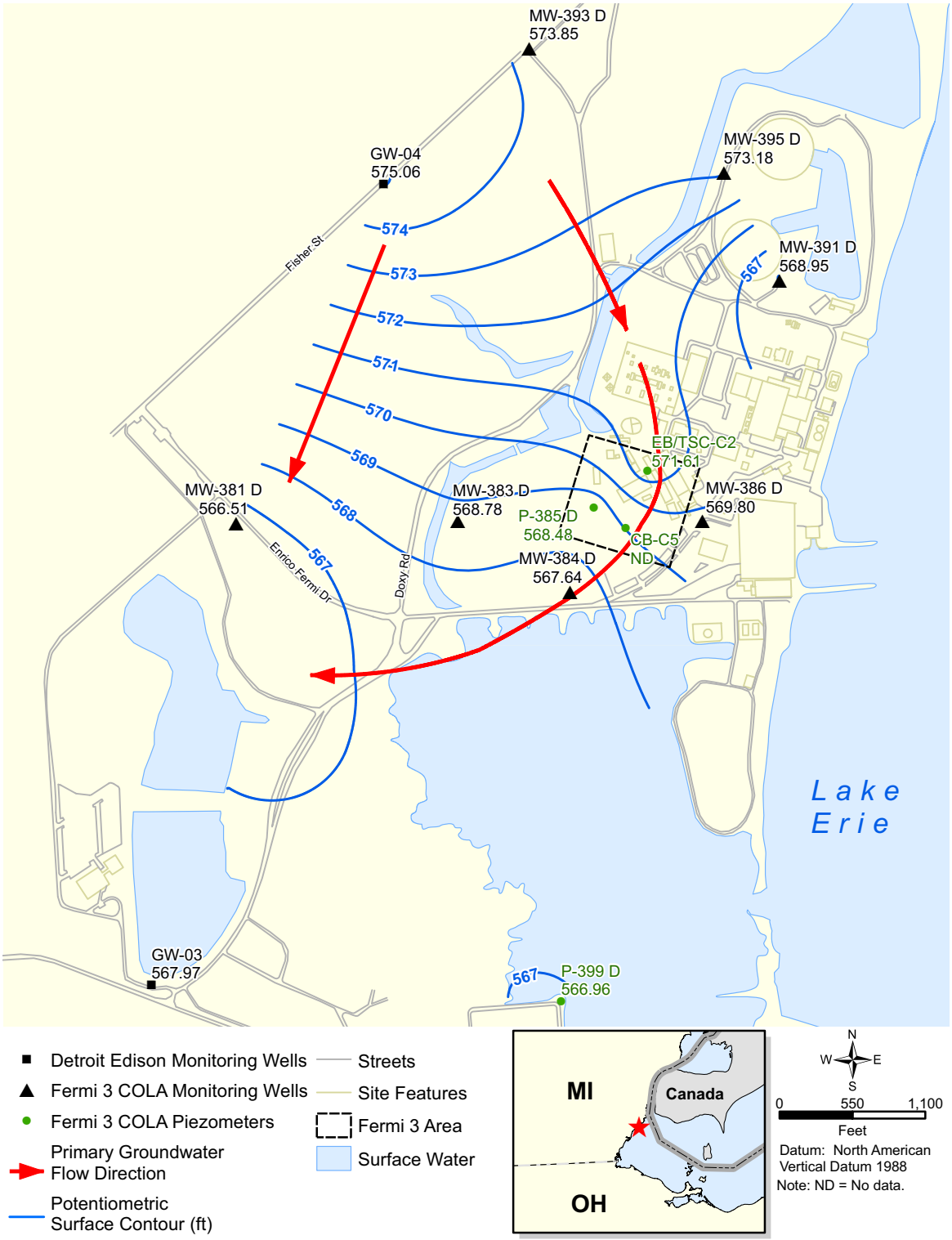

Figure 2.4-250 Fermi 3 Paired Hydrographs

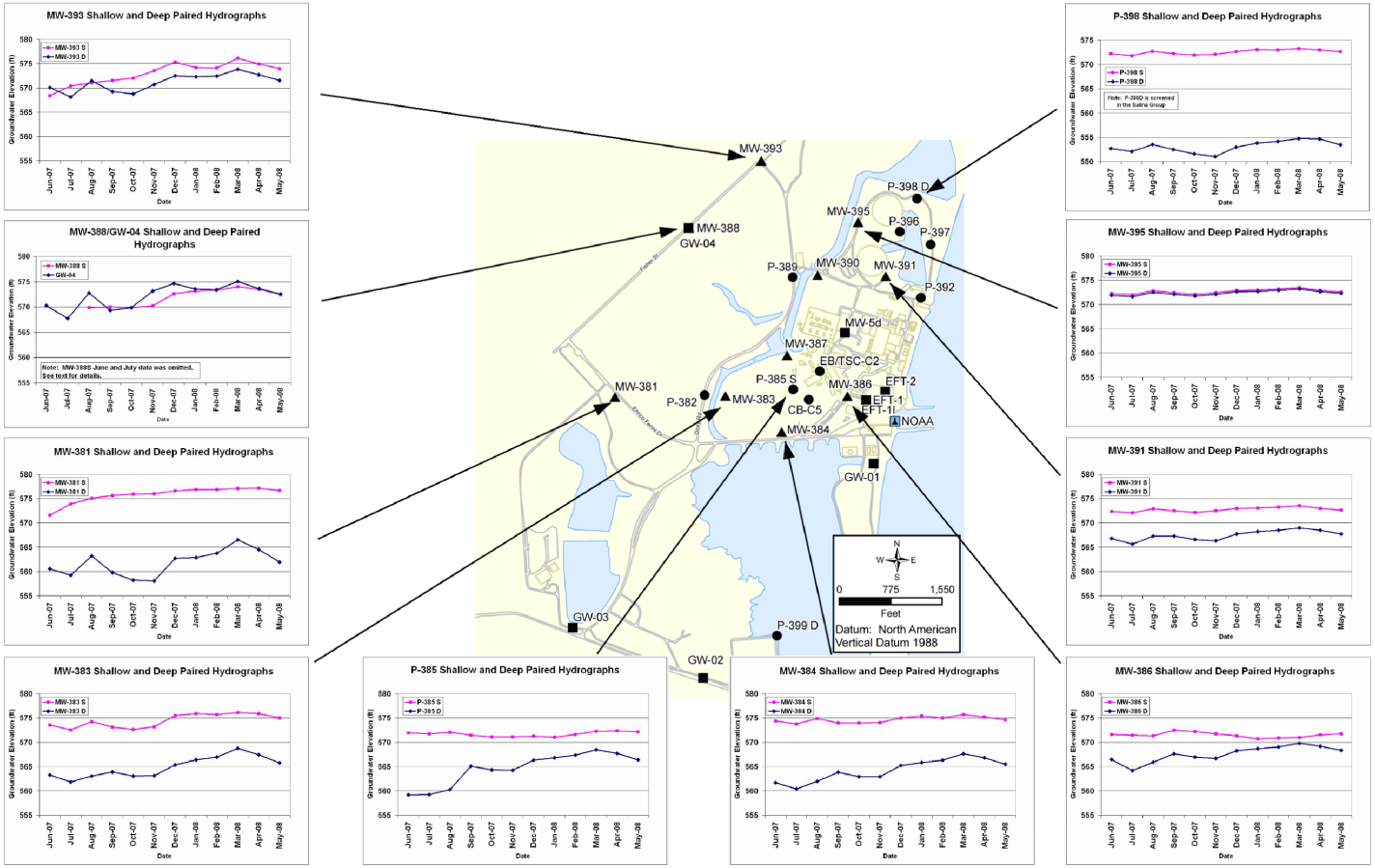

Figure 2.4-251 Monroe County Water Level Hydrographs

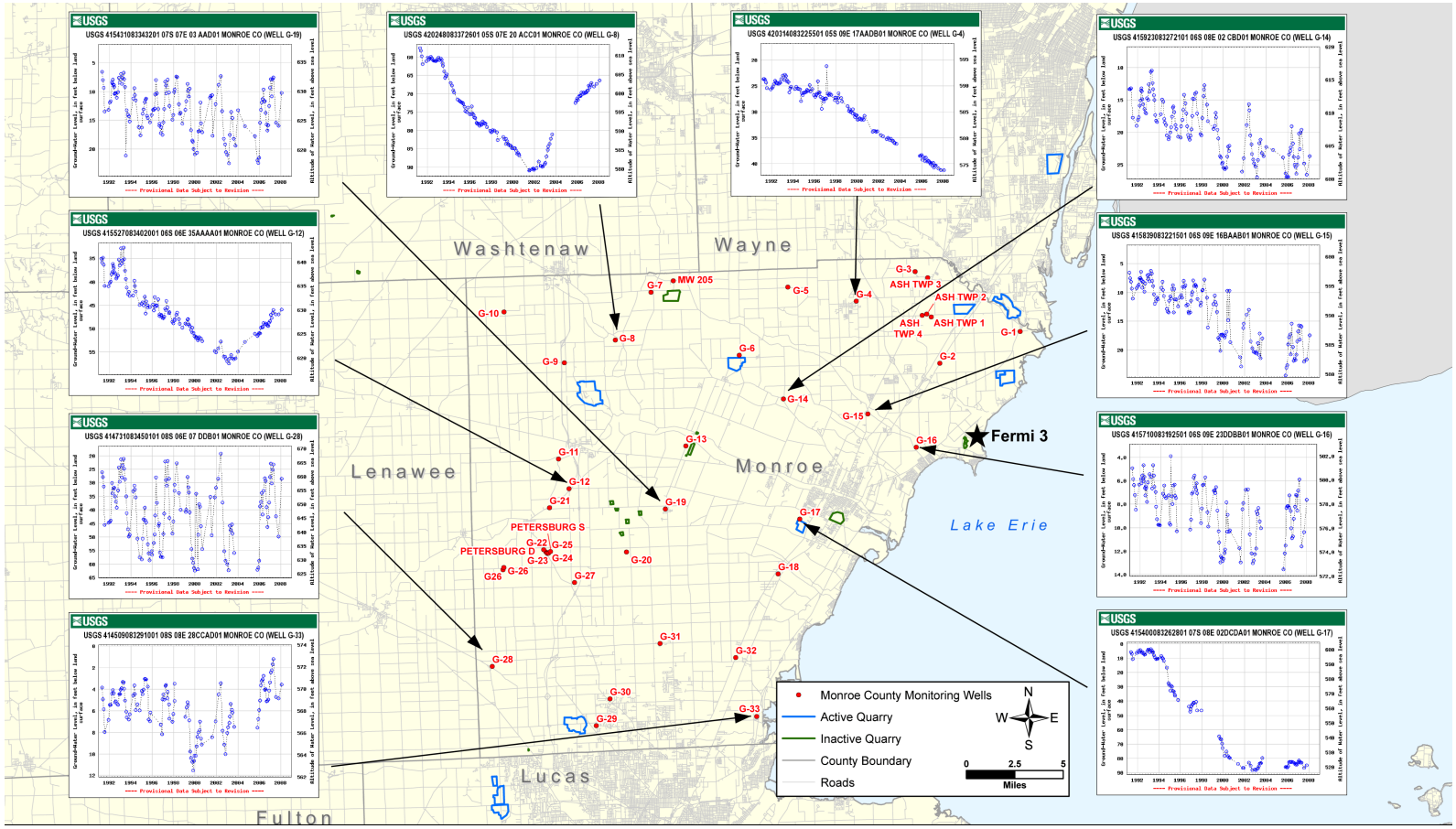

Source: Reference 2.4-278

Figure 2.4-252 Fermi 3 Overburden Hydraulic Conductivity

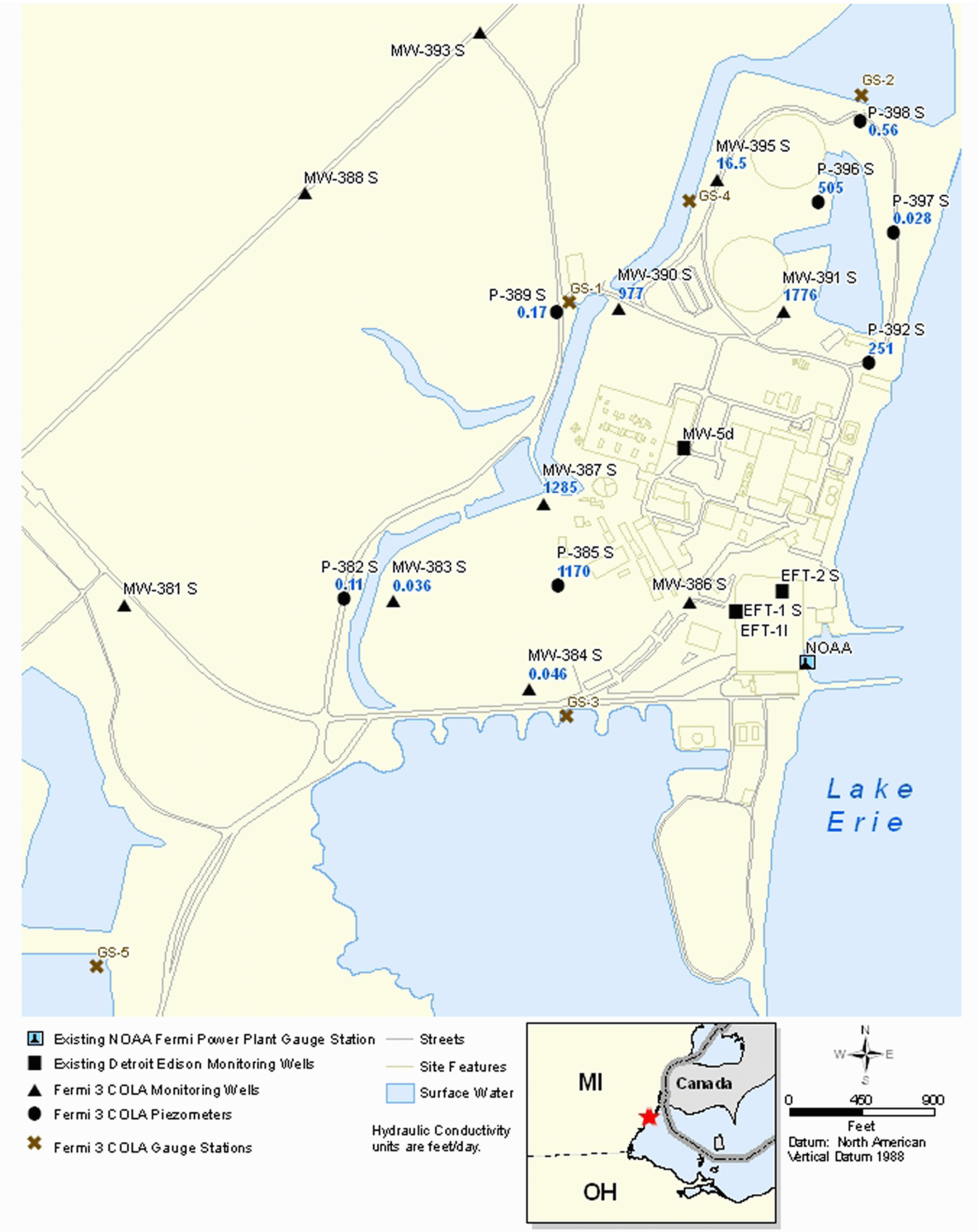

Figure 2.4-253 Fermi 3 Bedrock Hydraulic Conductivity

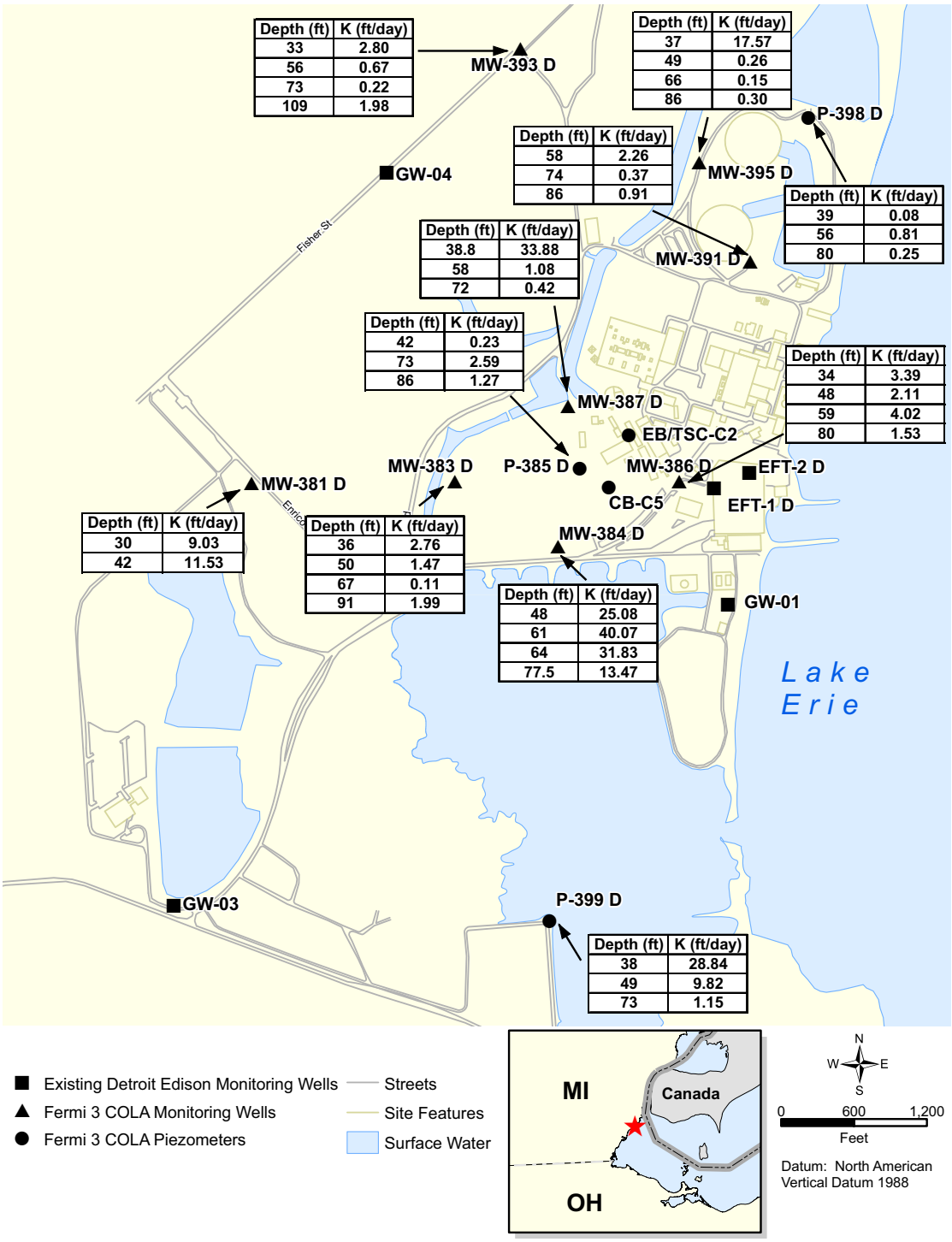

Figure 2.4-254 Groundwater Model Grid Refinement

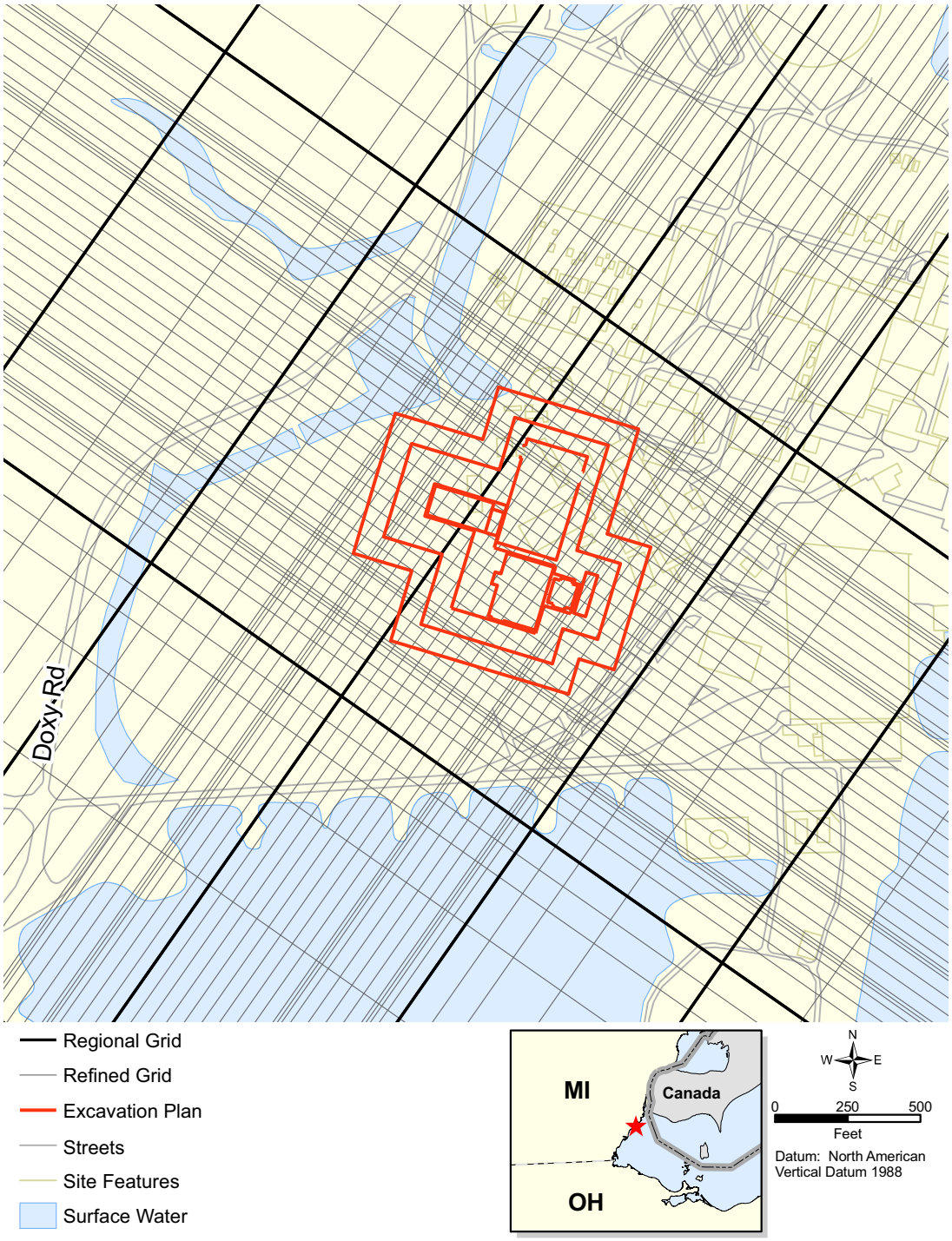

Figure 2.4-255 Dewatering Bass Islands Group: Drawdown Contours - Reinforced Diaphragm Concrete Wall With Grouted Base Combination

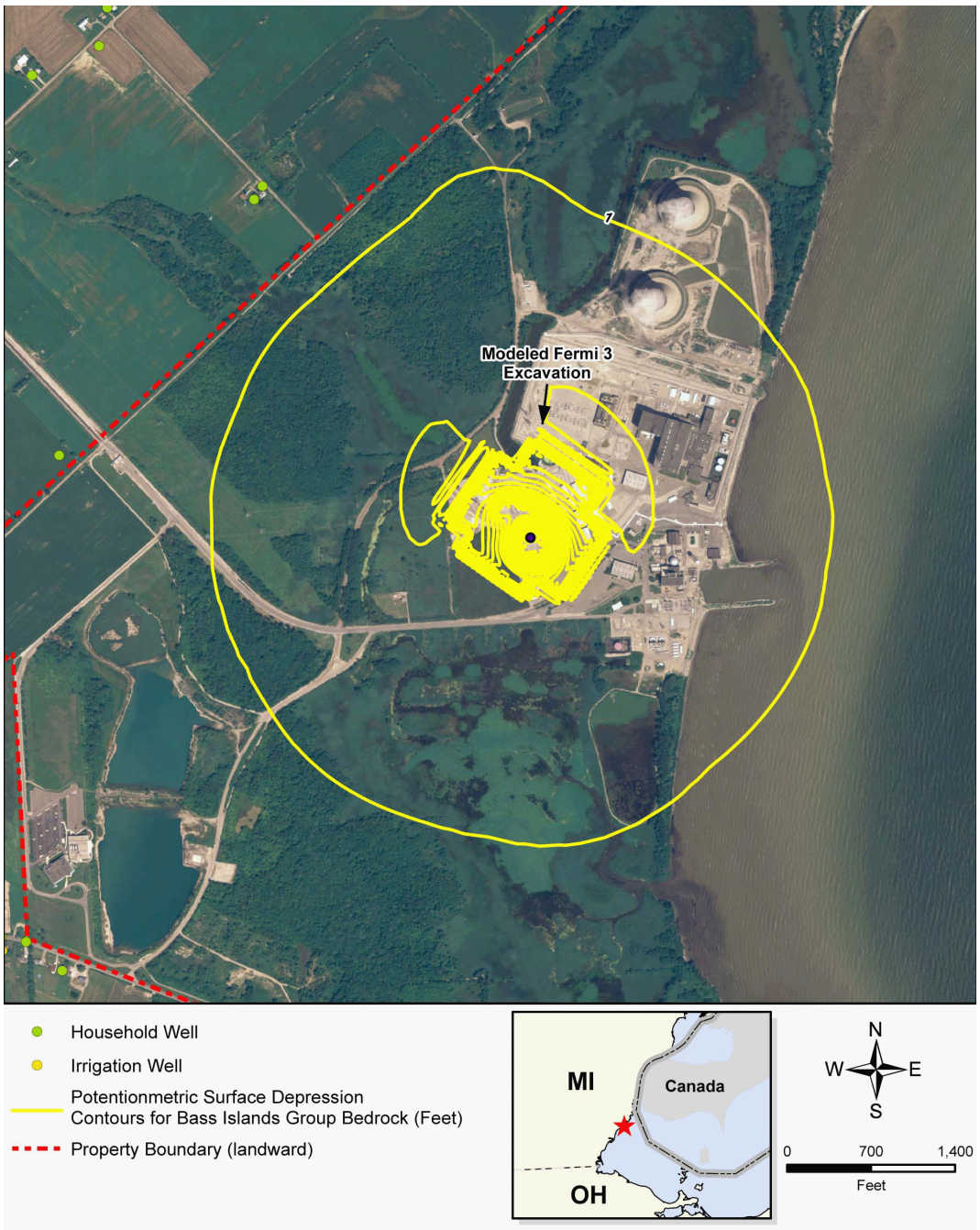

Figure 2.4-256 Dewatering Bass Islands Group: Drawdown Contours – Grout Curtain/Freeze Wall Combination with a Grouted Base

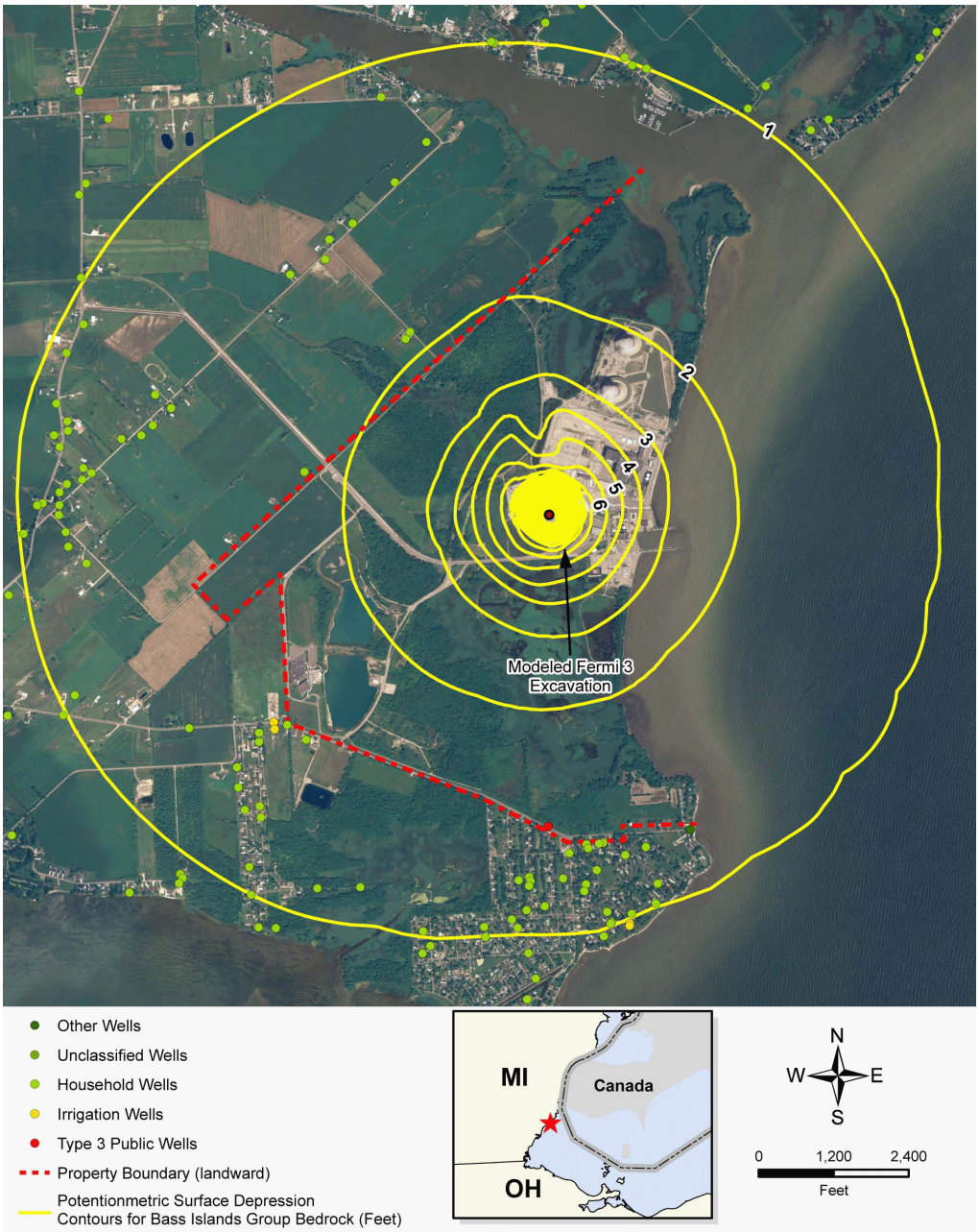

Figure 2.4-257 Effective Monitoring Intervals For Bedrock Wells At The Fermi Site

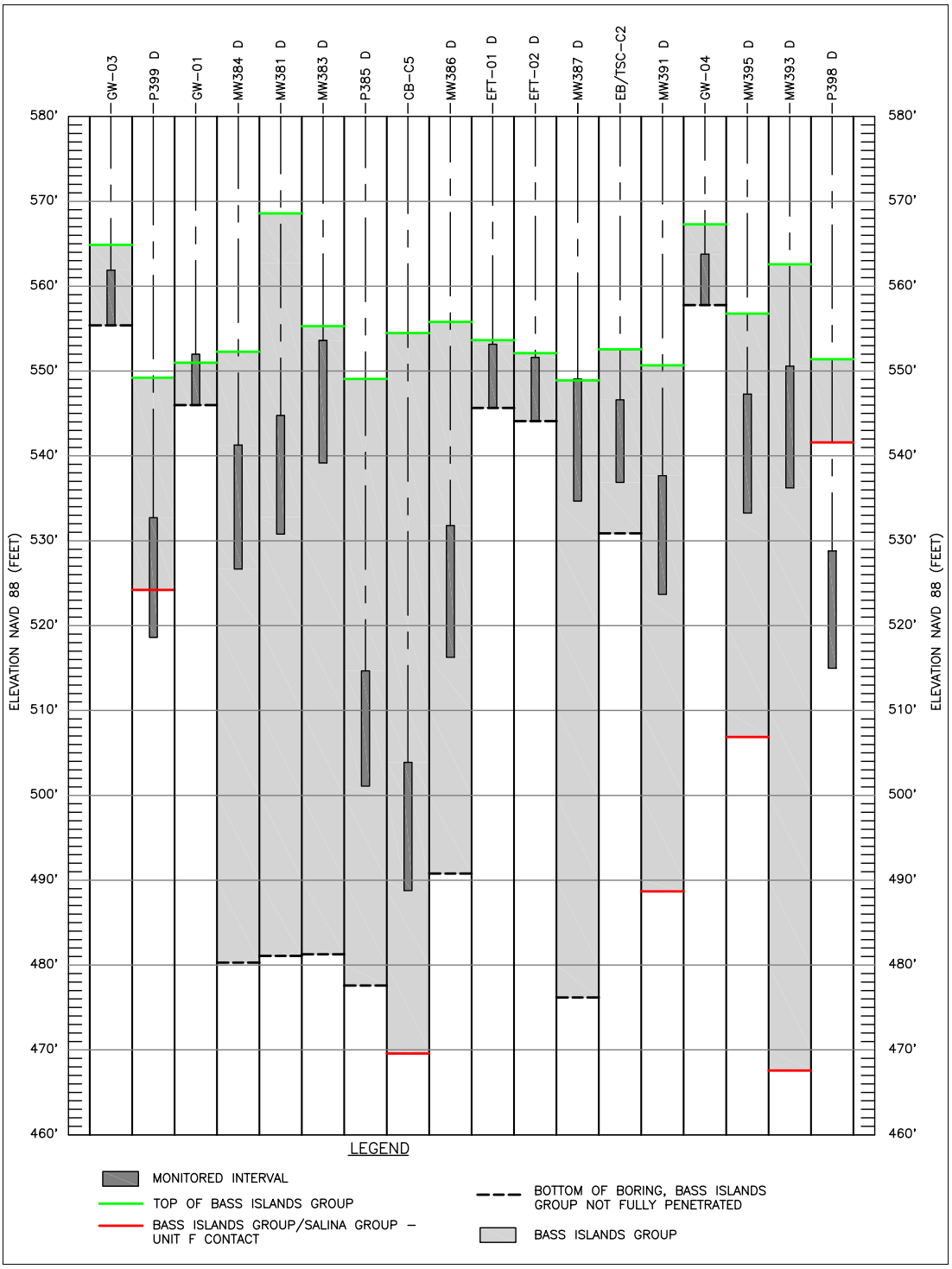

Figure 2.4-258 Watershed Boundary

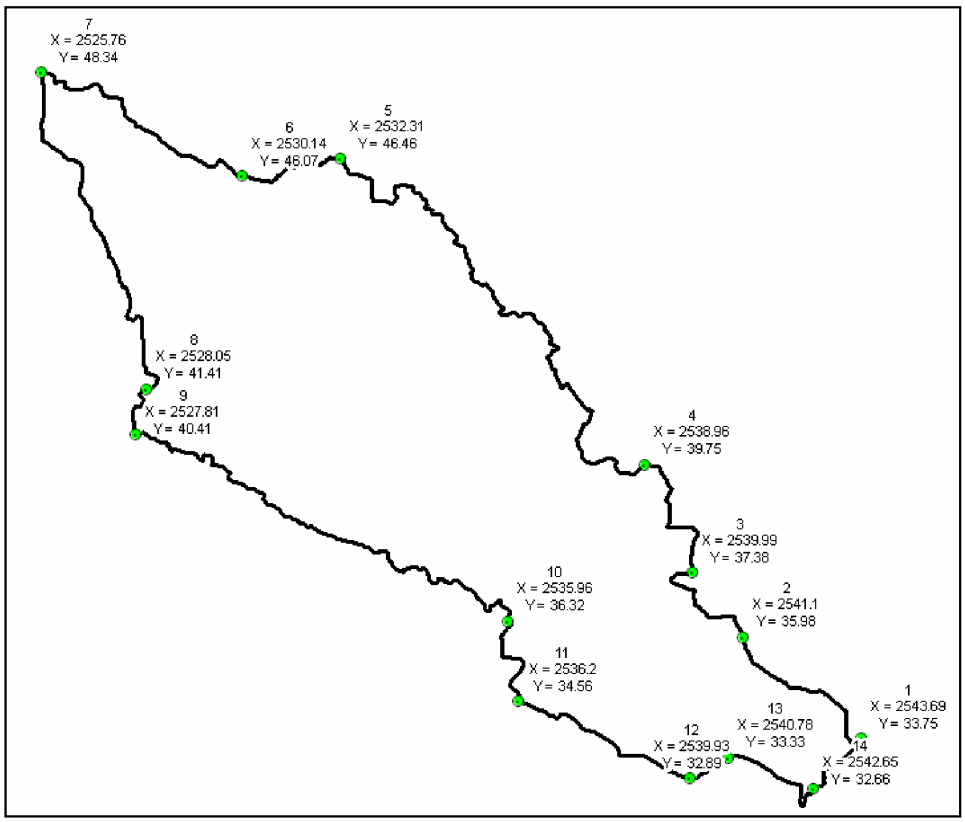

Figure 2.4-259 PMP Hyetograph

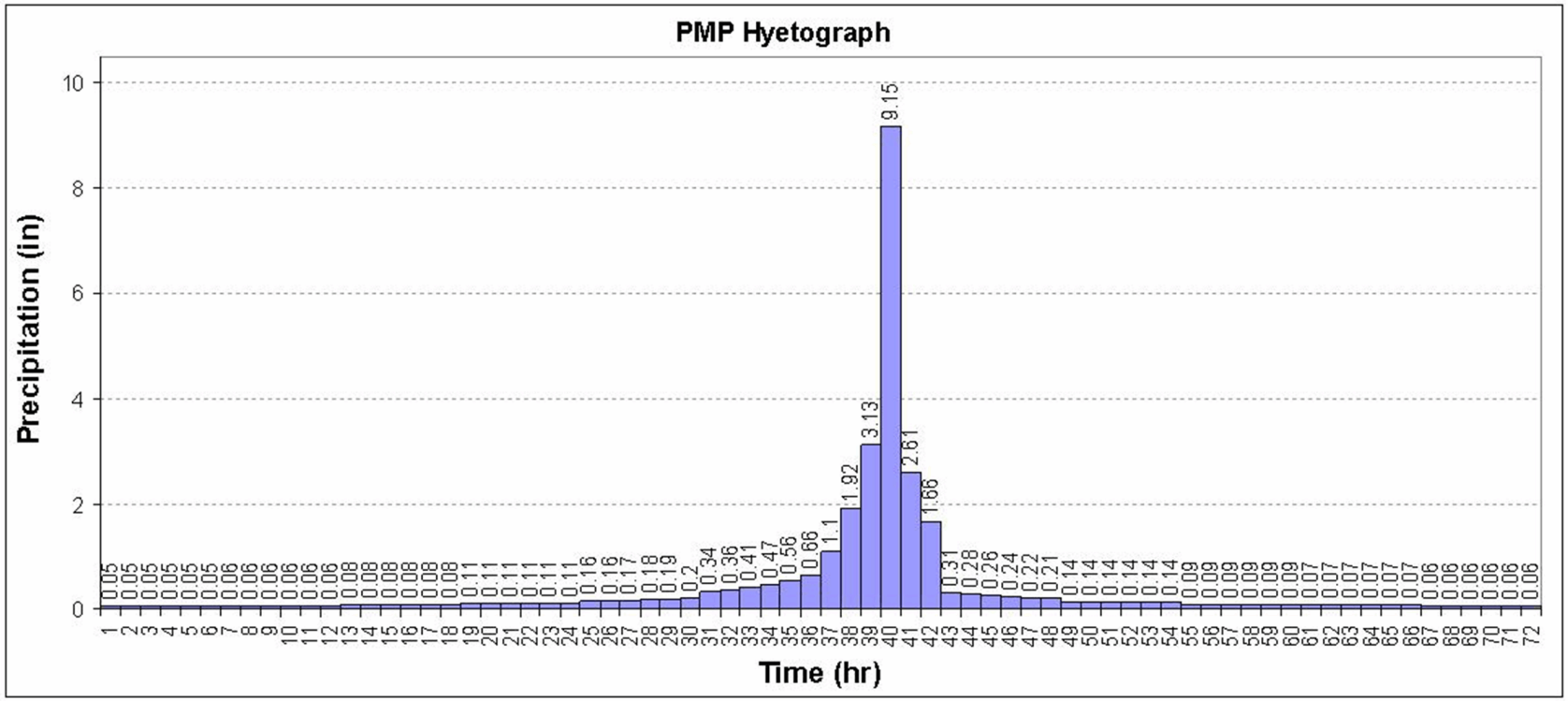

Figure 2.4-260 Results of the Snowmelt Analysis - Total Depth of Rain and Snowmelt Available for Runoff

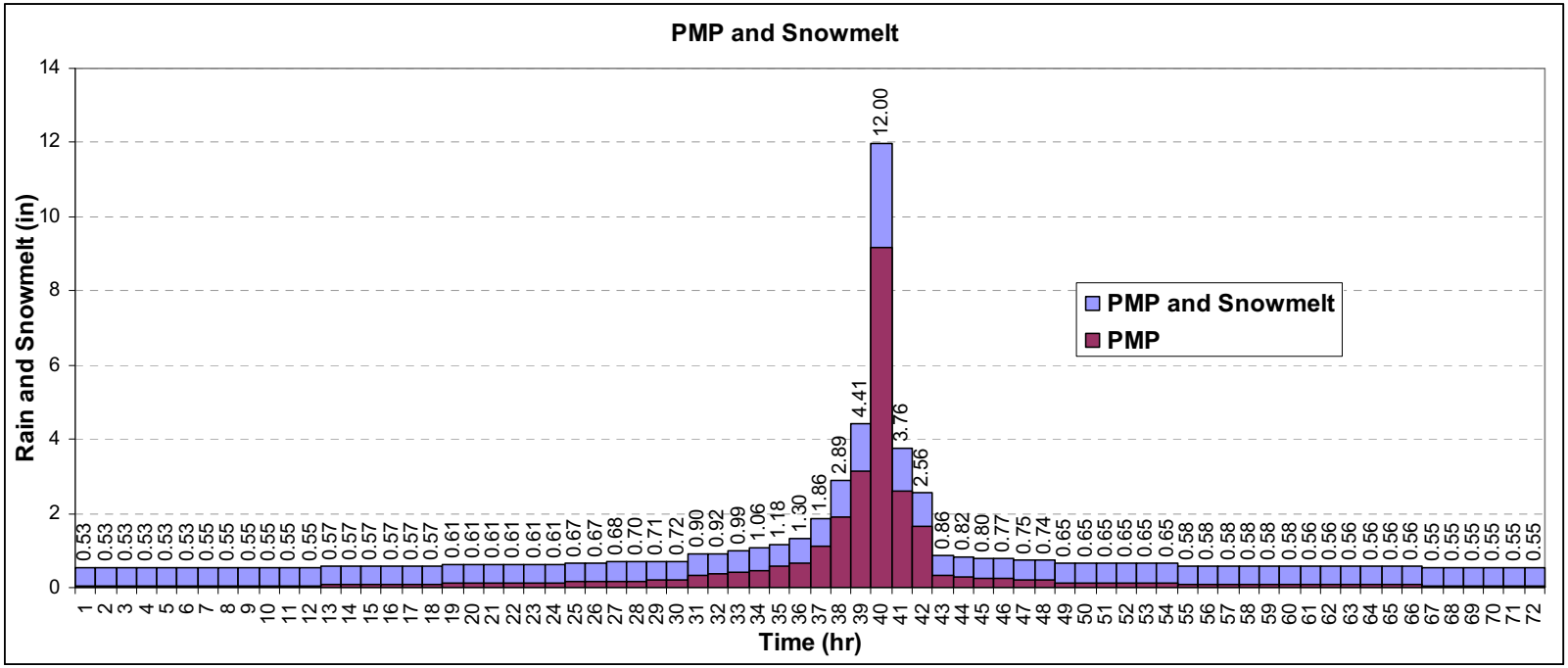

Figure 2.4-261 Summary of HEC-HMS Results

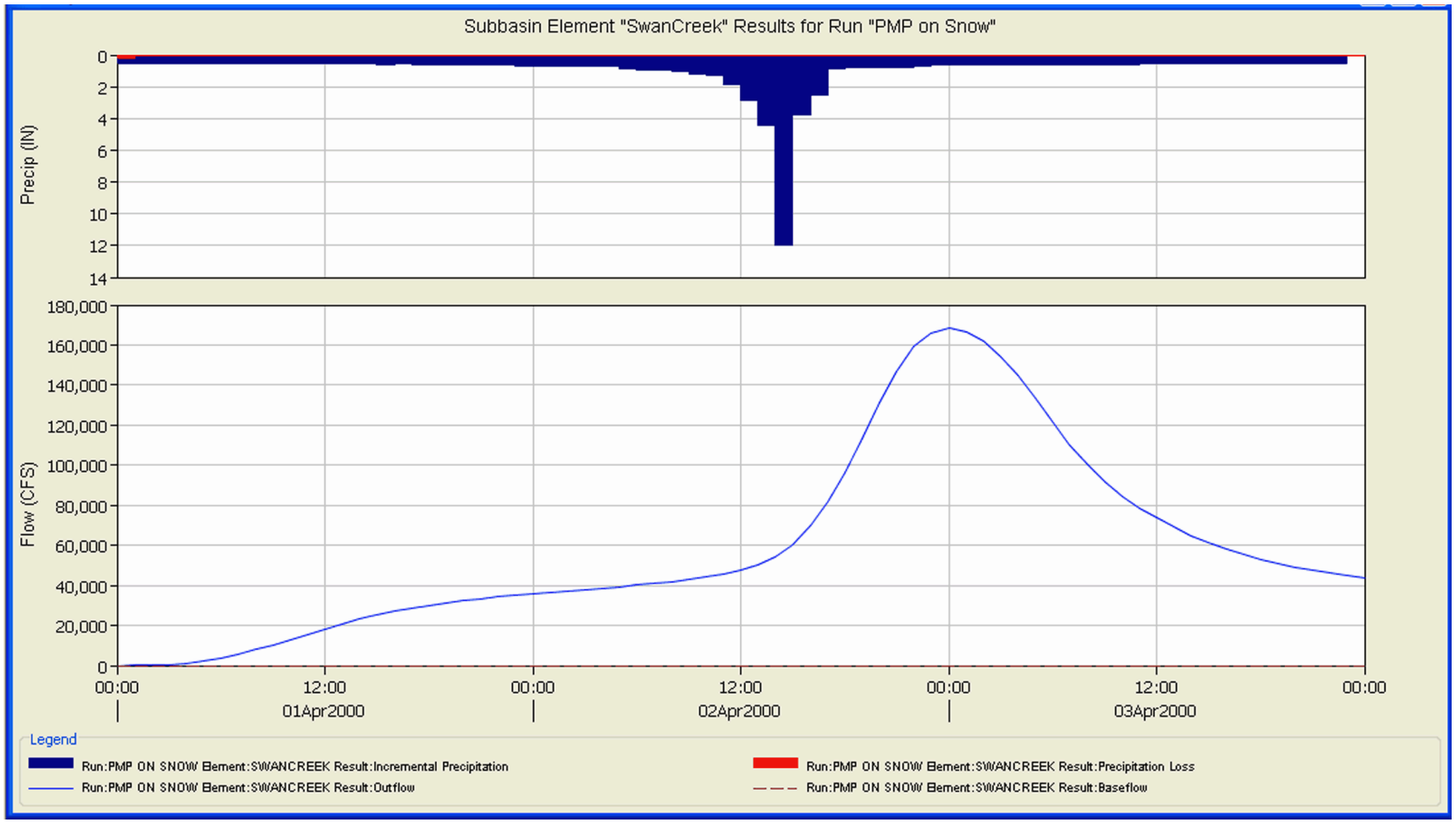

Figure 2.4-262 Water Surface Elevation at Plant

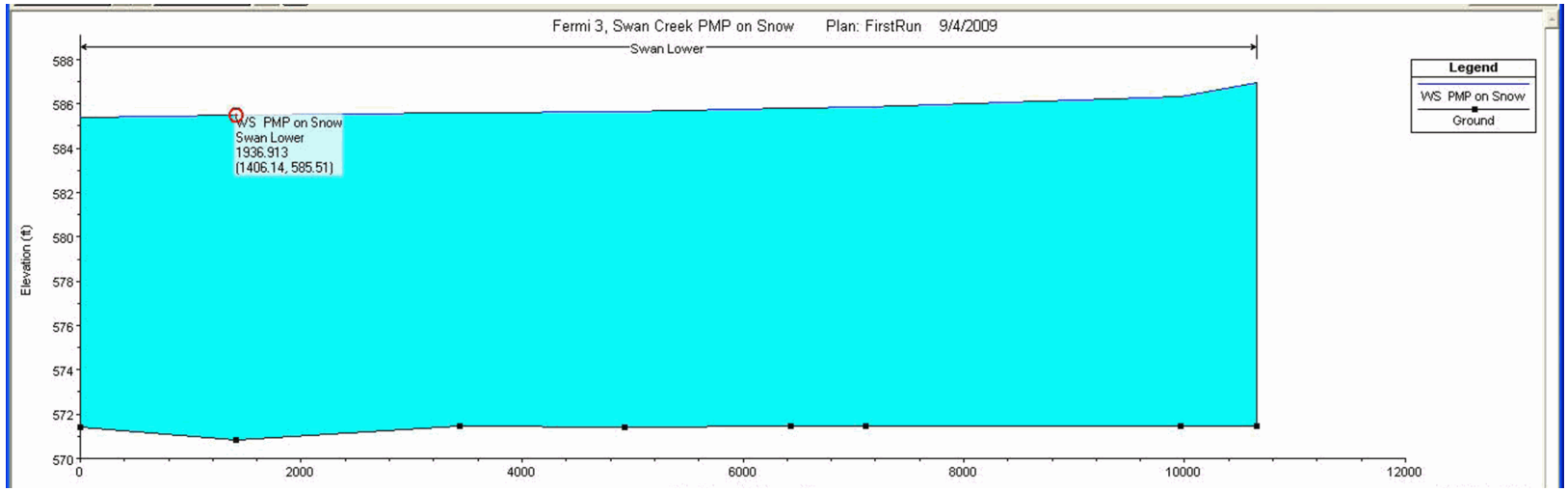

Figure 2.4-263 Still Water Elevations

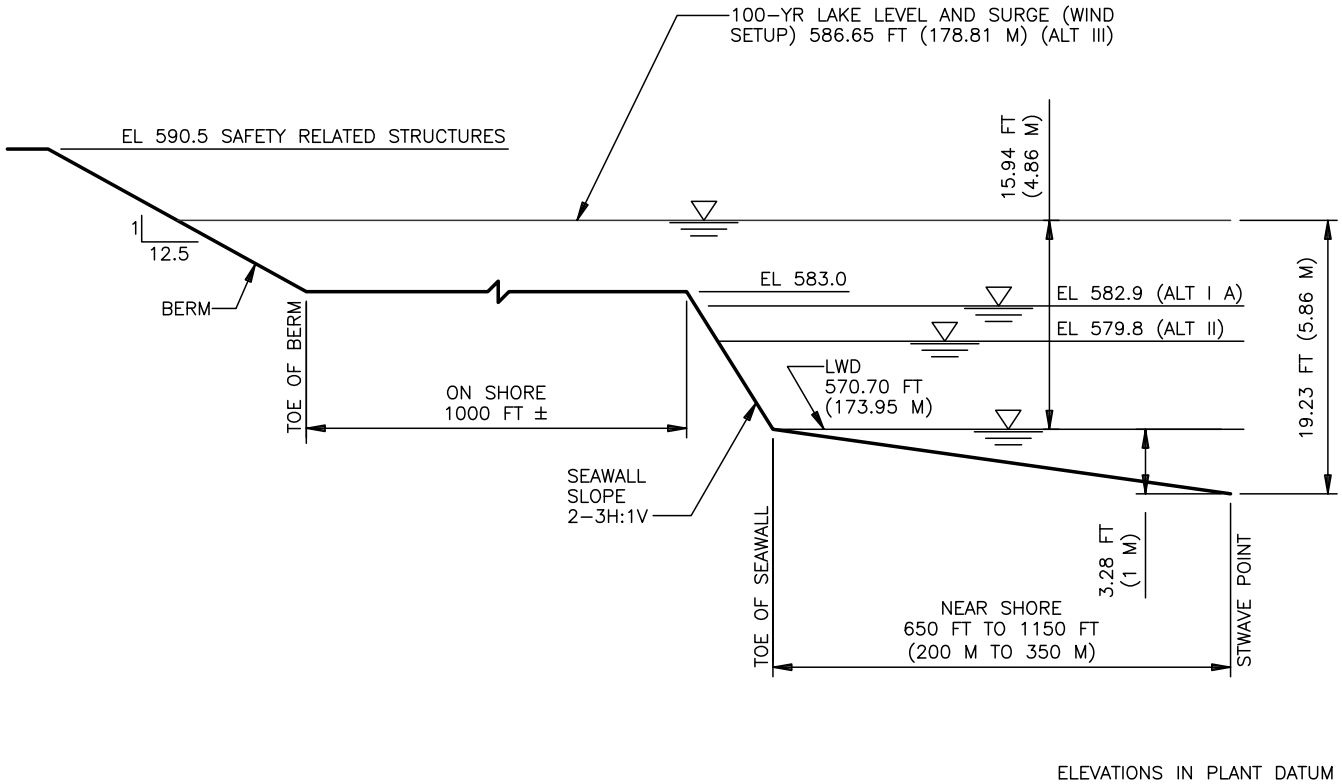

Figure 2.4-264 Wave Height and Bathymetry – Fermi Site

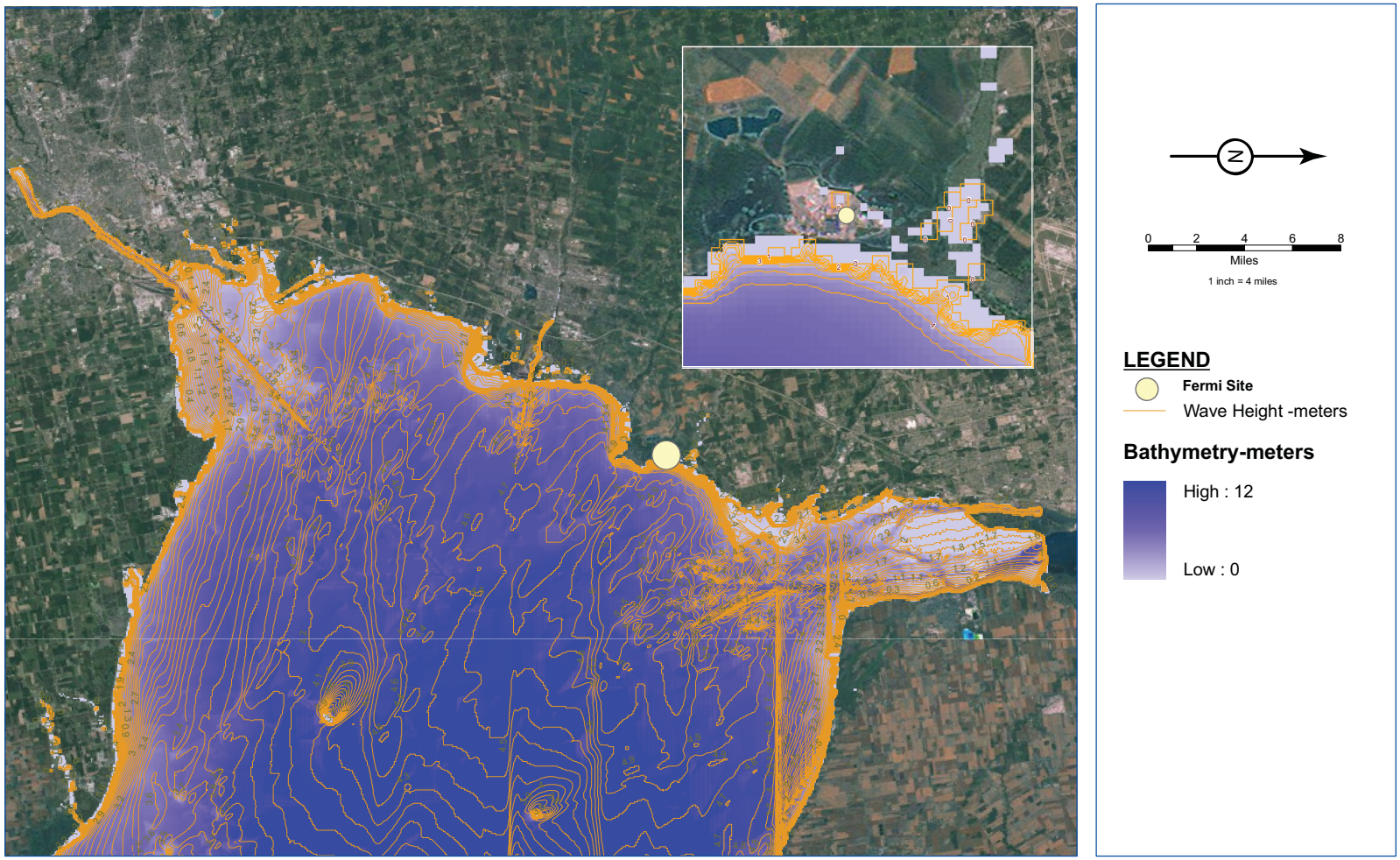

Figure 2.4-265 Wave Run-Up (Vertical exaggeration is approximately 5 to 1)

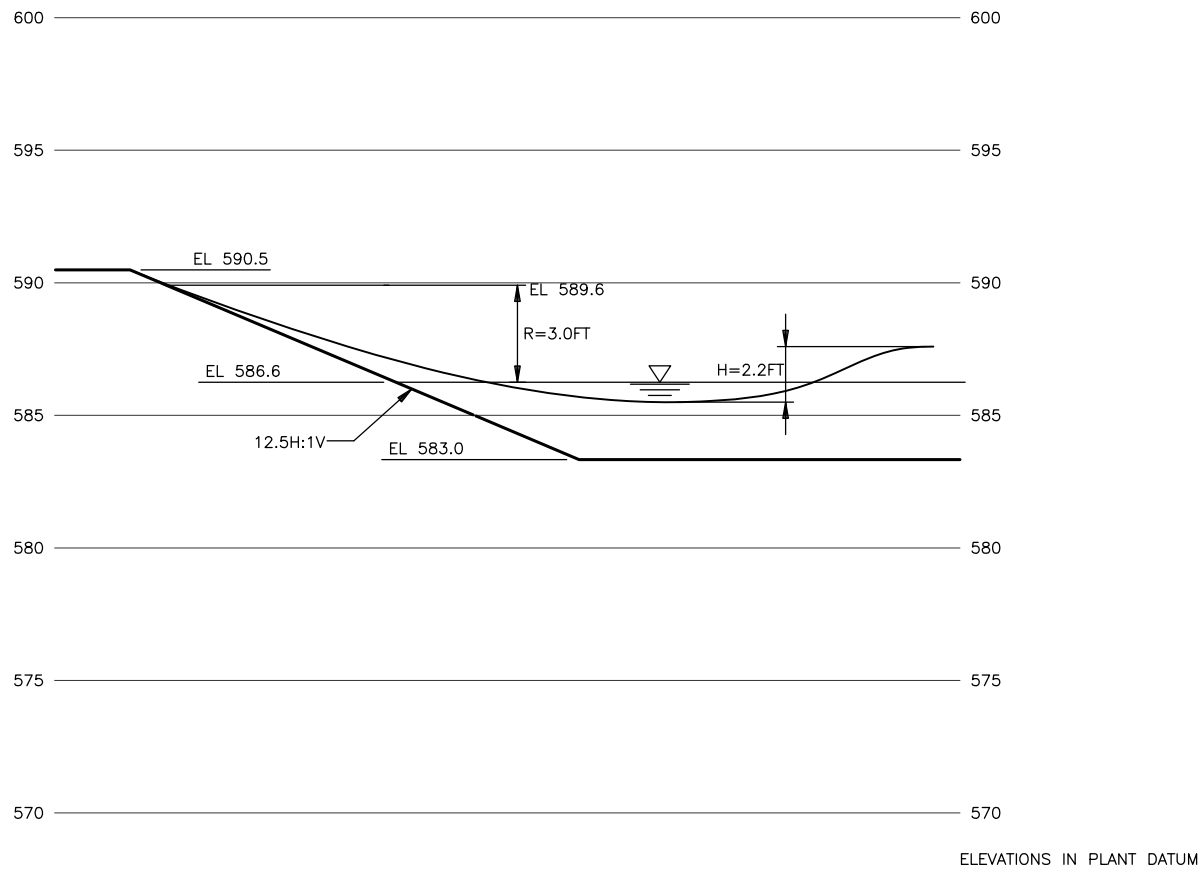

Figure 2.4-266 Conceptual Model for Groundwater Transport Analysis

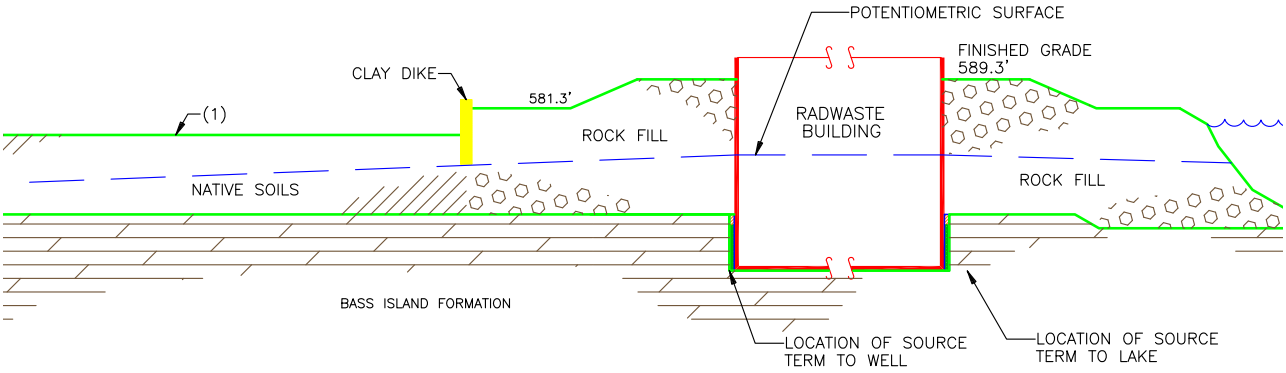

OF NATIVE SOILS NOT PER SCALE.
GRADIENT NOT PER SCALE